A Modeling Study of Effects of Flow Reduction on Salinity and Thermal Habitats in the Chassahowitzka River

XinJian Chen, Ph.D., P.E.

Southwest Florida
Water Management District

7601 US 301 North
Tampa, Florida 33637

May 2019

(Final Draft)

Table of Contents

Summary

The Chassahowitzka River is a spring-fed estuary located in Citrus County, on the Gulf coast of central Florida. The river is about 9 kilometers long from its headwaters to the Gulf of Mexico and receives a small amount of freshwater runoff from its 230 square kilometers of watershed. Most of the hydrologic loading to the Chassahowitzka River comes from its 492 square kilometer springshed, in forms of submarine groundwater discharges (SGDs) out of numerous spring vents in its headspring area and in several of its tributaries.

To evaluate minimum flows and levels (MFLs) for this relatively small and narrow estuarine system, a laterally averaged hydrodynamic model has been applied to study how reductions of SGD would affect salinity and thermal distributions in the Chassahowitzka River. The hydrodynamic model, named LAMFE, is a flux-based finite difference model that uses z-level in the vertical direction and fits bottom elevation with a cut-cell method. It is a semi-implicit model that uses a free-surface correction method, a very efficient numerical scheme that is unconditionally stable with respect to gravity waves, wind and bottom shear stresses, and vertical eddy viscosity terms. The LAMFE model is especially effective in simulating hydrodynamics in narrow and meandering rivers or estuaries such as the Chassahowitzka River.

The simulation domain extends from the mouth of the Chassahowitzka River to the headspring area, with the actual longitudinal length of 8.04 kilometers of the main stem being included in the simulation domain, along with all tributaries to the river. The model was driven by measured real-time data of water elevation, salinity, and temperature at its mouth, measured meteorological data in the region, and measured and estimated SGDs entering the estuarine system. Based on the availability of these data at the time when the Chassahowitzka River LAMFE model was developed, the model was calibrated and verified against real-time water elevations, salinities, and temperatures measured at three locations within the simulation domain during 11/18/2012 – 3/28/2017. The period prior to 1/1/2016 was for model calibration, while the period between 1/1/2016 – 3/28/2017 was for model verification.

The model was used to simulate hydrodynamics, salinity transport, and thermal dynamics in the estuary for over 10 years, from October 2007 to February 2018, to evaluate effects of the SGD reduction on salinity and thermal habitats in Chassahowitzka River, after the model was calibrated and verified. Impacts of the existing groundwater withdrawal were estimated to cause roughly a 1.40% SGD reduction based on a groundwater modeling effort. As such, the baseline flow scenario was about 1.0142 times of the existing flow condition. A series of model runs were conducted to simulate salinity and temperature in the estuary for various flow reductions from the baseline flow scenario, including 2.5%, 5%, 7.5%, 10%, …, 27.5%, and 30% reductions. Simulated salinity results were post-processed, with water volumes, bottom areas, and shoreline lengths for salinities less than or equal to 1, 2, 3, 5, 10, 15 psu being calculated based on known bathymetry. For temperature, water volumes and surface areas for temperature ≤ 15 ºC, 15 – 20 ºC, and ≥ 20 ºC were calculated. Manatees and Common Snook (*Centropomus undecimalis*) are

the primary animals to be considered in the thermal analysis. Because an adult manatee needs up to 3.8 ft (1.158 m) of a water layer to be totally submerged in, water volume and surface area of 15 – 20 °C and ≥ 20 °C with a constraint of a minimum of 1.158 m of water layer were also calculated.

Processed results of salinity habitats (water volumes, bottom areas and shoreline lengths for ≤ 1, 2, 3, 5, 10, 15 psu) and thermal habitats (water volume and surface area for ≤ 15 °C, 15 °C – 20 °C, and ≥ 20 °C) were further analyzed to generate a list of allowable flow reduction percentages based on a criterion that favorable salinity and thermal habitats should not suffer a loss of 15% or more from their baseline conditions due to a flow reduction. It was found that the most sensitive salinity habitat to flow reduction is ≤ 1 psu bottom area, which will be reduced by 15% with a 7.75% SGD reduction. The most sensitive manatee thermal habitat to the flow reduction is the 4-hour average of ≥ 15 °C surface area, which can be reduced by 15% with a 10.10% reduction of SGD. For Common Snook, the most sensitive thermal habitat is the single cold day average of ≥ 15 °C volume, which can be reduced 15% with an 8.47% SGD reduction. Based on model results of the scenario simulations, the MFL for the Chassahowitzka River was proposed to be 92% of the baseline flow condition, or a maximum of 8% reduction from the baseline condition.

The proposed MFL was evaluated for sea level rises in 2035. Three SLRs at the mouth of the Chassahowitzka River were estimated based on data obtained at the NOAA St. Petersburg and Cedar Key stations from the USACE web site http://www.corpsclimate.us/ccaceslcurves.cfm. Estimated low, intermediate, and high SLRs that could occur during 2012 – 2035 were 4.837, 8.723, and 21.105 cm, respectively. These SLRs were added to the mouth of the Chassahowitzka River to drive the hydrodynamic model in simulating the baseline flow and the MFL conditions. Habitat reductions caused by the proposed MFL with a SLR relative to those for the baseline flow condition with the same SLR were calculated and analyzed. Model results suggest that a sea level rise could significantly change salinity and thermal characteristics in the Chassahowitzka River. The proposed MFL does cross the threshold of 15% loss for ≤ 1 psu salinity volume and bottom area when the intermediate and/or low SLRs are concerned. The proposed MFL could also cause thermal habitats for both manatees (under the acute condition) and Common Snook to be reduced by more than 15% under all three sea level rise scenarios.

1. Introduction

The Chassahowitzka River is a spring-fed estuary located in Citrus County, on the Gulf coast of central Florida (Fig. 1). From its headspring to the Gulf of Mexico, the river is about 9 kilometers long and receives an insignificant amount of freshwater runoff from its 230 square kilometers of watershed. Most of the hydrologic loading to the Chassahowitzka River comes from its 492 square kilometer springshed, in forms of submarine groundwater discharges out of numerous spring vents in its headspring area and in several of its tributaries.

Like some other estuaries along the Gulf coast of Florida, the Chassahowitzka River estuary is generally well or partially mixed. The system is ecologically important for many marine species, including Florida manatees (*Trichechus manatus latirostris*) and Common Snook (*Centropomus undecimalis*), which use the spring-fed estuaries as thermal refuges in winters because a large amount of spring water with a relatively constant temperature of more than 22.0 ºC flows to the river. In order to protect this ecologically valuable springs/estuarine system, a regulatory minimum spring water flow rate was established in 2013. The adoption of the MFL rule for the Chassahowitzka River in 2013 required that the MFL is to be re-evaluated in 2019.

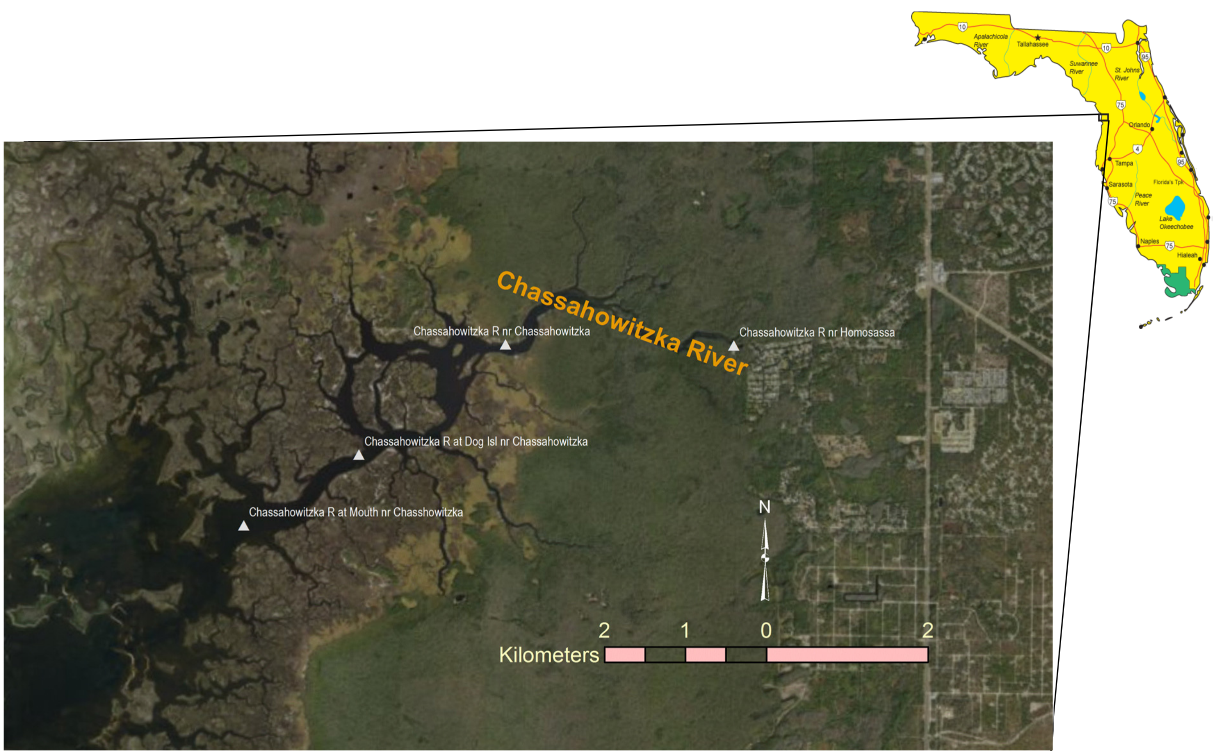

Figure 1. Aerial view of the Chassahowitzka River on the Gulf coast of Florida. Triangles mark locations of USGS real-time data stations along the river.

The objective of this modeling study is to support the MFL re-evaluation for the Chassahowitzka River. For this purpose, efforts have been made to improve model simulations for circulations, salinity transport processes, and thermal transport processes in the estuary. Improvement of the current modeling study over the previous one includes: the use of a more efficient hydrodynamic model for the riverine estuary than that used in the 2013 MFL establishment, a much longer calibration/verification period, more recent flow data, and a much longer simulation period for scenario runs.

Because the Chassahowitzka River is a narrow and meandering estuary, its circulation pattern as well as salinity and temperature distributions are normally vertically two-dimensional, which is typical for narrow estuaries (Prandle, 1985; Jay and Smith, 1990; Chen, 2004a). Therefore, the most suitable hydrodynamic model for the Chassahowitzka River is the Laterally Averaged Model for Estuaries, or LAMFE, developed by the author. The LAMFE model has been used in several previous MFL studies and has been extensively reviewed by numerous external experts over the last two decades. Examples of the LAMFE model application in the MFL evaluation include the lower Hillsborough River (Chen 1997; Chen, 1999; and Chen, 2004a), the lower Alafia River (Chen, 2005; Flannery et al., 2007), the lower Peace and Myakka Rivers (Chen, 2007a; Chen, 2008a; and Chen, 2010), and the lower Manatee/Braden Rivers (Chen, 2012a). Numerous peer-reviewed, LAMFE-related papers have been published in reputable journals (e.g., Chen, et al., 2000; Chen, 2003a; Chen, 2004b; Chen, 2004c; Chen, 2007b; Chen, 2007c; Chen, 2008b; Chen, 2012b) and international conference proceedings (e.g., Chen and Flannery, 1997; Chen, 2003b; Chen, 2006; Chen, 2008c; Chen, 2012c). Some of these peer-reviewed papers include validations of the LAMFE code. A user manual of the LAMFE model is also available (Chen, 2011) and contains all the details of testing of the LAMFE code.

As mentioned in Chen (2017), most previous coastal and estuarine hydrodynamic modeling studies did not consider effects of SGDs (Johnson et al, 1991; Blumberg and Kim, 2000), partly because SGDs are much lower than river flows and precipitations for these estuaries and partly because SGDs are very difficult to quantify in many cases. There are only very limited estuarine and coastal hydrodynamic modeling studies which considered SGDs. Ganju et al. (2011) applied the 3D model ROMS (Warmer et al., 2008) to West Falmouth Harbor, Massachusetts to verify their tidal and groundwater flux estimates to the estuary based on velocity and salinity measurements. Chen (2017) estimated and considered SGDs in the hydrodynamic simulations for Crystal River/Kings Bay using the 3D model UnLESS3D for the MFL evaluation of the estuarine system.

Because SGDs constitute a majority of the hydrologic loading to the Chassahowitzka River, a good quantification of SGDs for the estuarine system is important for a successful simulation of the Chassahowitzka River. Although there are much more flow data available for the estuary now than several years ago when the previous MFL evaluation was conducted, a high-quality dataset for all the SGDs to the spring-fed estuarine system still does not exist at this moment. As a result, some of the SGD data had to be estimated based on limited data available to this modeling study.

In the following, a discussion of the physical characteristics of the Chassahowitzka River estuary is provided in Section 2, which also contains available field data collected in the estuary. Section 3 describes model setup and model calibration and verification, including comparisons of modeled water levels, salinities, and temperatures to measured real-time data, with a skill assessment of the model performance. Section 4 presents scenario simulations and analyses of model results of these scenario runs. Section 5 considers effects of the sea level rise on the MFL evaluation results. Conclusions of this modeling effort for the MFL re-evaluation of the Chassahowitzka River are summarized at the end of the report in Section 6.

2. Physical Characteristics of the Estuary and Field Data

2.1 Physical characteristics of the Chassahowitzka River

Chassahowitzka River (Fig. 1) is a short and narrow estuary, which originates in Citrus County and flows to the Gulf of Mexico at Chassahowitzka Bay. The river is about 9 km long, with a mean depth of 0.9 m, or 3 feet (Notestein et al. 2001). The width of the Chassahowitzka River varies between about 30 m or less in the upstream portion of the river and over 550 m near its mouth.

Although the river has a watershed of about 230 square kilometers, most of the watershed is self-percolating and barely contributes any quantifiable surface water runoff. The majority of its hydrologic loading comes from spring flows out of numerous spring vents located in the headspring area and in several of its tributaries. Submarine groundwater discharges from these spring vents are from the Upper Floridan aquifer, with a contributing springshed estimated at about 492 square kilometers.

Figure 2 shows locations of the spring vents that discharge groundwater flows to the Chassahowitzka River. The Chassahowitzka Main Spring, Chassahowitzka #1, Chassahowitzka #2, and several unnamed springs upstream of the headwaters for the Chassahowitzka River (Scott et al. 2004). Many spring flows discharging to the Chassahowitzka tributaries are insignificant, except for the Crab Creek spring, the Potters Creek spring (Ruth spring), Baird Creek springs, and flows to the Crawford Creek, possibly from Beteejay and Rita Marie springs.

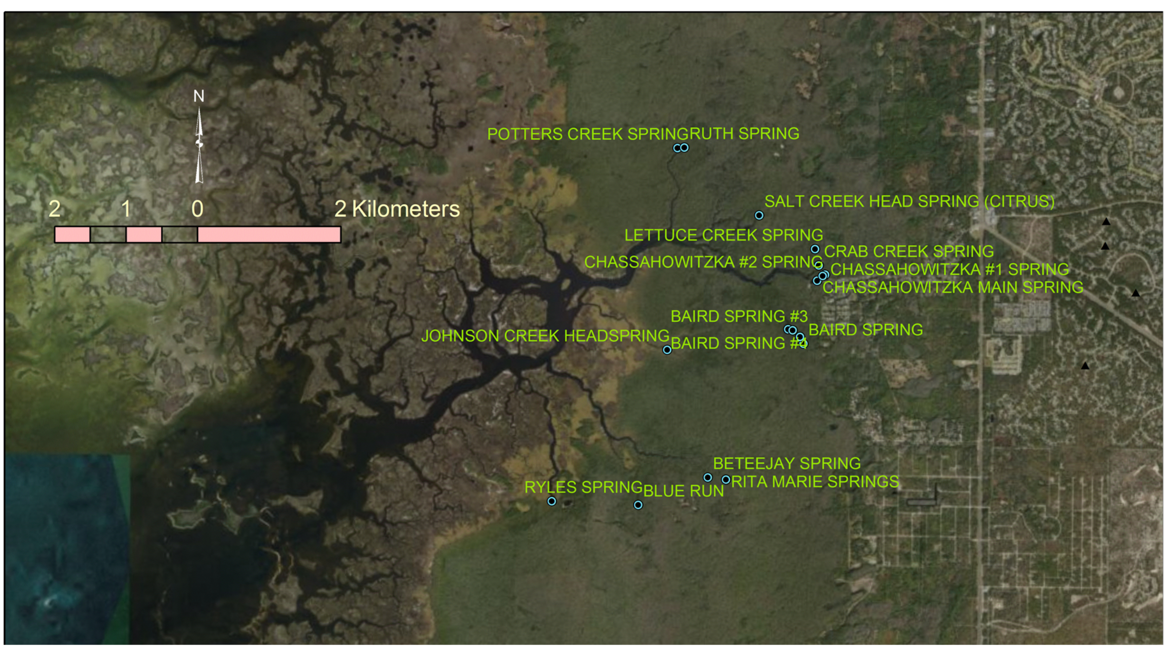

Figure 2. Spring locations of the Chassahowitzka River estuarine system.

Although the Chassahowitzka Main, Chassahowitzka #1, and Chassahowitzka #2 are considered as the headwaters of the river, there exists a channel network upstream of the headspring area, connecting to the Chassahowitzka River and allowing residents living along the channels to get access to the River. Although surface water runoff to this channel network is negligible, there are some relatively small SGDs entering the channels, which are eventually gauged at a United States Geological Survey (USGS) station just above the Crab Creek confluence in the Chassahowitzka River (the USGS Chassahowitzka River near Homosassa station). In addition to these small SGDs, there is also tidal flow, which comes from or enters to this channel network but contributes no net flow for the Chassahowitzka River.

3.2 Field data

Available field data for the hydrodynamic modeling of the Chassahowitzka River system using the LAMFE model included bathymetry survey and real-time data of water elevation, salinity (measured in the form of specific conductance), and temperature at four USGS stations in the estuary. Bathymetry survey was conducted by the University of South Florida (Wang, 2006). Figure 3 is a plot of Chassahowitzka River bathymetry from Wang (2006). In addition to the bathymetry survey, there are also Light Detection and Ranging (LIDAR) data available for the Chassahowitzka River system in this study.

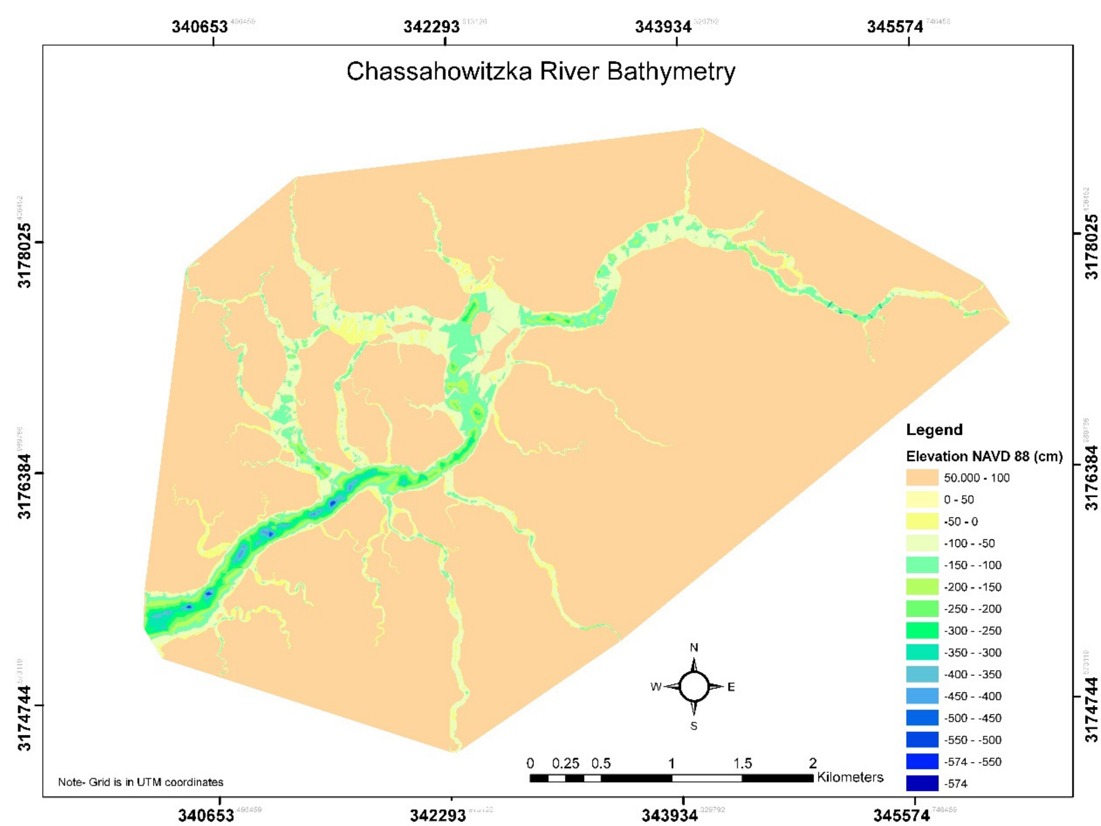

Figure 3. Bathymetry surveyed by Wang (2006) in the Chassahowitzka River system.

As can be seen from Figure 3, most of the tributaries of the Chassahowitzka River are very shallow. In the main stem of the Chassahowitzka River, most river segments are also shallow, except for the most downstream one quarter of the river, where the bottom elevation of the river are -3.0 m, NAVD88 or lower. There several deep areas in the downstream portion of the estuary, with the bottom elevation being -5 m, NAVD88 or lower. In the most upstream 10% of the river, the river bottom is generally shallower than -1 m, NAVD88, with most of the bottom being actually shallower than -0.5 m, NAVD88.

With funds provided by the Southwest Florida Water Management District (SWFWMD), the USGS installed measurement instruments at four stations along the river, showing with triangles in Figure 1. These USGS stations are, from downstream to upstream: (1) Chassahowitzka River at Mouth near Chassahowitzka, (2) Chassahowitzka River at Dog Island near Chassahowitzka, (3) Chassahowitzka River near Chassahowitzka, and (4) Chassahowitzka River near Homosassa. Rea-time water elevations, salinities, and temperatures were recorded every 15 minutes. Table 1 shows some general information about these USGS stations, including station name, station number, longitude, latitude, starting date of the data collection, datum, and sensor elevations for conductance and temperature. At the two downstream stations, conductance and temperature data have been collected at two depths, one near the top and the other near the bottom. At the Chassahowitzka River near Homosassa station and the Chassahowitzka River near Chassahowitzka station, conductance and temperature data at one depth have been collected.

Table 1. General information about the USGS data collection stations in the Chassahowitzka River.

Station Name	Chassahowitzka River			
	near Homosassa	near Chassahowitzka	at Dog Island near Chassahowitzka	at Mouth near Chassahowitzka
Station #	2310650	2310663	2310673	2310674
Longitude	82 34 38.38W	82 36 22.35W	82 37 28.35W	82 38 20.35W
Latitude	28 42 55.71N	28 42 54.95N	28 42 09.95N	28 41 40.95N
Available Since	10/11/2007	5/1/2003	9/12/2005	10/11/2005
Datum	NGVD29	-0.71 ft, NAVD88	NAVD88	NAVD88
Sensor Elevation (ft, NAVD88)	-2.42	-4.32	-2.06	-2.80
			-4.21	-6.25

In addition to water elevation, conductance, and temperature, cross-sectional flow data were also available from the USGS for the Chassahowitzka River near Homosassa station and the Chassahowitzka River near Chassahowitzka station. These flow data were calculated from regression relationships obtained by the USGS based on limited measured flow data. It was found that multivariable regression relationships exist among the Chassahowitzka flow, tides, water elevation change over the 15-minute interval (i.e., time derivative of water elevation), and the groundwater level in a Weeki Wachee well, which is about 13 miles, or about 21 kilometers, away from the headwaters of the Chassahowitzka River. From November 17, 2012 on, the USGS started flow data collection at the Chassahowitzka River near Homosassa station using the index velocity method.

Figure 4 shows measured water elevations at the four USGS stations during a 270-day period: 12/19/2009 – 3/18/2010 (top panel), 3/19/2010 – 6/16/2010 (middle panel), and 6/17/2010 – 9/14/2010 (bottom panel). In the figure, water level data were plotted with red lines for the Chassahowitzka River near Homosassa station, while water levels at the Chassahowitzka River near Chassahowitzka, at Dog Island near Chassahowitzka, and at mouth near Chassahowitzka stations were plotted with green, blue, and black lines, respectively. Graphics of time series plots of water elevations at the four USGS stations for other time periods are similar and not presented here. These plots are included in Appendix A.

Figure 5 shows measured salinities at the four USGS stations during a 90-day period between 12/19/2009 and 3/18/2010. In the top panel of the figure, salinity data were plotted with blue line for the Chassahowitzka River near Homosassa station and with green line for the Chassahowitzka River near Chassahowitzka station. The middle panel contains top-layer (blue line) and bottom-layer (green) salinities at the Chassahowitzka River near Chassahowitzka. Measured top-layer and bottom-layer salinities at the Chassahowitzka River at Dog Island near Chassahowitzka station are plotted with blue and green lines, respectively in the bottom panel of Figure 5. Plots of measured salinity time series at the four USGS stations for other time periods are similar and can be found in Appendix B.

Figure 6 shows measured temperatures at the four USGS stations during the same 90-day period between 12/19/2009 and 3/18/2010 in the same format as that for salinity data shown in Figure 5. Measured temperature time series at the four USGS stations for other time periods are similar and shown in Appendix C.

Although Figs. 4 - 6 only show several months of real-time data measured in Chassahowitzka, it can be seen from these figures that tidal signals are evident in water level, salinity, and temperature in the estuarine system. The high-frequency tidal variability includes both diurnal and semi-diurnal variations. There are also some non-tidal, low frequency signals in the real-time data, which are mainly influenced by meteorological and hydrological characteristics of the region.

Comparing water levels measured at the Chassahowitzka River near Homosassa station, which is located just upstream of the confluence with Crab Creek, with those measured at other three stations, which are all located downstream of the Crab Creek confluence, it is clear that the low tides near the headspring area is much higher than those at the three downstream stations. Although the upstream inflow and tidal attenuation typically cause low tides in the upstream reach higher than those in the downstream reach in an estuary, they are not able to keep the low tides at the Chassahowitzka River near Homosassa station at the level as high as that shown in the data.

The only reasonable explanation is that there is at least a shallow area or a shoal between the Chassahowitzka River near Homosassa and Chassahowitzka River near Chassahowitzka stations that causes a damming effect for the flow in the river, maintaining the water level upstream of this shallow area to a relatively high level during low tides. Although a field reconnaissance didn't identify any shoals in the upstream portion of the Chassahowitzka River, possibly due to fact that the field trip was during high tides, there is a long stretch in the upstream part of the river which is shallow. From the bathymetry data shown in Figure 3, it can also be seen that a shallow river segment of about 480 meters long exists in the Chassahowitzka River and is located just downstream of the confluence with the Crab Creek. Physically parameters such as the water level and salinity at the Chassahowitzka River near Homosassa station are greatly affected by this shallow river segment.

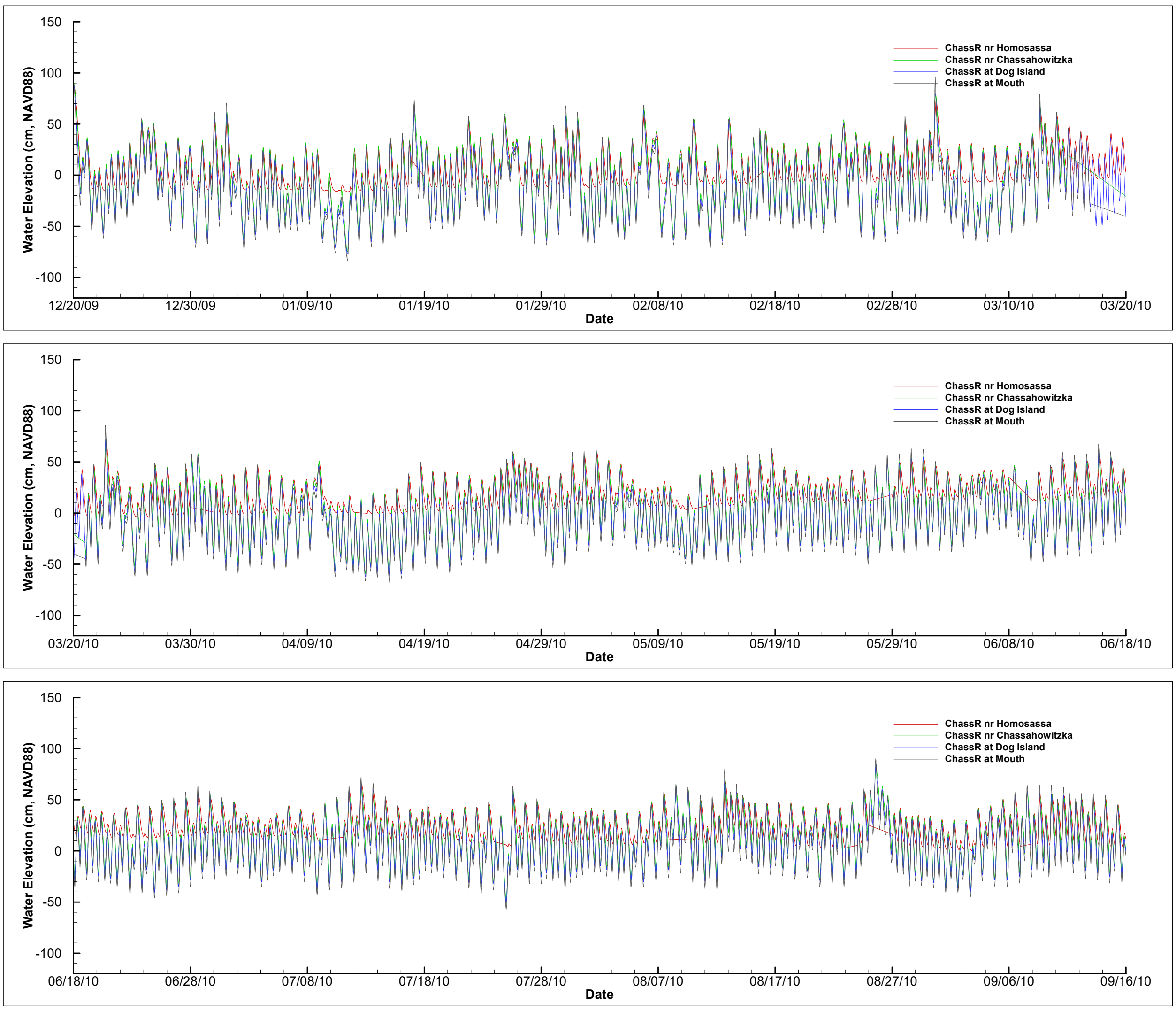

Figure 4. Measured water elevations at the Chassahowitzka River near Homosassa (red lines), near Chassahowitzka (green lines), at Dog Island near Chassahowitzka (blue lines), and at mouth

near Chassahowitzka (black lines) during a 270-day period: 12/20/2009 – 3/20/2010 (top panel), 3/20/2010 – 6/18/2010 (middle panel), and 6/18/2010 – 9/16/2010 (bottom panel).

Figure 5. Measured salinities at the Chassahowitzka River near Homosassa (top panel, blue line), near Chassahowitzka (top panel, green line), at Dog Island near Chassahowitzka (middle panel, top layer blue line, bottom layer green line), and at mouth near Chassahowitzka (bottom panel, top layer blue line, bottom layer green line) during a 90-day period: 12/20/2009 – 3/20/2010.

Measured salinity at the Chassahowitzka River near Homosassa station also behaves quite differently from other stations. In addition to the fact that salinity is lower than those at the other three stations, it exhibits only short-term tidal variations that are diurnal and semi-diurnal. Long-term variations seen at salinity data measured at other three stations almost do not exist at the Chassahowitzka River near Homosassa station. The peak salinities during tidal cycles vary within a small range between about 4 psu to 5 psu, while the lowest salinity values during tidal cycle stay within about 0.5 psu to 1 psu. As a result, both salinity peaks and salinity troughs are quite stable. This salinity variability at the Chassahowitzka River near Homosassa station is mainly due to the relatively low and stable salinity in the SGDs near the headwaters and the shallow stretch of the river in the Chassahowitzka River, which acts like salinity barriers prohibiting salt water from the downstream segment to be transported upstream. It is likely that salinity in spring vents upstream of the Crab Creek conference behaves with similar variabilities as that measured at the Chassahowitzka River near Homosassa station.

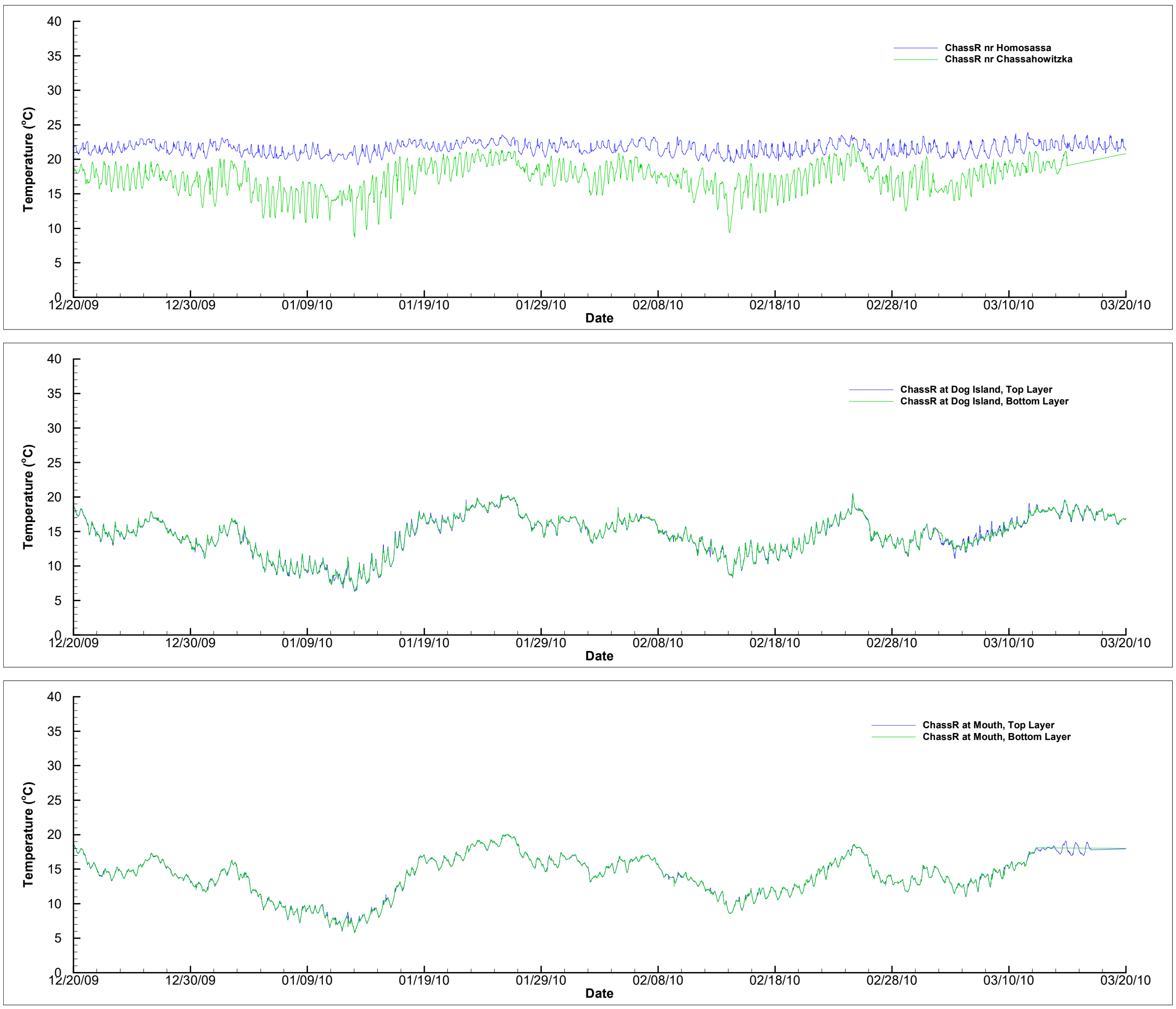

Figure 6. Measured temperatures at the Chassahowitzka River near Homosassa (top panel, blue line), near Chassahowitzka (top panel, green line), at Dog Island near Chassahowitzka (middle panel, top layer blue line, bottom layer green line), and at mouth near Chassahowitzka (bottom panel, top layer blue line, bottom layer green line) during a 90-day period: 12/20/2009 – 3/20/2010.

The 90-day period in the temperature time series shown in Figure 6 includes some cold days in 2010, which broke and still is the record for the number of consecutive days with daily minimum air temperature below 0 ºC for the region since air temperature data first available more than 73 years ago. During these cold days, water temperature dropped to about 5 ºC in the downstream portion of the river, especially downstream of the Dog Island. Upstream of the Dog Island, water was warmer due to SGDs from all the spring vents in the headspring area and in tributaries such as the Crab Creek and the Potters Creek. Because the Chassahowitzka River near Homosassa station is located just below the Chassahowitzka Main Spring, measured temperature there represents mostly SGD temperature from the ground, with temperature having very small diurnal variations around an average of about 22.5 ºC. Because of fact that the measurement location is a few hundred feet downstream of the Chassahowitzka Main, it is likely that the actual temperature of the SGD is slightly warmer than the data shown and has a smaller temperature variability.

Meteorological data (wind speed, wind direction, air temperature, air humidity, and solar radiation) used for this modeling study were hourly readings at a SWFWMD weather station near Inglis, Florida for days prior to 7/2/2013. For days since 7/2/2013, meteorological data collected with a 15-minute interval at a Florida Automated Weather Network (FAWN) station by the University of Florida's Institute of Food and Agricultural Science (UF/IFAS) were used. The Inglis station is about 22 miles (35.4 KM) north of the Chassahowitzka River, while the FAWN station of UF/IFAS is located at the Lecanto High School, about 10 miles (16.1 KM) northeast of the Chassahowitzka River.

Similar to the Crystal River/Kings Bay system (Chen, 2017), the climatology in the region has distinct winter and summer patterns. Winter is characterized by frequent frontal incursions and extratropical cyclones that can produce large shifts in wind speed and wind direction in response to rapidly changing atmospheric pressure and thermal gradients. Summer is generally characterized by light and variable winds originating from the northeast trade wind circulation. Sea/land breezes are typical due to the strong differential heating of the land and adjacent waters along the coast during the summer months. Occasional tropical storms can move to the area during summer, causing a temporal but sometimes intense modification to the meteorological conditions of the region.

Figure 7 shows time series of wind at 10 m above the ground at a FAWN station at the Lecanto High School during a 270-day period, from November 19, 2015 to August 15, 2016. Solar radiation, air temperature, and air humidity measured at the Lecanto High School station are shown in Figure 8 during the same 270-day period. Temporal variabilities of solar radiation, air temperature, air humidity, and wind speed and wind direction for other time periods are similar to Figures 7 and 8. As such, time series plots of the measured meteorological parameters for other time periods are omitted here.

As the objective of this modeling study is to support the MFL re-evaluation for the Chassahowitzka River, good SGD data for the river are important. Although much more flow data is now available than several years ago when the MFL evaluation was first conducted for the estuary, there are still many uncertainties in quantifying SGDs, especially for those entering to the tributaries. The best flow dataset available in this study is that for flow through the cross section at the USGS Chassahowitzka River near Homosassa station.

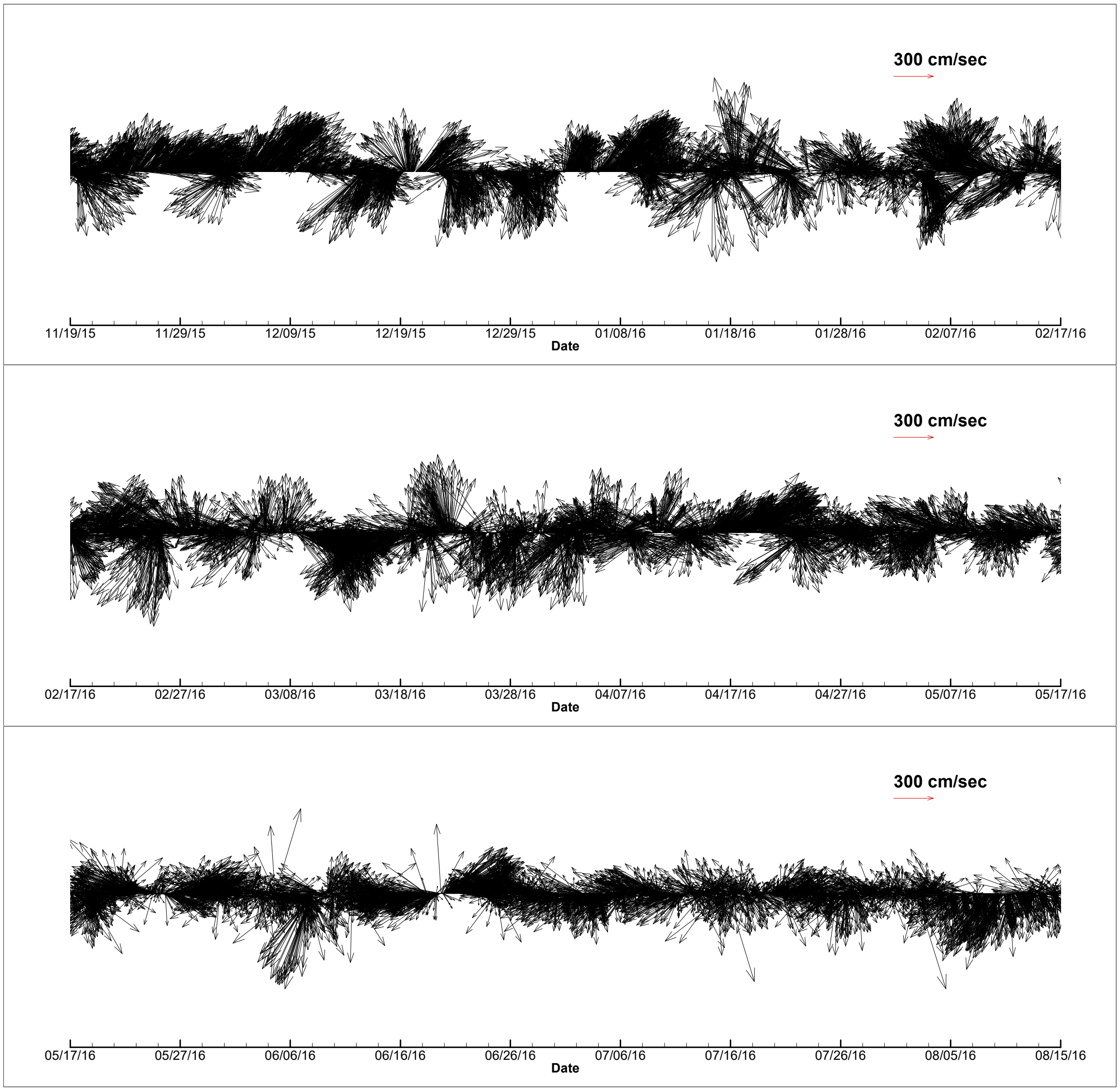

Figure 7. Vector plots of measure wind at a FAWN station at the Lecanto High School during 11/19/2015 – 8/15/2016.

As mentioned before, the USGS developed a multivariable relationship correlating discharge through the cross section of the USGS Chassahowitzka River near Homosassa station with the surface water elevation, elevation change over the recording interval (time derivative of water elevation), and groundwater level at a well in Weeki Wachee (roughly 21 kilometers away from the Chassahowitzka River), based on a limited number of discharge data measured at this cross section. The relationship takes the following form

$$Q_{ch} = 31.3378 - 6.1376GH + 2.4394W - 905.3087DelRate \quad (1)$$

where Q_{ch} (in cfs) is the total SGD entering Chassahowitzka above the confluence with the Crab Creek (or through the cross section at the Chassahowitzka near Homosassa station,) GH is gage height (feet, NGVD29), W is Weeki Wachee well level (feet, NGVD29), and $DelRate$ is the change of gage height over the 15-minute interval of data collection.

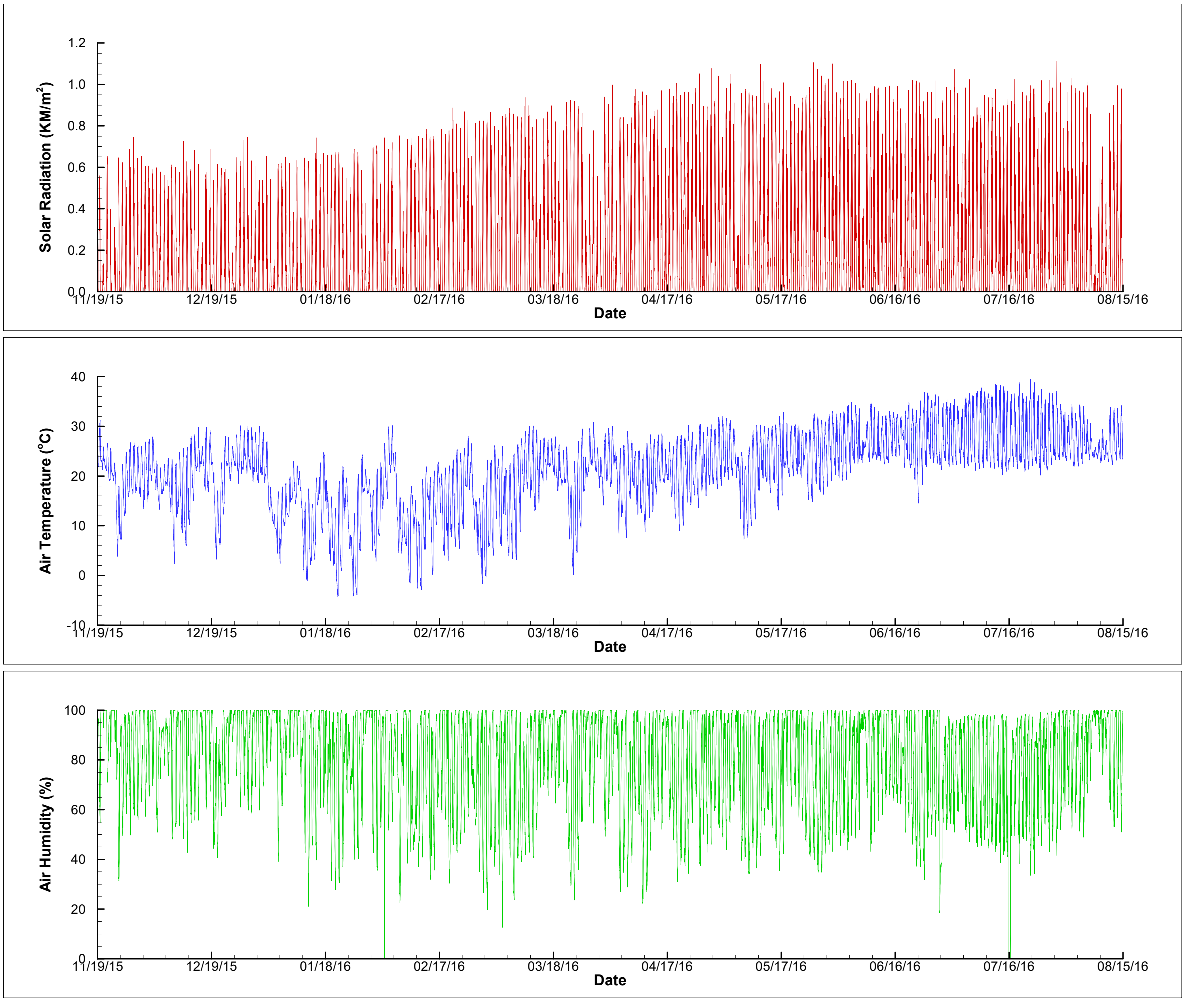

Figure 8. Measured solar radiation, air temperature, and air humidity at a FAWN station at the Lecanto High School during 11/19/2015 – 8/15/2016.

Since 11/17/2012, the USGS has been measuring the index velocity at the cross section of the Chassahowitzka River near Homosassa station. The discharge rate through the cross section was computed using a rating curve relating the index velocity with discharge, which includes not only all the SGDs out of the spring vents upstream of the cross section but also the tidal flow through the cross section. Figure 9 shows gaged USGS flow through the cross section of the Chassahowitzka River near Homosassa station using the index velocity method during a 270-day period from 11/19/2015 to 8/15/2016. As can be seen from the figure, there are some missing and bad data periods in the flow data; nevertheless, tidal signals, with a range of less than 0 cfs to more than 100 cfs, are evident.

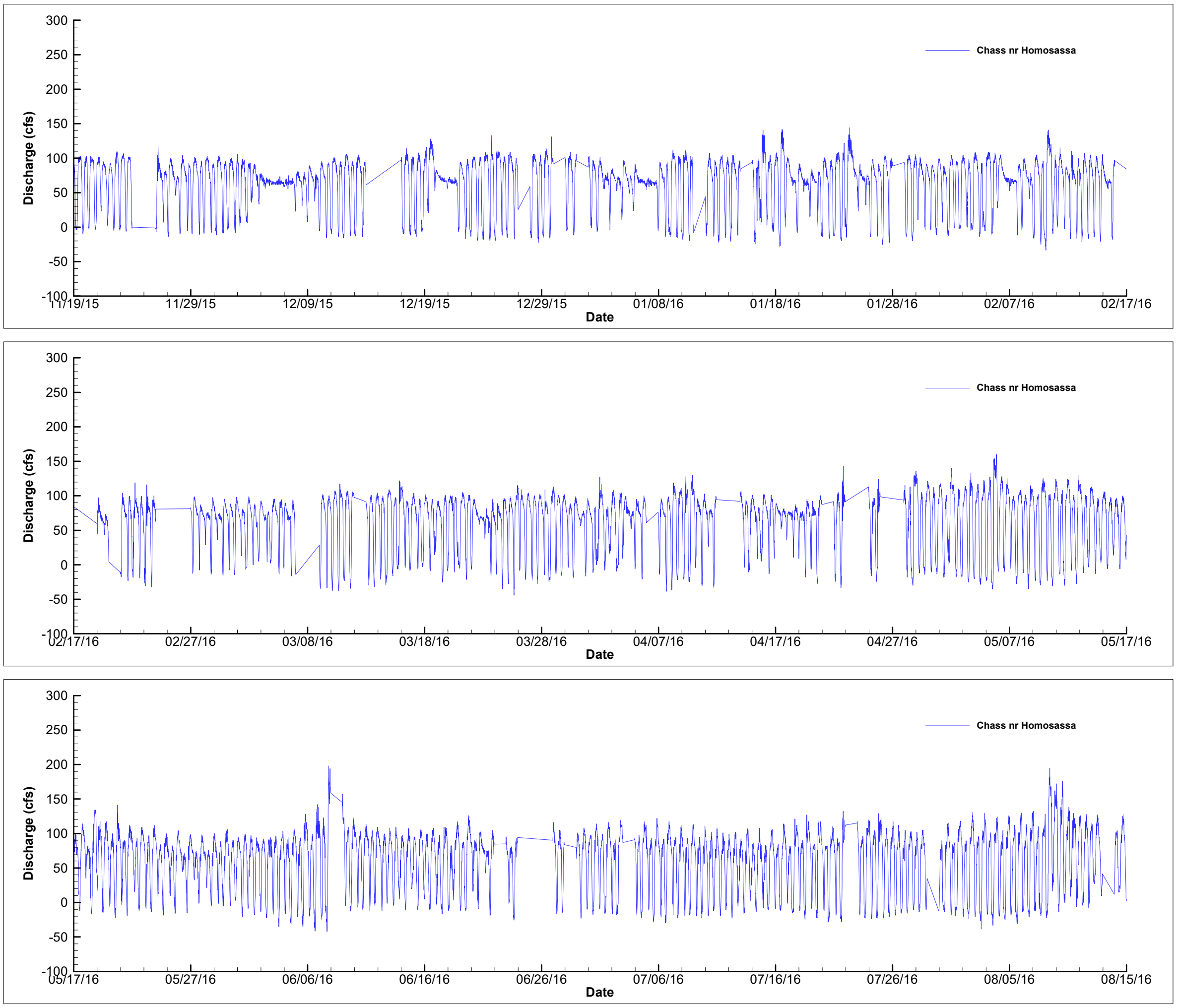

Figure 9. Gaged discharge through the cross section of the USGS Chassahowitzka River near Homosassa station during a 270-day period from 11/19/2015 to 8/15/2016.

Overall, real-time data of water elevation, salinity, temperature, and discharge measured by the USGS on the Chassahowitzka River are of good quality, despite the fact that there are a few missing data periods and a number of problematic data points in the dataset. The meteorological data collected at the Inglis station by the SWFWMD and at the Lecanto High station by the FAWN are good enough for a successful application of the LAMFE model to the Chassahowitzka River.

3. Model Development

This section is a brief description of the LAMFE model development for the MFL re-evaluation of the Chassahowitzka River system. The model theory and numerical methods used in the model are not discussed here but can be found in several previous publications (e.g., Chen, 2003a; Chen, 2004c).

3.1 Model Setup

Based on its physical characteristics, the Chassahowitzka River system was discretized with 348 grids along the river main stem and its 19 branches. The horizontal spacing of the grids varies between 10 m to 370 m. Figure 10 shows cross sections that form the 348 LAMFE grids along the main stem of the Chassahowitzka River and its branches. The water body was discretized with 15 layers between elevations -5.1 m, NAVD88 and 3.3 m, NAVD88, with the layer thickness varying from 0.3 m to 1.2 m.

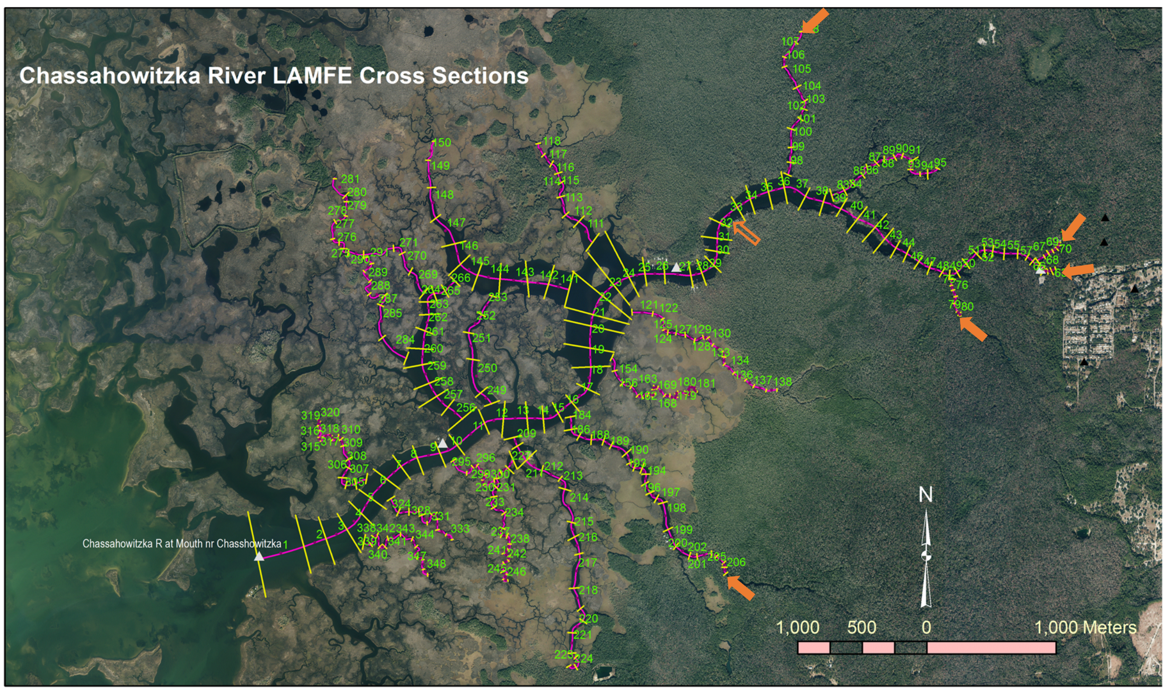

Figure 10. Cross sections (yellow segments) that form the LAMFE grids for the Chassahowitzka River and its branches. Numbers in green are grid numbers in the longitudinal direction. Orange arrows are locations where SGDs enter the model domain (the unfilled arrow indicates the location that was randomly chosen for an unidentified SGD source.)

Based on the availability of measured data which were used to drive the model at the time of the model development, a 52-month period between 11/18/2012 and 3/28/2017 was chosen for model calibration and verification. The period prior to 1/1/2016 was for model calibration, while the period between 1/1/2016 – 3/28/2017 was for model verification. A variable time step (Δt)

between 25 and 75 seconds was used in model runs, with Δt = 75 sec being used 99.27% for the 52-month simulation period.

As mentioned in the previous sections, data used as boundary conditions to drive the model include those measured for water level, salinity, and temperature at the downstream open boundary (the USGS Chassahowitzka River at Mouth near Chassahowitzka), meteorological data collected at Inglis Dam (before 7/2/2013) and Lecanto High (on and after 7/2/2013), SGDs entering the estuarine system. While available data are good enough to specify boundary conditions at the downstream open boundary and at the free surface, there is not enough data to quantify all the SGDs for the estuary. The only available real-time discharge data that are continuously collected for a long period of time and useful for this modeling study are those measured by the USGS at the Chassahowitzka River near Homosassa station (Figures 1 and 11) since October 8, 2012. Measured discharge through the cross section of this station includes both SGDs upstream of it and the tidal flow through the cross section.

Figure 11. Location of the USGS Chassahowitzka River near Homosassa and a channel network upstream of the headwaters of the estuary.

By taking away the tidal flow, the net flow, which represents all SGDs upstream of the cross section, can be calculated. Because the upstream portion of the Chassahowitzka River near Homosassa station is a relatively small area, any spatial variations of tides in the area are negligible and temporal variations of tides can be assumed to be the same as those at the measurement station. As such, the tidal flow can be approximated as follows

$$q_t = -A\frac{\partial \eta}{\partial t} \tag{2}$$

where q_t is the tidal flow, with the positive flow pointing toward downstream, η is measured water elevation, t is time, and A is the surface water area upstream of the cross section.

Figure 12 shows a comparison of net flow with measured discharge at the USGS Chassahowitzka River near Homosassa station during 1/18/2016 through 2/17/2016. The difference between the blue line, which represents measured discharge, and the red line, which represents the net flow (SGD), is the tidal flow, which is calculated by the above equation. As can be seen from the figure, SGDs also have strong tidal signals, just like measured total flow through the cross section at the USGS station. As the surface area upstream of the cross section is relatively small, the amplitude of the tidal flow is only about one half of that variability of the SGD gauged at the cross section.

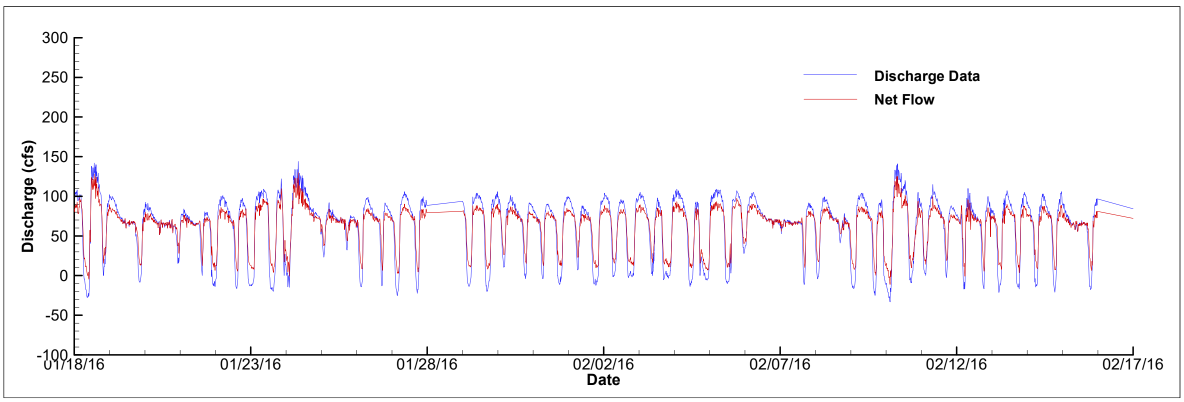

Figure 12. Comparison of measured discharge with net flow at the USGS Chassahowitzka River near Homosassa station during 1/18/2016 through 2/17/2016.

The USGS also gages discharge through its Chassahowitzka River near Chassahowitzka station using the index velocity method and the period of record started on May 4, 2003, which was much earlier than the starting date for the Chassahowitzka River near Homosassa station. Nevertheless, gaged discharge data at this station are not as useful as these at the USGS Chassahowitzka River near Homosassa station in this modeling study. There are at least the following four reasons that limit the use of gauged discharge at the Chassahowitzka River near Chassahowitzka station in the current hydrodynamic modeling of the river:

1. The measured discharge through the cross section of the Chassahowitzka River near Chassahowitzka is mostly tidal flow, because the water area upstream of this cross section is large, as it gages about 40% of the river (Figure 1). Figure 13 shows time series of gaged discharge through the USGS Chassahowitzka River near Chassahowitzka station (black line) during 10/1/2006 through 3/28/2017. For comparison, gaged discharge through the USGS Chassahowitzka River near Homosassa station since the is plotted in Figure 13, with a blue line. The average discharges during the period between 11/17/2012 and 3/28/2017 through the

Chassahowitzka River near Homosassa station was 61.6 cfs, while the average through the Chassahowitzka River near Chassahowitzka River was 94.1 cfs during the same period. Because tidal flow contributes zero net flow over a long period of time, 61.6 cfs and 94.1 cfs are also gaged SGD averages upstream of the Chassahowitzka River near Homosassa and near Chassahowitzka stations, respectively. Because the net flow of the upstream station varies with an amplitude roughly two times of its long-term average (Figure 12), it is likely that the net flow, which is measured discharge with tidal flow being taken away, roughly varies between around 0 cfs to 188 cfs. From Figure 13, measured discharge through the Chassahowitzka River near Chassahowitzka varies from about -1,000 cfs to about 1,000 cfs, with many data points > 2,000 cfs or < -2,000 cfs. As such, the tidal flow through this station has a much large variability than the net flow does. In other words, the SGD through the cross section is only a small portion of the gaged discharge. As a result, taking tidal flow away from gaged discharge to obtain the net flow involves large errors.

2. Equation (2), which is only suitable for a small upstream area, cannot be used to estimate tidal flow anymore, because the tidal reach upstream of the cross section is a few kilometers long. To obtain a good estimate of the tidal flow, a well-calibrated hydrodynamic model will be needed.
3. Although the calculated net flow through the Chassahowitzka River near Chassahowitzka station represents all the SGDs upstream the cross section, it gives no information on how SGDs are partitioned among different sources. The difference between calculated net flows at the two cross sections is the total SGD entering the river between the two cross sections.
4. Because the Chassahowitzka River near Chassahowitzka station is a few kilometers downstream from different SGD sources, it takes time for water particles to be transported from spring vents to the cross section and thus the calculated net flow represents spring flows out of spring vents a number of hours ago. This time difference is the age of the water particle at the cross section since flowing out of the ground.

Because of the above limitations, measured discharge at the Chassahowitzka River near Chassahowitzka station could not be used as input data for the model. They were used for model calibration and verification.

For a better estimate of SGDs from spring vents downstream of the Chassahowitzka River near Homosassa station, available discharge data (Vanasse Hangen Brustlin, Inc., 2014 & 2018) measured in the downstream tributaries and obtained from previous studies (Dynamic Solutions, 2009) were analyzed, including the Crab, Potters Creek, Baird, and Crawford Creeks. Most of these discharge data measured in the tributaries are collected manually during a short time period on selected days, except for the most recent data collected in Potters and Crawford, where real-time discharges with a 15-minute interval were measured since December 2017 (Vanasse Hangen Brustlin, Inc., 2018), after the model calibration and verification processes were completed.

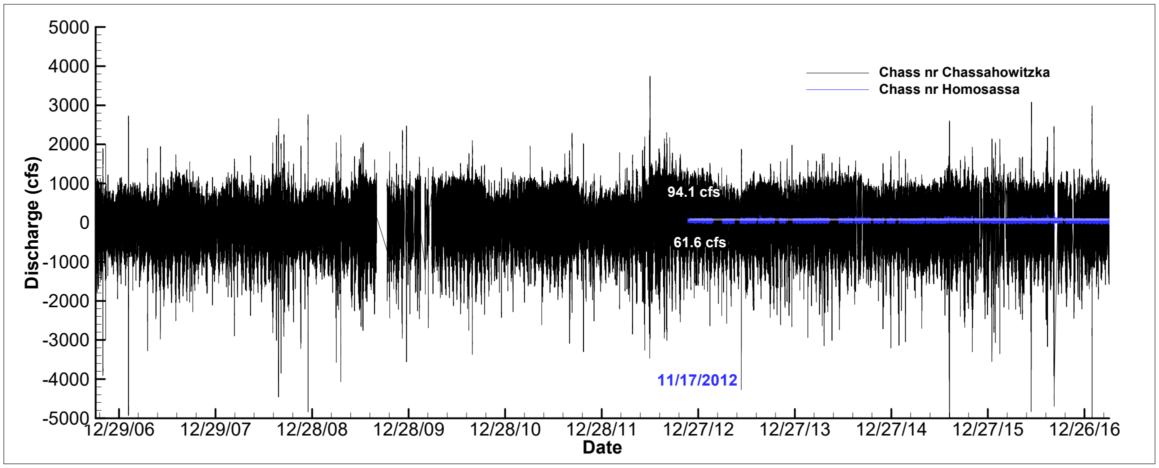

Figure 13. Gaged discharges through the USGS Chassahowitzka River near Homosassa (blue line) and near Chassahowitzka River near Chassahowitzka (black line) stations.

Because available discharges measured in the tributaries were mainly short-term data that were collected manually within only a few hours (generally less than 6 hours), they do not contain any continuous recordings that allows for a comprehensive analysis of the tidal effect on the SGD. The best way to estimate SGDs from spring vents in these tributaries was to assume that the effects of groundwater level and tides on SGDs in the tributaries are similar to these on SGDs gaged at the Chassahowitzka River near Homosassa station. As a result, it is reasonable to assume that tributary SGDs are proportional to those at this station. This assumption may not be true in a short time scale (hours) as tides may have some time lags or leads for different locations but should hold if these time lags/leads were included in the consideration.

With this assumption, the question now becomes to find the best estimate of the ratio of total SGD entering the river segment between the two USGS index velocity gage stations to that through the upstream cross section at the Chassahowitzka River near Homosassa station. Table 2 lists different ratios of Q_1 over Q, where Q_1 represents the total SGD entering the segment between the two stations, including SGDs from Crab, Potters, and Baird Creeks, and Q represents SGD through the cross section at the upstream USGS station. These ratios were calculated from all the available discharge data to date, which were either measured or estimated by models. Data sources used in the ratio calculation included the USGS, a withdrawal impact study by the SWFWMD, Dynamic Solutions, LLC, and VHB. It can be seen from the table that the ratio varies between 52.76 and 110.26, with a median of 79.13%, a mean of 82.83% and an average of max and min of 81.51%.

Table 2. Ratio of SGDs entering the river segment between the Chassahowitzka River near Homosassa station and near Chassahowitzka station to SGD through the former station.

Source	Q_1/Q (%)
USGS	52.76

Withdrawal Impact	79.13
Dynamic Solutions, 2009	110.26
Vanasse Hangen Brustlin (VHB), Inc., 2014	108.13
Vanasse Hangen Brustlin, Inc., 2018	63.88

After several trials and errors, the most reasonable choice is the mean ratio (82.83%) with the following partitioning:

$$Q_{cc} = 0.64Q_1 = 0.5301Q \tag{3}$$

$$Q_{bc} = 0.07Q_1 = 0.0580Q \tag{4}$$

$$Q_{pc} = 0.27Q_1 = 0.2236Q \tag{5}$$

$$Q_r = 0.02Q_1 = 0.0166Q \tag{6}$$

where Q_{cc}, Q_{bc}, and Q_{pc} are SGDs for the Crab, Baird, and Potters Creeks, respectively, Q_r is an unidentified SGD source which was treated as randomly located between the two cross sections. For the Crawford Creek, it was found that the ratio of its SGD to Q is 0.225.

Although the tidal flux calculated using Equation (2) contributes zero net flow to the Chassahowitzka River, this discharge rate is needed for the specification of the upstream flow boundary condition of the model. The blue line in the bottom panel of Figure 14 shows the time series plot of estimated tidal flow through the most upstream cross section of the simulation domain for the river during 10/12/2007 – 2/16/2018. The net SGD entering the most upstream grid of the simulation domain (Q in the above equations) is shown with the red line in the top panel of the Figure 14. Discharge at the Chassahowitzka River near Homosassa station prior to 11/17/2012 was estimated using a regression equation provided by the USGS. Net SGDs entering the Crab Baird, Potters, and Crawford Creeks are similar to the red line shown in Figure 4, with various scaling factors applied to Q. Orange arrows in Figure 10 indicate locations where SGDs enter the model domain. The unfilled arrow indicates the location that was randomly chosen for the unidentified SGD source (Q_r).

Because no direct measurements of salinity in the spring vents were available for this modeling study, salinity in SGD was an unknown. This piece of information is needed as the boundary condition for the LAMFE model. To obtain a reasonably estimate of salinities in all SGDs, this study used a trial and error approach. Based on measured salinity at the Chassahowitzka River near Homosassa station and other available salinity data measured in the Chassahowitzka River system, numerous salinity estimates were tested in model runs. After a careful analysis of simulated salinity results for all salinity estimates for SGDs, it was found that the following set of salinity estimate is the most reasonable

$$s_{cm} = min(max(s_0/1.025,0.5), 5.0) \tag{7}$$

$$s_{cc} = s_{br} = s_{pc} = max(s_{cm} + 0.25, 2.0) \tag{8}$$

$$s_{cf} = 0.95 \tag{9}$$

$$s_r = max(s_{cm} + 0.25, 2.0) + 1.0 \tag{10}$$

where s_0 represents measured salinity at the Chassahowitzka River near Homosassa station, s_{cm} is the estimated SGD salinity in the headwaters, s_{cc}, s_{br}, s_{pc}, s_r, and s_{cf} are estimated salinities in SGDs for the Crab, Baird, Potters Creeks, and Crawford Creeks, respectively, and s_r is estimated salinity for the unidentified SGD source.

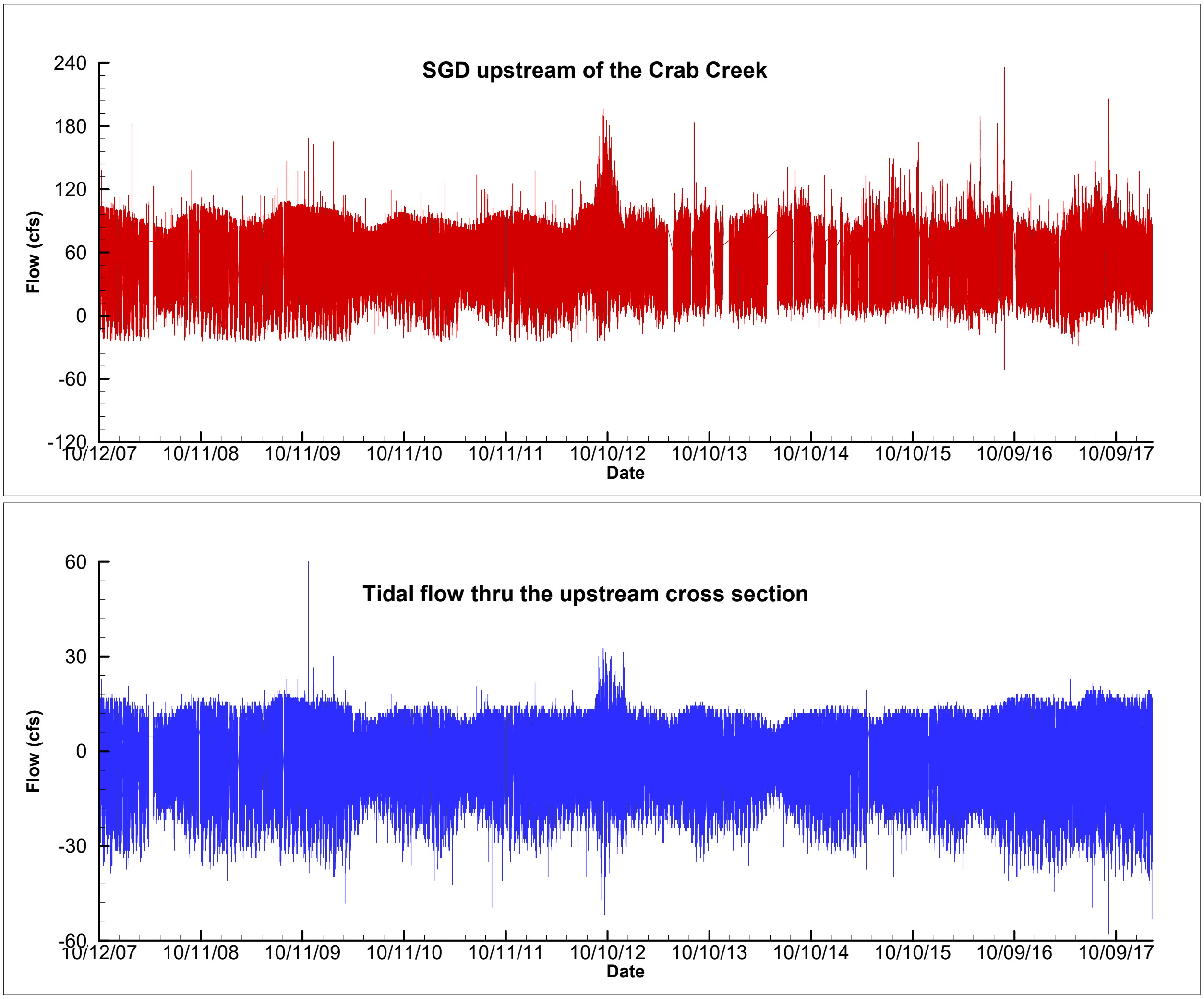

Figure 14. Time series of the net SGD (red line) through the USGS Chassahowitzka River near Homosassa station (upstream of the Crab Creek) and estimated tidal flow (blue line) through the most upstream cross section of the simulation domain for the Chassahowitzka River.

Similarly, information about temperatures in spring vents is also needed as the boundary condition for the LAMFE model. Generally, SGD temperature is very stable and barely contains any tidal variations. From temperature data collected in springs vents in Kings Bay, it was found that spring water is slightly colder in winter than in other seasons. This kind of seasonal variability is also expected to exist for SGD temperature in the Chassahowitzka River system and contained in the temperature data at the Chassahowitzka River near Homosassa station. This study used a combination of measured temperature and a constant temperature value as the estimate of water temperature in all spring vents in the Chassahowitzka River system, as follows:

$$T_{SGD} = \alpha T_{cm} + (1 - \alpha)T_0 \tag{11}$$

where T_{SGD} is estimated temperature in SGD, T_{cm} is measured temperature at the Chassahowitzka River near Homosassa station, T_0 is a constant value of 23.5 ºC, and α is a model parameter and was determined to be 0.7 during the model calibration process.

Figures H - 1 through H - 6 in Appendix H show time series plots of upstream boundary conditions of SGD, SGD salinity, and SGD temperature, which were used in the Chassahowitzka River hydrodynamic model.

3.2 Model Calibration and Verification

Model calibration involves a series of adjustment of model parameters within certain allowable ranges to obtain the best match of simulated water levels, salinities, and temperatures with measured data in the field. Similar to hydrodynamic models developed for other estuarine systems (e.g., Chen, 2012b), a series of model runs indicates that the most sensitive model parameter to simulated water levels in the upstream portion of the Chassahowitzka River is the bottom roughness, while the most sensitive model parameter to simulated salinities is the ambient eddy diffusivity. For temperature simulation, the most sensitive model parameter is the light attenuation coefficient.

As already mentioned above, the LAMFE model was calibrated against measured real-time data at the USGS Chassahowitzka River near Homosassa, near Chassahowitzka, and at Dog Island near Chassahowitzka stations. Only limited input parameters had to be tuned in the calibration process, including the bottom roughness, ambient vertical eddy viscosity and diffusivity, and ranges of salinity variation in spring discharges.

Comparisons of model results of water level, salinity, temperature, and discharge with measured field data at the three measurement stations in the Chassahowitzka River are presented in Figs. 15 -18, respectively. In these figures, red lines are model results, while dashed green lines are measured data. For simplicity and clarity, only 90 days of model results during 2/17/2013 through 5/18/2013 for water level are shown in Figure 15. For the same reasons, only 60 days of model results during March 19, 2013 through May 18, 2013 of salinity, temperature, and discharge are presented in Figures 16, 17, and 18, respectively. The choice of these 90-day or 60-day period is arbitrary. Comparisons of model results with real-time field data during other time periods are similar, with some having a slightly better match and some a slightly worse match. Time series plots showing comparisons of model results with field data of water level, salinity, and temperature during other time periods are included in Appendixes E, F, G, and H, respectively.

As can be seen in Figures 15 and 18, simulated water elevations at all three USGS stations and simulated discharge at the Chassahowitzka River near Chassahowitzka station agree very well with measured data. Simulated water levels at the three USGS stations have the same long-term and short-term variations as measured data. Simulated discharge at the Chassahowitzka River near Chassahowitzka station generally match measured discharge very well, except some misses of negative peaks. Simulated discharges during the neap and spring tides have almost the same variabilities.

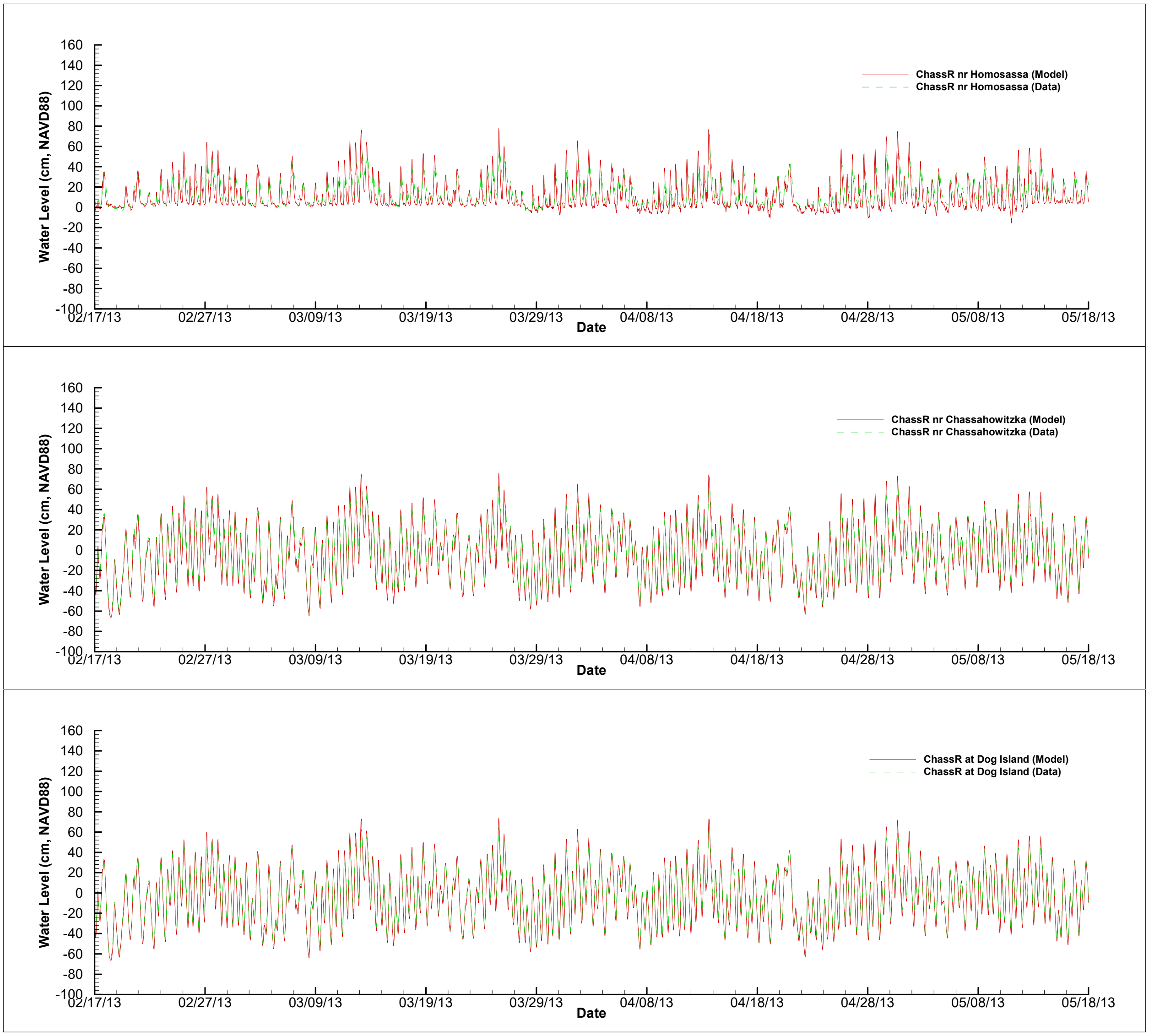

Figure 15. Comparison of measured and simulated water levels at the Chassahowitzka River near Homosassa station (top panel), Chassahowitzka River near Chassahowitzka (middle panel), and Chassahowitzka River at Dog Island near Chassahowitzka (bottom panel) during 2/17/2013 through 5/18/2013.

Modeled salinity and temperature results also have good agreement with field data (Figures 16 and 17), both in terms of long-term and short-term variations. Because of the uncertainties included in the input data that drive salinity and temperature simulations, it is expected that the match between model results and data for salinity or temperature is not as good as that for water level simulation. Nevertheless, simulated salinity and temperature results are satisfactorily well matched with measured real-time data. More details about comparisons of model results with field are shown in the next subsection, where skill assessment for the model is described.

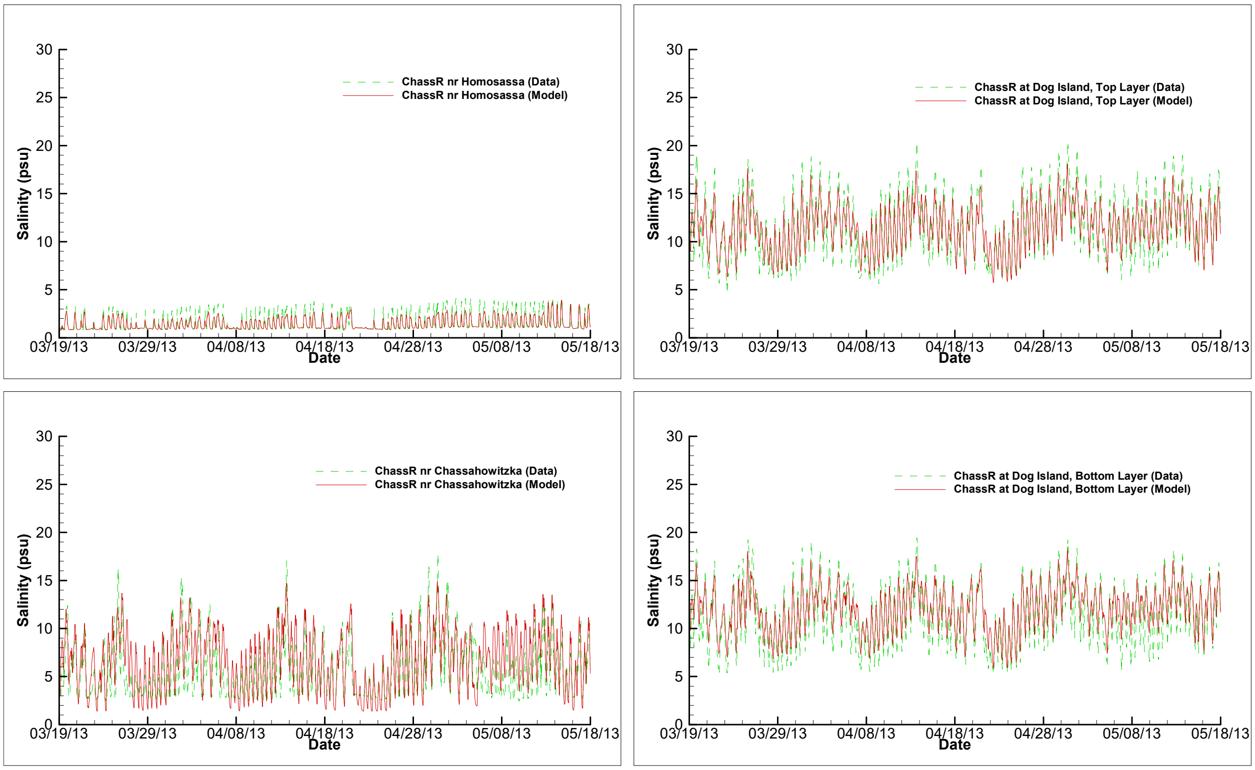

Figure 16. Comparison of measured and simulated salinities at the Chassahowitzka River near Homosassa station (top left panel), Chassahowitzka River near Chassahowitzka station (bottom left panel), and Chassahowitzka River at Dog Island near Chassahowitzka station (top right panel for top layer, bottom right panel for bottom layer) during 3/19/2013 through 5/18/2013.

3.3 Model Performance Metrics

The performance of the LAMFE model for the Chassahowitzka River is accessed quantitatively with several statistics, including the mean error (ME), mean absolute error (MAE), root-mean-square error (RMSE), normalized root-mean-square error (NRMSE), the coefficient of determination (R^2), and a skill assessment parameter introduced by Willmott (1981). The Willmott skill assessment parameter was used by Warner et al. (2005) to assess the performance of a hydrodynamic model for the Hudson River estuary. It also was used by the author to examine performances of the LAMFE model for the Lower Alafia River estuary (Chen, 2005), a multi-block, dynamically coupled 3D-2DV model for the lower Peace River – Lower Myakka River –

Upper Charlotte Harbor estuarine system (Chen, 2010) and an unstructured Cartesian grid model for Crystal River/Kings Bay (Chen, 2012d; Chen, 2017.)

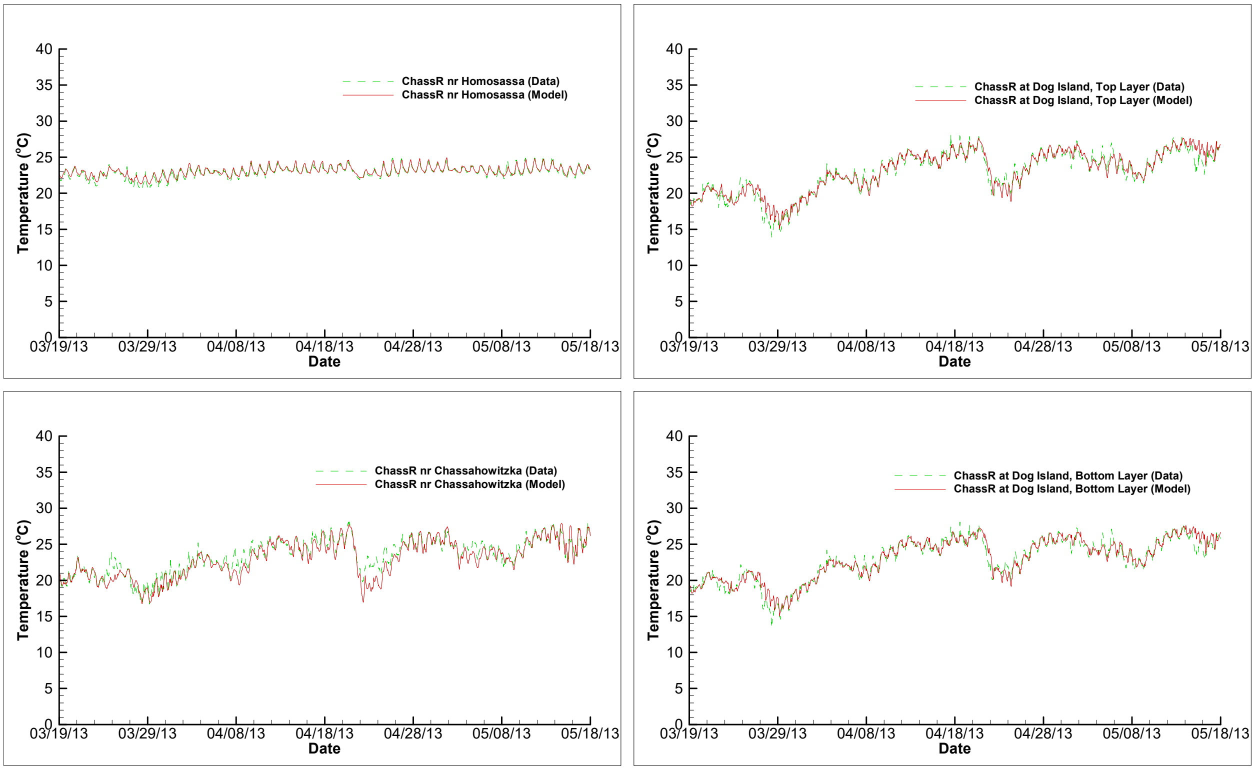

Figure 17. Comparison of measured and simulated temperatures at the Chassahowitzka River near Homosassa station (top left panel), Chassahowitzka River near Chassahowitzka station (bottom left panel), and Chassahowitzka River at Dog Island near Chassahowitzka station (top right panel for top layer, bottom right panel for bottom layer) during 3/19/2012 through 5/18/2013.

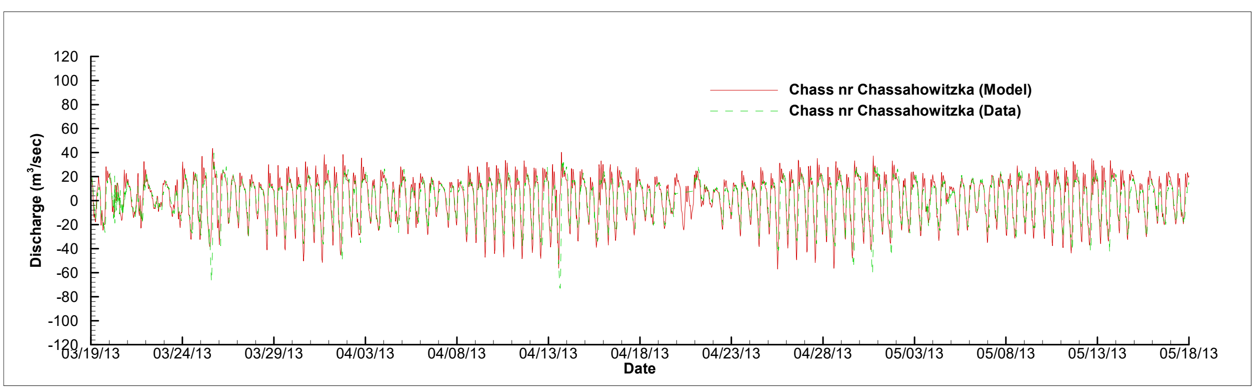

Figure 18. Comparison of measured and simulated discharge at the Chassahowitzka River near Chassahowitzka station during 3/19/2012 through 5/18/2013.

This Willmott skill assessment parameter takes the following form

$$S_k = 1 - \frac{\sum (y^M - y^D)^2}{\sum (|y^M - \overline{y^D}| + |y^D - \overline{y^D}|)^2} \tag{12}$$

where S_k is the skill assessment parameter (or simply the skill); y^M and y^D represent simulated and measured variables (water level, salinity, etc.); and $\overline{y^D}$ is the expectation of y^D. S_k in the above equation varies between 0 and 1, with one being a perfect agreement and zero being a complete disagreement between simulated results and measured data.

Mean errors, mean absolute errors, root-mean-square errors, normalized root-mean-square errors, coefficients of determination and Willmott skills for simulated water elevations, salinities, and temperatures are listed in Table 3, 4, 5, and 6, respectively, during the calibration period (11/18/2012 – 12/31/2015), the verification period (1/1/2016 – 3/28/2017), and the entire simulation period (11/18/2012 – 3/28/2017).

As can be seen from Table 3, the mean error between simulated and measured water elevations ranges between -5.20 cm and -1.69 cm among the three USGS stations in the Chassahowitzka River during the calibration period, between -2.82 cm and -0.96 cm during the verification period, and between -4.53 cm and -1.51 cm during the entire period. The MAE between simulated and measured water elevations is between 4.97 cm and 7.24 cm among the three USGS stations during the calibration period, between 4.59 cm and 6.35 cm during the verification period, and between 4.87 cm and 6.99 cm during the entire period. The RMSE between simulated and measure water levels varies in the ranges of 6.12 cm - 8.88 cm for the calibration period, 5.81 cm – 7.95 cm for the verification period, and 6.04 cm – 8.61 cm for the entire period. Accordingly, normalized RMSEs are in the ranges of 0.034 – 0.083, 0.030 – 0.043, and 0.031 – 0.047, respectively for the calibration period, the verification period, and the entire period, respectively. The R^2 value and Willmott skill parameter for simulated water elevations are in the ranges of 0.82 - 0.95 and 0.92 – 0.99, respectively for the calibration period. They are in the ranges of 0.84 – 0.96 and 0.95 – 0.99, respectively for the verification period. For the entire period, the R^2 value and Willmott skill parameter for water level simulation in the Chassahowitzka River are in the range of 0.82 – 0.96 and 0.93 – 0.99 respectively. Overall, the ME, MAE, RMSE, NRMSE, R^2, and skill parameter for simulated water elevations are respectively -3.21 cm, 6.13 cm, 7.81 cm, 0.031, 0.92, and 0.97 among the three USGS stations for the entire period.

From Table 4, it can be seen that simulated salinities at the three USGS stations have a mean error between -0,32 psu and 0.31 psu and a mean absolute error in the range of 0.29 psu to 1.24 psu for the calibration period. During the verification period, ME and MAE of simulated salinities range between -0.53 psu and 0.06 psu and between 0.33 psu and 1.47 psu, respectively, while during the entire period, ME and MAE ranges are from -0.39 psu to 0.24 psu and from 0.30 psu to 1.29 psu, respectively. RMSE and NRMSE between simulated and measured salinities are respectively in the ranges of 0.41 psu – 1.58 psu and 0.068 – 0.087 for the calibration period, 0.51 psu – 1.99 psu and 0.033 – 0.106 for the verification period, and 0.44 psu – 1.71 psu and 0.029 –

0.088 for the entire period. R^2 values of simulated salinities at the three USGS stations vary between 0.64 and 0.83, between 0.62 and 0.76, and between 0.65 and 0.80, respectively for the calibration, verification, and entire periods. Willmott skills for simulated salinities at the three stations range between 0.89 and 0.93 for the calibration period, between 0.88 and 0.91 for the verification period, and between 0.89 and 0.93 for the entire period. Overall, ME, MAE, RMSE, NRMSE, R^2, and skill parameter for simulated salinities are -0.04 psu, 1.02 psu, 1.45 psu, and 0.060, 0.89, and 0.97, respectively among the three USGS stations.

Table 3. MEs, MAEs, RMSEs, NRMSEs, R^2 values, and Willmott skill assessment parameters for simulated water levels in comparison with real-time field data measured at the Chassahowitzka River near Homosassa, near Chassahowitzka, and at Dog Island stations during the calibration period, the verification period, and the entire simulation period.

Water Level (cm)	**ME**	**MAE**	**RMSE**	**NRMSE**	R^2	**Skill**
	Calibration Period					
Chass R near Homosassa	-5.201	7.236	8.867	0.083	0.816	0.919
Chass R near Chassahowitzka	-3.840	6.648	8.524	0.051	0.924	0.973
Chass R at Dog Island	-1.688	4.966	6.121	0.034	0.954	0.986
Overall for all stations	-3.612	6.307	7.959	0.044	0.918	0.972
	Verification Period					
Chass R near Homosassa	-2.821	6.346	7.931	0.043	0.844	0.952
Chass R near Chassahowitzka	-2.394	5.802	7.947	0.043	0.923	0.977
Chass R at Dog Island	-0.958	4.590	5.807	0.030	0.958	0.989
Overall for all stations	-2.132	5.648	7.383	0.030	0.921	0.978
	Entire Simulation (Calibration & Verification) Period					
Chass R near Homosassa	-4.531	6.986	8.614	0.047	0.817	0.931
Chass R near Chassahowitzka	-3.442	6.416	8.369	0.046	0.923	0.974
Chass R at Dog Island	-1.506	4.873	6.044	0.031	0.955	0.987
Overall for all stations	-3.214	6.13	7.808	0.031	0.918	0.973

Table 5 shows that simulated temperatures have a mean error between -0,46 ºC and 0.16 ºC and a mean absolute error between 0.25 ºC and 1.02 ºC for the calibration period at the three USGS stations. During the verification period, ME and MAE of simulated temperatures range between –0.36 ºC and 0.16 ºC and between 0.27 ºC and 0.97 ºC, respectively, while during the entire period, ME and MAE ranges are from -0.43 ºC to 0.16 psu and from 0.26 ºC to 1.01 ºC, respectively. RMSE and NRMSE between simulated and measured temperatures are respectively in the ranges of 0.32 ºC – 1.38 ºC and 0.032 – 0.068 for the calibration period, 0.35 ºC – 1.26 ºC and 0.025 – 0.060 for the verification period, and 0.33 ºC – 1.36 ºC and 0.027 – 0.063 for the entire period. R^2 values of simulated temperatures at the three USGS stations vary between 0.93 and

0.98, between 0.89 and 0.98, and between 0.91 and 0.98, respectively for the calibration, verification, and entire periods. Willmott skills for simulated temperatures at the three stations range between 0.97 and 0.99 for the calibration period, between 0.957 and 0.995 for the verification period, and between 0.96 and 0.99 for the entire period. Overall, ME, MAE, RMSE, NRMSE, R^2, and skill parameter for simulated temperatures are -0.04 ºC, 0.59 ºC, 0.89 ºC, and 0.031, 0.96, and 0.99, respectively among the three USGS stations.

Simulated discharge at the Chassahowitzka River near Chassahowitzka station has a mean error of -0.002 m^3/s, a mean absolute error of 0.02 m^3/s, a root-mean-square error of 0.03 m^3/s, a normalized RMSE of 0.037, a R^2 value of 0.96, and the Willmott skill of 0.99 during the calibration period. These statistics are 0.001 m^3/s, 0.02 m^3/s, 0.02 m^3/s, 0.029, 0.97, and 0.99, respectively during the verification period. During the entire simulation period, ME, MAE, RMSE, NRMSE, R2, and the skill parameter are -0.001 m^3/s, 0.02 m^3/s, 0.02 m^3/s, 0.031, 0.96, and 0.99, respectively.

Table 4. MEs, MAEs, RMSEs, NRMSEs, R^2 values, and Willmott skill assessment parameters for simulated salinities in comparison with real-time field data measured at the Chassahowitzka River near Homosassa, near Chassahowitzka, and at Dog Island stations during the calibration period, the verification period, and the entire simulation period.

Salinity (psu)	**ME**	**MAE**	**RMSE**	**NRMSE**	R^2	**Skill**
	Calibration Period					
Chass R nr Homosassa	0.011	0.285	0.412	0.087	0.833	0.929
Chass R nr Chassahowitzka	0.314	1.168	1.581	0.081	0.654	0.893
Chass R at Dog Island	-0.320	1.203	1.537	0.068	0.792	0.930
Chass R at Dog Island	0.015	1.239	1.581	0.071	0.766	0.929
Overall for all stations	0.007	0.967	1.367	0.057	0.889	0.970
	Verification Period					
Chass R nr Homosassa	0.042	0.330	0.509	0.033	0.735	0.890
Chass R nr Chassahowitzka	0.062	1.468	1.988	0.106	0.620	0.883
Chass R at Dog Island	-0.534	1.383	1.778	0.086	0.757	0.907
Chass R at Dog Island	-0.220	1.401	1.780	0.099	0.730	0.907
Overall for all stations	-0.160	1.138	1.617	0.077	0.887	0.967
	Entire Simulation (Calibration & Verification) Period					
Chass R nr Homosassa	0.021	0.299	0.443	0.029	0.801	0.918
Chass R nr Chassahowitzka	0.239	1.257	1.712	0.088	0.651	0.894
Chass R at Dog Island	-0.385	1.257	1.614	0.068	0.79	0.927
Chass R at Dog Island	-0.058	1.289	1.645	0.074	0.767	0.927
Overall for all stations	-0.044	1.019	1.447	0.060	0.889	0.969

Table 5. MEs, MAEs, RMSEs, NRMSEs, R^2 values, and Willmott skill assessment parameters for simulated temperatures in comparison with real-time field data measured at the Chassahowitzka River near Homosassa, near Chassahowitzka, and at Dog Island stations during the calibration period, the verification period, and the entire simulation period.

Temperature (°C)	**ME**	**MAE**	**RMSE**	**NRMSE**	***R*²**	**Skill**
	Calibration Period					
Chass R nr Homosassa	0.157	0.252	0.321	0.055	0.925	0.965
Chass R nr Chassahowitzka	-0.464	1.022	1.388	0.068	0.935	0.972
Chass R at Dog Island	0.053	0.555	0.806	0.032	0.978	0.994
Chass R at Dog Island	0.022	0.571	0.821	0.034	0.977	0.994
Overall for all stations	-0.059	0.600	0.917	0.037	0.959	0.988
	Verification Period					
Chass R nr Homosassa	0.160	0.270	0.354	0.056	0.887	0.957
Chass R nr Chassahowitzka	-0.357	0.965	1.264	0.060	0.950	0.979
Chass R at Dog Island	0.144	0.511	0.718	0.025	0.984	0.995
Chass R at Dog Island	0.157	0.522	0.717	0.031	0.984	0.995
Overall for all stations	0.028	0.564	0.826	0.029	0.968	0.991
	Entire Simulation (Calibration & Verification) Period					
Chass R nr Homosassa	0.158	0.257	0.331	0.052	0.913	0.962
Chass R nr Chassahowitzka	-0.434	1.006	1.355	0.063	0.939	0.974
Chass R at Dog Island	0.079	0.542	0.782	0.027	0.98	0.994
Chass R at Dog Island	0.061	0.557	0.792	0.032	0.979	0.994
Overall for all stations	-0.035	0.59	0.892	0.031	0.962	0.989

Table 6. MEs, MAEs, RMSEs, NRMSEs, R^2 values, and Willmott skill assessment parameters for simulated discharges in comparison with real-time field data measured at the Chassahowitzka River near Homosassa, near Chassahowitzka, and at Dog Island stations during the calibration period, the verification period, and the entire simulation period.

Discharge (m^3/s)	**ME**	**MAE**	**RMSE**	**NRMSE**	***R*²**	**Skill**
	Calibration Period					
Chass R nr Chassahowitzka	-0.002	0.017	0.026	0.037	0.959	0.988
	Verification Period					
Chass R nr Chassahowitzka	0.001	0.016	0.023	0.029	0.968	0.991
	Entire Simulation (Calibration & Verification) Period					
Chass R nr Chassahowitzka	-0.001	0.017	0.025	0.031	0.962	0.989

4. Scenario Simulations

4.1 Scenarios

An effort was made to run the LAMFE model that was calibrated and verified for the Chassahowitzka River as long as possible for various flow reduction conditions. Based on all the available data that could be used to drive the LAMFE model continuously, the longest time span that the model can be run is a 123-month (10.25 years) period during October 11, 2007 through February 15, 2018. The USGS has real-time data of water elevation, salinity, and temperature at the open boundary at the mouth of the river during these 123 months. The USGS also has water elevation data at the Chassahowitzka River near Homosassa station during the same time span, allowing the tidal flux through the most upstream cross section of the simulation domain to be calculated. Real-time Meteorological data (wind speed, wind direction, air temperature, air humidity, and solar radiation) were also available during these 123 months, either from the SWFWMD weather station near Inglis, Florida or from the UF/IFAS FAWN station at the Lecanto High School. The same method described in Section 3.2 was used to estimated submarine groundwater discharges for the Crab, Baird, Potters, Crawford Creeks, based on available discharge data measured or estimated at the cross section of the USGS Chassahowitzka River near Homosassa station.

A total of 14 flow scenarios were simulated and analyzed, including the baseline flow (BSL) condition, the existing flow condition, and 2.5%, 5%, 7.5%, 10%, 12.5%, 15%, 17.5%. 20%, 22.5%, 25%, 27.5%, and 30% reductions from the BSL condition. The BSL condition is an imaginary flow condition that would exist if no ground water were withdrawn in the springshed. It is estimated that the existing withdrawal causes about 1.4% reduction of SGDs in Chassahowitzka. As such, the BSL is obtained by dividing the existing SGDs by 0.986. Table 7 lists details on how flow is calculated for each flow scenarios.

Table 7. Flow reduction scenarios conducted for the Chassahowitzka River MFL re-evaluation.

Scenario No.	Scenario Name	Flow Calculation
1	Baseline	(No. 2 SGDs)/0.986, or 1.0142×(No. 2 SGDs)
2	Existing	SGDs were obtained using method described in Section 3.2
3	2.5%	0.975×(No. 1 SGDs), or 0.9888(No. 2 SGDs)
4	5%	0.95×(No. 1 SGDs), or 0.9635×(No. 2 SGDs)
5	7.5%	0.925×(No. 1 SGDs), or 0.9381×(No. 2 SGDs)
6	10%	0.9×(No. 1 SGDs), or 0.9128×(No. 2 SGDs)
7	12.5%	0.875×(No. 1 SGDs), or 0.8874×(No. 2 SGDs)

8	15%	0.85×(No. 1 SGDs), or 0.8621×(No. 2 SGDs)
9	17.5%	0.825×(No. 1 SGDs), or 0.8367×(No. 2 SGDs)
10	20%	0.8×(No. 1 SGDs), or 0.8114×(No. 2 SGDs)
11	22.5%	0.775×(No. 1 SGDs), or 0.7860×(No. 2 SGDs)
12	25%	0.75×(No. 1 SGDs), or 0.7606×(No. 2 SGDs)
13	27.5%	0.775×(No. 1 SGDs), or 0.7353×(No. 2 SGDs)
14	30%	0.7×(No. 1 SGDs), or 0.7099×(No. 2 SGDs)

Simulated salinities and temperatures at the centers of all grid cells were written out to output files with an interval of 30 minutes for all 14 scenarios. These model results were processed to calculate volumes, bottom areas, and shoreline lengths for various salinity ranges and volumes and surface areas of various temperature ranges at each time point. Salinity and thermal habitats calculated and analyzed are listed in Table 8 below.

Table 8. Salinity and temperature ranges used in the post-processes of model results of the scenario runs.

	Ranges	**Habitats**
Salinity	1. ≤ 1 psu 2. ≤ 2 psu 3. ≤ 3 psu 4. ≤ 5 psu 5. ≤ 10 psu 6. ≤ 15 psu 7. ≤ 20 psu	Salinity habitats calculated: 1. Water volume, 2. Bottom area, and 3. Shoreline length.
Temperature	1. < 15 ºC 2. ≥ 15 ºC 3. ≥ 20 ºC	Thermal habitats calculated were water volume and surface area. Habitats of ≥ 15 ºC and ≥ 20 ºC were calculated both with and without the 3.8 ft (1.158 m) requirement for depth or layer thickness.

Because the downstream boundary of the model domain for the Chassahowitzka River is at the mouth of the river, it is possible that a flow reduction may cause salinity at the open boundary to slightly increase. To consider this factor in the scenario simulations, a series test runs of the LAMFE model with an extended simulation domain were conducted to figure out how much salinity increase could occur with various flow reductions. The extended simulation domain has five extra grids that cover an offshore area below the mouth of the Chassahowitzka River.

Figure 19 shows the cross sections of the LAMFE model for the extended simulation domain of the Chassahowitzka River. The downstream open boundary in the extended simulation domain is 5.48 km offshore of the mouth of the Chassahowitzka River and it is expected that any flow reductions in the Chassahowitzka River only have very insignificant effect on salinity increase there. Bathymetry data for this offshore area were obtained from the U.S. Coastal Relief Model Vol. 3 – Florida and East Gulf of Mexico of NOAA's National Center for Environmental Information. The following is its website link

https://www.ngdc.noaa.gov/docucomp/page?xml=NOAA/NESDIS/NGDC/MGG/DEM/iso/xml/307.xml&view=getDataView&header=none

In the test runs, it was assumed that the water level and water temperature at the offshore open boundary is the same as these at the mouth of the Chassahowitzka River, but the salinity is a little higher than that at the river mouth and roughly takes the following form

$$S_1 = S_0 + \min(\max(0.1(30 - S_0), 0.0), 2.5) \tag{13}$$

where S_0 is measured salinity at the mouth of Chassahowitzka River and S_1 is estimated salinity at the offshore open boundary. The above equation for estimating S_1 is obtained through a trial and error process with a goal to reach a best match between simulated and measured salinities at the mouth of the Chassahowitzka River for the existing flow scenario. It is interesting to note that the above equation is also valid for the Homosassa LAMFE model, which was developed for the MFL re-evaluation of the Homosassa River (Chen, 2019a).

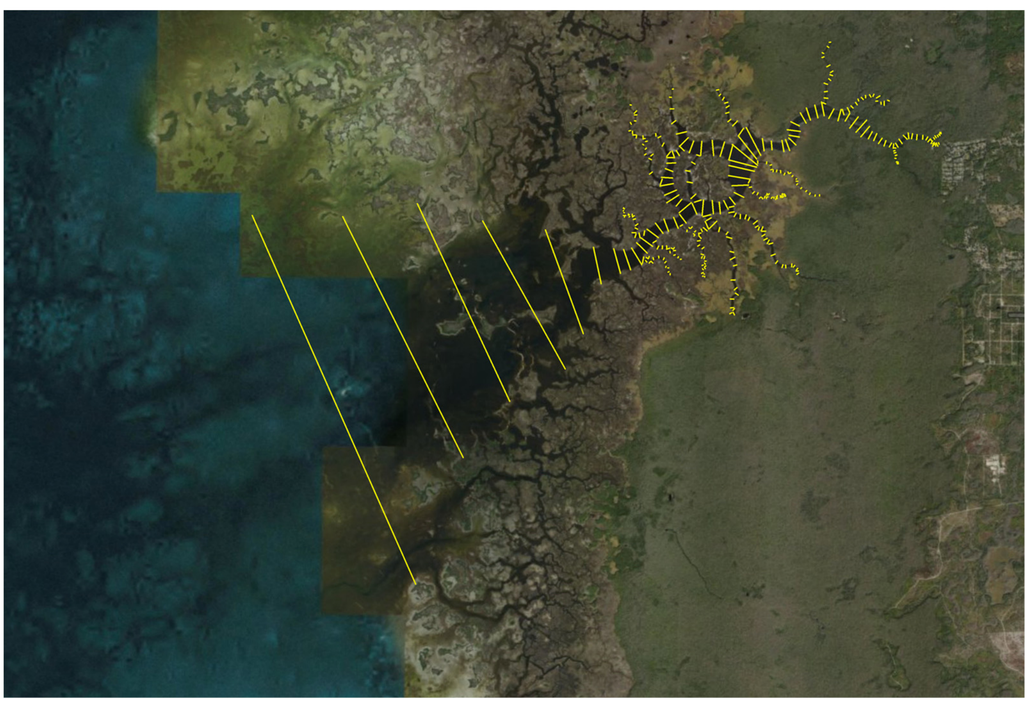

Figure 19. An extended simulation domain for the Chassahowitzka River, which has five extra grids coving an offshore area below the mouth of the river.

Figure 20 shows the average salinity increases in different layers of the model for different flow reductions. The low case k on the right side of the figure is an index for vertical layers, counting from the bottom to the top. From the figure, it is clear that salinity increase at the mouth of the Chassahowitzka River due to upstream flow reduction is generally very small. A 30% flow reduction causes a salinity increase of about 0.3 psu at the top layer of the mouth but only a < 0.02 psu increase at the bottom layer. At the same depth, the salinity increase at the river mouth is linearly increase with the flow reduction percentage. Near the bottom of the river mouth, flow reduction in the Chassahowitzka has barely any effects on salinity.

Although the effect of flow reduction on salinity at the river mouth is very small, the scenario runs take these small salinity increases into consideration. Salinity boundary conditions at the open boundary at the mouth of the river were adjusted according to the salinity increases shown in Figure 20.

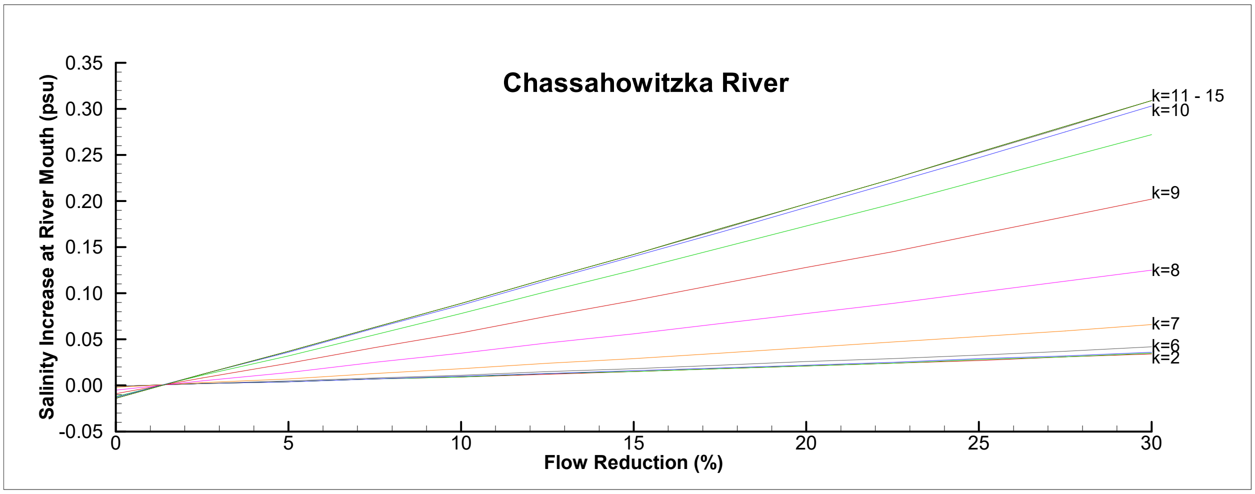

Figure 20. Effects of flow reduction on salinities in different layers at the mouth of the Chassahowitzka River.

With effects of reduced SGD on salinity at the mouth of the Chassahowitzka River being considered, one may wonder if a reduction of SGD will cause a change of salinity in the spring discharge itself. Because there is not a subterranean estuary model available for the region, a comprehensive modeling study on how groundwater withdrawal affects salinity distributions in the groundwater, especially in the proximity of spring vents of the Chassahowitzka River, is impossible. An analysis of discharge and salinity measured at the Chassahowitzka River near Homosassa station (Chen, 2019b) shows that although salinity and SGD are weakly correlated (R^2 = 0.37,) they do not have the true cause-and-effect relationship, because both SGD and salinity are highly affected by tides. After tidal signals in both SGD and salinity are taken out using a low-pass filter, the correlation between tidally filtered SGD and tidally-filtered salinity has no correlation at all (R^2 = 0.0004.) In other words, a reduction of SGD will likely not cause salinity in spring discharges to change.

4.2. Results of Salinity Habitats

Direct comparisons and analyses of 30-minute results of water volume, bottom area, and shoreline length for different flow reductions are very tedious and not necessary, because one would easily lose the forest for the trees. Instead, daily mean values of salinity habitats are typically analyzed in the MFL evaluation. Figures 21 & 22 show daily mean volumes, bottom area, and shoreline lengths for salinity ≤ 1, 2, 3, 5, 10, and 15 for the baseline and 10% flow reductions, respectively. In the figures, model results during the first 20 days of the simulation period were excluded, because these first 20 days were considered as a spin-up period. Time series of simulated daily salinity habitats for other flow reduction scenarios have the similar temporal variabilities and thus are omitted here.

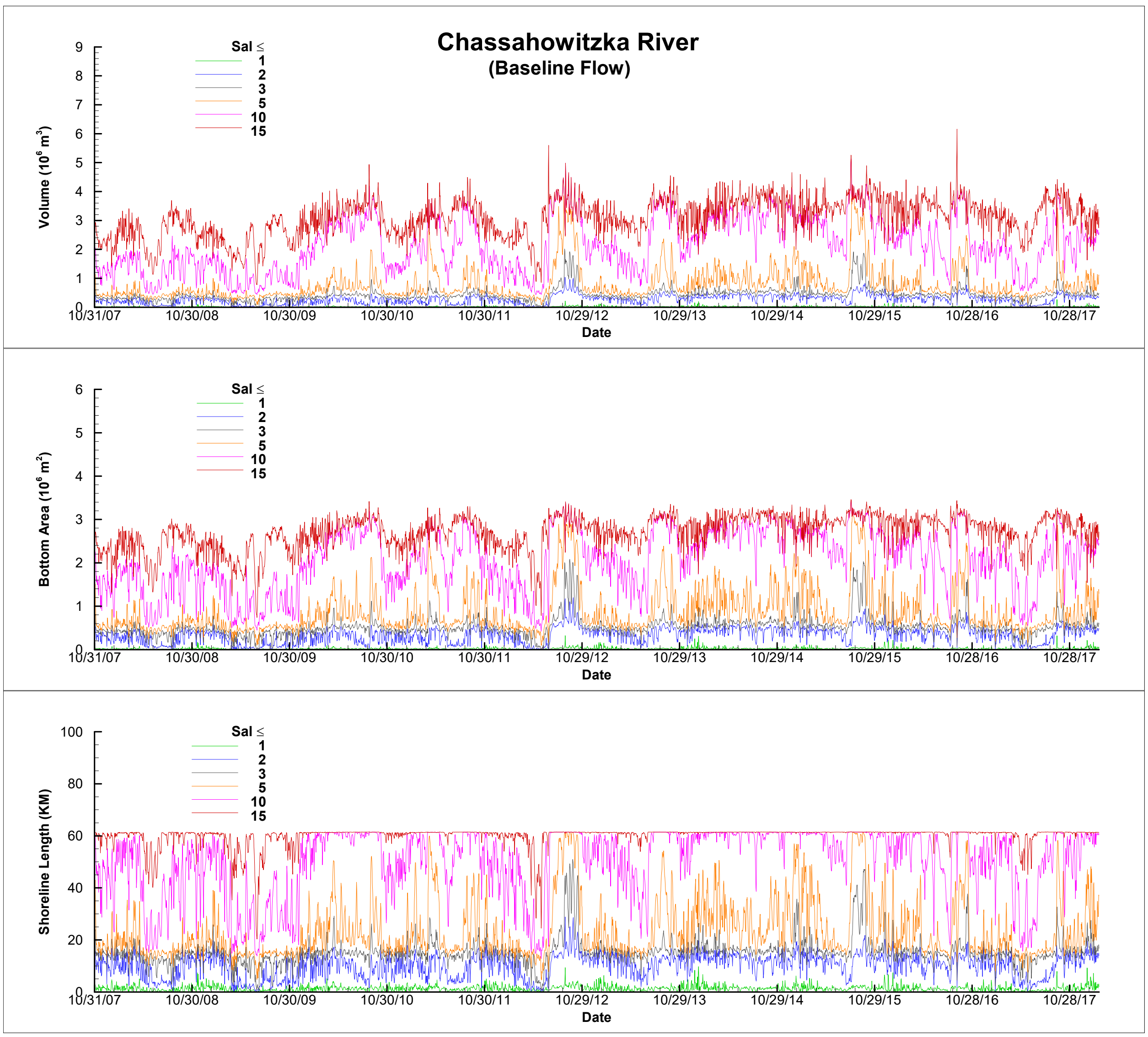

Figure 21. Simulated daily salinity habitats for salinity ≤ 1, 2, 3, 5, 10, and 15 psu for the baseline flow scenario during the 123-month simulation period.

Time series plots of simulated salinity habitats for the baseline scenario and the 10% flow reduction scenario look similar, with low salinity habitats being reduced when all SGDs entering the system are reduced 10%; however, these salinity habitat reductions are only evident when Figure 21 & 22 are overlaid together. To get a better overall picture of the effects of flow reduction on salinity habitats, cumulative distribution functions are plotted. Figures 23 -25 show CDFs of water volume, bottom area, and shoreline length for various salinity ranges and flow reduction scenarios.

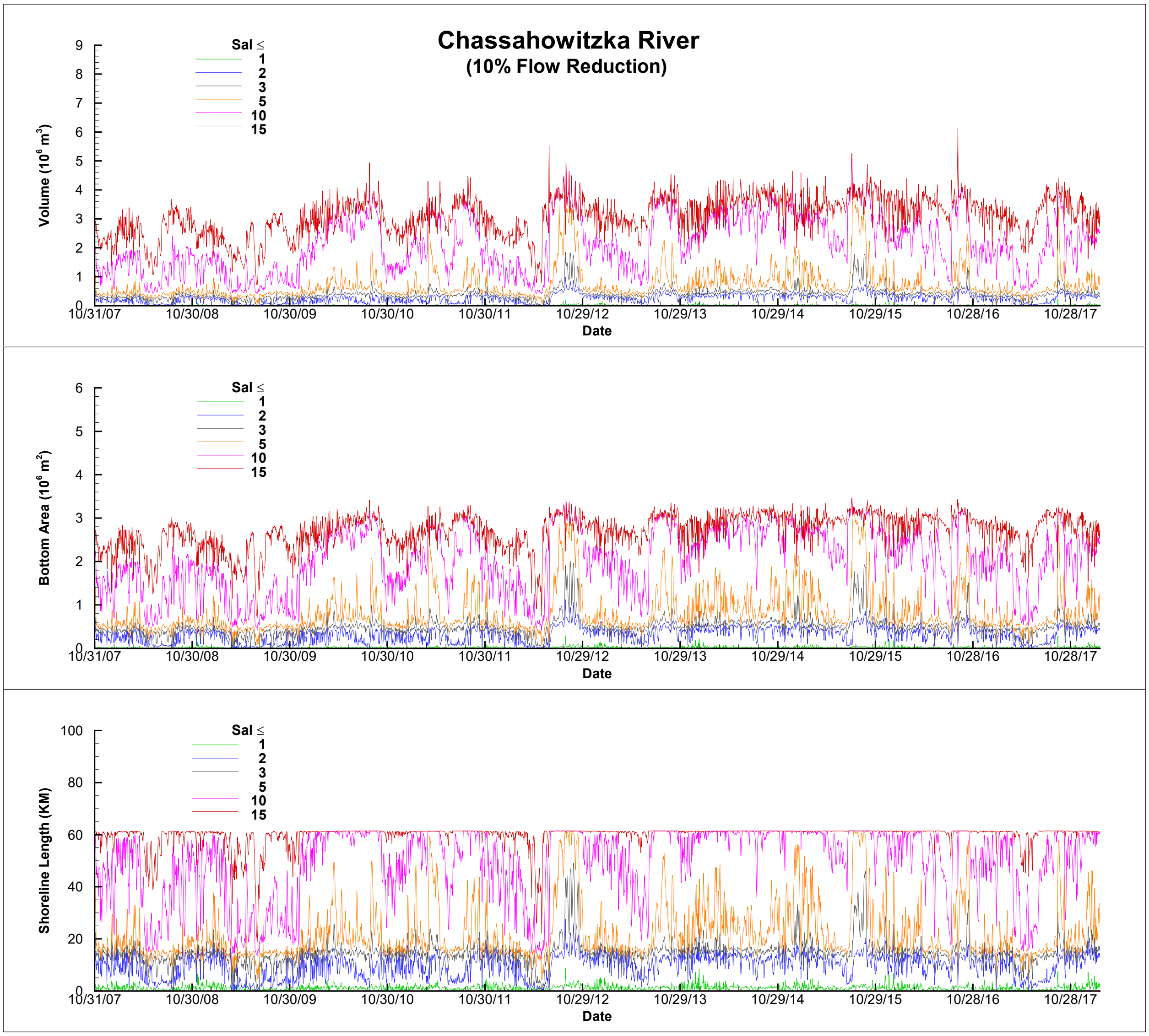

Figure 22. Simulated daily salinity habitats for salinity ≤ 1, 2, 3, 5, 10, and 15 psu for the 10% flow reduction scenario during the 123-month simulation period.

For a clear inspection of the differences among different CDFs for different flow reductions, only the baseline, existing, 2.5%, 5%, 10%, 15%, 20%, 25%, and 30% flow reduction scenarios are included in Figures 23 - 25. Because ≤ 20 psu habitats only have very small relative changes when SGDs are reduced, their CDF plots are not included in Figures 23 - 25. Generally, the response of ≤ 20 psu habitats to the SGD reduction is similar to but smaller than that of ≤ 15 psu habitats. As such, ≤ 20 psu habitats are not included in the following discussions.

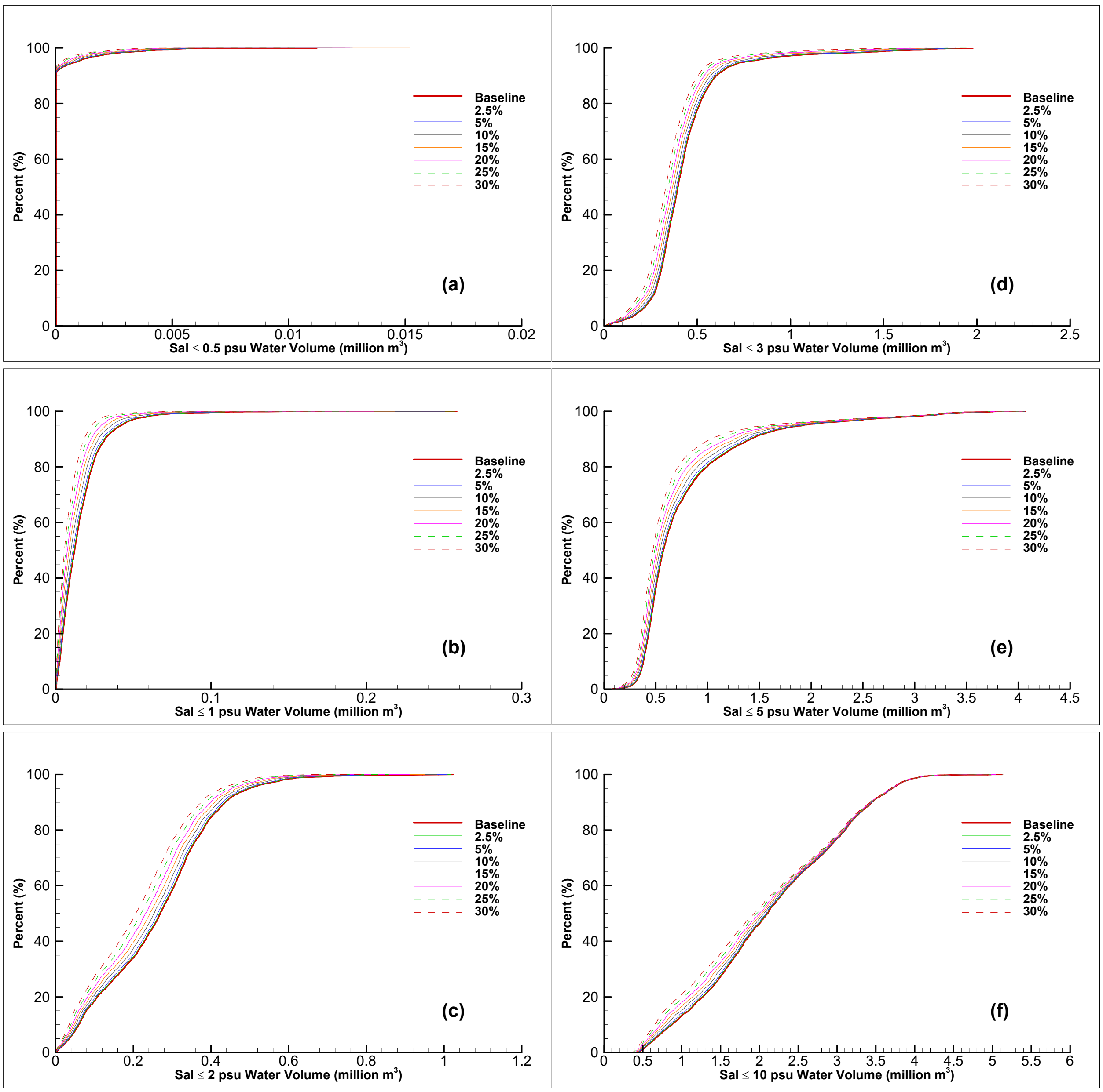

Figure 23. Cumulative distribution functions of simulated water volume for various flow reductions for salinity ≤ 1 psu (a), ≤ 2 psu (b), ≤ 3 psu (c), ≤ 5 psu (d), ≤ 10 psu (e), and ≤ 15 psu (f).

From Figures 23 - 25, it is apparent that the low salinity habitats for ≤ 1 psu, ≤ 2 psu, or ≤ 3 psu are usually much more sensitive to these for ≤ 10 psu and ≤ 15 psu. This is consistent with many other estuarine systems we've studied in the SWFWMD. To quantify the relative changes of salinity habitats caused by any flow reduction, average water volume, bottom area, and shoreline length for different salinity ranges can be calculated, which are graphically areas between the *y*-axis and CDF curves in Figures 23 - 25.

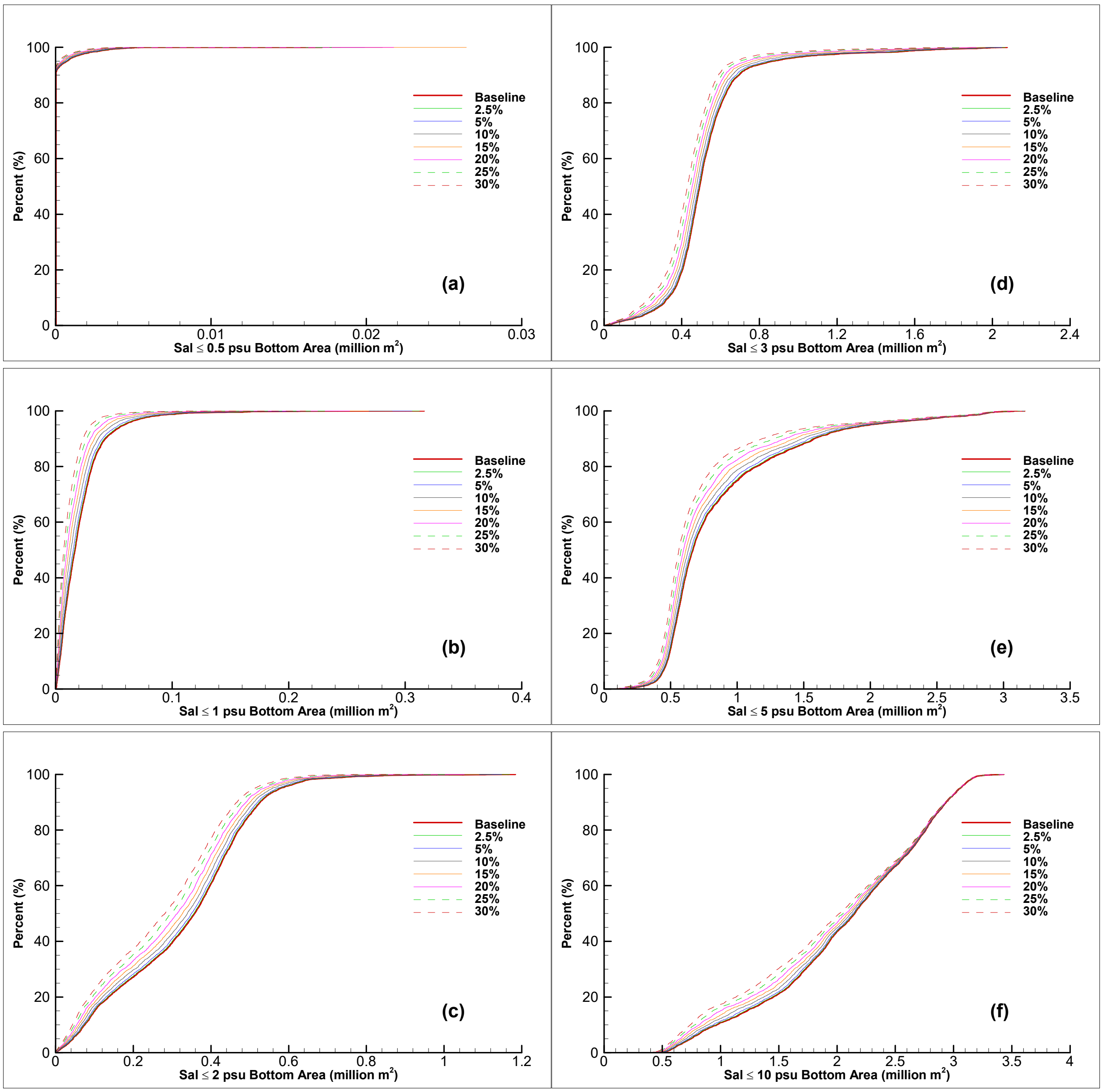

Figure 24. Cumulative distribution functions of simulated bottom area for various flow reductions for salinity ≤ 1 psu (a), ≤ 2 psu (b), ≤ 3 psu (c), ≤ 5 psu (d), ≤ 10 psu (e), and ≤ 15 psu (f).

Table 9, 10, and 11 list averages of salinity volume, bottom area, and shoreline length, respectively for salinity ≤ 1, 2, 3, 5, 10, and 15 psu under various flow reduction conditions. As can be seen from Table 9, ≤ 1 psu salinity volumes are more than one order of magnitude smaller than ≤ 2 psu volumes, which are about 60% of those for ≤ 3 psu, for all the flow reductions

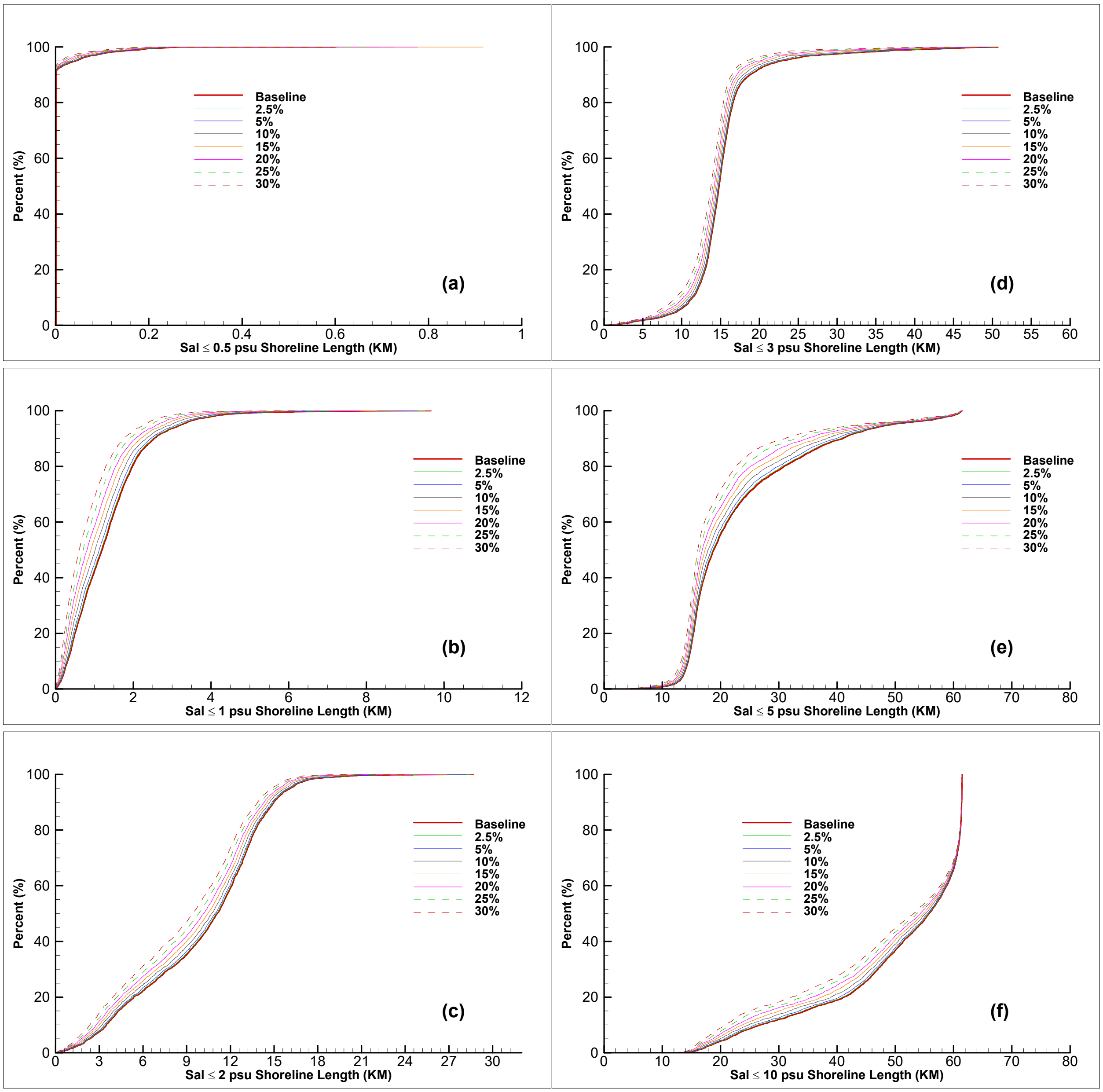

Figure 25. Cumulative distribution functions of simulated shoreline length for various flow reductions for salinity ≤ 1 psu (a), ≤ 2 psu (b), ≤ 3 psu (c), ≤ 5 psu (d), ≤ 10 psu (e), and ≤ 15 psu (f).

Similar scale differences among bottom areas and shoreline lengths of different salinity ranges can also be seen in Tables 10 and 11. Table 10 shows that ≤ 1 psu bottom areas are also more than one order of magnitude smaller than ≤ 2 psu bottom areas, which are about 62% of ≤ 3 psu bottom areas. Table 11 shows that ≤ 1 psu shoreline lengths are roughly one order of magnitude smaller than ≤ 2 psu shoreline lengths, which are about 66% of ≤ 3 psu shoreline lengths.

Table 9. Average water volumes of different salinity ranges for 14 flow reduction scenarios.

Reduction Scenario	**Average Water Volumes (million m^3)**					
	≤ 1	*≤ 2*	*≤ 3*	*≤ 5*	*≤ 10*	*≤ 15*
Baseline	0.016198	0.263063	0.435535	0.784724	2.162329	3.089820
Existing	0.015776	0.260723	0.431793	0.777789	2.156556	3.088459
2.5%	0.015454	0.258839	0.428751	0.772098	2.151654	3.087235
5.0%	0.014732	0.254587	0.421994	0.759602	2.140959	3.084672
7.5%	0.014001	0.250177	0.415048	0.746741	2.129661	3.081909
10.0%	0.013280	0.245716	0.408070	0.733988	2.118223	3.079149
12.5%	0.012585	0.241105	0.400866	0.720899	2.106145	3.076178
15.0%	0.011908	0.236455	0.393571	0.707927	2.093950	3.073200
17.5%	0.011249	0.231654	0.386168	0.694582	2.081221	3.070020
20.0%	0.010605	0.226720	0.378777	0.681275	2.068265	3.066729
22.5%	0.009979	0.221679	0.371197	0.667839	2.054889	3.063376
25.0%	0.009370	0.216452	0.363511	0.654206	2.040948	3.059810
27.5%	0.008785	0.211103	0.355692	0.640625	2.026704	3.056136
30.0%	0.008232	0.205592	0.347637	0.626871	2.011824	3.052291

Table 10. Average bottom areas of different salinity ranges for 14 flow reduction scenarios.

Reduction Scenario	**Average Bottom Areas (million m^2)**					
	≤ 1	*≤ 2*	*≤ 3*	*≤ 5*	*≤ 10*	*≤ 15*
Baseline	0.022207	0.330551	0.527002	0.876135	2.077281	2.709745
Existing	0.021585	0.327955	0.523146	0.869005	2.072247	2.708788
2.5%	0.021114	0.325856	0.519999	0.863188	2.068010	2.707942
5.0%	0.020052	0.321137	0.513006	0.850383	2.058658	2.706131
7.5%	0.018983	0.316216	0.505811	0.837255	2.048757	2.704193
10.0%	0.017927	0.311229	0.498554	0.824243	2.038682	2.702242
12.5%	0.016911	0.306028	0.491004	0.810863	2.028022	2.700141
15.0%	0.015921	0.300760	0.483339	0.797568	2.017203	2.698007
17.5%	0.014957	0.295289	0.475545	0.783851	2.005884	2.695720
20.0%	0.014019	0.289633	0.467747	0.770147	1.994326	2.693346

22.5%	0.013107	0.283817	0.459703	0.756323	1.982370	2.690909
25.0%	0.012225	0.277750	0.451522	0.742266	1.969928	2.688305
27.5%	0.011376	0.271487	0.443165	0.728251	1.957148	2.685595
30.0%	0.010576	0.265004	0.434489	0.714106	1.943738	2.682746

Table 11. Average shoreline lengths of different salinity ranges for 14 flow reduction scenarios.

Reduction Scenario	**Average Shoreline Lengths (KM)**					
	≤ 1	*≤ 2*	*≤ 3*	*≤ 5*	*≤ 10*	*≤ 15*
Baseline	1.376323	10.147712	15.374695	23.627028	50.446408	60.081444
Existing	1.350584	10.089992	15.295891	23.449689	50.332133	60.064883
2.5%	1.330310	10.044143	15.231626	23.306337	50.236242	60.051244
5.0%	1.284592	9.940482	15.089545	22.990200	50.020780	60.020330
7.5%	1.237434	9.832148	14.943922	22.669881	49.790695	59.988317
10.0%	1.190222	9.720639	14.799675	22.359874	49.557828	59.955350
12.5%	1.143269	9.602665	14.649671	22.040847	49.312147	59.919948
15.0%	1.096250	9.483931	14.497181	21.722581	49.059561	59.883075
17.5%	1.049472	9.360411	14.342203	21.397008	48.797474	59.842884
20.0%	1.002739	9.231385	14.190015	21.074463	48.535291	59.800255
22.5%	0.956130	9.096124	14.030081	20.751576	48.260389	59.757134
25.0%	0.909541	8.954379	13.866613	20.422693	47.974719	59.710917
27.5%	0.863057	8.804956	13.698764	20.096217	47.678593	59.662081
30.0%	0.817820	8.649255	13.524590	19.770612	47.368027	59.611275

From Tables 9 - 11, relative reductions of salinity habitats from these of the BSL condition caused by flow reductions can be easily calculated and are presented in Tables 12 - 14. It can be seen from Tables 12 - 14, the relative reduction of any salinity habitats increases with the increase of flow reduction, with low salinity habitats being more sensitive than those for salinity ≤ 10 psu or higher. In each table, the percent flow reduction that would trigger a 15% reduction of each individual salinity habitat is listed at the bottom row. The most sensitive salinity habitat is ≤ 1 psu bottom area, which has a decline of 15% if SGDs are reduced by 7.75%. In other words, if the flow reduction is less than 7.75%, none of the salinity habitats that are considered here will be reduced 15% or more.

Table 12. Relative reductions of water volume for various salinity ranges under different flow reduction scenarios.

Reduction Scenario	**Relative Reduction (Water Volume)**					
	Sal ≤ 1	*≤ 2*	*≤ 3*	*≤ 5*	*≤ 10*	*≤ 15*

Existing	2.61%	0.89%	0.86%	0.88%	0.27%	0.04%
2.5%	4.59%	1.61%	1.56%	1.61%	0.49%	0.08%
5.0%	9.05%	3.22%	3.11%	3.20%	0.99%	0.17%
7.5%	13.56%	4.90%	4.70%	4.84%	1.51%	0.26%
10.0%	18.01%	6.59%	6.31%	6.47%	2.04%	0.35%
12.5%	22.31%	8.35%	7.96%	8.13%	2.60%	0.44%
15.0%	26.48%	10.11%	9.64%	9.79%	3.16%	0.54%
17.5%	30.55%	11.94%	11.33%	11.49%	3.75%	0.64%
20.0%	34.53%	13.82%	13.03%	13.18%	4.35%	0.75%
22.5%	38.39%	15.73%	14.77%	14.90%	4.97%	0.86%
25.0%	42.15%	17.72%	16.54%	16.63%	5.61%	0.97%
27.5%	45.76%	19.75%	18.33%	18.36%	6.27%	1.09%
30.0%	49.18%	21.85%	20.18%	20.12%	6.96%	1.21%
Trigger (%)	***8.31%***	***21.55%***	***22.82%***	***22.65%***	***>30%***	***>30%***

Table 13. Relative reductions of bottom areas for various salinity ranges under different flow reduction scenarios.

Reduction Scenario	**Relative Reduction (Bottom Area)**					
	Sal ≤ 1	*≤ 2*	*≤ 3*	*≤ 5*	*≤ 10*	*≤ 15*
Existing	2.80%	0.79%	0.73%	0.81%	0.24%	0.04%
2.5%	4.92%	1.42%	1.33%	1.48%	0.45%	0.07%
5.0%	9.70%	2.85%	2.66%	2.94%	0.90%	0.13%
7.5%	14.52%	4.34%	4.02%	4.44%	1.37%	0.20%
10.0%	19.27%	5.85%	5.40%	5.92%	1.86%	0.28%
12.5%	23.85%	7.42%	6.83%	7.45%	2.37%	0.35%
15.0%	28.31%	9.01%	8.29%	8.97%	2.89%	0.43%
17.5%	32.65%	10.67%	9.76%	10.53%	3.44%	0.52%
20.0%	36.87%	12.38%	11.24%	12.10%	3.99%	0.61%
22.5%	40.98%	14.14%	12.77%	13.68%	4.57%	0.70%
25.0%	44.95%	15.97%	14.32%	15.28%	5.17%	0.79%
27.5%	48.77%	17.87%	15.91%	16.88%	5.78%	0.89%
30.0%	52.38%	19.83%	17.55%	18.49%	6.43%	1.00%
Trigger (%)	***7.75%***	***23.67%***	***26.07%***	***24.56%***	***>30%***	***>30%***

Table 14. Relative reductions of shoreline length for various salinity ranges under different flow reduction scenarios.

Reduction Scenario	**Relative Reduction (Shoreline Length)**					
	Sal ≤ 1	*≤ 2*	*≤ 3*	*≤ 5*	*≤ 10*	*≤ 15*
Existing	1.87%	0.57%	0.51%	0.75%	0.23%	0.03%

2.5%	3.34%	1.02%	0.93%	1.36%	0.42%	0.05%
5.0%	6.66%	2.04%	1.85%	2.70%	0.84%	0.10%
7.5%	10.09%	3.11%	2.80%	4.05%	1.30%	0.16%
10.0%	13.52%	4.21%	3.74%	5.36%	1.76%	0.21%
12.5%	16.93%	5.37%	4.72%	6.71%	2.25%	0.27%
15.0%	20.35%	6.54%	5.71%	8.06%	2.75%	0.33%
17.5%	23.75%	7.76%	6.72%	9.44%	3.27%	0.40%
20.0%	27.14%	9.03%	7.71%	10.80%	3.79%	0.47%
22.5%	30.53%	10.36%	8.75%	12.17%	4.33%	0.54%
25.0%	33.92%	11.76%	9.81%	13.56%	4.90%	0.62%
27.5%	37.29%	13.23%	10.90%	14.94%	5.49%	0.70%
30.0%	40.58%	14.77%	12.03%	16.32%	6.10%	0.78%
Trigger (%)	***11.08%***	***>30%***	***>30%***	***27.60%***	***>30%***	***>30%***

Based on the review comments received for the Crystal River/Kings Bay MFL report, effects of flow reduction on shoreline length were further analyzed for both altered (seawalls and ripraps) and natural (herbaceous, forest, rock, or shell) shores for the Chassahowitzka River. Data on Chassahowitzka River shoreline survey was collected by Water & Air Research, Inc. (2018). Tables 15 and 16 shows relative reductions of altered and natural shoreline lengths from these of the BSL condition caused by flow reductions.

Table 15. Relative reductions of altered shoreline length for various salinity ranges under different flow reduction scenarios.

Reduction Scenario	**Relative Reduction (Altered Shoreline Length)**					
	Sal ≤ 1	*≤ 2*	*≤ 3*	*≤ 5*	*≤ 10*	*≤ 15*
Existing	0.71%	1.44%	1.07%	0.52%	0.09%	0.01%
2.5%	1.22%	2.54%	1.90%	0.95%	0.15%	0.01%
5.0%	2.52%	5.14%	3.80%	1.94%	0.31%	0.02%
7.5%	3.48%	7.74%	5.80%	2.96%	0.48%	0.03%
10.0%	4.31%	10.33%	7.82%	4.01%	0.67%	0.04%
12.5%	5.06%	12.98%	9.89%	5.13%	0.86%	0.05%
15.0%	5.76%	15.68%	12.00%	6.30%	1.07%	0.07%
17.5%	6.38%	18.44%	14.14%	7.50%	1.29%	0.08%
20.0%	7.10%	21.21%	16.32%	8.77%	1.54%	0.10%
22.5%	7.75%	23.99%	18.54%	10.07%	1.79%	0.12%
25.0%	8.42%	26.80%	20.81%	11.44%	2.07%	0.14%
27.5%	9.06%	29.57%	23.14%	12.86%	2.37%	0.16%
30.0%	9.75%	32.36%	25.53%	14.37%	2.69%	0.19%
Trigger (%)	***>30%***	***14.37%***	***18.49%***	***>30%***	***>30%***	***>30%***

Table 16. Relative reductions of natural shoreline length for various salinity ranges under different flow reduction scenarios.

Reduction Scenario	Relative Reduction (Natural Shoreline Length)					
	Sal ≤ 1	*≤ 2*	*≤ 3*	*≤ 5*	*≤ 10*	*≤ 15*
Existing	0.12%	0.61%	0.54%	0.64%	0.21%	0.02%
2.5%	0.22%	1.11%	0.98%	1.15%	0.37%	0.04%
5.0%	0.45%	2.26%	1.95%	2.29%	0.76%	0.08%
7.5%	0.67%	3.45%	2.94%	3.46%	1.17%	0.13%
10.0%	0.88%	4.67%	3.95%	4.65%	1.60%	0.18%
12.5%	1.06%	5.95%	5.00%	5.86%	2.06%	0.23%
15.0%	1.23%	7.27%	6.04%	7.07%	2.51%	0.28%
17.5%	1.38%	8.68%	7.12%	8.31%	2.98%	0.34%
20.0%	1.53%	10.14%	8.24%	9.55%	3.47%	0.40%
22.5%	1.66%	11.66%	9.42%	10.80%	3.96%	0.46%
25.0%	1.79%	13.21%	10.64%	12.05%	4.49%	0.53%
27.5%	1.91%	14.85%	11.90%	13.32%	5.04%	0.60%
30.0%	2.03%	16.55%	13.21%	14.62%	5.63%	0.68%
Trigger (%)	***>30%***	***27.72%***	***>30%***	***>30%***	***>30%***	***>30%***

4.3. Results of Manatee Thermal Habitats

One of the purposes for considering thermal habitats (water volumes and surface areas of certain temperature ranges) is to protect manatees during the coldest days in winter, so that the warm-water refuge in the estuary won't be significantly reduced because of the SGD reduction. Manatees cannot survive in water colder than 20 ºC for a prolonged period, because of their inability to increase their metabolic rates in cold water to compensate the increased rate of body heat loss, as they have a high thermal conductance, or poor insulation (Worthy et al., 2000). Because SGDs have a relatively stable temperature of 22.0 ºC or higher during winter, they provide a quite big area of warm-water refuge for manatees when water temperature in the Gulf dips to 20 ºC or lower.

Following the similar MFL-evaluation procedure used during the previous MFL evaluations for the Chassahowitzka River and for other spring-fed estuaries in the District (e.g. Weeki Wachee River, Crystal River/Kings, and Homosassa River), water volumes and surface areas of three temperature ranges, namely < 15 ºC, between 15 and 20 ºC, and ≥ 20 ºC, were calculated for various flow reduction scenarios. Figure 26 shows time series (30-minute interval) plots of water volumes and surface areas for temperature < 15 ºC, ≥ 15 ºC, and ≥ 20 ºC under the BSL condition (the ≥ 15 ºC thermal habitats are sums of those for temperature ≥ 20 ºC and for temperature between 15 and 20 ºC). For comparison, time series of the < 15 ºC, ≥ 15 ºC, and ≥ 20 ºC thermal habits for the 10% flow reduction scenario are shown in Figure 27. Time series plots of thermal habitats for other flow reduction scenarios are similar and are omitted here.

It should be noted that the computation of ≥ 15 ºC (between 15 and 20 ºC in the actual computation) or ≥ 20 ºC volume and surface area for manatee thermal habitat analysis only includes grids containing at least one continuous noncold (≥ 15 ºC) or warm water (≥ 20 ºC) layer with a thickness of 1.158 m (3.8 feet) or more in the water column. This 1.158 m thickness constrain for the warm water layer is determined from the size of an adult manatee to ensure that the animal is fully enclosed in warm water. Any water columns that do not meet the 1.158 m criterion are excluded from the computation of ≥ 15 ºC and ≥ 20 ºC volumes and surface areas.

As expected, during the warm months of the year, water temperature in the Chassahowitzka River is ≥ 20 ºC and there exist no water volume and surface area that are < 20 ºC. As a result, ≥ 15 ºC habitats and ≥ 20 ºC habitats are identical. During the manatee season, which is defined as November – March in this MFL evaluation, water temperature in the Chassahowitzka River can drop to 10 ºC or lower, a significant amount of < 15 ºC water volume and surface area exist in the estuary. During the coldest days of the year, the total ≥ 20 ºC volume with a layer thickness of 1.158 m or more became significantly smaller than warm days.

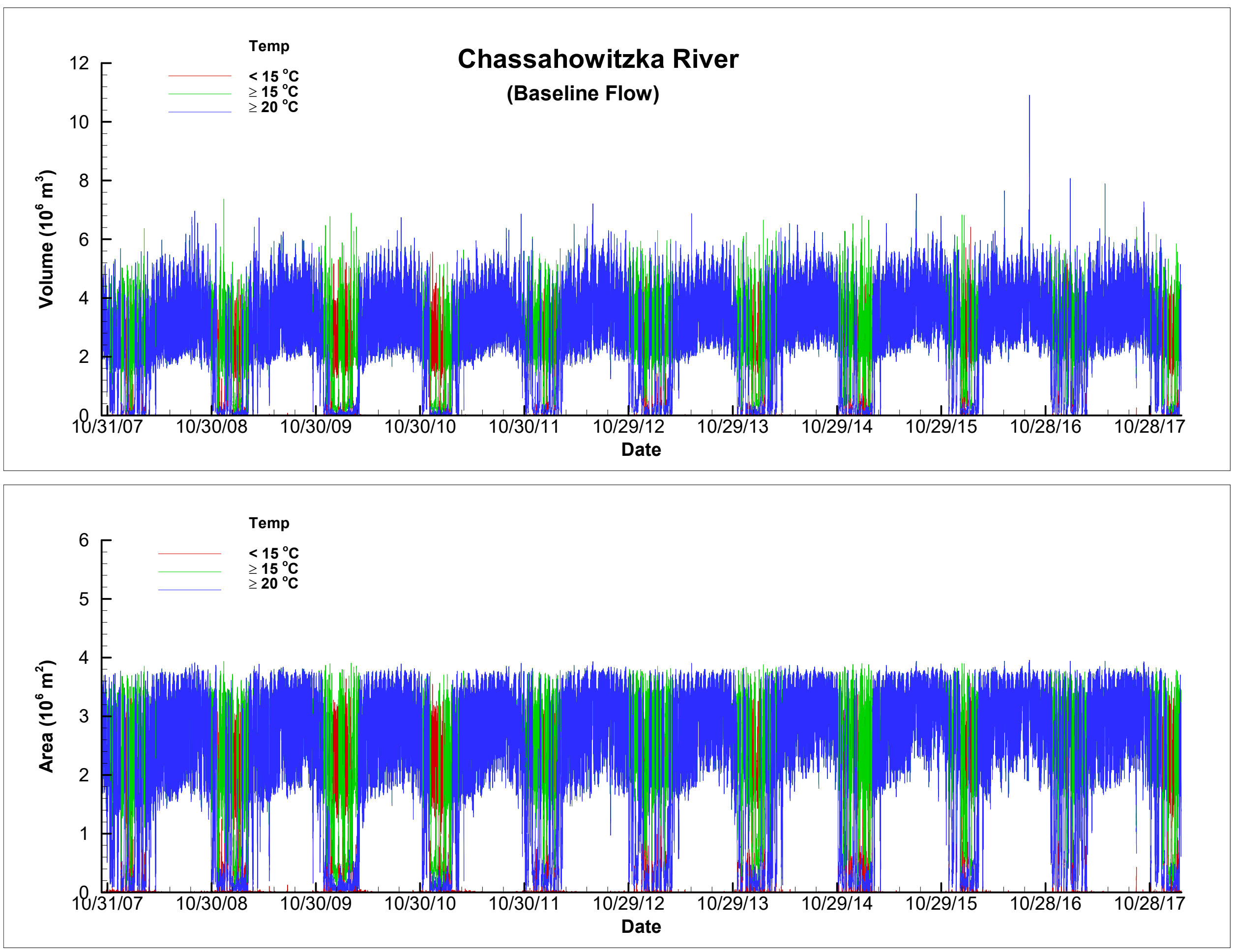

Figure 26. Time series of simulated water volumes (top panel) and surface areas (bottom panel) for temperature < 15 ºC, ≥ 15 ºC, and ≥ 20 ºC under the baseline condition during the 123-month simulation period.

Although the manatee season lasts five months long, warm water refuge for manatee are critical only during or right after a cold front event. The Gulf water during the manatee season generally varies between 15 – 25 ºC most of the time; however, during severe cold front days, Gulf water can drop to a couple of degree below 10 ºC. When the Gulf water is only a few degrees warmer or colder than the spring flow temperature, reducing spring flow won't have much an effect on thermal habitats. As such, the only time period when thermal habitats are sensitive to SGD reduction would be during the cold days when the Gulf water is much colder than spring flows out of the vents. Clearly, considering the overall warm thermal habitat reduction for the entire manatee season or several manatee seasons is meaningless, because such a parameter barely responds to flow reduction. As a result, thermal analysis in this study considers only short time scales, in the order of several days or several hours when warm water or noncold water thermal habitats become less available to manatees during or right after cold front events.

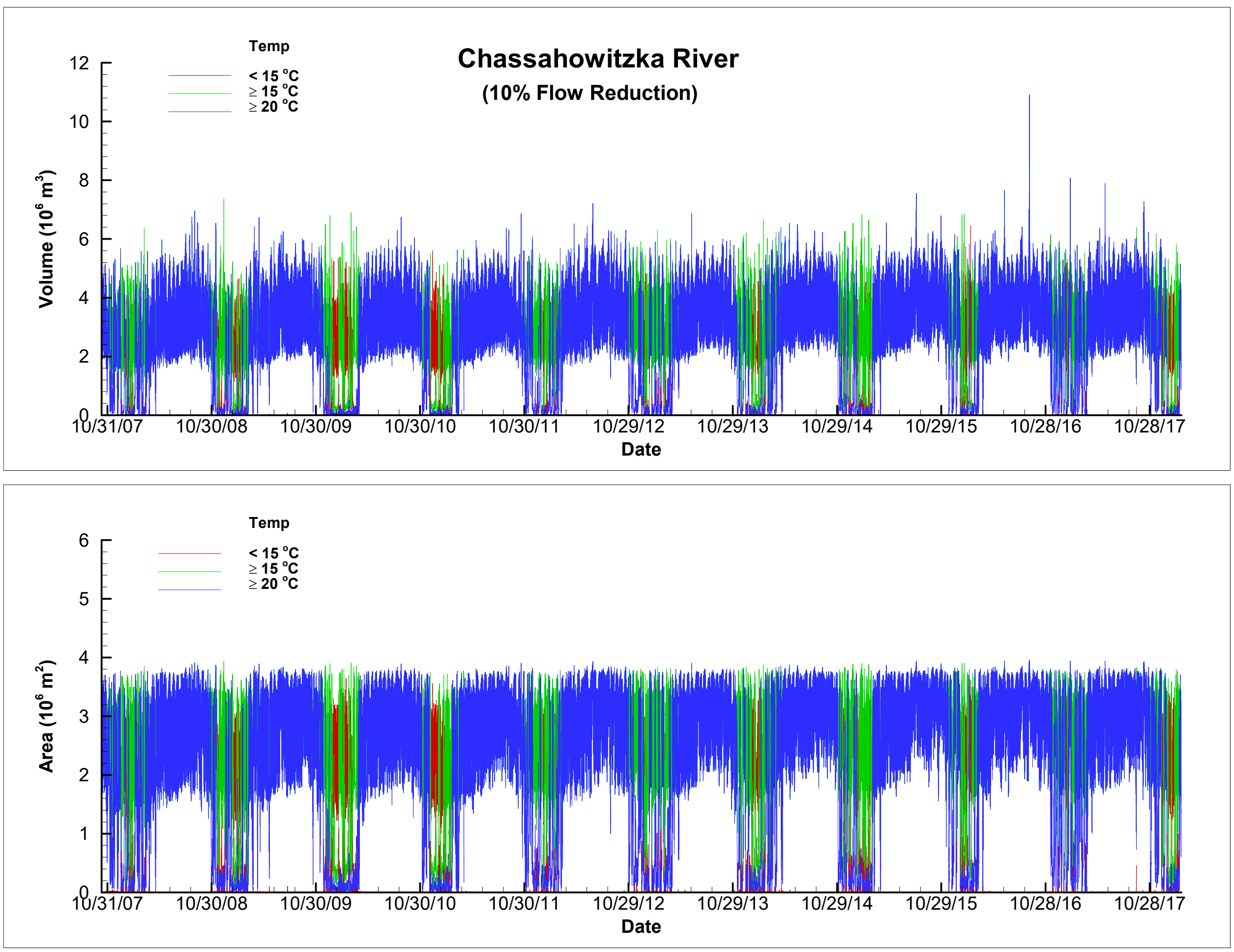

Figure 27. Time series of simulated water volumes (top panel) and surface areas (bottom panel) for temperature < 15 ºC, ≥ 15 ºC, and ≥ 20 ºC under the 10% flow reduction during the 123-month simulation period.

There are also physiological reasons for considering a relatively short time scale in studying effects of flow reduction to thermal habitats. Manatees have a low metabolic rate and high thermal conductance, and they have a limited ability to raise their metabolic rate to keep them warm during cold days. Consequently, manatees are not capable of surviving in cold environment for a long time. Any exposure to water below 20 ºC for longer than 4 – 7 days could result in disastrous losses to the manatee population (Rouhani et al., 2007). When water temperature is further drops to below 15 ºC, manatees cannot withstand the cold for more than 4 hours (Janicki Environmental and Applied Technology & Management, 2007).

Because of these physiological constraints for manatees, the MFL evaluation generally takes two temporal scales into consideration. One is no longer than 4 days (96 hours) for the warm water habitats, with temperature 20 ºC or higher, and the other is about 4 hours for the noncold water habitats, with temperature 15 ºC or higher. The former is considered as a chronic condition for manatees, while the latter is an acute condition for manatee. To be conservative and consistent with previous MFL evaluations (e.g., Rouhani et al., 2007; Janicki Environmental and Applied Technology & Management, 2007; Chen, 2017), the time scale for the chronic condition is further reduced to 72 hours.

In the analysis of thermal habitats for the chronic and acute conditions for manatees, 72-hour and 4-hour moving averages of simulated water volumes and surface areas for temperature ≥ 20 ºC and ≥ 15 ºC, respectively were first calculated, with the consideration of the 3.8 ft depth (or layer thickness) requirement. The 72-hour and 4-hour moving averages at a time point t (in hours) were simply calculated as the arithmetic means during [t-36, t+36] and [t-2, t+2], respectively. Figure 28 shows time series of 72-hour moving averages of volume (top panel) and surface area (bottom panel) for temperature ≥ 20 ºC under various flow conditions, including the baseline, existing, 5%, 10%, 15%, 20%, 25%, and 30% flow reductions. The small inserts are plots showing available warm water (≥ 20 ºC) volumes and surface areas during and after a typical cold front in the January 2010. Time series of 4-hour moving averages of water volume and surface area for temperature ≥ 15 ºC under various flow conditions are shown in Figure 29, in which noncold water habitats during and after a typical cold front are also plotted in small inserts.

An analysis of the 72-hour moving averages of warm water volume and surface area for all the time points simulated during manatee season is neither practical nor necessary. Similar to the procedure used in the Crystal River/Kings Bay MFL evaluation (Chen, 2017), 72-hour averages of warm water volume and surface area at several critical time points were chosen to examine the effect of flow reduction on thermal habitats with temperature ≥ 20 ºC. These critical time points included times when the lowest air temperatures were recorded at the weather stations in 2010 and 2018 and the time when the lowest overall water temperature in the Chassahowitzka River occurred. Times at or around which ≥ 20 ºC volume and surface area reached their minima were also examined.

The coldest air temperature measured in the Homosassa/Chassahowitzka River area during the entire 123 months of the simulation period was -9.13 ºC, which was recorded at 7:30 AM on January 18, 2018 at the Lecanto High School. The area also experienced a couple of severe cold fronts during the first couple of months in 2010. The most severe cold front event was during January 4, 2010 - January 15, 2010, when daily lows of air temperature were all below 0 ºC during these 12 days, making the longest period on record for consecutive days with freezing air temperature in the area. The coldest air temperature recorded was -7.78 ºC during these 12 days and recorded at 6:00 AM on January 11, 2010. Although -7.78 ºC is not the coldest air temperature on record for the area, the longevity of the coldness makes this time point and several hours around it to be critical about the availability of the useable thermal habitats for manatees. Figure 30 shows measured air temperatures during the coldest days in 2010 (top panel) and 2018 (bottom panel).

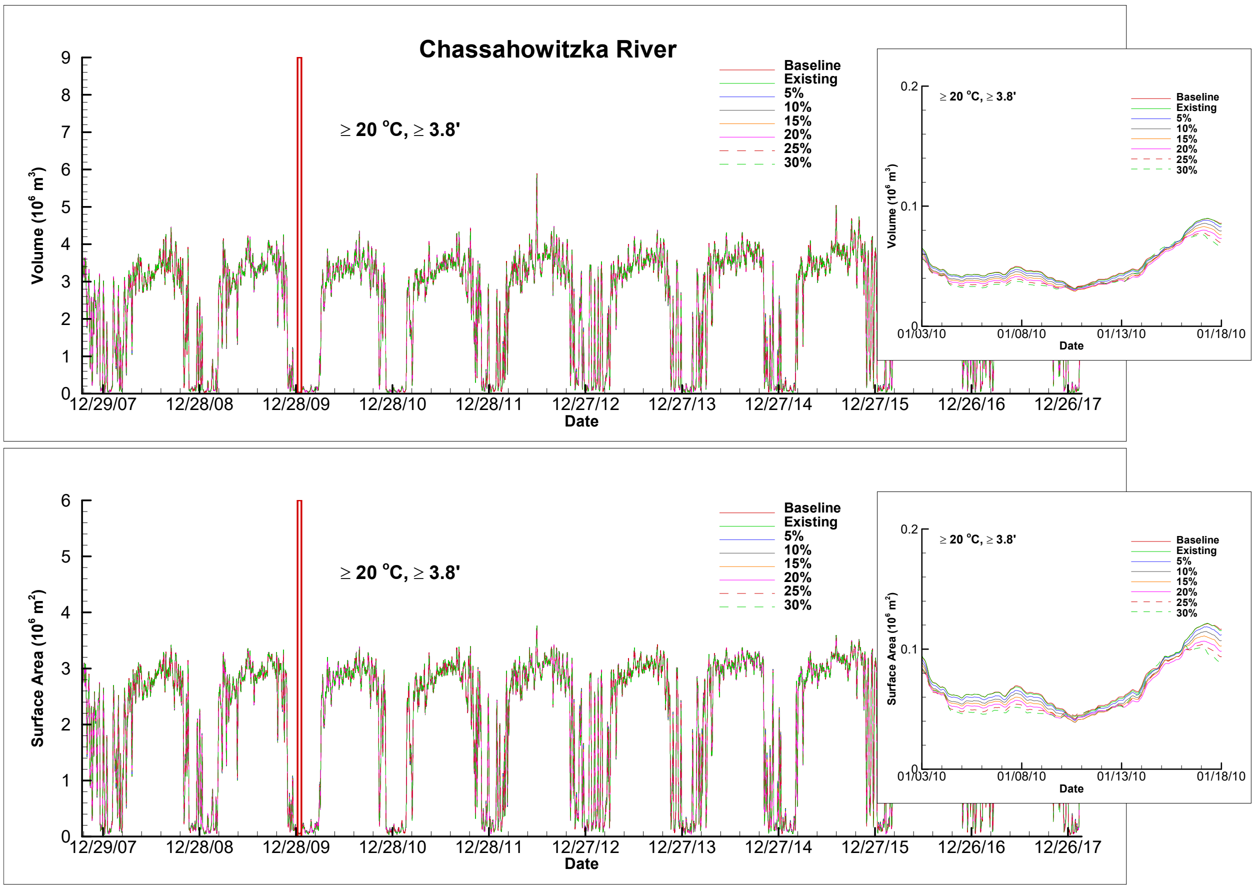

Figure 28. Comparisons of time series of 72-hour moving averages of ≥ 20 ºC volume (top panel) and surface area (bottom panel) for the baseline, existing, 5%, 10%, 15%, 20%, 25%, and 30% flow reduction scenarios during the 123-month simulation period.

In general, water temperature in the Chassahowitzka River has a delay of response when a cold front moves in. Other factors such as the temperature boundary conditions at the downstream boundary, SGDs, heat fluxes at the free surface, and transport processes within the water body also affect temperature distributions in the river. As a result, water temperature in the Chassahowitzka River does not necessarily correlate well with air temperature. Based on available temperature data, the overall lowest water temperature during the 123-month simulation period in the Chassahowitzka River is found to be at 1:00 AM on January 12, 2010.

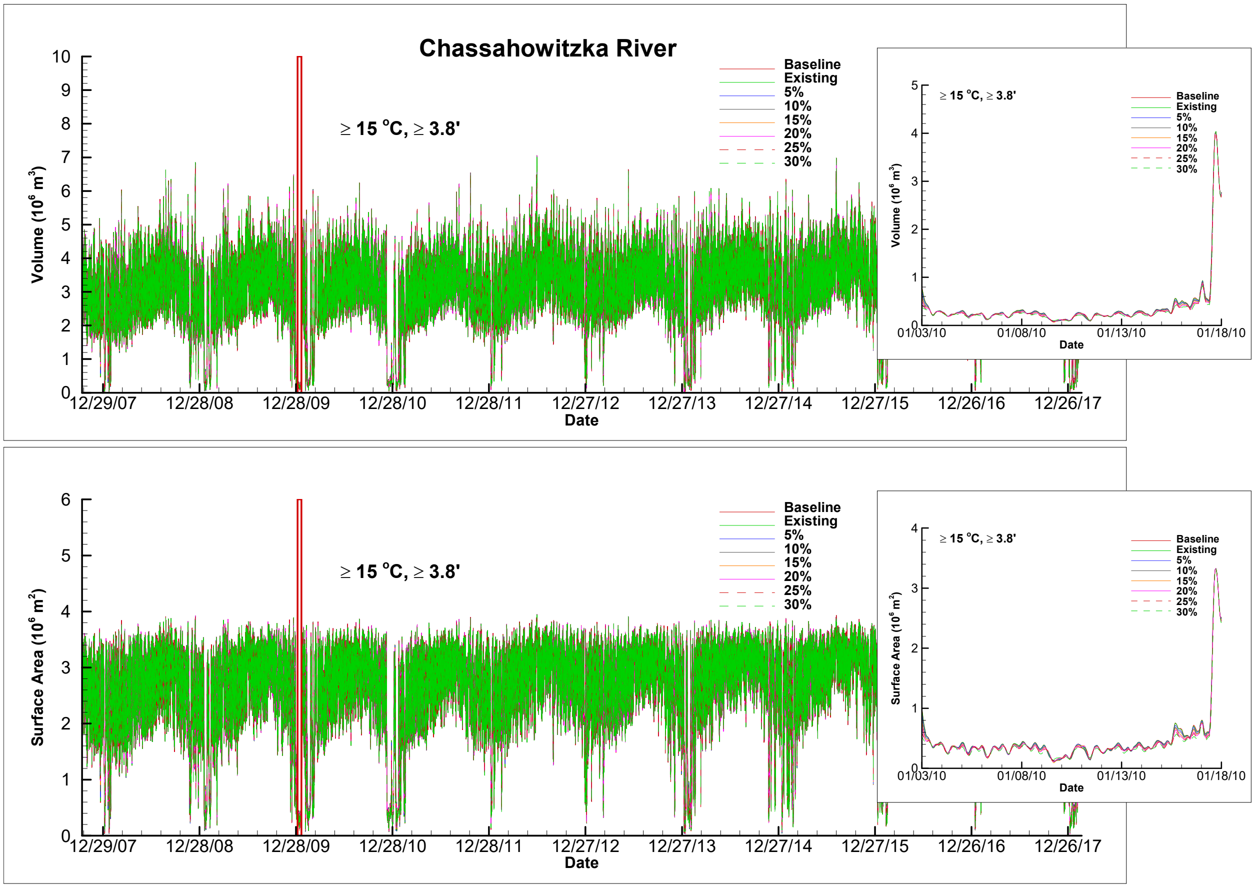

Figure 29. Comparisons of time series of 4-hour moving averages of ≥ 15 ºC volume (top panel) and surface area (bottom panel) for the baseline, existing, 5%, 10%, 15%, 20%, 25%, and 30% flow reduction scenarios during the 123-month simulation period.

Table 17 shows 72-hour averages of water volume for the chronic condition for manatees at five critical time points in the Chassahowitzka River. Besides the coldest air in 2010 (at 6:00 AM, 1/11/2010, or during 6:00 PM, 1/9/2010 - 6:00 PM, 1/12/2010) and in 2018 (at 7:30 AM, 1/18/2018, or 7:30 PM, 1/16/2018 – 7:30 PM, 1/19/2018) as well as the coldest water in the river (at 1:00 AM, 1/12/2010, or 1:00 PM, 1/10/2010 – 1:00 PM, 1/13/2010), the time point at which the river had the smallest amount of 72-hour average of ≥ 20 ºC volume was also included in the table. During the 72-hour period centered at 10:30 AM, 1/1/2018, or during 10:30 AM, 1/1/2018 – 10:30 AM, 1/4/2018, the river had the smallest amount of 72-hour average of ≥ 20 ºC volume at 26,133 m^3 under the BSL condition. Two hours later, during a 72-hour time window centered at 12:30 AM, 1/3/2018 (or 12:30 PM, 1/1/2018 - 12:30 PM, 1/4/18), the 72-hour average of ≥ 20 ºC volume had the most sensitive reaction to the SGD reduction among the lowest 0.02% warm water volumes in the river. With a 30% SGD reduction, the lowest 72-hour average of ≥ 20 ºC volume during the 123 months was reduced to 20,795 m^3, or 734,369 cubic feet (5,493,456 gallons) in the Chassahowitzka River.

Because a reduction of SGD not only reduces the amount of warm water entering the estuarine system but also more or less affects other physical processes and parameters (e.g., density distribution, mixing, baroclinic forces, heat exchanges at the free surface, velocities, elevations, etc.) in the river, which eventually affect the temperature distribution in the water body. As the interaction among these processes and parameters are highly nonlinear, the relationship between water temperature and the percentage of the SGD reduction at a fixed spatial location and a fixed time point is not necessarily monotonic. A close examination of Figures 28 and 29 shows that due to the nonlinear interactions, a SGD reduction can cause the time series of the 72-hour moving averages of ≥ 20 ºC volume and surface area to have a time drift.

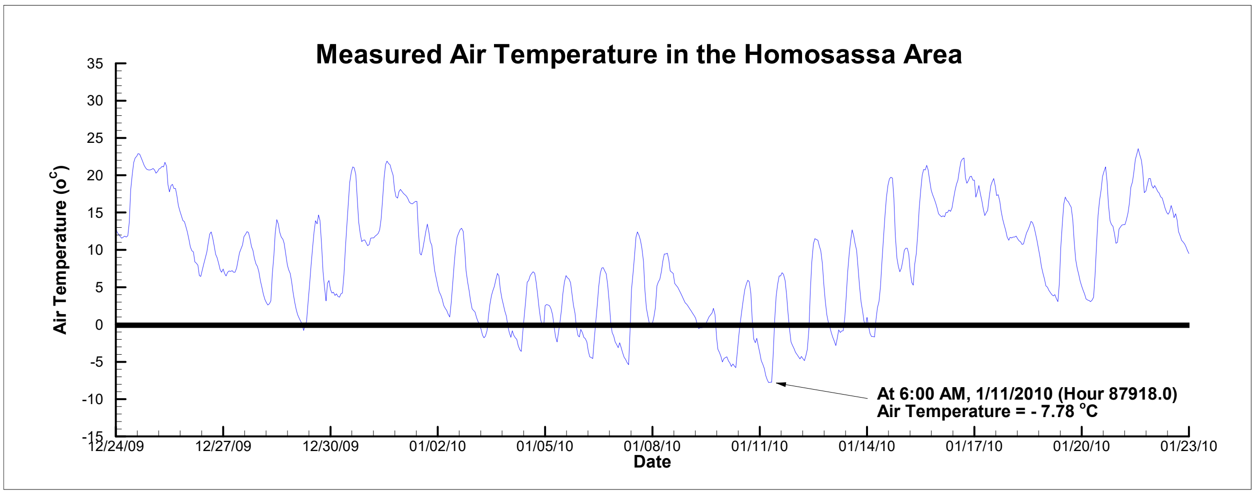

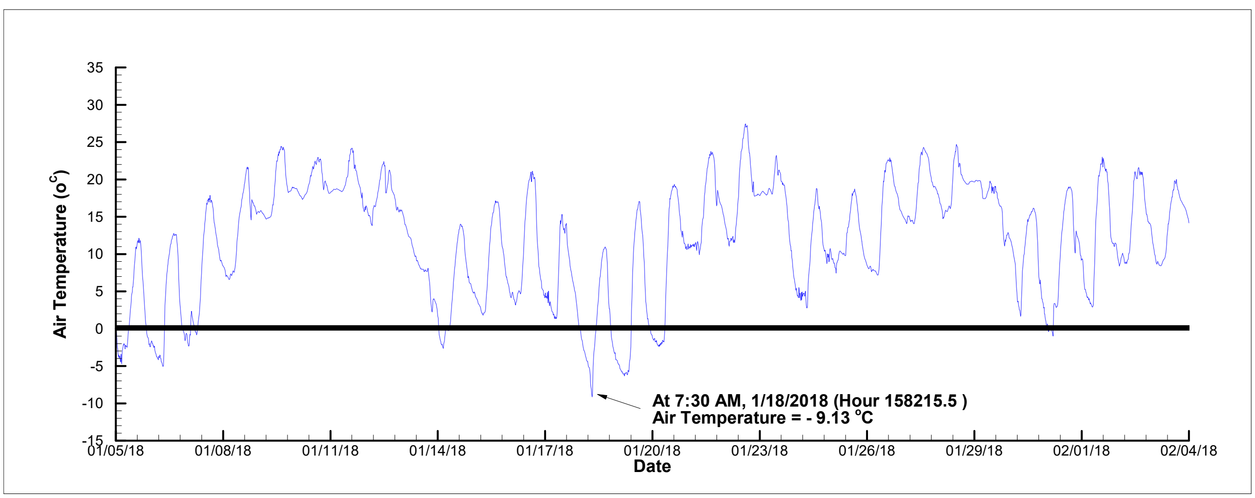

Figure 30. Coldest days with the lowest air temperatures measured in 2010 and 2018 in the Homosassa/Chassahowitzka River area.

Table 17. Water volumes (in m^3) for the chronic condition for five 72-hour time windows in the Chassahowitzka River.

	72-Hour Time Window				
	#1	*#2*	*#3*	*#4*	*#5*
	1/9/10 18:00 - 1/12/10 18:00	*1/10/10 13:00 - 1/13/10 13:00*	*1/1/18 10:30 - 1/4/18 10:30*	*1/1/18 12:30 - 1/4/18 12:30*	*1/16/18 19:30 - 1/19/18 19:30*
Baseline	34778	39166	26133	26719	55523
Existing	34213	38500	25909	26493	54964
2.5%	34040	38213	25732	26331	54418
5.0%	33405	37348	25525	26106	53377
7.5%	32708	36447	25298	25815	52335
10.0%	32024	35591	25007	25514	51714
12.5%	31399	34910	24406	24876	50610
15.0%	31672	34876	23901	24390	50388
17.5%	31947	34977	23421	23898	50111
20.0%	32355	35303	23023	23435	49119
22.5%	33643	36251	22725	23098	49235
25.0%	34026	36398	22029	22394	48801
27.5%	33795	36100	21375	21744	48467
30.0%	33664	35913	20795	21097	48525

Relative changes of the 72-hour average of the ≥ 20 ºC water volume from the baseline volumes at the five critical time points are shown in Table 18, in the form of percentage reduction. From Tables 17 & 18, it can be seen that the 72-hour average of warm water volume reduces monotonically with the SGD reduction in time windows #3 and #4, but not monotonically with at other three 72-hour time windows, when either the air temperature was lowest or when the water temperature was lowest. Only during 10:30 AM, 1/1/2018 – 10:30 AM, 1/4/2018 and 12:30 PM, 1/1/2018 - 12:30 PM, 1/4/2018 was the 72-hour average of ≥ 20 ºC water volume reduced by more than 15%, as the SGD reduction increased from 0% to 30%.

Table 18. Percentage reductions of the ≥ 20 ºC water volume relative to the corresponding baseline volumes for five 72-hour time windows in the Chassahowitzka River.

	72-Hour Time Window				
	#1	*#2*	*#3*	*#4*	*#5*
Scenario	*1/9/10 18:00 - 1/12/10 18:00*	*1/10/10 13:00 - 1/13/10 13:00*	*1/1/18 10:30 - 1/4/18 10:30*	*1/1/18 12:30 - 1/4/18 12:30*	*1/16/18 19:30 - 1/19/18 19:30*
Existing	1.62%	1.70%	0.86%	0.85%	1.01%
2.5%	2.12%	2.43%	1.53%	1.45%	1.99%
5.0%	3.95%	4.64%	2.33%	2.29%	3.87%
7.5%	5.95%	6.94%	3.20%	3.38%	5.74%

10.0%	7.92%	9.13%	4.31%	4.51%	6.86%
12.5%	9.72%	10.87%	6.61%	6.90%	8.85%
15.0%	8.93%	10.95%	8.54%	8.72%	9.25%
17.5%	8.14%	10.70%	10.38%	10.56%	9.75%
20.0%	6.97%	9.86%	11.90%	12.29%	11.53%
22.5%	3.26%	7.44%	13.04%	13.55%	11.33%
25.0%	2.16%	7.07%	15.70%	16.19%	12.11%
27.5%	2.83%	7.83%	18.21%	18.62%	12.71%
30.0%	3.20%	8.31%	20.43%	21.04%	12.60%
Triger			***24.34%***	***23.87%***	

Like Table 17, Table 19 lists 72-hour averages of surface area for the chronic condition for manatees at five critical time points in the Chassahowitzka River. The time window when the river had the least 72-hour average of ≥ 20 ºC surface area was during 10:30 AM, 1/1/2018 – 10:30 AM, 1/4/2018, the same as that for the ≥ 20 ºC volume. During the 72 hours from 1:30 PM, 1/1/2018 to 1:30 PM, 1/4/2018 (time window #4 in Table 19), the most sensitive reaction to the SGD reduction occurred among the lowest 0.02% warm water surface area. The smallest warm water surface area for the entire 123 months of simulation was 33,653 m^2 under the BSL condition. With a 30% flow reduction, this amount was reduced to 27,001 m^2, or 290,636 square feet, which is about 6.67 acres.

Relative percentage changes of ≥ 20 ºC surface area from the baseline surface area are presented in Table 20, in a similar way as that in Table 18. Among the five time windows only during #3 and #4 was the average ≥ 20 ºC surface area reduced by more than 15%, as the SGD reduction increased from 0% to 30%. Furthermore, the 72-hour average of ≥ 20 ºC surface area declines monotonically with the SGD reduction only during time windows #4 and #5 (Table 20), but not monotonically at other three time points, when either the air temperature was the lowest or when the water temperature was the lowest.

Table 19. Surface areas (in m^2) for the chronic condition for five 72-hour time windows in the Chassahowitzka River.

	72-Hour Time Window				
	#1	*#2*	*#3*	*#4*	*#5*
	1/9/10 18:00 - 1/12/10 18:00	*1/10/10 13:00 - 1/13/10 13:00*	*1/1/18 10:30 - 1/4/18 10:30*	*1/1/18 13:30 - 1/4/18 13:30*	*1/16/18 19:30 - 1/19/18 19:30*
Baseline	47030	53014	33653	35196	78579
Existing	46139	51981	33386	34925	77848
2.5%	45967	51708	33182	34731	77212
5.0%	45312	50660	32919	34475	75530
7.5%	44342	49498	32737	34162	73922

10.0%	43336	48273	32447	33886	72946
12.5%	42635	47338	31600	32956	71111
15.0%	43115	47449	30979	32267	70674
17.5%	43993	48012	30345	31517	70548
20.0%	44794	48775	29829	30984	68580
22.5%	47360	50745	29575	30566	69316
25.0%	48098	51085	28707	29680	68849
27.5%	48137	51029	27802	28707	68170
30.0%	47833	50644	27001	27821	68026

Table 20. Percentage reductions of the ≥ 20 ºC surface area relative to the corresponding baseline surface areas for five 72-hour time windows in the Chassahowitzka River.

	72-Hour Time Window				
	#1	*#2*	*#3*	*#4*	*#5*
	1/9/10 18:00 - 1/12/10 18:00	*1/10/10 13:00 - 1/13/10 13:00*	*1/1/18 10:30 - 1/4/18 10:30*	*1/1/18 13:30 - 1/4/18 13:30*	*1/16/18 19:30 - 1/19/18 19:30*
Existing	1.89%	1.95%	0.79%	0.77%	0.93%
2.5%	2.26%	2.46%	1.40%	1.32%	1.74%
5.0%	3.65%	4.44%	2.18%	2.05%	3.88%
7.5%	5.72%	6.63%	2.72%	2.94%	5.93%
10.0%	7.85%	8.94%	3.58%	3.72%	7.17%
12.5%	9.35%	10.71%	6.10%	6.36%	9.50%
15.0%	8.32%	10.50%	7.95%	8.32%	10.06%
17.5%	6.46%	9.44%	9.83%	10.45%	10.22%
20.0%	4.75%	8.00%	11.36%	11.97%	12.72%
22.5%	-0.70%	4.28%	12.12%	13.15%	11.79%
25.0%	-2.27%	3.64%	14.70%	15.67%	12.38%
27.5%	-2.35%	3.74%	17.39%	18.44%	13.25%
30.0%	-1.71%	4.47%	19.77%	20.95%	13.43%
Triger			***25.28%***	***24.33%***	***>30%***

As stated above, when water temperature drops to below 15 ºC, the condition for manatees becomes very severe, as it becomes very harsh for manatees in an environment with water lower than 15 ºC for more than four hours. Naturally, manatees try to avoid < 15 ºC habitats and find warmer habitats to survive in these acute conditions. As such, the existence and extension of ≥ 15 ºC habitats are critical and the analysis of thermal habitats under the acute condition becomes the analysis of thermal habitats ≥ 15 ºC, which are not supposed to be reduced more than 15% in the 4-hour period. This approach is consistent with analyses of salinity and thermal habitats in our previous MFL evaluations, as we focus on reductions of favorable habitats, not on the increases of unfavorable habitats.

The ≥ 15 ºC thermal habitats are simply the summations of ≥ 20 ºC habitats and those between 15 and 20 ºC, as shown in Figure 29. Similar to the analysis for the chronic condition, five critical time points were examined, including those when the air temperature were lowest in 2010 and 2018, water temperature in the river was coldest, the 4-hour average of ≥ 15 ºC thermal habitats were lowest, and noncold habitats were most sensitive to the SGD reduction among the lowest 0.02% of thermal habitats.

Table 21 shows 4-hour averages of water volume for the acute condition for manatees at five critical time points in the Chassahowitzka River. During the 4-th 4-hour time window, centered at Hour 157830, the river had the smallest amount of 4-hour average of ≥ 15 ºC volume. The 4-hour average of ≥ 15 ºC volume had the most sensitive reaction to the SGD reduction among the lowest 0.02% noncold water volumes in the river during 6:30 AM – 10:30 AM on 1/7/2014. With a 30% SGD reduction, the lowest 4-hour average of ≥ 15 ºC volume during the 123 months was 34,095 cubic meters, or 1,204,054 cubic feet (9,006,946 gallons).

Table 21. Four-hour averages of ≥ 15 ºC water volumes (in m^3) for the acute condition during five time windows in the Chassahowitzka River.

	4-Hour Time Window				
	#1	*#2*	*#3*	*#4*	*#5*
	1/11/10 4:00 – 1/11/10 8:00	*1/11/10 23:00 – 1/12/10 3:00*	*1/7/14 6:30 – 1/7/14 10:30*	*1/2/18 4:00 – 1/2/18 8:00*	*1/18/19 5:30 – 1/18/18 9:30*
Baseline	132890	198853	25158	23944	136020
Existing	133483	199784	26054	23867	131646
2.5%	136371	202083	26321	23808	131760
5.0%	136961	203475	27084	23698	126020
7.5%	146782	206210	28093	23940	124852
10.0%	147570	207845	30190	23958	118184
12.5%	161240	208516	32364	24487	114509
15.0%	168904	207553	34095	24673	110189
17.5%	175493	206390	38596	24745	107896
20.0%	179134	203635	45024	26153	104041
22.5%	180040	199329	46963	27530	99643
25.0%	178857	197539	49801	30466	99245
27.5%	178497	191717	50057	32422	96169
30.0%	176508	189220	49922	34095	93456

Relative changes of the 4-hour average of the ≥ 15 ºC water volume from the baseline volumes at the five critical time points are shown in Table 22, in the form percentage reduction. As shown in the table, during time window #5 centered at 7:30 AM, 1/18/2018, a 11.75% SGD reduction would trigger a 15% reduction of the 4-hour average of ≥ 15 ºC water volume. Unlike the 72-hour average of ≥ 20 ºC water volume shown in Table 18, the most sensitive time point for the noncold water volume under the acute condition was when the air temperature was the lowest in 2010.

Table 22. Percentage reductions of the 4-hour average of the ≥ 15 ºC water volume relative to the corresponding baseline volumes during five time windows in the Chassahowitzka River.

	4-Hour Time Window				
	#1	*#2*	*#3*	*#4*	*#5*
	1/11/10 4:00 – 1/11/10 10:00	*1/11/10 23:00 – 1/12/10 3:00*	*1/7/14 6:30 – 1/7/14 10:30*	*1/2/18 4:00 – 1/2/18 8:00*	*1/18/19 5:30 – 1/18/18 9:30*
Existing	-0.45%	-0.47%	-3.56%	0.32%	3.22%
2.5%	-2.62%	-1.62%	-4.62%	0.57%	3.13%
5.0%	-3.06%	-2.32%	-7.66%	1.03%	7.35%
7.5%	-10.45%	-3.70%	-11.67%	0.02%	8.21%
10.0%	-11.05%	-4.52%	-20.00%	-0.06%	13.11%
12.5%	-21.33%	-4.86%	-28.64%	-2.27%	15.81%
15.0%	-27.10%	-4.38%	-35.52%	-3.04%	18.99%
17.5%	-32.06%	-3.79%	-53.41%	-3.35%	20.68%
20.0%	-34.80%	-2.40%	-78.96%	-9.23%	23.51%
22.5%	-35.48%	-0.24%	-86.67%	-14.98%	26.74%
25.0%	-34.59%	0.66%	-97.95%	-27.24%	27.04%
27.5%	-34.32%	3.59%	-98.97%	-35.41%	29.30%
30.0%	-32.82%	4.84%	-98.43%	-42.39%	31.29%
Triger					***11.75%***

Similar to Tables 21 and 22, 4-hour averages of ≥ 15 ºC surface areas for the acute condition at five critical time points and their percentage changes relative to the corresponding baseline noncold surface areas are listed in Tables 23 and 24. The lowest noncold surface area with a 30% SGD reduction was 116,695 m2, or 1,256,095 square feet (28.84 acres). Among the five critical time windows, only during time window #5 would a reduction of SDG between 0% to 30% trigger a 15% reduction of the 4-hour average of ≥ 15 ºC surface area.

Table 23. Four-hour averages of ≥ 15 ºC surface areas (in m^2) for the acute condition during five time windows centered in the Chassahowitzka River.

	4-Hour Time Window				
	#1	*#2*	*#3*	*#4*	*#5*
	1/11/10 4:00 – 1/11/10 10:00	*1/11/10 23:00 – 1/12/10 3:00*	*1/8/14 2:00 – 1/8/14 6:00*	*1/2/18 4:00 – 1/2/18 8:00*	*1/18/19 5:30 – 1/18/18 9:30*

Baseline	227108	254634	32891	32721	217725
Existing	227833	256339	32810	32646	209706
2.5%	233375	256923	32746	32584	209654
5.0%	234222	262044	32598	32465	199373
7.5%	249060	261343	33787	32813	196881
10.0%	250544	265076	38500	32666	185271
12.5%	271200	266640	39723	33484	180217
15.0%	280367	265916	40140	33682	171349
17.5%	290988	264922	40596	33524	168843
20.0%	297674	262252	41468	35488	160700
22.5%	299988	257024	43378	37903	152056
25.0%	297924	254619	47405	42961	151744
27.5%	297334	243447	49359	46640	146374
30.0%	295304	241175	52080	49010	141667

Table 24. Percentage reductions of the 4-hour average of the ≥ 15 ºC surface area relative to the corresponding baseline volumes during five time windows in the Chassahowitzka River.

	4-Hour Time Window				
	#1	*#2*	*#3*	*#4*	*#5*
	1/11/10 4:00 – 1/11/10 10:00	*1/11/10 23:00 – 1/12/10 3:00*	*1/8/14 2:00 – 1/8/14 6:00*	*1/2/18 4:00 – 1/2/18 8:00*	*1/18/19 5:30 – 1/18/18 9:30*
Existing	-0.32%	-0.67%	0.25%	0.23%	3.68%
2.5%	-2.76%	-0.90%	0.44%	0.42%	3.71%
5.0%	-3.13%	-2.91%	0.89%	0.78%	8.43%
7.5%	-9.67%	-2.63%	-2.72%	-0.28%	9.57%
10.0%	-10.32%	-4.10%	-17.05%	0.17%	14.91%
12.5%	-19.41%	-4.72%	-20.77%	-2.33%	17.23%
15.0%	-23.45%	-4.43%	-22.04%	-2.94%	21.30%
17.5%	-28.13%	-4.04%	-23.43%	-2.45%	22.45%
20.0%	-31.07%	-2.99%	-26.08%	-8.46%	26.19%
22.5%	-32.09%	-0.94%	-31.88%	-15.84%	30.16%
25.0%	-31.18%	0.01%	-44.13%	-31.29%	30.30%
27.5%	-30.92%	4.39%	-50.07%	-42.54%	32.77%
30.0%	-30.03%	5.29%	-58.34%	-49.78%	34.93%
Triger		***>30%***			***10.10%***

4.4. Results of Common Snook Thermal Habitats

Another purpose for considering thermal habitats is to protect Common Snook during the coldest days in winter by ensuring that the favorite thermal habitats for Common Snook in the estuary won't be significantly reduced because of an SGD reduction. Stevens et al. (2016)

suggested the importance of the warm water sources to Common Snook during the coldest days of the winter in coastal estuaries. According to studies conducted by Schafland and Foote (1983) and Blewett and Stevens (2014), Common Snook need 15 ºC or warmer to survive during winter. There were documented evidence of Common Snook die off during severe cold fronts in the region. As such, this study calculated water volumes and surface areas of ≥ 15 ºC in the Chassahowitzka River for all the scenario runs. Unlike the thermal habitat calculation for manatees, no warm water layer thickness restriction was used in the calculation.

As water warmer than 15 ºC appears to be a threshold for Common Snook, measured water temperature data during the simulation period for the scenario runs were analyzed to find out the starting and ending times when water temperature was below 15 ºC for each winter. Table 25 shows these starting and ending time points. If we call the time span from the time point when the first < 15 ºC water temperature was recorded to the time point when the last < 15 ºC water temperature was recorded a Common Snook season for the winter, then the duration of the Common Snook season can vary quite significantly, from only 53.36 days to 149.10 days for the estuary, during the 123-month simulation period. We name this kind of variable duration from one winter to the next winter the varying Common Snook season.

Table 25. Starting and ending time points when water temperature in Chassahowitzka dropped to below 15 ºC during each winter of the scenario simulation period.

Season	Starting Time	Ending Time	Duration (Days)
1	12/17/07 9:30	3/9/08 15:00	83.23
2	10/30/08 6:45	3/5/09 17:15	126.44
3	11/29/09 3:45	3/9/10 12:15	100.35
4	11/7/10 6:30	2/15/11 11:45	100.22
5	12/8/11 9:00	2/15/12 10:30	69.06
6	10/30/12 7:15	3/28/13 9:45	149.10
7	11/28/13 4:45	3/8/14 10:45	100.25
8	11/19/14 2:30	2/22/15 14:15	95.49
9	1/5/16 23:15	2/28/16 8:00	53.36
10	12/10/16 8:30	3/17/17 9:15	97.03
11	12/10/17 3:45	2/3/18 9:45	55.25

Table 26 shows percentage reductions of ≥ 15 ºC thermal habitats for all scenario runs during the 11 varying Common Snook seasons of the 123-month simulation period. The most sensitive Common Snook season to SGD reduction was during 11/29/09 3:45 – 3/9/10 12:15 and the percentage reduction results of ≥ 15 ºC water volume and surface area during this period are also included in the table. It can be seen that as the SGD reduction increases, both ≥ 15 ºC volume and ≥ 15 ºC surface area decrease linearly with the SGD. With a 30% reduction of SGD, ≥ 15 ºC volume and ≥ 15 ºC surface area are reduced by 5.44% and 5.61%, respectively during the most sensitive varying Common Snook season.

Table 26. Percentage reductions of ≥ 15 ºC water volume and surface area for all the 11 varying Common Snook seasons and for most sensitive season during 11/29/09 3:45 – 3/9/10 12:15.

Scenario	Volume Reduction	Surface Area Reduction	Volume Reduction	Surface Area Reduction
	All 11 Varying Common Snook Seasons		*11/29/09 3:45 – 3/9/10 12:15*	
Existing	0.08%	0.07%	0.21%	0.20%
2.5%	0.14%	0.12%	0.37%	0.36%
5.0%	0.28%	0.26%	0.77%	0.75%
7.5%	0.44%	0.40%	1.17%	1.12%
10.0%	0.60%	0.55%	1.56%	1.51%
12.5%	0.76%	0.71%	1.98%	1.92%
15.0%	0.93%	0.88%	2.42%	2.37%
17.5%	1.12%	1.07%	2.87%	2.83%
20.0%	1.32%	1.28%	3.34%	3.33%
22.5%	1.52%	1.50%	3.84%	3.85%
25.0%	1.74%	1.74%	4.36%	4.42%
27.5%	1.97%	1.99%	4.90%	5.01%
30.0%	2.21%	2.25%	5.44%	5.61%

Alternatively, one may define a snook season as a fixed duration for all the years, simply using the period from the earliest calendar day when < 15 ºC occurred to the latest calendar day when < 15 ºC occurred for all the winters. From Table 25, the earliest such day was October 30 in both 2008 and 2012, while the latest such day was March 28 in 2013. Therefore, the fixed snook season would be a 150-day (or 151-day if a leap year is involved) period from October 30 of the current year to March 28 of the next year. Table 27 shows results of the percentage reduction of ≥ 15 ºC thermal habitats for all scenario runs during the 11 fixed Common Snook seasons. The most sensitive Common Snook season to the SGD reduction was during 10/30/2009 – 3/28/2010, which was the same winter for the varying Common Snook season (Table 26). Results of the percentage reduction of ≥ 15 ºC water volume and surface area during this period are also included in the table. As expected, a 15% reduction of the seasonally averaged thermal habitats also did not occur, even when the SGD was reduced by 30% during the most sensitive Common Snook season.

Table 27. Percentage reductions of ≥ 15 ºC water volume and surface area for all the 11 fixed Common Snook seasons and for most sensitive fixed season during 10/30/2009 – 3/28/2010.

Scenario	Volume Reduction	Surface Area Reduction	Volume Reduction	Surface Area Reduction
	All Seasons		*10/30/2009 – 3/28/2010*	
Existing	0.04%	0.04%	0.11%	0.10%
2.5%	0.08%	0.07%	0.20%	0.19%
5.0%	0.16%	0.14%	0.41%	0.41%
7.5%	0.25%	0.22%	0.62%	0.60%
10.0%	0.35%	0.31%	0.83%	0.81%
12.5%	0.44%	0.40%	1.06%	1.04%
15.0%	0.55%	0.51%	1.30%	1.29%
17.5%	0.66%	0.62%	1.55%	1.55%
20.0%	0.78%	0.75%	1.81%	1.83%
22.5%	0.90%	0.88%	2.08%	2.12%
25.0%	1.03%	1.02%	2.36%	2.44%
27.5%	1.17%	1.18%	2.66%	2.78%
30.0%	1.32%	1.34%	2.96%	3.11%

The main differences between Tables 26 and 27 came from the fact that a fixed Common Snook season has more days than a varying Common Snook season. As a result, more noncold days with water temperature ≥ 15 ºC were included in the former than in the later. Excluding these noncold days from the calculation will make the calculated average thermal habitats more sensitive to the SGD reduction. It was found that there were 406 cold days with water temperature below 15 ºC at one measurement station or more in the Chassahowitzka River. Many cold days occurred consecutively, making 83 cold-day blocks out of the 406 cold days.

Table 28 shows results of percentage reduction of ≥ 15 ºC water volume and surface area for all 83 cold day blocks, (same as those for all 406 cold days), the most sensitive cold-day block, and the most sensitive single cold day during the 123-month scenario simulation period. It can be seen from the table that average ≥ 15 ºC water volume and surface during all the 406 cold days would not be reduced by 15%, even with a 30% SGD reduction; however, during the cold-day block of 12/10/2017 – 12/15/2017, an 18.51% SGD reduction would trigger a 15% reduction of ≥ 15 ºC water volume in the Chassahowitzka River, while a 21.37% reduction of SGD would cause a 15% reduction of ≥ 15 ºC surface area. If we look at the most sensitive single cold day to the SGD reduction, on 1/4/2014 an 8.47% SGD reduction would cause a 15% reduction of ≥ 15 ºC water volume and on 12/16/2014 a 11.38% SGD reduction would reduce ≥ 15 ºC surface area by 15%.

Table 28. Percentage reductions of ≥ 15 ºC water volume and surface area for all 82 cold day blocks (or 401 cold days), the most sensitive cold-day block, and the most sensitive single cold day during the 123-month scenario simulation period.

Scenario	Volume Reduction	Surface Area Reduction	Volume Reduction	Surface Area Reduction	Volume Reduction	Surface Area
	All <15 ºC Days		Cold-Day Block: 12/10/2017 – 12/15/2017		Single Cold Day:	
					1/4/2014	12/16/20
Existing	0.30%	0.24%	1.11%	1.02%	5.49%	6.36%
2.5%	0.53%	0.43%	1.96%	1.92%	6.74%	7.52%
5.0%	1.08%	0.91%	3.86%	3.65%	12.98%	14.92%
7.5%	1.67%	1.40%	5.86%	5.48%	20.84%	22.37%
10.0%	2.26%	1.91%	7.84%	7.31%	28.93%	30.26%
12.5%	2.87%	2.46%	9.87%	9.09%	39.47%	41.10%
15.0%	3.51%	3.05%	12.02%	10.69%	45.39%	46.77%
17.5%	4.20%	3.68%	14.15%	12.24%	46.66%	48.51%
20.0%	4.92%	4.37%	16.24%	13.99%	47.51%	49.89%
22.5%	5.67%	5.09%	18.29%	15.83%	48.21%	50.04%
25.0%	6.48%	5.87%	20.35%	17.75%	48.72%	50.33%
27.5%	7.31%	6.70%	22.51%	19.90%	49.26%	50.61%
30.0%	8.16%	7.57%	24.53%	22.06%	49.45%	50.76%
Trigger			***18.51%***	***21.37%***	***5.64%***	***5.03%***

4.5 A Summary of Model Results of Scenario Runs

As described above, the percentages of flow reduction that would trigger a 15% reduction of salinity and thermal habitats in the Chassahowitzka River have been obtained through a series of model simulations for various flow reduction scenarios. Table 29 is a summary of the triggering percentages of the flow reduction that would cause significant harms to the Chassahowitzka River system.

From Table 29, it can be seen that except for salinity ≤ 1 psu, salinity volume is generally more sensitive to flow reduction than salinity bottom area, which is more sensitive to flow reduction than salinity shoreline length. The 15% reduction threshold is only crossed for salinity habitats of 5 psu or below with a flow reduction of 30% or less. The most sensitive salinity habitat to flow reduction is ≤ 1 psu bottom area, which is reduced 15% with a 7.75% SGD reduction.

The acute condition for manatee is more sensitive than the chronic condition for manatees to the SGD reduction in the Chassahowitzka River. The most sensitive thermal habitat is the 4-hour average of ≥ 15 ºC surface area, which can be reduced by 15% with a 10.10% reduction of

SGD when this thermal habitat is low. The most sensitive Common Snook thermal habitat is ≥ 15 ºC water volume during a single cold day. With an 8.47% reduction of the SGD, the daily ≥ 15 ºC water volume could drop 15%.

Table 29. A summary of the percentage flow reduction that would cause 15% reductions of salinity and thermal habitats in the Chassahowitzka River.

	Salinity Habitats					
Salinity (psu) ≤	*1*	*2*	*3*	*5*	*10*	*15*
Volume	8.31%	21.55%	22.82%	22.65%	>30%	>30%
Bottom Area	7.75%	23.67%	26.07%	24.56%	>30%	>30%
Shoreline Length	11.08%	>30%	>30%	27.60%	>30%	>30%
	Manatee Thermal Habitats					
Thermal Conditions	*Chronic*			*Acute*		
Volume	23.87%			11.75%		
Surface Area	24.33%			10.10%		
	Common Snook Thermal Habitats					
Thermal Conditions	*Cold-Day Block*			*Single Cold Day*		
Volume	18.51%			8.47%		
Surface Area	21.37%			11.38%		

5. Effects of Sea Level Rises

Because the analysis of effects of the SGD reduction on salinity and thermal habitats in the previous section used measured data collected during the previous 10.25 years, it is possible that the proposed MFL may not be valid if the hydrological, meteorological, and other physical conditions which affect salinity and thermal habitats in the Chassahowitzka River differ significantly from those during the 10.25-year simulation period. One of the physical conditions that are expected to be change and could alter the salinity and thermal characteristics in the estuary is the sea level rise caused by global warming. It is meaningful to see if the proposed MFL still holds a number of years later, when a SLR relative to the average sea level during the 10.25-year simulation period occurs.

This section describes how sea level rises are considered in the hydrodynamic modeling of the Chassahowitzka River and how SLRs would affect salinity and thermal habitat in the spring-fed estuary. As the objective is to verify the proposed MFL with a SLR in the future, the LAMFE model for the Chassahowitzka River was run for both the BSL condition with a SLR and the proposed MFL condition with the same SLR. Simulated salinity and thermal habitats between the two model runs were compared to check if the 15% habitat reduction criterion would be violated by the proposed MFL with the SLR.

5.1 Sea Level Rise Estimates

To be consistent with the SWFWMD's regional water supply planning horizon, sea level conditions in 2035 are evaluated. The United States Army Corps of Engineers (USACE) provides SLR estimates at their web site, http://www.corpsclimate.us/ccaceslcurves.cfm, where three types of the SLR can be obtained at several NOAA stations along the Florida Gulf coast: a low estimate, an intermediate estimate, and a high estimate. The closest NOASS stations to the mouth of the Chassahowitzka River are #8726724 (Clearwater Beach FL) and #8727520 (Cedar Key FL), with the Clearwater Beach station being about 81,693 m south - southwest of mouth of the Chassahowitzka River and the Cedar Key station about 61,996 m northwest of the mouth of the Chassahowitzka River, respectively. The St. Petersburg station is further south from the mouth of the Chassahowitzka River with a distance of about 103,794 m but has a longer period of record of water level data than the Clearwater Beach station does. As such, the St. Petersburg station is considered as a better station for the SLR estimation than the Clearwater Beach station. Based on this consideration, the low, intermediate, and high sea level rise estimates at the mouth of the Chassahowitzka River in 2035 were calculated from those at the St. Petersburg and Cedar Key stations using an inverse distance weighting method.

Table 30 lists the low, intermediate, and high SLRs from 2012 to 2015 at the NOAA St. Petersburg and Cedar Key stations as well as at the mouth of Chassahowitzka River. Because 2012 is the middle year of the scenario simulation period, during which there was also sea level rise, adding the same sea level rise estimates to the water level data at the mouth of the Chassahowitzka River during the 123 months of the simulation period is reasonable.

Table 30. Sea level rise estimates at NOAA St. Petersburg and Cedar Key stations as well as the mouth of the Chassahowitzka River. SLRs at the St. Petersburg and Cedar Key stations were obtained from a USACE website, while SLRs at the mouth of the Chassahowitzka River were estimated based on those at the former two stations.

	NOAA Station		***Estimated for***
	St. Petersburg	***Cedar Key***	***Chassahowitzka Mouth***
Low SLR (cm)	5.791	4.267	4.837
Intermediate SLR (cm)	10.058	7.925	8.723
High SLR (cm)	22.250	20.422	21.105

5.2 Model Results for SLR Scenarios

In the SLR model runs, 4.837, 8.723, and 21.105 cm were added to the water level data measured at the open boundaries for the entire 123-month simulation period for the low, intermediate and high SLR estimates, respectively. The added layer of water is assumed to have the same salinity and temperature values as measured top-layer salinity and temperature during the simulation period. The modified boundary conditions at these open boundaries were used to drive the model to simulate effects of low, intermediate, and high SLR estimates on salinity and temperature distributions in the system. The added SLR not only increases the average depth of the estuary and thereby the volume of the estuary, but also causes more Gulf water to be transported to the system.

It should be acknowledged that the above treatment of the SLR in the model is far from perfect when considering its effects on hydrodynamics and salinity and thermal transport processes in the Chassahowitzka River, because a SLR could modify several factors controlling physical processes in the estuary. For example, the rainfall pattern in the region could be altered by the SLR, the salinity and temperature characteristics in the Gulf could be quite different with or without a SLR, and the potentiometric surface in the coastal region could be pushed upward by a SLR. Because of the SLR, SGDs to the Chassahowitzka River system would likely be reduced to a certain degree. Clearly, our treatment only considered the direct effect of the SLR on the estuary and didn't consider other consequences caused by the SLR, which are virtually unknown to us because of the lack of data or research on the topics for the region.

The SLR runs were conducted for the BSL scenario and the MFL (8% reduction from the BSL) scenario. Model results for these runs are presented and discussed below. For simplicity, time series plots of daily means of simulated salinity habitats similar to Figs. 21 & 22 are omitted here, and only the CDF plots of simulated salinity habitats for various flow reductions are presented in the following discussion. For thermal habitats, time series plots water volumes and surface areas of < 15 ºC, ≥15 ºC , and ≥ 20 ºC are omitted and time series plots of 72-hour and 4-hour moving average similar to Figs. 28 & 29 are also omitted here.

5.2.1 Salinity Habitats

Cumulative distribution functions for water volumes, bottom areas, and shoreline lengths are depicted in Figs. 31, 32, and 33, respectively for salinity ≤ 1, 2, 3, 5, 10, and 15 psu for the BSL condition and for BSL with SLRs (high, intermediate, and low estimates). It can be seen from these figures that the shape of CDFs has been greatly modified by SLR. For salinity volumes, CDF curves of ≤ 1, 2, 3, and 5 psu all shift to the left, while CDF curves of ≤ 10 psu and 15 psu shift to the right. As mentioned before, the area between the *y*-axis and the CDF curve numerically represents the average value of the variable for the given sample used to generate the CDF curve. From Figure 31, it can be seen that average water volumes for salinity ≤ 2, 3, and 5 psu are all reduced with the increase of the SLR. However, ≤ 10 and 15 psu salinity volumes increase as a result of the SLR.

For salinity bottom areas, CDF curves of ≤ 1, 2, 3, and 5 psu all shift to the left, while CDF curves of ≤ 15 psu shift to the right. CDF curves of ≤ 10 psu shift to the left when ≤ 10 psu bottom areas are low but to the right when ≤ 10 psu bottom areas are high. For shoreline lengths, CDF curves all shift to the left, with ≤ 15 psu shoreline length CDFs being almost no change with different SLRs.

CFDs for water volumes, bottom areas, and shoreline lengths for salinity ≤ 1, 2, 3, 5, 10, and 15 psu for the MFL condition and for MFL with SLRs (high, intermediate, and low estimates) are plotted in Figures 34 - 36, which clearly demonstrate effects of high, intermediate, and low SLRs on CDFs of water volumes, bottom areas, and shoreline lengths of different salinity ranges under a 8% flow reduction condition. Comparing Figs. 34, 35, and 36 with Figs. 31, 32, and 33, respectively, it can be seen that the SLR has the similar effects on CDFs of various salinity habitats under the MFL flow condition as on those under the BSL condition. The biggest relative volume, bottom area, or shoreline length reduction occurs for low salinity ranges such ≤ 1, 2, or 3 psu in the Chassahowitzka River.

As Figures 31 - 33 and Figures 34 - 36 demonstrate SLR effects on salinity habitats for both the BSL condition and the MFL condition, it is more desirable to see the MFL effects on various salinity habitats for the three SLRs. Figures 37 - 39 show comparisons of CDFs of water volume, bottom area, and shoreline length, respectively for salinity ≤ 1, 2, 3, 5, 10, and 15 psu under BSL condition with those under the MFL condition, with the high, intermediate, and low SLRs being added to the downstream open boundary of the Chassahowitzka River. In these figures, the black solid and dashed lines are respectively for BSL and MFL conditions with a high SLR estimate. The red solid and dashed lines are respectively for BSL and MFL conditions with an intermediate SLR, while the blue solid and dashed lines are respectively for BSL and MFL conditions with a low SLR. It can be seen from Figures 37 - 39 that MFL has relatively large effects on low salinity habitats when a SLR is considered.

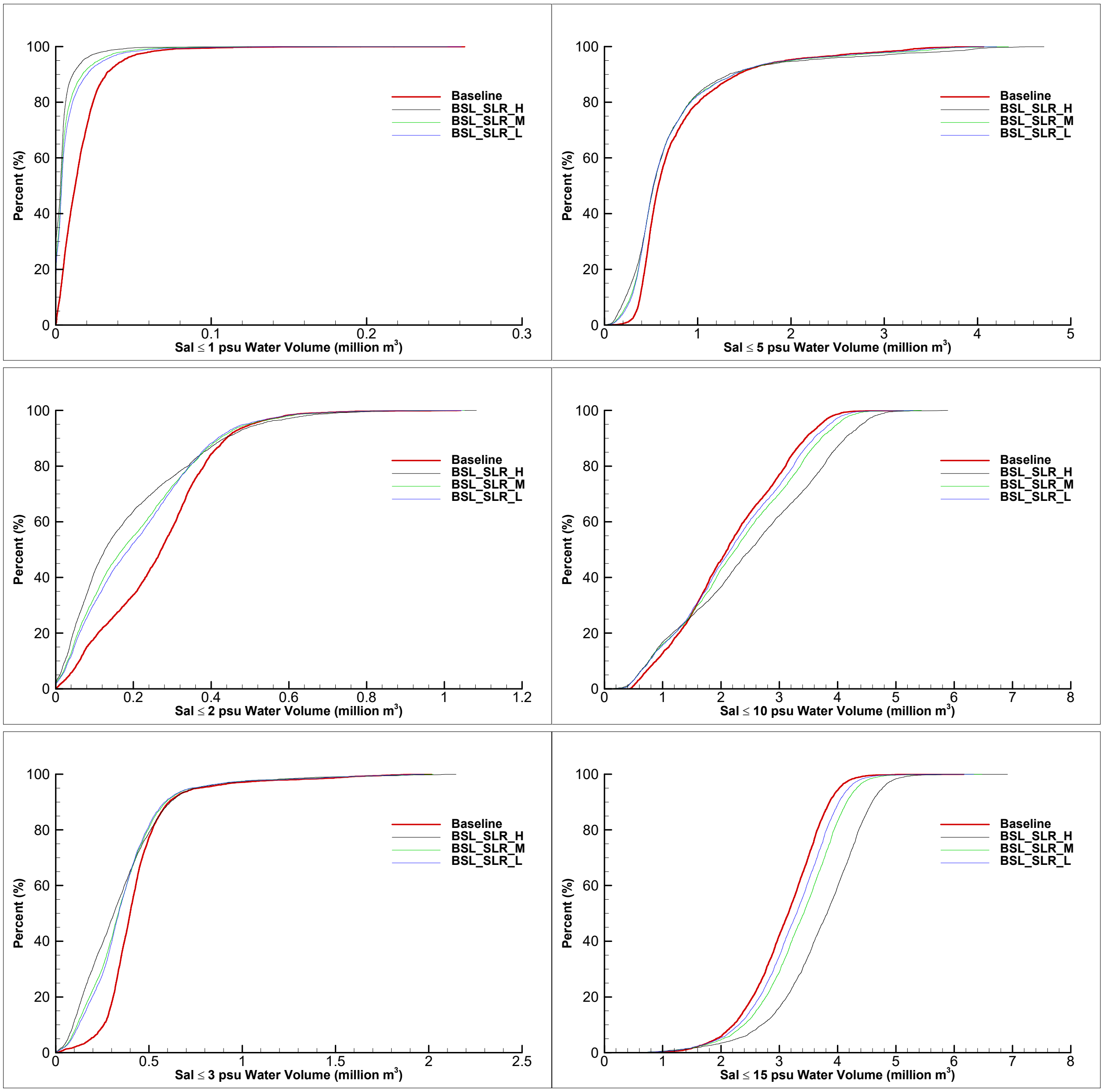

Figure 31. CDFs of water volume for salinity ≤ 1, 2, 3, 5, 10, and 15 psu for the BSL condition (red lines) and for the BSL with the high SLR (black lines), the intermediate SLR (green lines), and low SLR (blue lines) in the Chassahowitzka River.

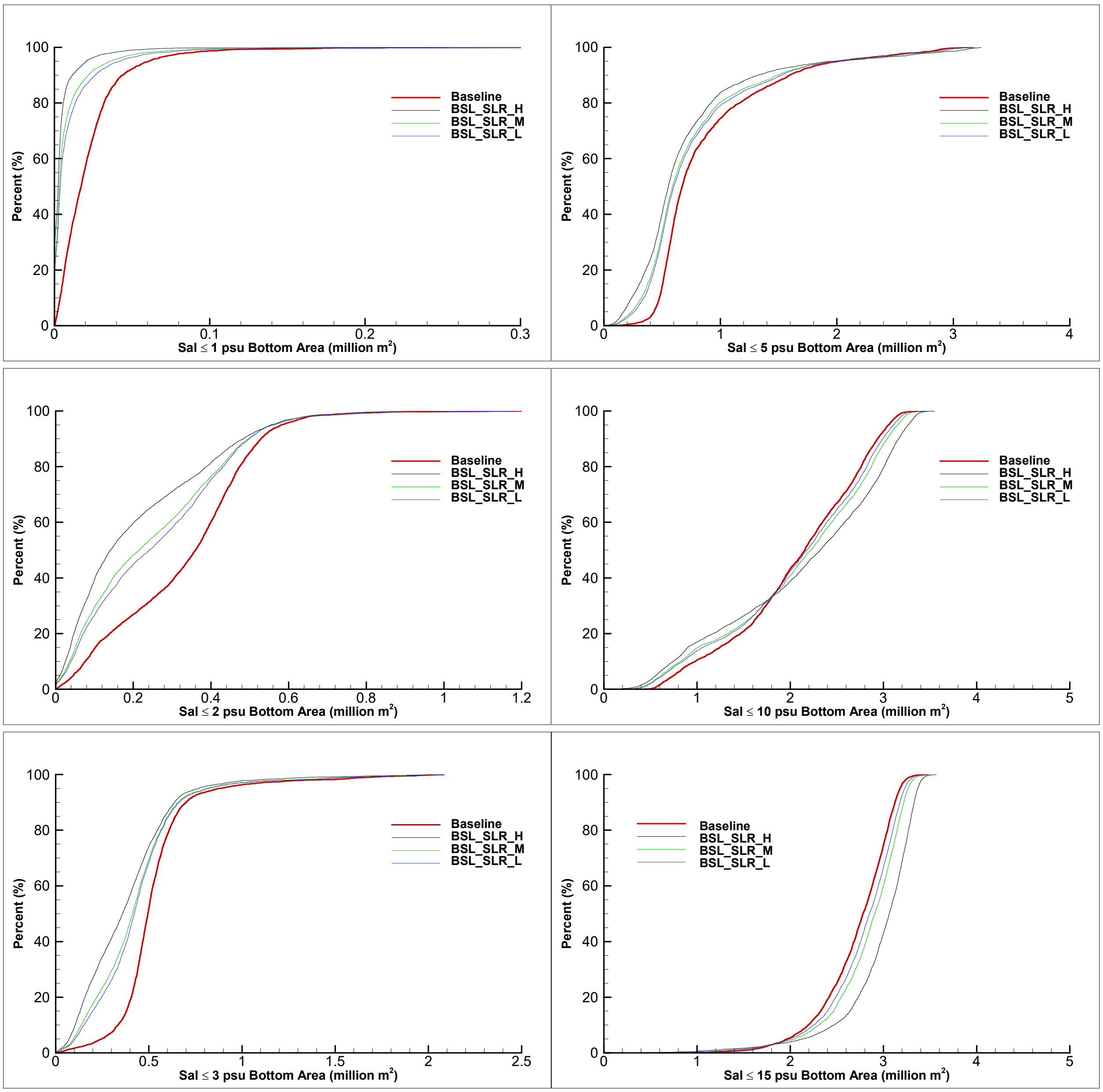

Figure 32. CDFs of bottom areas for salinity ≤ 1, 2, 3, 5, 10, and 15 psu for the BSL condition (red lines) and for the BSL with the high SLR (black lines), the intermediate SLR (green lines), and low SLR (blue lines) in the Chassahowitzka River.

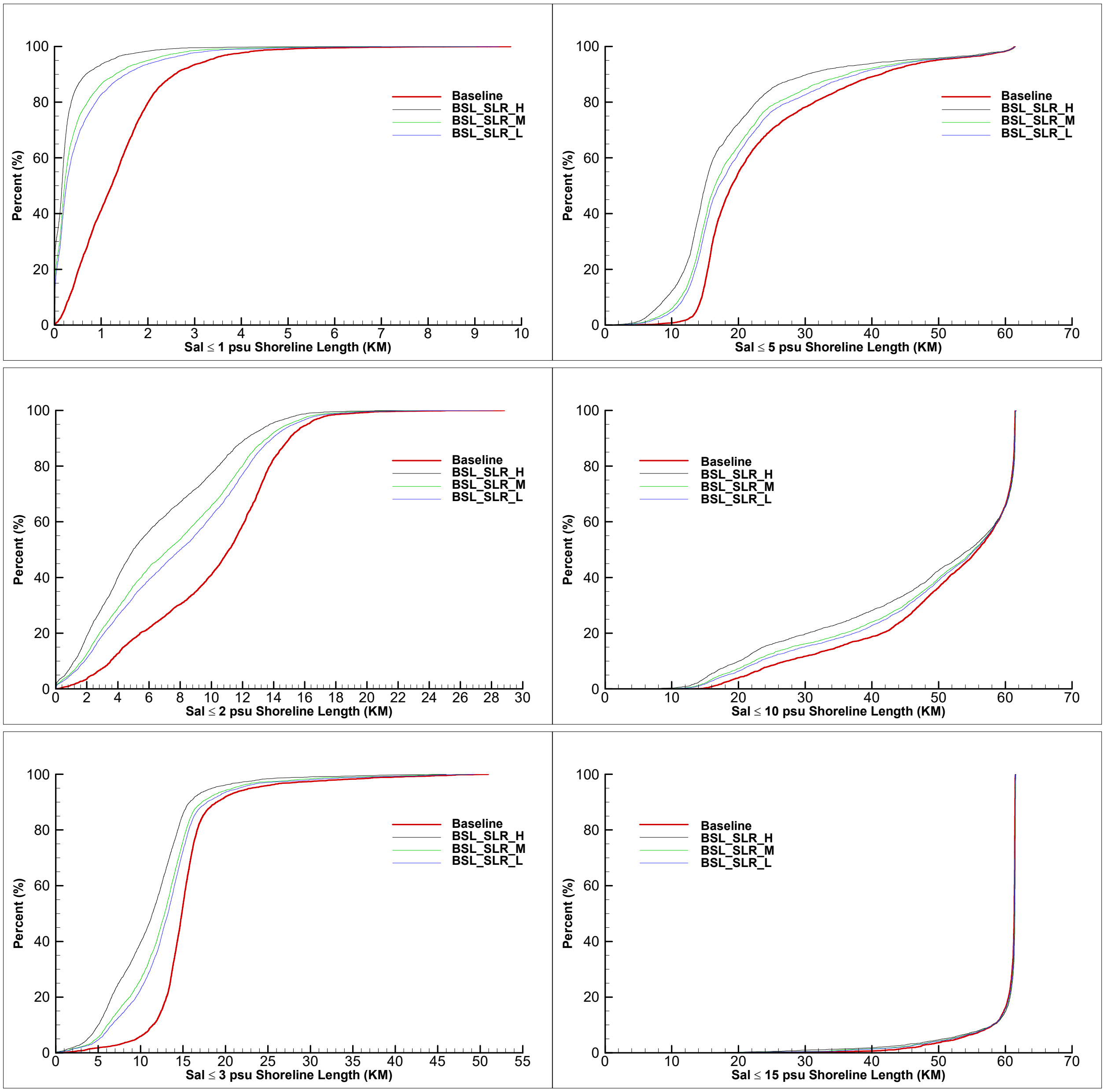

Figure 33. CDFs of shoreline length for salinity ≤ 1, 2, 3, 5, 10, and 15 psu for the BSL condition (red lines) and for the BSL with the high SLR (black lines), the intermediate SLR (green lines), and low SLR (blue lines) in the Chassahowitzka River.

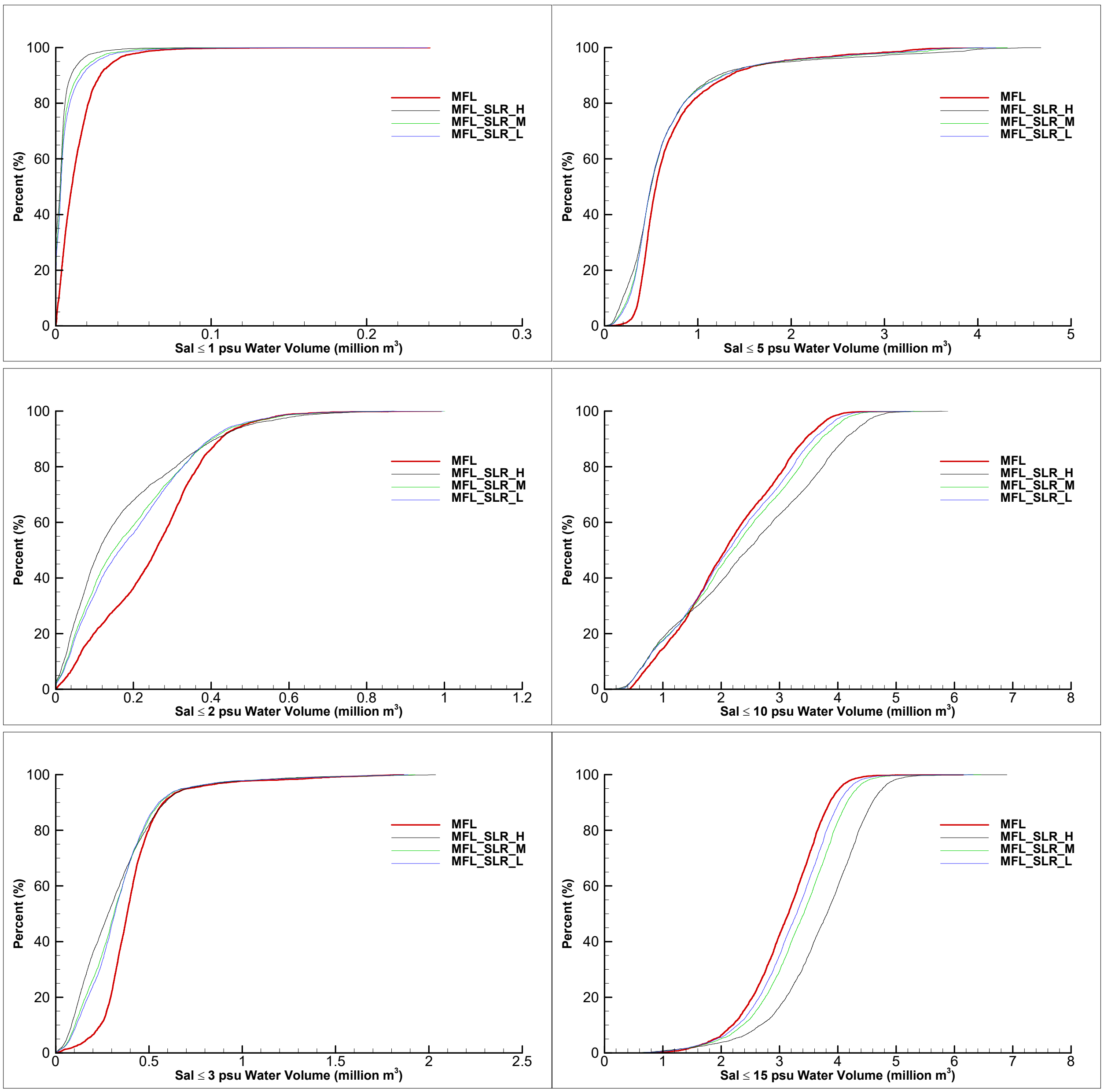

Figure 34. CDFs of water volume for salinity ≤ 1, 2, 3, 5, 10, and 15 psu for the MFL flow condition (red lines) and for MFL with high SLR (black lines), the intermediate SLR (green lines), and low SLR (blue lines) in the Chassahowitzka River.

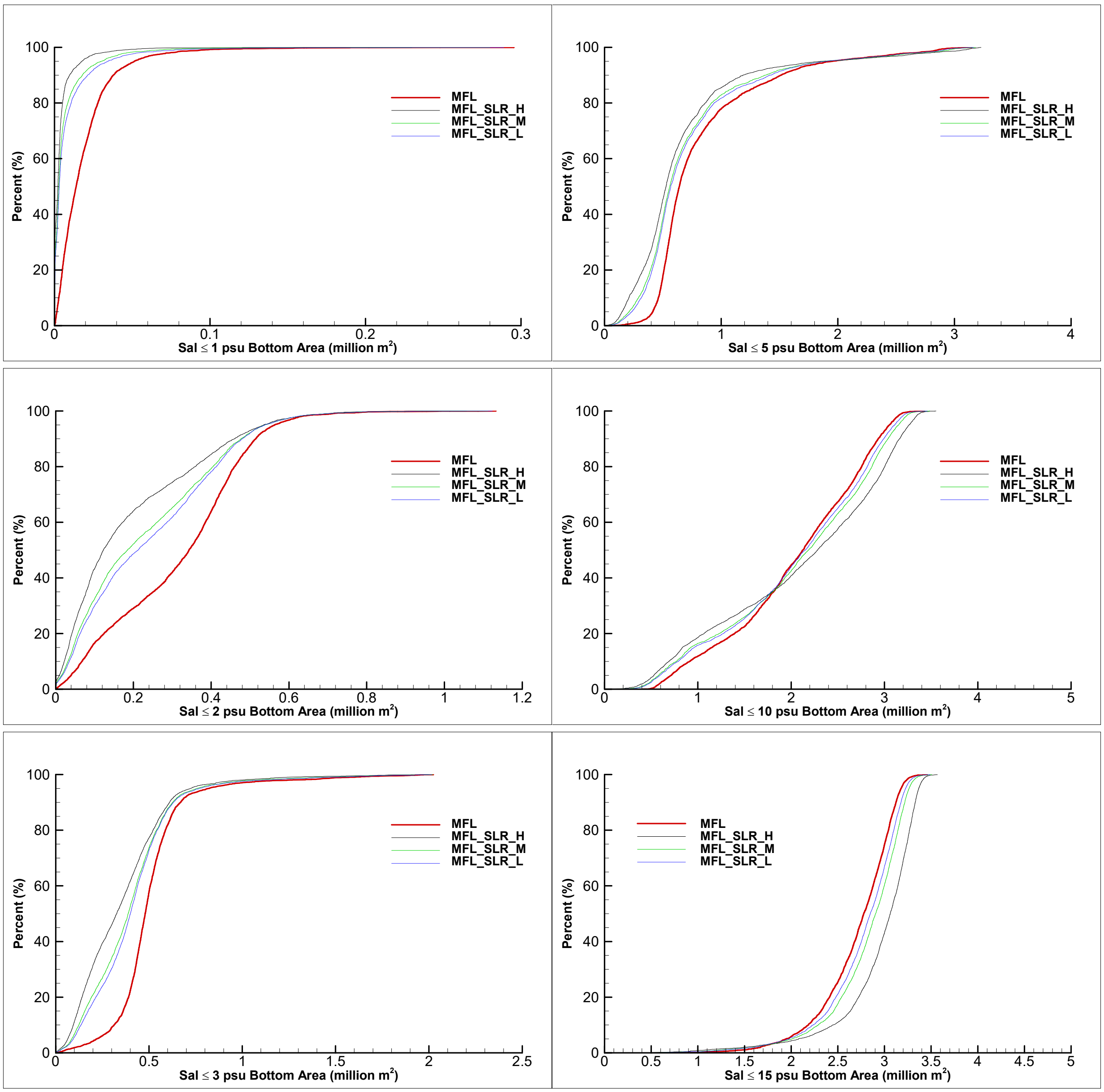

Figure 35. CDFs of bottom area for salinity ≤ 1, 2, 3, 5, 10, and 15 psu for the MFL flow condition (red lines) and for MFL with high SLR (black lines), the intermediate SLR (green lines), and low SLR (blue lines) in the Chassahowitzka River.

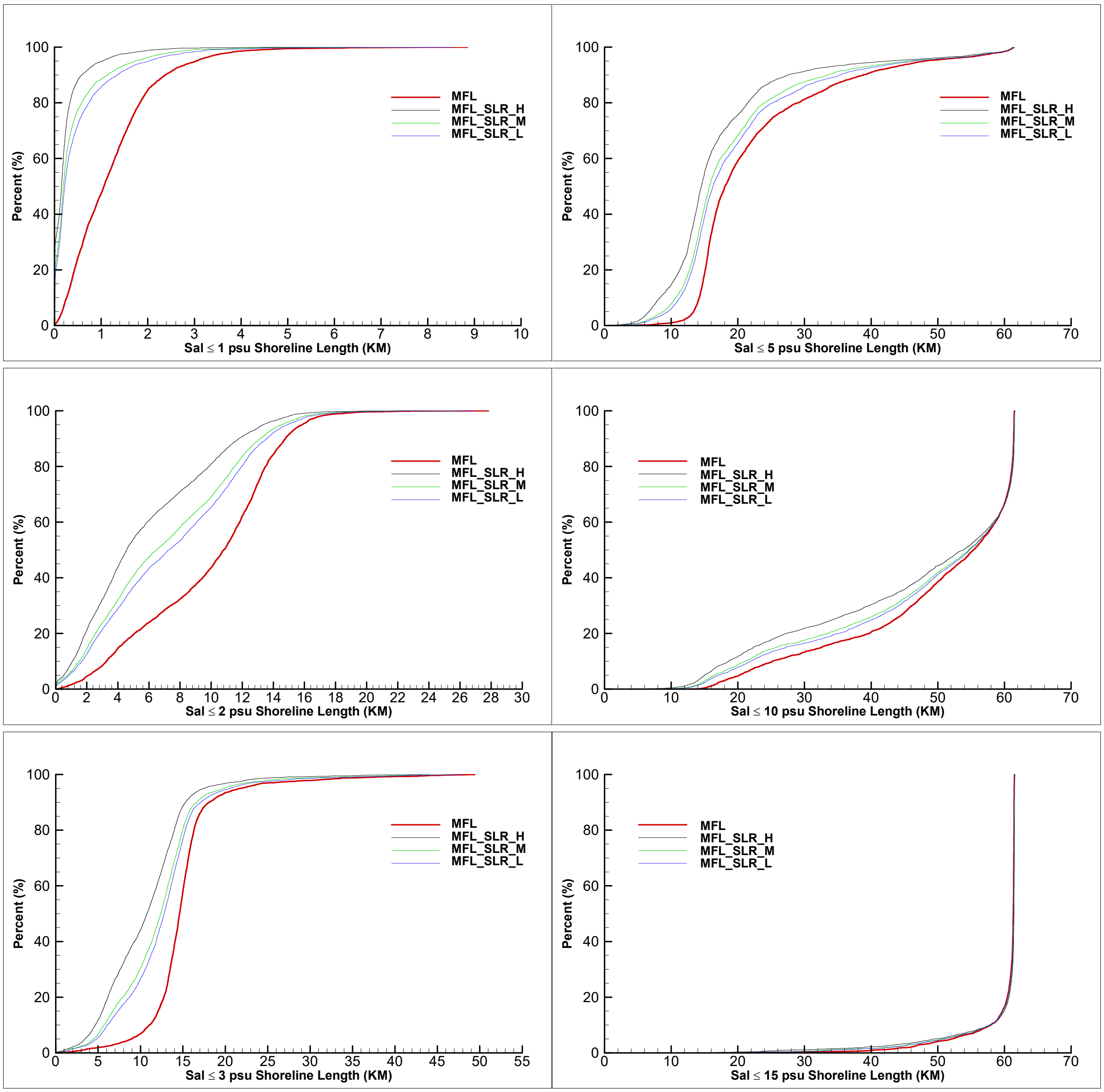

Figure 36. CDFs of shoreline length for salinity ≤ 1, 2, 3, 5, 10, and 15 psu for the MFL flow condition (red lines) and for MFL with high SLR (black lines), the intermediate SLR (green lines), and low SLR (blue lines) in the Chassahowitzka River.

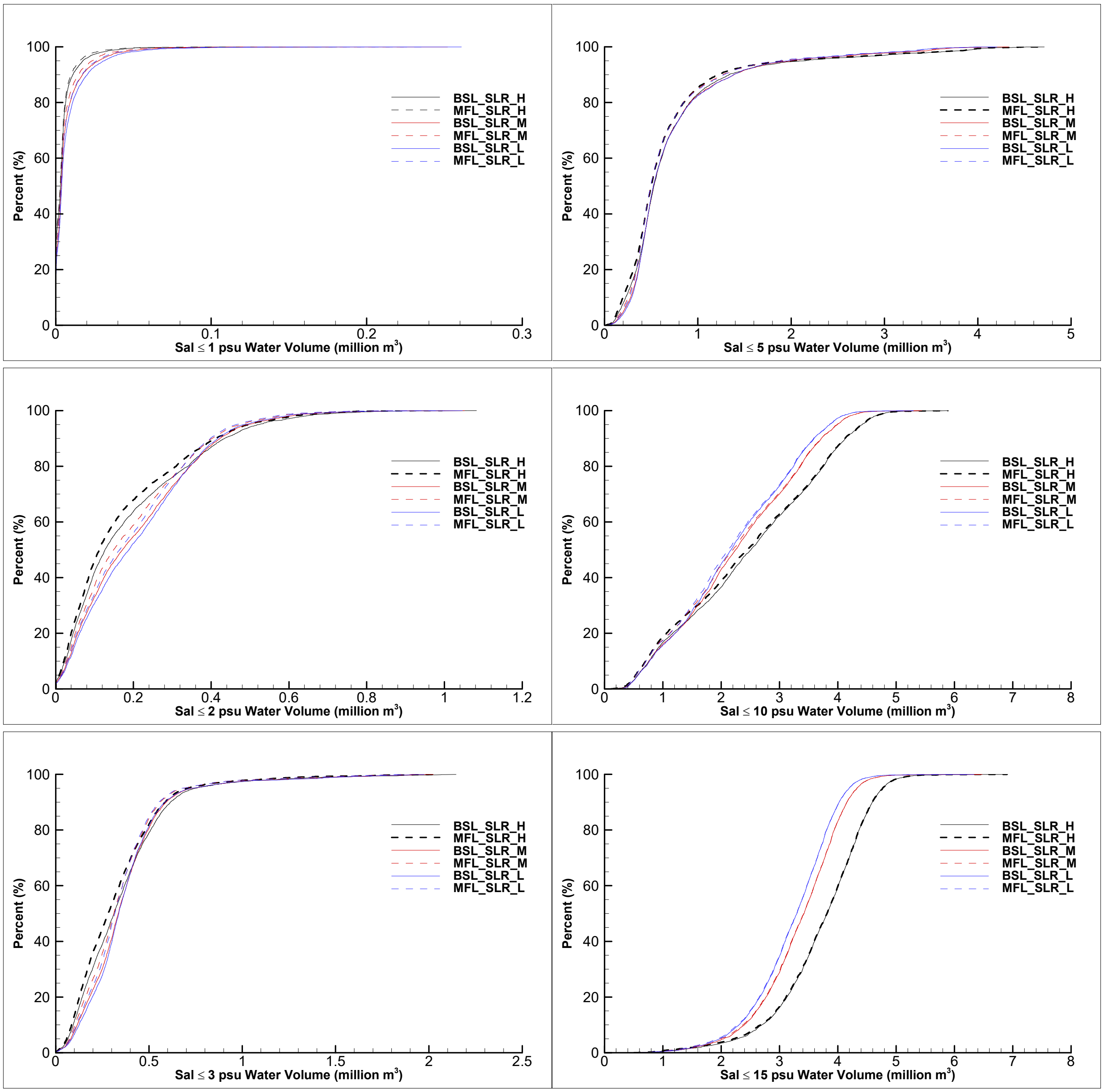

Figure 37. Comparisons of CDFs of water volume for salinity ≤ 1, 2, 3, 5, 10, and 15 psu under BSL condition (solid lines) with those under the MFL condition (dashed lines). High (black), intermediate (red), and low (blue) SLRs were added to the downstream open boundary of the Chassahowitzka River.

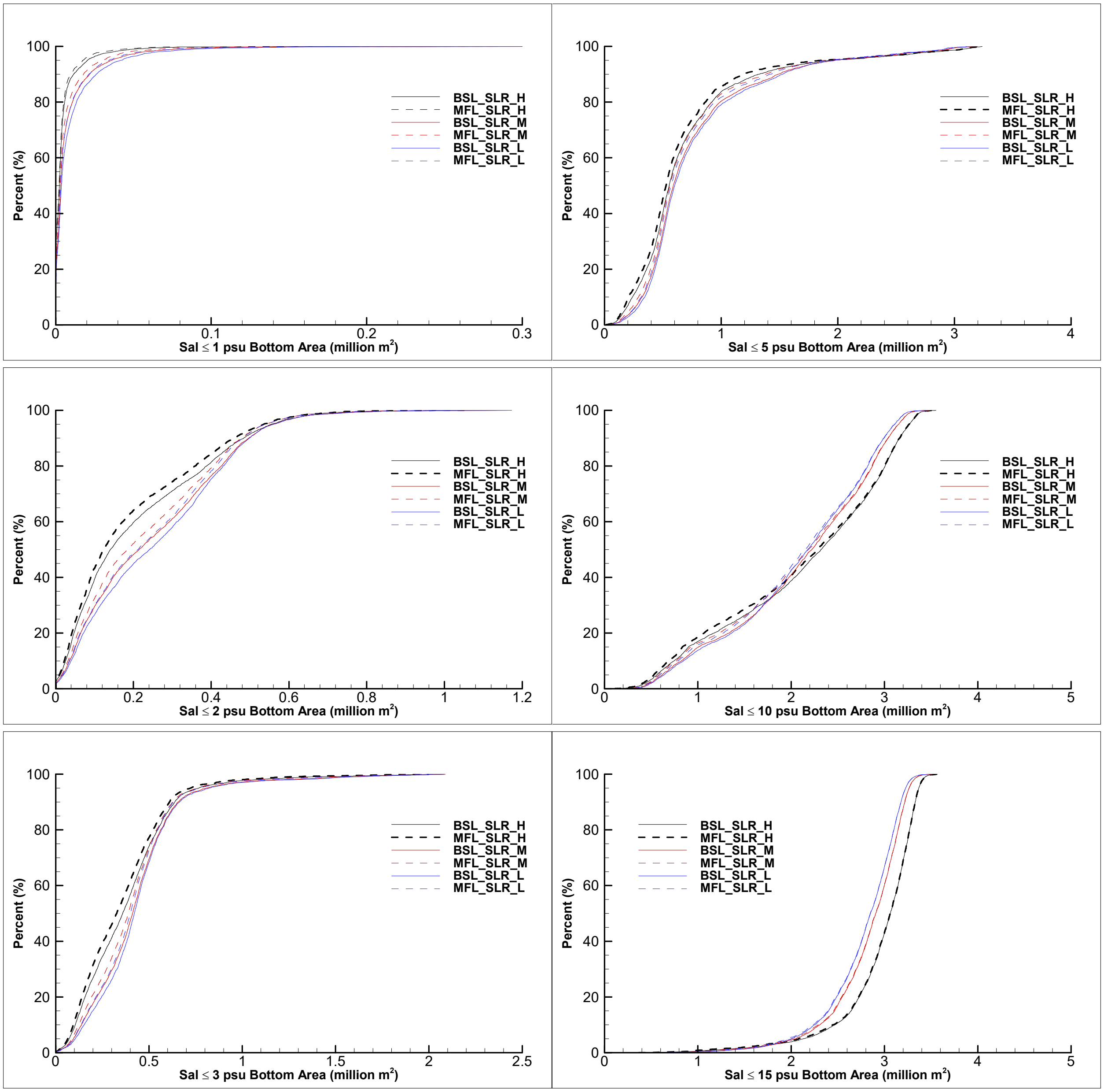

Figure 38. Comparisons of CDFs of bottom area for salinity ≤ 1, 2, 3, 5, 10, and 15 psu under BSL condition (solid lines) with those under the MFL condition (dashed lines). High (black), intermediate (red), and low (blue) SLRs were added to the downstream open boundary of the Chassahowitzka River.

Table 31 shows model results of water volume, bottom area, and shoreline length for salinity ≤ 1, 2, 3, 5, 10, and 15 psu under the BSL condition, BSL with high SLR, BSL with intermediate SLR, BSL with low SLR, MFL, MFL with high SLR, MFL with intermediate SLR, and MFL with low SLR in the Chassahowitzka River. The units for water volume, bottom area, and shoreline length results in the table are respectively million cubic meter, million square meters, and kilometers. The percentage reductions of water volume, bottom area, shoreline length caused by the MFL for the four SLR conditions (no SLR consideration is considered as 0 SLR, or SLR #0) are shown in Table 32.

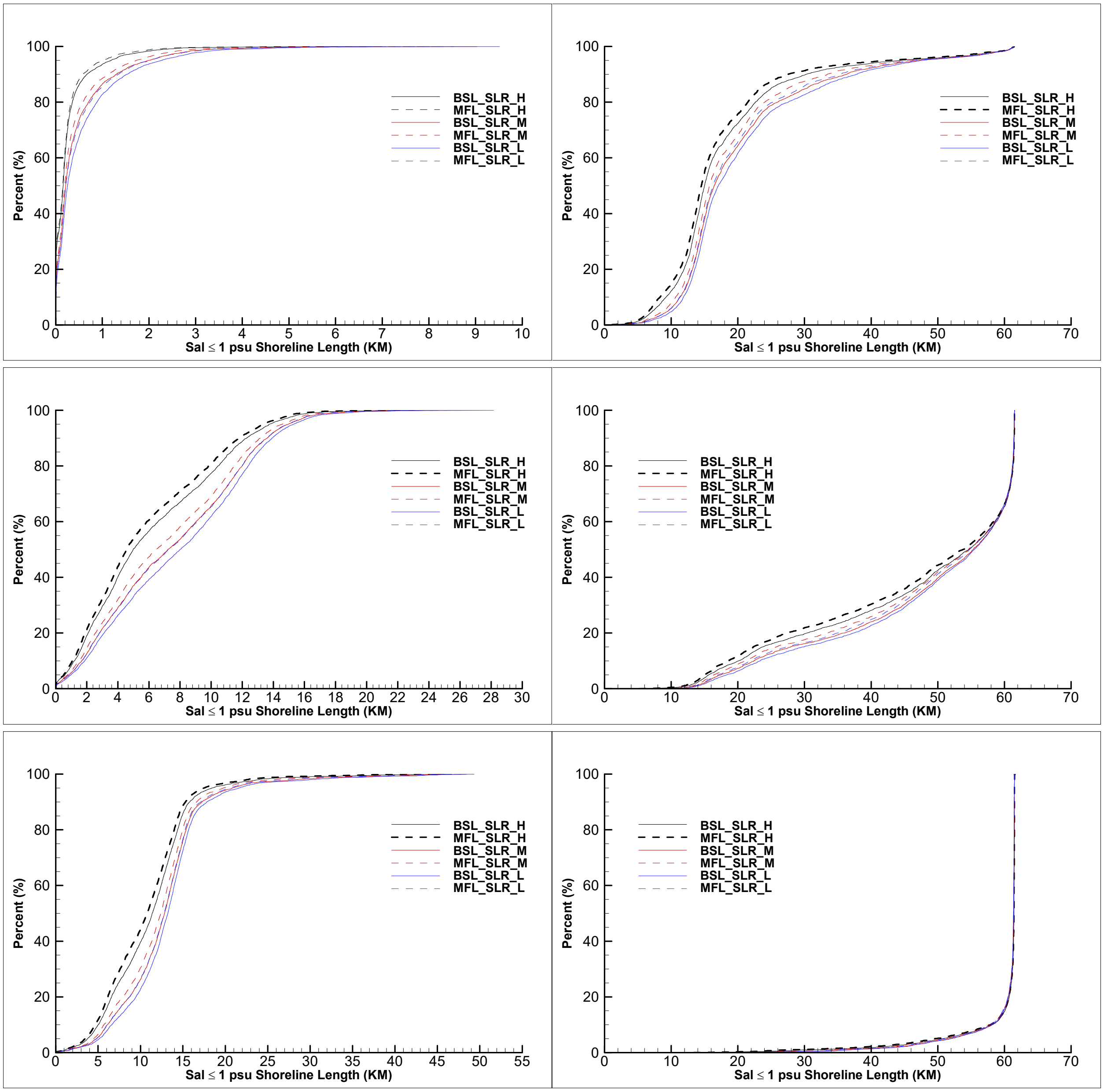

Figure 39. Comparisons of CDFs of shoreline length for salinity ≤ 1, 2, 3, 5, 10, and 15 psu under BSL condition (solid lines) with those under the MFL condition (dashed lines). High (black), intermediate (red), and low (blue) SLRs were added to the downstream open boundary of the Chassahowitzka River.

Table 32 shows that the biggest relative reduction of water volume caused by the MFL is 15.72%, for salinity ≤ 1 psu and with the low SLR. For bottom areas and shoreline length, the biggest relative reductions caused by the MFL are 18.49% and 14.06%, respectively, and occur for salinity ≤ 1 psu and with the low SLR, too. With all three SLRs, MFL- caused reductions of ≤

1 psu habitats are higher than those of ≤ 2 psu habitats, which are higher than ≤ 3 psu habitats, and so on. Table 32 clearly shows that the proposed MFL for the Chassahowitzka River cannot guarantee that ≤ 1 psu volume and bottom area in the river won't lose more than 15% with the consideration of intermediate and low SLRs.

Table 31. Water volumes, bottom areas, and shoreline lengths for salinity ≤ 1, 2, 3, 5, 10, and 15 psu under BSL condition, BSL with high SLR, BSL with intermediate SLR, BSL with low SLR, MFL, MFL with high SLR, MFL with intermediate SLR, and MFL with low SLR in the Chassahowitzka River.

Salinity (psu) ≤	**1**	**2**	**3**	**5**	**10**	**15**
	Water Volume (10^6 m^3)					
Baseline	0.016198	0.263063	0.435535	0.784724	2.162329	3.089820
BSL with high SLR	0.004844	0.188613	0.353022	0.733513	2.495421	3.712832
BSL with interm. SLR	0.006907	0.207007	0.368098	0.728931	2.274506	3.334076
Baseline with low SLR	0.007933	0.211880	0.371518	0.726195	2.205572	3.218913
MFL	0.013857	0.249326	0.413739	0.744401	2.127788	3.081524
MFL with high SLR	0.004340	0.171873	0.325369	0.687975	2.446675	3.701186
MFL with interm. SLR	0.005881	0.190707	0.341844	0.684714	2.233388	3.324162
MFL with low SLR	0.006686	0.195890	0.345774	0.682829	2.166299	3.209402
	Bottom Area (10^6 m^2)					
Baseline	0.022207	0.330551	0.527002	0.876135	2.077281	2.709745
BSL with high SLR	0.005028	0.208818	0.379314	0.716504	2.138893	2.953842
BSL with interm. SLR	0.008409	0.247638	0.425581	0.772424	2.091893	2.816907
Baseline with low SLR	0.010036	0.259089	0.438705	0.788028	2.070623	2.767489
MFL	0.018772	0.315264	0.504452	0.834848	2.047047	2.703899
MFL with high SLR	0.004328	0.190865	0.352146	0.674832	2.098799	2.945764
MFL with interm. SLR	0.006904	0.229145	0.398199	0.728426	2.056436	2.809926
MFL with low SLR	0.008180	0.240709	0.411346	0.743948	2.036058	2.760715
	Shoreline Length (KM)					
Baseline	1.376323	10.147712	15.374695	23.627028	50.446408	60.081444
BSL with high SLR	0.284256	6.124174	11.124488	18.405325	47.442159	59.862284
BSL with interm. SLR	0.478532	7.510608	12.673569	20.576810	48.799239	59.950483
Baseline with low SLR	0.571575	7.966469	13.176783	21.314326	49.205364	59.969833
MFL	1.228097	9.811171	14.916486	22.612185	49.749744	59.982830
MFL with high SLR	0.253965	5.707060	10.542236	17.512108	46.580390	59.723178
MFL with interm. SLR	0.413112	7.061401	12.095930	19.564799	48.010680	59.829010
MFL with low SLR	0.491195	7.517429	12.587689	20.277056	48.424457	59.850609

Percentage reductions of altered and natural shorelines for various salinity ranges caused by the MFL, relative to their corresponding shoreline lengths under the baseline flow condition, for no SLR, high SLR, intermediate SLR, and low SLR are shown in Table 33. It can be seen from the table that neither altered nor natural shores for salinity ≤ 1, 2, 3, 5, 10, and 15 psu are reduced by the proposed MFL for more than 15%. In other words, the proposed MFL is valid under various SLR scenarios when altered and natural shoreline lengths are concerned.

Table 32. Percentage reductions of water volume, bottom area, and shoreline length for salinity ≤ 1, 2, 3, 5, 10, and 15 psu caused by the MFL, relative to those under the BSL condition for different SLR scenarios.

Salinity (psu) ≤	**1**	**2**	**3**	**5**	**10**	**15**
SLR Scenario	Water Volume					
No SLR (#0)	14.45%	5.22%	5.00%	5.14%	1.60%	0.27%
High SLR (#1)	10.40%	8.88%	7.83%	6.21%	1.95%	0.31%
Interm. SLR (#2)	14.85%	7.87%	7.13%	6.07%	1.81%	0.30%
Low SLR (#3)	15.72%	7.55%	6.93%	5.97%	1.78%	0.30%
	Bottom Area					
No SLR	15.47%	4.62%	4.28%	4.71%	1.46%	0.22%
High SLR	13.92%	8.60%	7.16%	5.82%	1.87%	0.27%
Interm. SLR	17.90%	7.47%	6.43%	5.70%	1.69%	0.25%
Low SLR	18.49%	7.09%	6.24%	5.59%	1.67%	0.24%
	Shoreline Length					
No SLR	10.77%	3.32%	2.98%	4.30%	1.38%	0.16%
High SLR	10.66%	6.81%	5.23%	4.85%	1.82%	0.23%
Interm. SLR	13.67%	5.98%	4.56%	4.92%	1.62%	0.20%
Low SLR	14.06%	5.64%	4.47%	4.87%	1.59%	0.20%

Table 33. Relative reductions of altered shoreline length for salinity ≤ 1, 2, 3, 5, 10, and 15 psu caused by the MFL, relative to those under the BSL condition for different SLR scenarios.

Salinity (psu) ≤	**1**	**2**	**3**	**5**	**10**	**15**
SLR Scenario	Altered Shore					
No SLR (#0)	9.94%	4.97%	3.77%	2.32%	0.39%	0.03%
High SLR (#1)	7.06%	8.10%	6.84%	4.59%	0.79%	0.05%
Interm. SLR (#2)	10.54%	7.75%	6.07%	3.79%	0.64%	0.04%
Low SLR (#3)	10.64%	7.42%	5.80%	3.55%	0.58%	0.04%
	Natural Shore					
No SLR	10.15%	2.86%	2.54%	3.57%	1.17%	0.14%
High SLR	9.84%	6.09%	4.64%	4.14%	1.56%	0.20%
Interm. SLR	13.02%	5.23%	3.97%	4.12%	1.38%	0.17%
Low SLR	13.37%	4.91%	3.87%	4.08%	1.35%	0.17%

5.2.2 Thermal Habitats for Manatees

Table 34 shows simulated 72-hour moving averages of ≥ 20 ºC water volume, in cubic meters, at the same five critical time points as those shown in Table 17 for the BSL condition, BSL with the high, intermediate, and low SLRs, MFL, and MFL with the high, intermediate, and low SLRs. Percentage reductions of warm water volume caused by the MFL for no SLR and for high, intermediate, and low SLRs are listed in Table 35. From Table 35, it can be seen that with the consideration of the SLR, the proposed MFL will cause warm water volume for manatees to be reduced by 4.64% - 7.96% at the five critical time points.

Table 34. Seventy-two-hour averages of warm water volume (in m^3) under the chronic condition for manatees for various SLR scenarios under the BSL and MFL conditions at five critical time points.

	72-Hour Time Window				
	#1	*#2*	*#3*	*#4*	*#5*
	1/9/10 18:00 1/12/10 18:00	*1/10/10 13:00 1/13/10 13:00*	*1/1/18 10:30 1/4/18 10:30*	*1/1/18 12:30 1/4/18 12:30*	*1/16/18 19:30 1/19/18 19:30*
Baseline	34778	39166	26133	26719	55523
BSL with high SLR	44725	48696	32926	33358	81421
BSL with interm. SLR	39888	43170	27843	28473	65242
Baseline with low SLR	38351	41570	27291	27961	61114
MFL	32582	36277	25277	25779	52049
MFL with high SLR	41565	45351	30957	31352	74943
MFL with interm. SLR	37091	39906	26550	27125	61162
MFL with low SLR	35713	38452	25773	26437	57178

Table 35. Percentage reductions of the 72-hour average of ≥ 20 ºC water volume caused by the MFL at the five critical time points, relative to the corresponding ≥ 20 ºC volumes under the BSL condition for different SLR scenarios.

SLR Scenario	72-Hour Time Window				
	#1	*#2*	*#3*	*#4*	*#5*
	1/9/10 18:00 1/12/10 18:00	*1/10/10 13:00 1/13/10 13:00*	*1/1/18 10:30 1/4/18 10:30*	*1/1/18 12:30 1/4/18 12:30*	*1/16/18 19:30 1/19/18 19:30*
No SLR (#0)	6.31%	7.38%	3.28%	3.52%	6.26%
High SLR (#1)	7.07%	6.87%	5.98%	6.01%	7.96%
Interm. SLR (#2)	7.01%	7.56%	4.64%	4.73%	6.25%
Low SLR (#3)	6.88%	7.50%	5.56%	5.45%	6.44%

Table 36 shows simulated 72-hour moving averages of ≥ 20 ºC surface area, in square meters, at the same five critical time points as those shown in Table 19 for the BSL condition, BSL with the high, intermediate, and low SLRs, MFL, and MFL with the three SLRs. Percentage reductions of ≥ 20 ºC surface area caused by the MFL for no SLR and for high, intermediate, and low SLR estimates are listed in Table 37. From the table, it can be seen that the MFL causes warm water surface area to be reduced by 4.38% - 8.46% in the Chassahowitzka River at the five critical time points, with the consideration of the three SLRs.

Table 36. Seventy-two-hour averages of ≥ 20 ºC surface area (in m^2) under the chronic condition for manatees for various SLR scenarios under the BSL and MFL conditions at five critical time points.

	72-Hour Time Window				
	#1	*#2*	*#3*	*#4*	*#5*
	1/9/10 18:00 1/12/10 18:00	*1/10/10 13:00 1/13/10 13:00*	*1/1/18 10:30 1/4/18 10:30*	*1/1/18 13:30 1/4/18 13:30*	*1/16/18 19:30 1/19/18 19:30*
Baseline	47030	53014	33653	35196	78579
BSL with high SLR	59716	64389	42728	44296	105546
BSL with interm. SLR	54009	58038	35829	37826	89278
Baseline with low SLR	52026	56075	35288	37111	84698
MFL	44152	49265	32718	34123	73539
MFL with high SLR	55784	60078	40168	41456	96620
MFL with interm. SLR	50285	53756	34261	35950	83280
MFL with low SLR	48403	51857	33324	35036	78978

Table 37. Percentage reductions of the 72-hour average of ≥ 20 ºC surface area caused by the MFL at the five critical time points, relative to the corresponding ≥ 20 ºC surface areas under the BSL condition for different SLR scenarios.

SLR Scenario	72-Hour Time Window				
	#1	*#2*	*#3*	*#4*	*#5*
	1/9/10 18:00 - 1/12/10 18:00	*1/10/10 13:00 - 1/13/10 13:00*	*1/1/18 10:30 - 1/4/18 10:30*	*1/1/18 13:30 - 1/4/18 13:30*	*1/16/18 19:30 - 1/19/18 19:30*
No SLR (#0)	6.12%	7.07%	2.78%	3.05%	6.41%
High SLR (#1)	6.58%	6.70%	5.99%	6.41%	8.46%
Interm. SLR (#2)	6.90%	7.38%	4.38%	4.96%	6.72%
Low SLR (#3)	6.96%	7.52%	5.57%	5.59%	6.75%

Table 38 shows simulated 4-hour moving averages of ≥ 15 ºC water volume, in cubic meters, at the same five critical time points as those shown in Table 21 for the BSL condition, BSL with the high, intermediate, and low SLRs, MFL, and MFL with the three SLRs. Percentage reductions of noncold water volume caused by the MFL for no SLR and for high, intermediate, and low SLRs are listed in Table 39, which shows that the largest percentage reduction of ≥ 15 ºC water volume caused by the MFL is 16.25% at Hour 87937, with the high SLR estimate. Table 39 contains several negative percentage reductions, suggesting that the proposed MFL causes warm water volume to temporally increase with 0 SLR, intermediate SLR, and low SLR at some of the five critical time points. This phenomenon should not be a surprise, as the SGD reduction could cause other factors contributing to the temperature distribution in the river to be altered.

Table 38. Four-hour averages of ≥ 15 ºC water volume (in m^3) under the acute condition for manatees for various SLR scenarios under the BSL and MFL conditions at five critical time points.

	4-Hour Time Window				
	#1	*#2*	*#3*	*#4*	*#5*
	1/11/10 4:00 – 1/11/10 8:00	*1/11/10 23:00 – 1/12/10 3:00*	*1/7/14 6:30 – 1/7/14 10:30*	*1/2/18 4:00 – 1/2/18 8:00*	*1/18/19 5:30 – 1/18/18 9:30*
Baseline	132890	198853	25158	23944	136020
BSL with high SLR	247594	233211	114975	68064	180483
BSL with interm. SLR	*188665*	207954	35308	37430	146093
Baseline with low SLR	174499	201918	28713	26689	142226
MFL	146421	206417	28776	23980	124528
MFL with high SLR	235509	195320	105357	63284	155053
MFL with interm. SLR	190832	203183	35714	37477	128915
MFL with low SLR	177983	197227	29505	28186	126635

Table 39. Percentage reductions of 4-hour average of ≥ 15 ºC water volume caused by the MFL at the five critical time points, relative to the corresponding ≥ 15 ºC water volumes under the BSL condition for different SLR scenarios.

SLR Scenario	4-Hour Time Window				
	#1	*#2*	*#3*	*#4*	*#5*
	1/11/10 4:00 – 1/11/10 8:00	*1/11/10 23:00 – 1/12/10 3:00*	*1/7/14 6:30 – 1/7/14 10:30*	*1/2/18 4:00 – 1/2/18 8:00*	*1/18/19 5:30 – 1/18/18 9:30*
No SLR (#0)	-10.18%	-3.80%	-14.38%	-0.15%	8.45%
High SLR (#1)	4.88%	16.25%	8.37%	7.02%	14.09%
Interm. SLR (#2)	-1.15%	2.29%	-1.15%	-0.13%	11.76%
Low SLR (#3)	-2.00%	2.32%	-2.76%	-5.61%	10.96%

Table 40 shows simulated 4-hour moving averages of ≥ 15 ºC surface area, in square meters, at the same five critical time points as those shown in Table 23 for the BSL condition, BSL with the high, intermediate, and low SLRs, MFL, and MFL with the three SLRs. Percentage reductions of noncold surface area caused by the MFL for no SLR and for high, intermediate, and low SLR estimates are listed in Table 41, which shows that the largest percentage reduction of ≥ 15 ºC surface area caused by the MFL is 17.30% and also occurs at Hour 87937, with the high SLR. Several negative reductions are contained in Table 41, for the same reasons mentioned above.

Table 40. Four-hour averages of ≥ 15 ºC surface area (in m^2) under the acute condition for manatees for various SLR scenarios under the BSL and MFL conditions at five critical time points.

	4-Hour Time Window				
	#1	*#2*	*#3*	*#4*	*#5*
	1/11/10 4:00 – 1/11/10 10:00	*1/11/10 23:00 – 1/12/10 3:00*	*1/8/14 2:00 – 1/8/14 6:00*	*1/2/18 4:00 – 1/2/18 8:00*	*1/18/19 5:30 – 1/18/18 9:30*
Baseline	227108	254634	32891	32721	217725
BSL with high SLR	382606	270591	118914	97731	258244
BSL with interm. SLR	311701	253734	55160	52651	220741
Baseline with low SLR	287799	250900	37755	36248	221326
MFL	249025	260630	34700	32809	196854
MFL with high SLR	369987	223792	112233	90792	218264
MFL with interm. SLR	316184	247406	56719	52906	193607
MFL with low SLR	294855	246426	39898	39084	194452

Table 41. Percentage reductions of 4-hour average of ≥ 15 ºC surface area caused by the MFL at the five critical time points, relative to the corresponding ≥ 15 ºC surface areas under the BSL condition for different SLR scenarios.

SLR Scenario	4-Hour Time Window				
	#1	*#2*	*#3*	*#4*	*#5*
	1/11/10 4:00 – 1/11/10 10:00	*1/11/10 23:00 – 1/12/10 3:00*	*1/8/14 2:00 – 1/8/14 6:00*	*1/2/18 4:00 – 1/2/18 8:00*	*1/18/19 5:30 – 1/18/18 9:30*
No SLR (#0)	-9.65%	-2.35%	-5.50%	-0.27%	9.59%
High SLR (#1)	3.30%	17.30%	5.62%	7.10%	15.48%
Interm. SLR (#2)	-1.44%	2.49%	-2.83%	-0.48%	12.29%
Low SLR (#3)	-2.45%	1.78%	-5.68%	-7.82%	12.14%

Tables 35, 37, 39, and 41 show that when the three see level rises are considered, the 15% reduction criterion for manatee thermal habitats under the chronic condition is not violated by the proposed MFL; however, the 15% reduction criterion for manatee thermal habitats under the acute condition will be violated by the proposed MFL for the Chassahowitzka River.

5.2.3 Thermal Habitats for Common Snook

Percentage reductions of ≥ 15 ºC water volume and surface area caused by the MFL, relative to those under the BSL condition for no SLR, high SLR, intermediate SLR, and low SLR during the 11 varying Common Snook seasons are shown in Table 42. The table also lists the largest MFL-induced percentage reductions of ≥ 15 ºC water volume and surface area among the 11 varying Common Snook seasons. They all occurred during 11/29/09 3:45 – 3/9/10 12:15, the same most sensitive Common Snook season to the MFL without considering any SLRs (see Table 26). From Table 42, it can be seen that the proposed MFL does not cause ≥ 15 ºC water volume and surface area to be reduced by 15% for any of the three SLRs, when a time scale of a varying Common Snook season is concerned.

Table 42. MFL-induced percentage reductions of ≥ 15 ºC water volume and surface area, relative to those under the BSL condition for different SLR scenarios during all the 11 varying Common Snook seasons and during most sensitive Common Snook season (11/29/09 3:45 – 3/9/10 12:15.)

SLR Scenario	Volume Reduction	Surface Area Reduction	Volume Reduction	Surface Area Reduction
	All 11 Varying Common Snook Seasons		11/29/09 3:45 – 3/9/10 12:15	
No SLR (#0)	0.47%	0.43%	1.24%	1.20%
High SLR (#1)	0.66%	0.71%	1.60%	1.75%
Interm. SLR (#2)	0.58%	0.59%	1.45%	1.54%
Low SLR (#3)	0.54%	0.52%	1.39%	1.39%

Similar to these shown in Table 42 with a time scale of a varying Common Snook season, percentage reductions of ≥ 15 ºC water volume and surface area caused by the MFL, relative to those under the BSL condition for various SLRs during the 11 fixed Common Snook seasons and the most sensitive Common Snook season are listed in Table 43. Because a fixed Common Snook season contains more noncold days than a varying Common Snook season, thermal habitats for Common Snook are less sensitive to the MFL for all the SLR scenarios, in comparison with the results using varying Common Snook seasons. Again, the proposed MFL doesn't cause ≥ 15 ºC water volume and surface area to be reduced by 15% for any of the three SLRs, when a time scale of a fixed Common Snook season is used.

Table 43. MFL-induced percentage reductions of ≥ 15 ºC water volume and surface area, relative to those under the BSL condition for different SLR scenarios during all the 11 fixed Common Snook seasons and during most sensitive Common Snook season (10/30/2009 – 3/28/2010.)

Scenario	Volume Reduction	Surface Area Reduction	Volume Reduction	Surface Area Reduction
	All 11 Fixed Common Snook Seasons		10/30/2009 – 3/28/2010	
No SLR (#0)	0.27%	0.24%	0.66%	0.64%
High SLR (#1)	0.39%	0.42%	0.88%	0.98%
Interm. SLR (#2)	0.35%	0.35%	0.79%	0.86%
Low SLR (#3)	0.32%	0.30%	0.75%	0.77%

When the time scale is shortened to cold-day blocks or individual cold days, the MFL effect on Common Snook thermal habitats become more significant for all the SLR scenarios. Percentage reductions of ≥ 15 ºC water volume and surface area caused by the MFL, relative those under the BSL condition for various SLRs during the cold days only are shown in Table 44. For all the 406 cold days during the 10.25 years, the average ≥ 15 ºC volume and surface reductions caused by the MFL are all less than 2.5%. Among the 83 cold-day blocks, the maximum percentage reductions of ≥ 15 ºC volume caused by the MFL for no SLR, low SLR, intermediate SLR, and high SLR are 6.20%, 6.03%, 6.17%, and 7.03%, respectively, while the maximum percentage reductions of ≥ 15 ºC surface area are 5.84%, 5.18%, 5.39%, and 6.66%, respectively.

From Table 44, it can be seen that on the daily time scale, the maximum ≥ 15 ºC volume reductions caused by the MFL can reach 18.16%, 22.79%, and 15.26%, respectively for the low, intermediate, and high SLRs, while the maximum ≥ 15 ºC surface area reductions are all between 13.0% and 13.5% for the three SLRs. As such, the proposed MFL can be invalid, because it could cause ≥ 15 ºC volume to be reduced by more than 15% on certain cold days, when the three SLRs are concerned.

Table 44. Overall percentage reductions during all cold days, maximum percentage reductions among all 82 cold day blocks, and maximum percentage reductions among all 401 days of ≥ 15 ºC water volume and surface area caused by the MFL, relative to those under the baseline condition for various SLR scenarios.

SLR Scenario	Volume Reduction	Surface Area Reduction	Max Vol Reduction	Max Surface Area Reduction	Max Vol Reduction	Max Surface Area Reduction
	All < 15 ºC Days		Among 82 <15 ºC Day Blocks		Among 401 < 15 ºC Days	
No SLR (#0)	1.78%	1.50%	6.20%	5.84%	14.47%	11.73%
High SLR (#1)	2.41%	2.36%	7.03%	6.66%	15.26%	13.42%
Interm. SLR (#2)	2.17%	2.02%	6.17%	5.39%	22.79%	13.34%
Low SLR (#3)	2.04%	1.80%	6.03%	5.18%	18.16%	13.08%

In summary, the proposed MFL is checked for estimated high, intermediate, and low sea level rises. It was found that the proposed MFL cannot hold for ≤ 1 psu volume and bottom area, with the 15% reduction criterion being violated for the intermediate and/or low SLRs. The proposed MFL could also cause thermal habitats for manatees under the acute condition to be reduced by more than 15%. For Common Snook thermal habitats, the proposed MFL would cause the maximum percentage reduction of daily ≥ 15 ºC volume area to be greater than 15% for the three SLR estimates.

6. Conclusions

The laterally averaged hydrodynamic model LAMFE (Chen et al., 2000; Chen, 2003a; Chen, 2004c; Chen, 2007b) was applied to the Chassahowitzka River to simulate circulations and salinity and thermal transport processes in the spring-fed estuary on the Gulf coast of Florida. The river is relatively short and narrow. It has a length of about 9 KM, with a mean depth of 0.9 m. The upstream part of the river is narrow and has a width of 30 m or less. As it runs westward to meet the Gulf of Mexico, it becomes wider and wider. At the mouth of the river, it is more than 550 m wide. The downstream portion of the Chassahowitzka River has many braided channels, which are interconnected and flow through many coastal marsh complexes. The estuarine system is generally well or partially mixed and receives submarine groundwater discharges in the headspring area of the Chassahowitzka River, including the Chassahowitzka Main, Chassahowitzka #1, Chassahowitzka #2, and several unnamed springs. SGDs from tributaries include the Crab Creek spring, the Potters Creek spring (Ruth spring), Baird Creek springs, and that flows to the Crawford Creek, possibly from Beteejay and Rita Marie springs.

In the model application, 348 longitudinal grids and 15 vertical layers were used to discretize the simulation domain, with grid length varying between 29 m to 281 m and layer thickness varying between 0.3 m to 1.2 m. The model was calibrated and verified against measured real-time data of water level, salinity, and temperature in the Chassahowitzka River during a 52-month period between 11/18/2012 and 3/28/2017.

The application of the LAMFE to the Chassahowitzka River estuary was a success. Willmott skills for water elevation, salinity, and temperature simulations are 0.96, 0.91, and 0.98, respectively, while R^2 values for water elevation, salinity, and temperature simulations are 0.9, 0.74, and 0.96, respectively. Overall mean errors for water level, salinity, and temperature simulations are -3.20 cm, -0.08 psu, and -0.02 ºC, respectively. Overall mean absolute errors for water level, salinity, and temperature simulations are 6.11 cm, 1.06 psu, and 0.57 ºC, respectively.

After the hydrodynamic model was calibrated and verified, it was used to conduct a series of flow reduction scenario runs, including the baseline and existing flow conditions and 2.5% – 30% flow reductions with a 2.5% increment. The scenario simulation period was about 123 months (~10.25 years,) from October 11, 2007 through February 15, 2018. Model results, including salinities and temperatures at all grid cells over the entire 123-month period, were analyzed. Different salinity and thermal habitats were calculated based on simulated salinity and temperature results and bathymetry data using a post-process program. These salinity and thermal habitats include water volumes, bottom areas, and shoreline lengths for salinity ≤ 1, 2, 3, 5, 10, 15, and 20 psu and water volume and surface areas for temperature < 15 ºC, ≥ 15 ºC, and ≥ 20 ºC. For ≥ 15 ºC and ≥ 20 ºC thermal habitats, the volume and surface area calculations were conducted both with and without a depth (or layer thickness) restriction of 3.8 feet (1.158 m.) Water volumes and surface areas for ≥ 15 ºC and ≥ 20 ºC with the 3.8 feet restriction were used in the analysis for manatee protection, while ≥ 15 ºC without the 3.8 ft restriction were used for in the analysis for Common Snook protection.

Calculated salinity and thermal habitats were analyzed to examine how flow reductions affect the availabilities of these habitats and what percentage of flow reduction would cause a significant reduction of a favorite habitat. It was found that the most sensitive salinity habitat to flow reduction is ≤ 1 psu bottom area, which will be reduced by 15% with a 7.75% SGD reduction. The most sensitive manatee thermal habitat to the flow reduction is the 4-hour average of ≥ 15 ºC surface area, which can be reduced by 15% with a 10.10% reduction of SGD when the thermal habitat under the acute condition is low. For Common Snook, the most sensitive thermal habitat is the single cold day average of ≥ 15 ºC volume, which can be reduced 15% with an 8.47% SGD reduction.

Sea level rises in 2035 relative to 2012, the middle of the 10.25-year scenario simulation period, at the mouth of the Chassahowitzka River were estimated based on those obtained from the USACE web site http://www.corpsclimate.us/ccaceslcurves.cfm for the NOAA St. Petersburg and Cedar Key stations by the inverse distance weighting method. The low, intermediate, and high SLRs were estimated to be 4.837, 8.723, and 21.105 cm, respectively over the 23-year span. These SLRs were added to open boundaries at the mouth of the Chassahowitzka River to drive the hydrodynamic model in simulating the BSL and the MFL (8% flow reduction) conditions. It should be noted that not all effects of a SLR on circulations and salinity and temperature transport processes in the river were considered in the analysis. Many other factors associated with a SLR were not included in the simulations, including the groundwater level rise that could be caused by the SLR.

The purpose for the consideration of SLRs in the MFL re-evaluation is to see if a proposed MFL is still valid when there is a SLR in the future. In consistence with the District planning horizon, it is desirable to find out if the MFL established using the 123-month period between 2007 and 2018 would be violated 23 years later if a 10.25-year period between 2030 and 2040 were used in the analysis. The assumption here is that the baseline conditions during the two 10.25-year periods were the same except for the sea level rise.

To analyze MFL effects on salinity and thermal habitats with a SLR, relative changes of the habitats caused by the proposed MFL with a SLR should be compared with those for the baseline flow condition with the same SLR. Model results suggest that a sea level rise could significantly change salinity and thermal characteristics in the Chassahowitzka River. Using the same 15% criterion to define a significant harm, the proposed MFL (8% reduction of SGDs) does not cross the threshold for salinity habitats. However, an 8% SGD reduction could cause thermal habitats for manatees under the acute condition to be reduced by more than 15% when the high SLR is to happen. For Common Snook thermal habitats (≥ 15 ºC volume and surface area), the 15% reduction criterion could be violated on some of coldest days in winter when any one of the three SLRs occurs.

7. References

Blewett, D.A. and Stevens, P.W., 2014. Temperature variability in a subtropical estuary and implications for common snook *Centropomus undecimalis*, a cold-sensitive fish. Gulf of Mexico Science, 32(1).

Blumberg, A.F., Kim, B.N., 2000. Flow Balance in St. Andrew Bay Revealed Through Hydrodynamic Simulations. *Estuaries*, 23, 21 – 33.

Chen, X., 1997. Simulating Salinity Distributions in the Lower Hillsborough River with a Laterally Averaged Two-Dimensional Hydrodynamic Model. Technical Report, Southwest Florida Water Management District, Brooksville, Florida.

Chen, X., 1999. Study of Salt Transport in the Lower Hillsborough River Using a Laterally Averaged Two-Dimensional Hydrodynamic Model. Technical Report, Southwest Florida Water Management District, Tampa, Florida.

Chen, X., M.S. Flannery and D.L. Moore. 2000. Response times of salinity in relation to changes in freshwater inflows in the Lower Hillsborough River. *Estuaries*. 23:735-742.

Chen, X., 2003a. An efficient finite difference scheme for simulating hydrodynamics in narrow rivers and estuaries. *International Journal for Numerical Methods in Fluids*, 42: 233-247.

Chen, X., 2003b. Coupling a 3D model with a 2DV model using a free-surface correction method. In (M. L. Spaulding, ed.) *Proceedings of ASCE Estuarine and Coastal Modeling 8*, 769-783.

Chen, X., 2004a. *Simulating Hydrodynamics and Salinity Transport in the Lower Hillsborough River During February 2001 - December 2002*. Technical Report, Southwest Florida Water Management District, Tampa, Fla.

Chen, X., 2004b. Modeling hydrodynamics and salt transport in the Alafia River estuary, Florida during May 1999–December 2001. *Estuarine, Coastal and Shelf Science*, 61 (3), 477-490.

Chen, X., 2004c. Using a piecewise linear bottom to fit the bed variation in a laterally averaged, z-coordinate hydrodynamic model. *International Journal for Numerical Methods in Fluids*. 44: 1185-1205.

Chen, X., 2005. *Simulating Hydrodynamics in the Lower Alafia River Estuary*. Technical Report, Southwest Florida Water Management District, Tampa, Fla.

Chen, X., 2006. Using a Dynamically Coupled 3D-2DV Model to Simulate Hydrodynamics in the Lower Peace River – Upper Charlotte Harbor System in Southwest Florida. In (M. L. Spaulding, ed.) *Proceedings of ASCE Estuarine and Coastal Modeling 9*, 72 -89.

Chen, X., 2007a. *Simulating Hydrodynamics in the Lower Peace River – Lower Myakka River - Upper Charlotte Harbor System, Florida during May 2003 – July 2004.* Technical Report, Southwest Florida Water Management District, Tampa, Florida.

Chen. 2007b. A laterally averaged two-dimensional trajectory model for estimating transport time scales in the Alafia River estuary, Florida. *Estuarine*, *Coastal and Shelf Science*, 75: 358-370, doi:10.1016/j.ecss.2007.04.020.

Chen. 2007c. Dynamic coupling of a three-dimensional hydrodynamic model with a laterally averaged, two-dimensional hydrodynamic model. *Journal of Geophysical Research*, 112, C07022, doi:10.1029/2006JC003805.

Chen, X., 2008a. *Hydrodynamic Simulations of the Lower Peace River – Lower Myakka River – Upper Charlotte Harbor System in Support of Determining Minimum Flows for the LPR and LMR in Southwest Florida*. Technical Report, Southwest Florida Water Management District, Tampa, Florida.

Chen, X., 2008b. Simulating Hydrodynamics in the Upper Charlotte Harbor and Its Major Tributaries in Florida. *Journal of Coastal Research*, SI 52: 149 – 162.

Chen, X., 2008c. Simulating Hydrodynamics in the Manatee and Braden River Estuaries in Southwest Florida using a Multi-Block Model. *Proceedings of ASCE Estuarine and Coastal Modeling 10*, 358 – 372.

Chen, X., 2010. *Hydrodynamic Simulations of the Lower Peace River – Lower Myakka River – Upper Charlotte Harbor System in Support of Determining Minimum Flows for the LPR and LMR in Southwest Florida*. Technical Report, Southwest Florida Water Management District, Tampa, Florida.

Chen, X., 2011. *User's Manual for a Laterally Averaged Model for Estuaries.* Technical Report, Southwest Florida Water Management District, Tampa, Florida.

Chen, X., 2012a. *Simulating Hydrodynamics and Salinity Transport Processes in the Manatee/Braden River Estuarine System Using a Multi-Block Model.* Technical Report, Southwest Florida Water Management District, Tampa, Florida.

Chen, X., 2012b. A sensitivity analysis of low salinity habitats simulated by a hydrodynamic model in the Manatee River estuary in Southwest Florida, USA. *Estuarine*, *Coastal and Shelf Science*, 104 - 105: 80-90, doi:10.1016/j.ecss.2012.03.023.

Chen, X., 2012c. Responses of simulated low salinity habitats to uncertainties of gauged and ungauged flows in the Myakka River estuary in Florida. *Proceedings of ASCE Estuarine and Coastal Modeling 12,* 435 – 456.

Chen, X., 2012d. Simulating hydrodynamics in a spring-fed estuary using a three-dimensional unstructured Cartesian grid model. *Estuarine, Coastal and Shelf Science 115*, 246 – 259, doi:10.1016/j.ecss.2012.09.007.

Chen, X., 2013. Evaluating the Response of the Residence Time to Flow in the Lower Peace River Estuary in Florida, USA. *Coastal Hazards, Trends in Engineering Mechanics Special Publication No.2, ASCE-EMI*. 149 -162.

Chen, X., 2017. *An Evaluation of Effects of Flow Reduction on Salinity and Thermal Habitats and Transport Time Scales in Crystal River/Kings Bay*. Technical Report, Southwest Florida Water Management District, Tampa, Florida. 130p.

Chen, X., 2019a. *A Modeling Study of Effects of Flow Reduction on Salinity and Thermal Habitats in the Homosassa River.* Technical Report, Southwest Florida Water Management District, Tampa, Florida. 100p.

Chen, X., 2019b. *Will A Reduction of Submarine Groundwater Discharge Cause Salinity in SGD to Increase in the Chassahowitzka and Homosassa Rivers?* Technical Article, Southwest Florida Water Management District, Tampa, Florida. 14p

Chen, X., Flannery, M.S., 1997. Use of a Hydrodynamic Model for Establishing a Minimum Freshwater Flow to the Lower Hillsborough River. In (M. L. Spaulding and A. F. Blumberg, eds.) *Proceedings of ASCE Estuarine and Coastal Modeling 5*, 663-678.

Dynamic Solutions, LLC, 2009. Impacts of Withdrawals on the Chassahowitzka River System. Report for the Southwest Florida Water Management District. 94p.

Flannery, M.S., Chen, X., Heyl, M., Munson, A., Dachsteiner, M., 2007. *The Determination of Minimum Flows for the Lower Alafia River Estuary*. Southwest Florida Water Management District, Brooksville, Florida.

Ganju, N.K., Hayn, M., Chen, S.-N., Howarth, R.W., Dickhudt, P.J., Aretxabaleta, A.L., Marino, R., 2012. Tidal and Groundwater Fluxes to a Shallow, Microtidal Estuary: Constraining Inputs Through Field Observations and Hydrodynamic Modeling. *Estuaries and Coasts* 35(5), 1285-1298, doi: 10.1007/s12237-012-9515-x.

Jay, D.A., Smith, J.D., 1990. Residual circulation in shallow estuaries, 2, Weakly stratified and partially mixed, narrow estuaries, *Journal of Geophysical Research*, 95, 733-748.

Janicki Environmental, Inc., Applied Technology & Management. 2007. *Impacts of Withdrawals on the Thermal Regime of the Weeki Wachee River*. Prepared for Southwest Florida Water Management District, Tampa, Fla 33637.

Johnson, B.H., Kim, K.W., Heath, R., Hsieh, B., Butler, L., 1991. Validation of a Three-Dimensional Hydrodynamic Model of Chesapeake Bay, *Journal of Hydraulic Engineering*, 117 (1), 2 – 20.

Notestein S.K., T.K. Frazer, M.V. Hoyer, and D.E. Canfield Jr. 2001. Nutrient limitation of periphyton in a spring-fed, coastal stream in Florida, USA. *Journal of Aquatic Plant Management*, 41: 57-60.

Prandle, D., 1985. On salinity regimes and the vertical structure of residual flows in narrow tidal estuaries. *Estuarine Coastal and Shelf Science*, 20, 615–635.

Rouhani, S., Sucsy, P., Hall, G., Osburn, W., Wild, M. 2007. *Analysis of Blue Spring Discharge Data to Determine a Minimum Flow Regime*. Prepared for St. Johns River Water Management District, Palatka, Fla. 32178.

Scott T.M., G.H. Means, R.P. Meegan, R.C. Means, S.B. Upchurch, R.E. Copeland, J. Jones, T. Roberts, and A. Willet. 2004. *Springs of Florida, Bulletin #66*. Florida Geological Survey, Tallahassee, Florida.

Shafland, P.L. and Foot, K. J. 1983. A lower lethal temperature for fingerling snook, *Centropomus undecimalis*. *Gulf of Mexico Science.* 6 (2).

Stevens, P.W., Blewett, D.A., Boucek, R.E., Rehage, J.S., Winner, B.L., Young, J.M., Whittington, J.A. and Paperno, R., 2016. Resilience of a tropical sport fish population to a severe cold event varies across five estuaries in southern Florida. *Ecosphere*, 7(8).

Vanasse Hangen Brustlin, Inc., 2014. *Chassahowitzka Discharge Measurement and Prediction*, Letter Report to the Southwest Florida Water Management District. 14p.

Vanasse Hangen Brustlin, Inc., 2018. *January 2018 Progress Report for Flow Monitoring in Springs Coast*. Memorandum to the Southwest Florida Water Management District. 2p.

Wang, P., 2006. *Shoreline Mapping and Bathymetric Survey for the Chassahowitzka and Manatee River Systems.* Final Report submitted to Southwest Florida Water Management District, Department of Geology, University of South Florida, Tampa, Fla. 33620.

Warner, J.C., Geyer, W.R., Lerczak, J.A., 2005. Numerical modeling of an estuary: A comprehensive skill assessment. *Journal of Geophysical Research* 110, C05001, doi:10.1029/2004JC002691.

Warner, J.C., Sherwood, C.R., Signell, R.P., Harris, C.K., Arango, H.G., 2008. Development of a three-dimensional, regional, coupled wave, current, and sediment-transport model. *Computers & Geosciences* 34: 1284–1306.

Water & Air Research, Inc., 2018. *Final Report for Shoreline Vegetation Assessment of the Chassahowitzka and Homosassa River Systems*, Prepared for: Southwest Florida Water Management District, Brooksville, Fla., 66p.

Willmott, C.J., 1981. On the validation of models. *Physical Geography* 2, 184-194.

Worthy, G.A.J., Miculka, T.A., Wright, S.D., 2000. Manatee Response to Cold: How Cold is Too Cold? *Florida Manatees and Warm Water, Proceedings of the Warm-Water Workshop*, Jupiter, Fla., pp. 1 - 6

Appendix A. Water Level Data Collected in the Chassahowitzka River

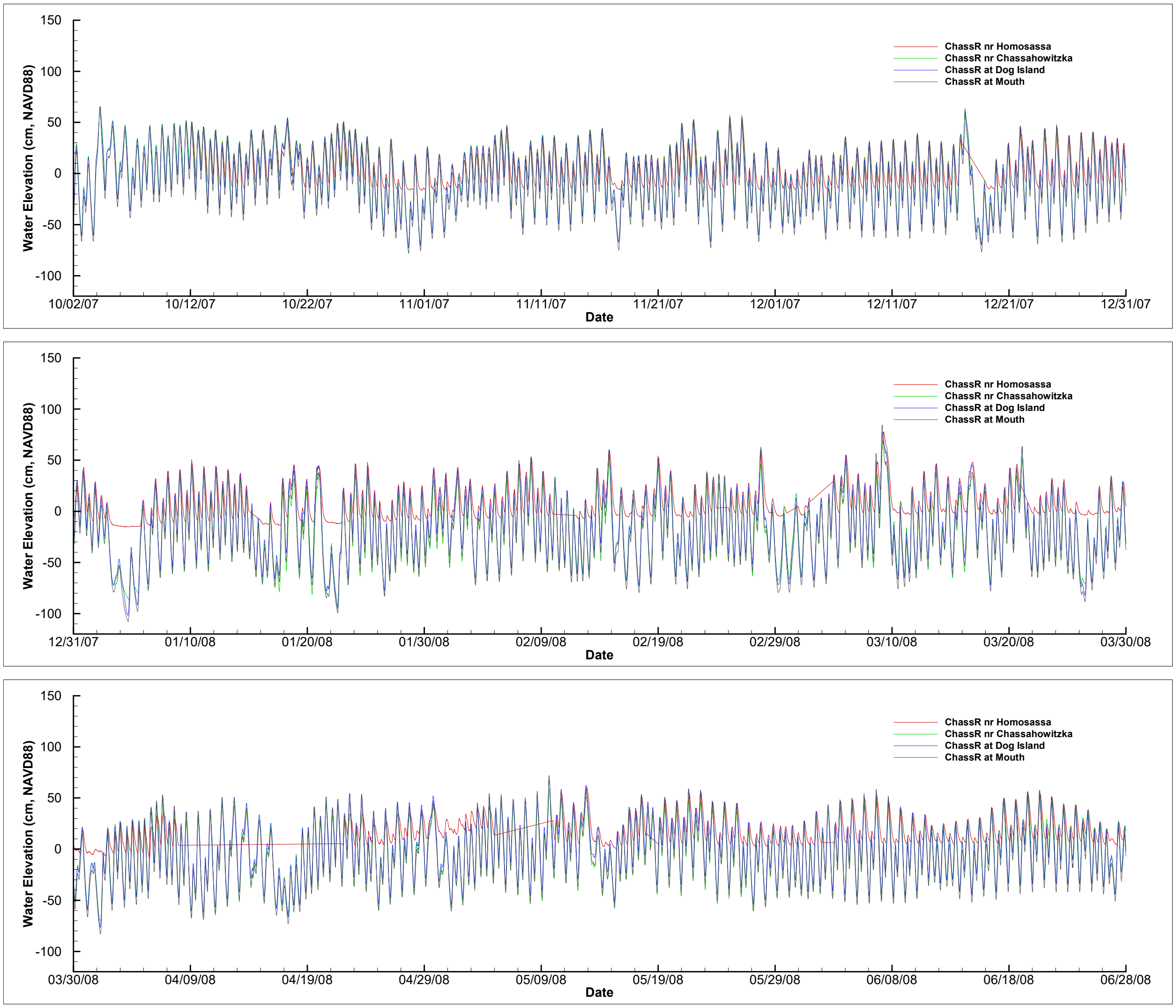

Figure A - 1. Measured real-time water levels at USGS Chassahowitzka near Homosassa (read lines), near Chassahowitzka (green lines), at Dog Island (blue lines), and at Mouth (black lines) stations in the Chassahowitzka River during 10/2/2007 – 6/28/2008.

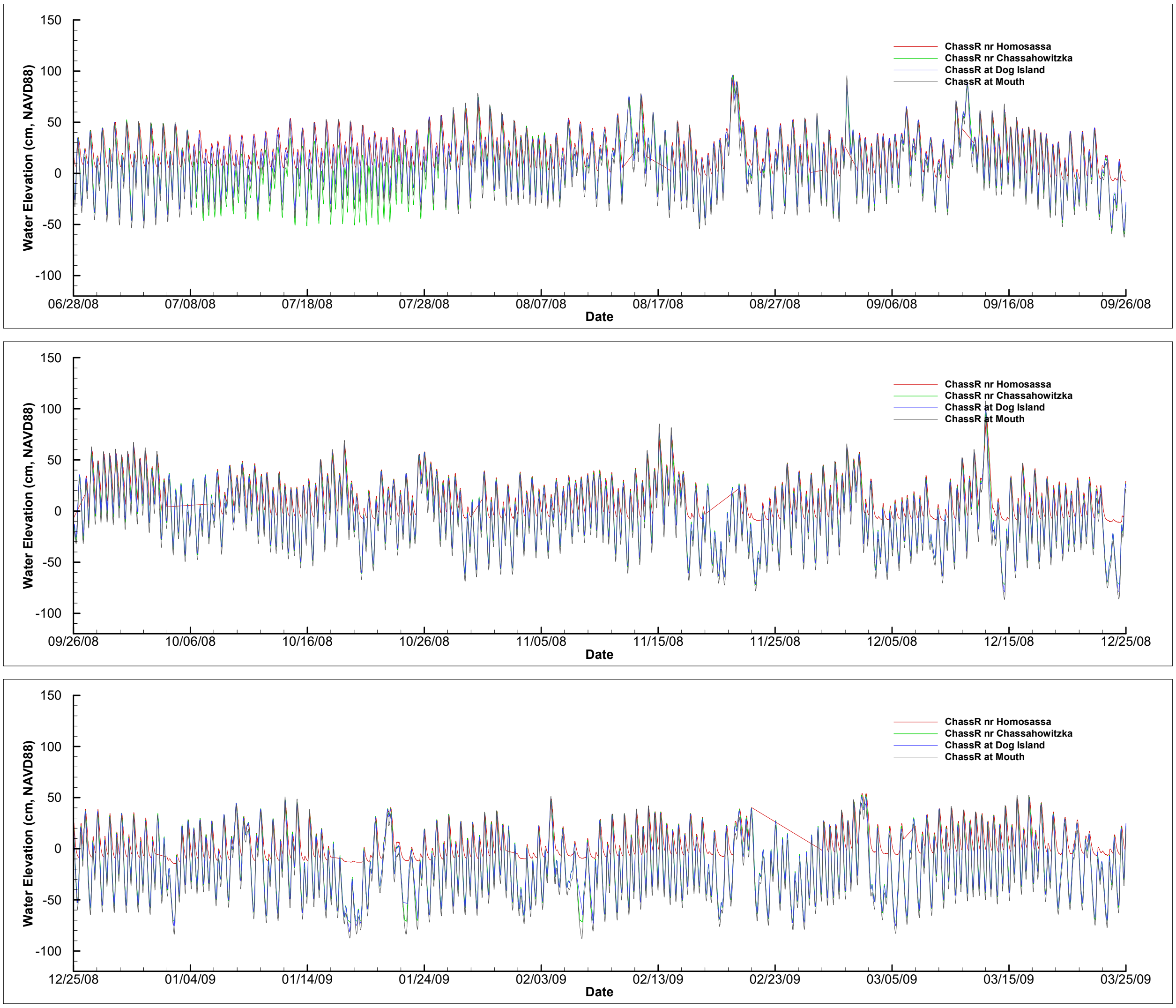

Figure A - 2. Measured real-time water levels at USGS Chassahowitzka near Homosassa (red lines), near Chassahowitzka (green lines), at Dog Island (blue lines), and at Mouth (black lines) in the Chassahowitzka River during 6/28/2008 – 3/25/2009.

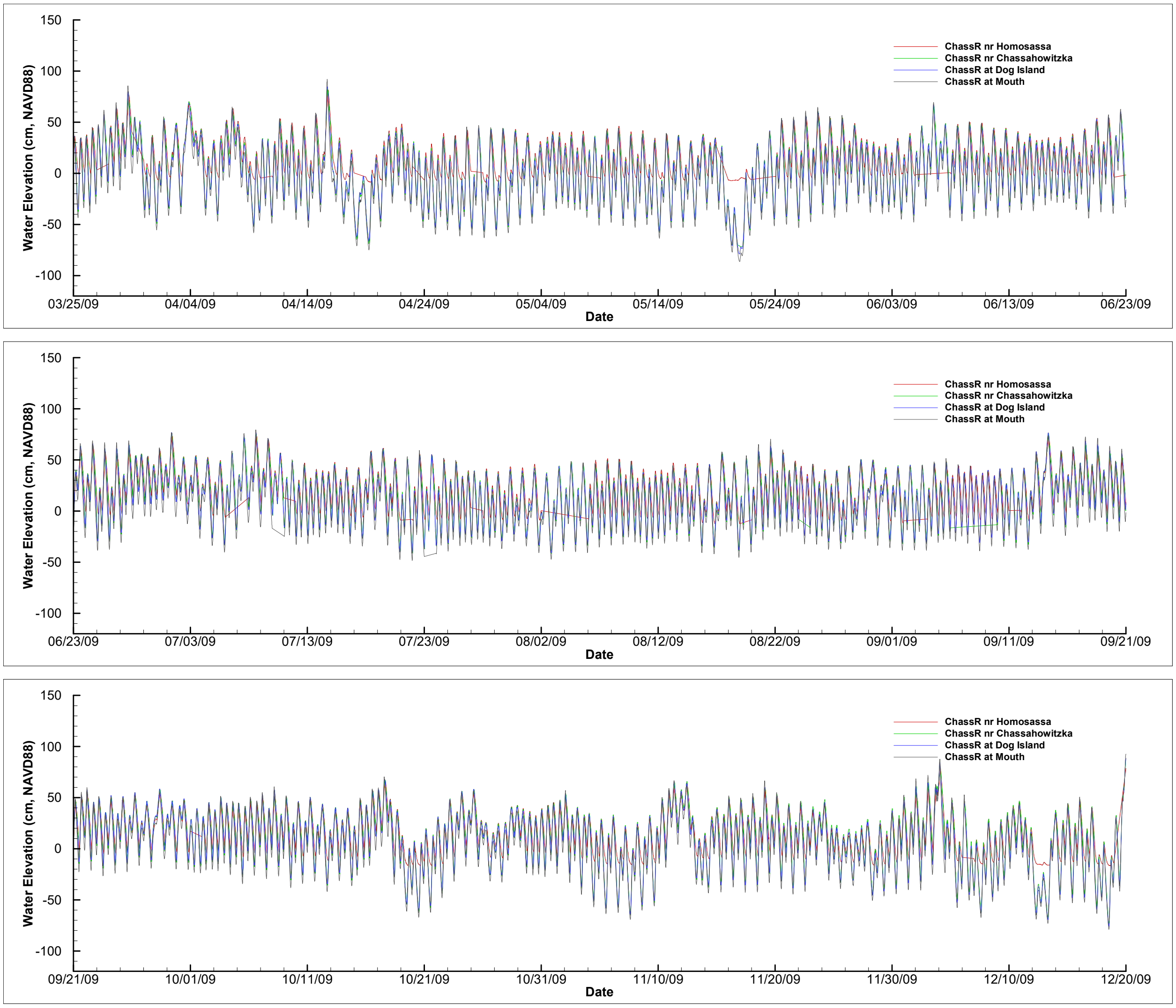

Figure A - 3. Measured real-time water levels at USGS Chassahowitzka near Homosassa (read lines), near Chassahowitzka (green lines), at Dog Island (blue lines), and at Mouth (black lines) stations in the Chassahowitzka River during 3/25/2009 – 12/20/2009.

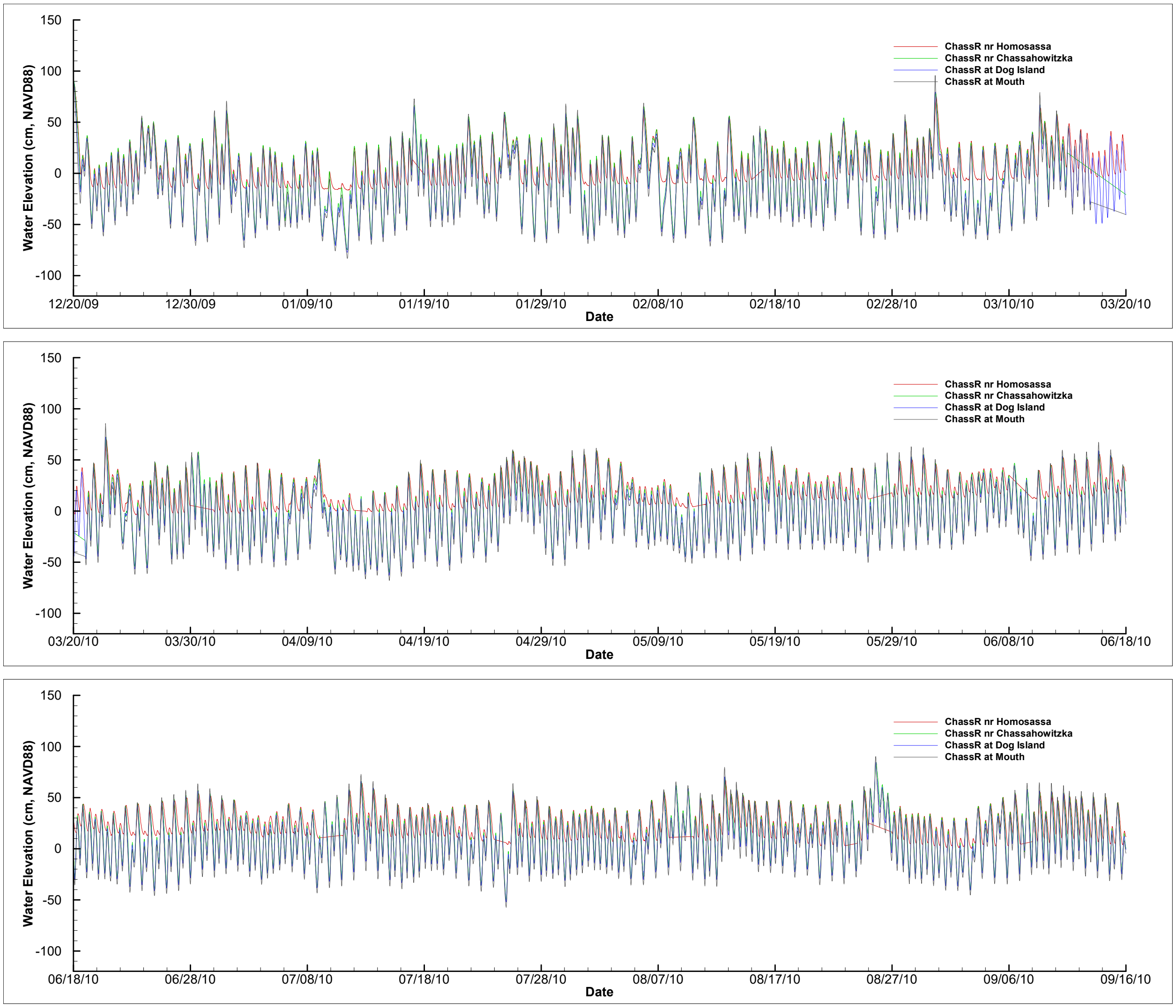

Figure A - 4. Measured real-time water levels at USGS Chassahowitzka near Homosassa (read lines), near Chassahowitzka (green lines), at Dog Island (blue lines), and at Mouth (black lines) stations in the Chassahowitzka River during 12/20/2009 – 9/16/2010.

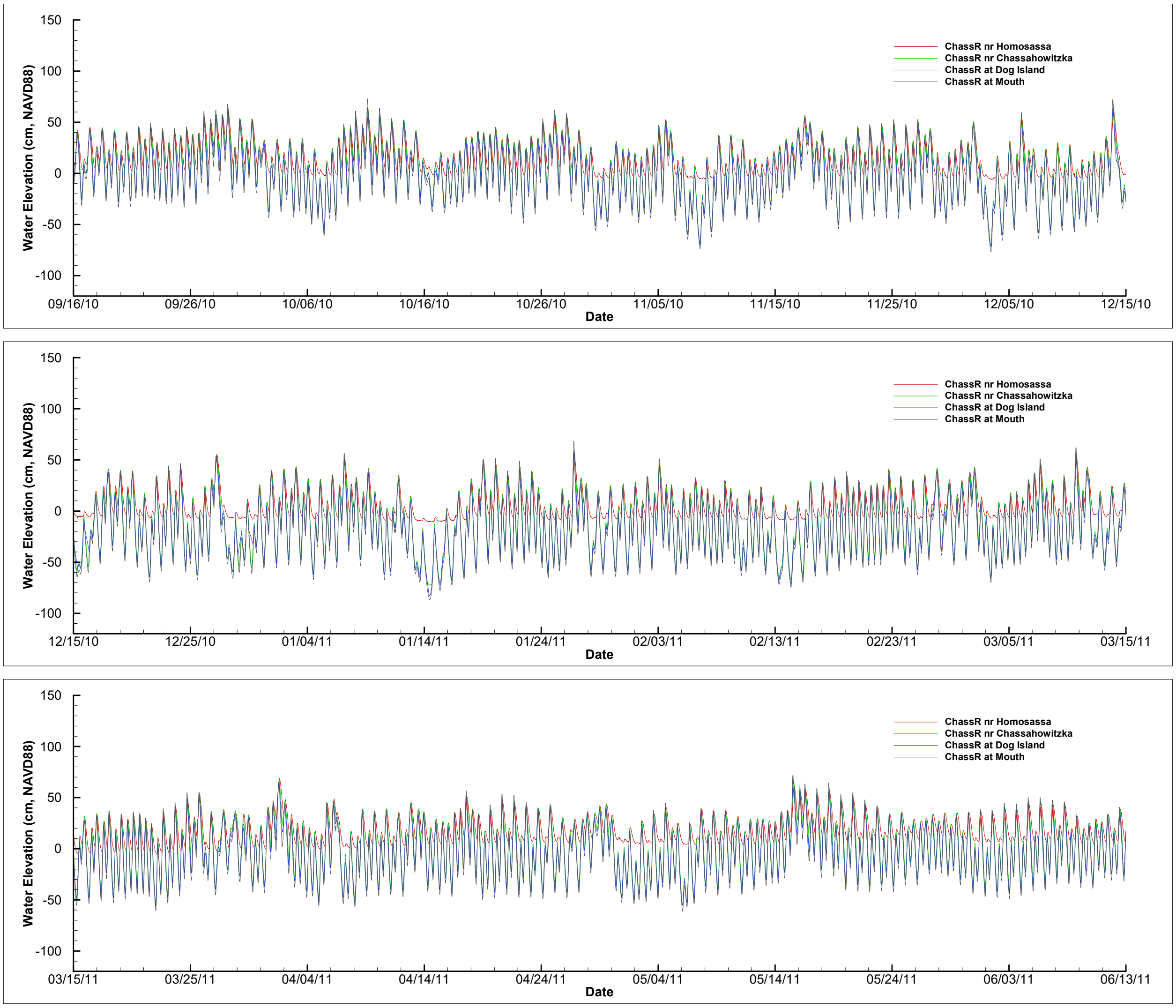

Figure A - 5. Measured real-time water levels at USGS Chassahowitzka near Homosassa (read lines), near Chassahowitzka (green lines), at Dog Island (blue lines), and at Mouth (black lines) stations in the Chassahowitzka River during 9/16/2010 – 6/13/2011.

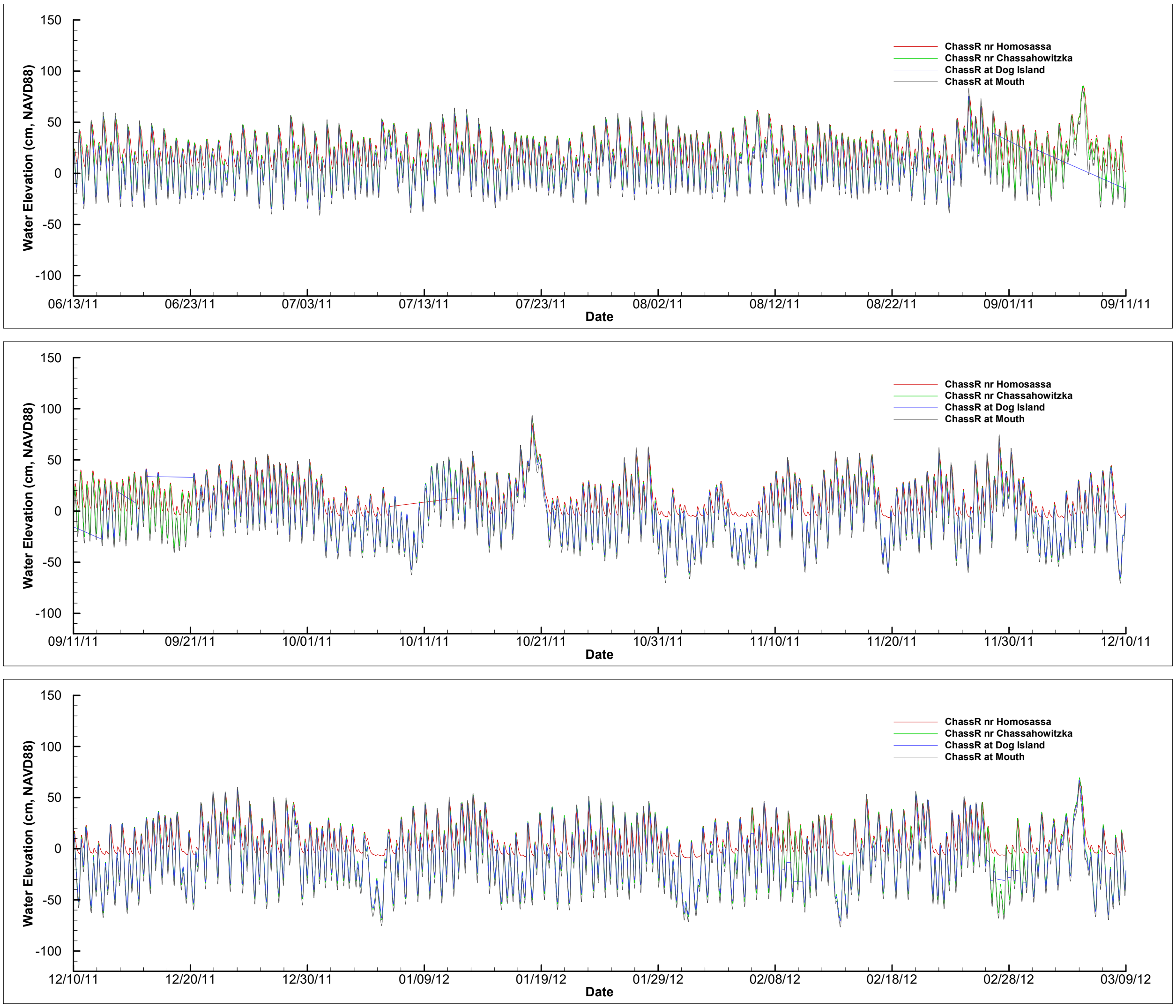

Figure A - 6. Measured real-time water levels at USGS Chassahowitzka near Homosassa (read lines), near Chassahowitzka (green lines), at Dog Island (blue lines), and at Mouth (black lines) stations in the Chassahowitzka River during 6/13/2011 – 3/9/2012.

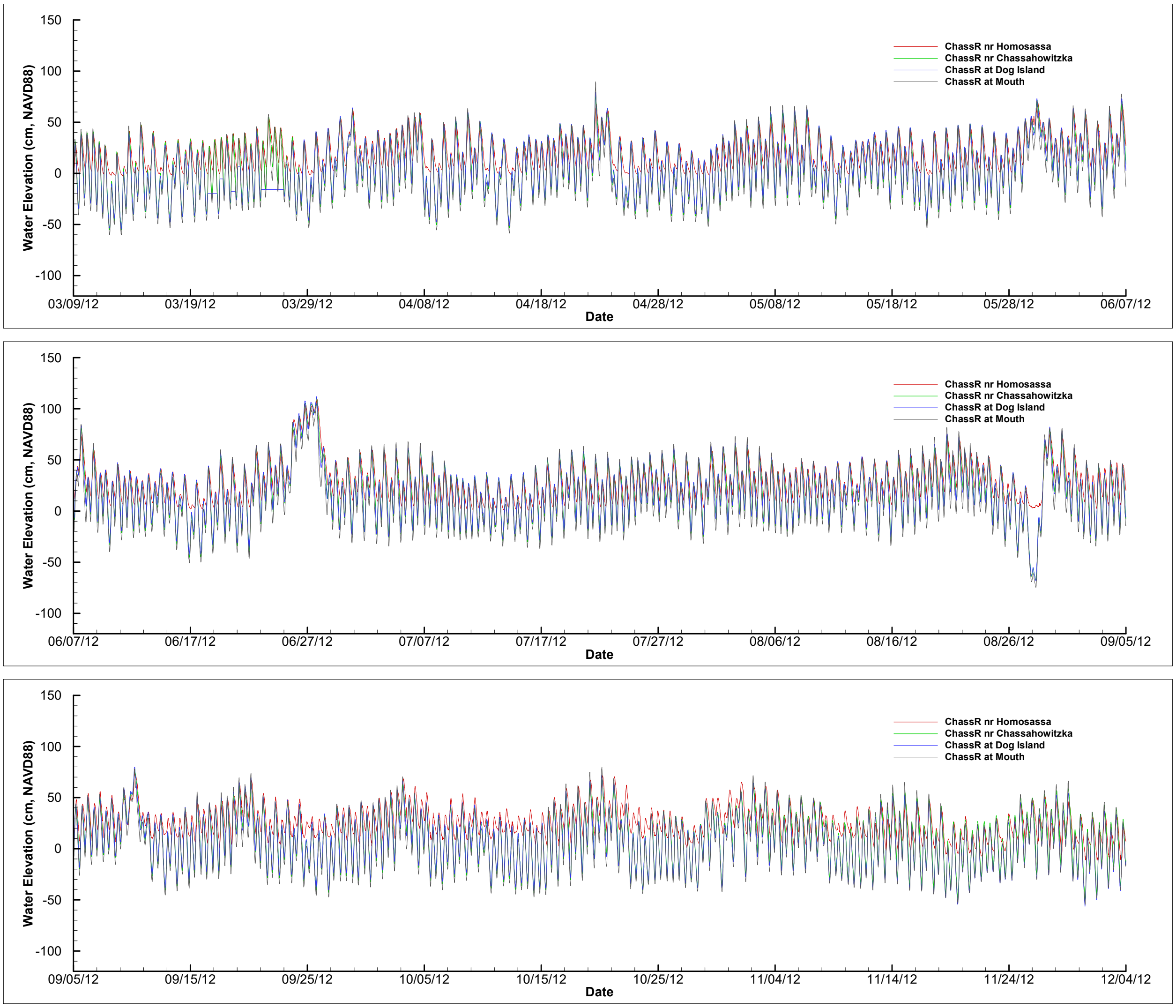

Figure A - 7. Measured real-time water levels at USGS Chassahowitzka near Homosassa (read lines), near Chassahowitzka (green lines), at Dog Island (blue lines), and at Mouth (black lines) stations in the Chassahowitzka River during 3/9/2012 – 12/4/2012.

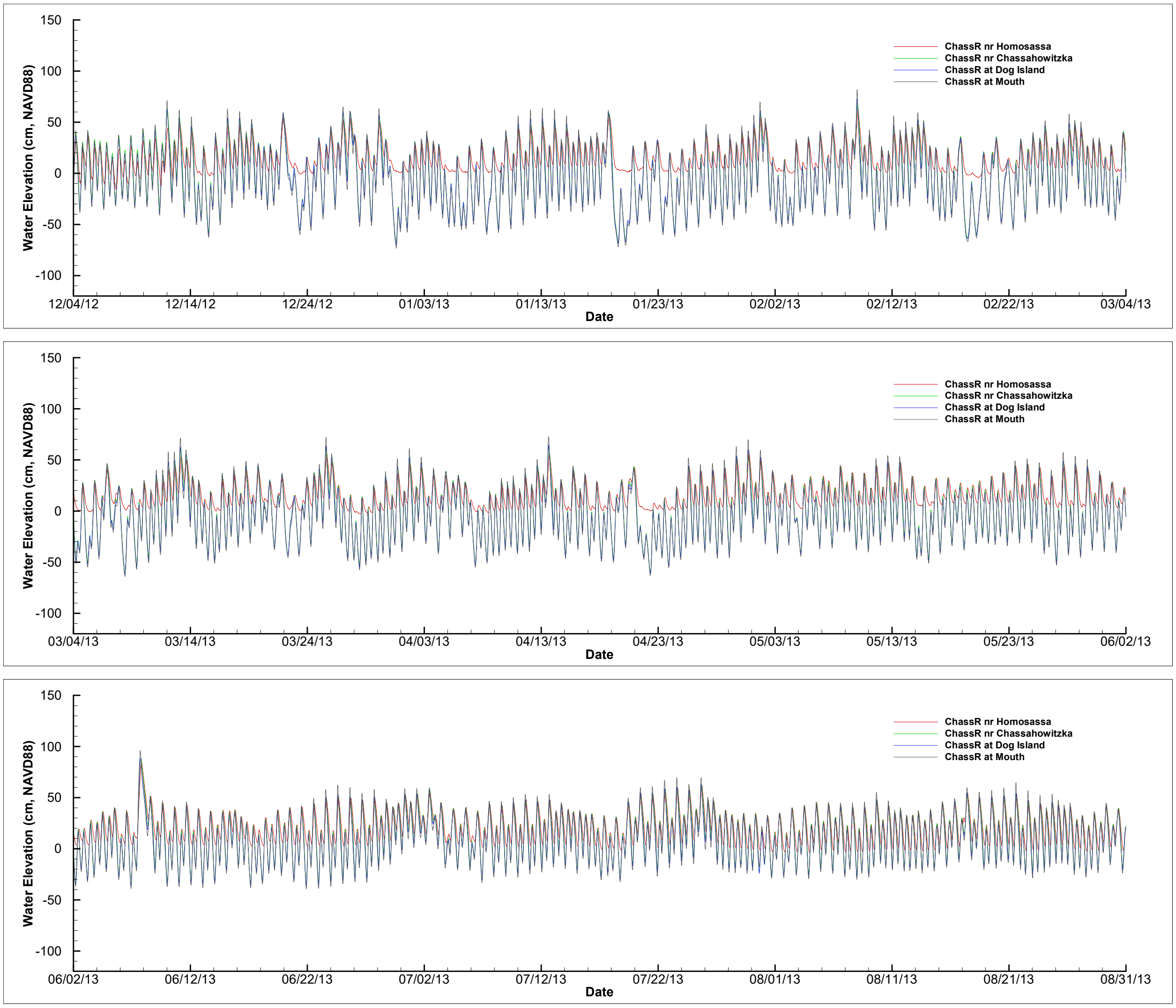

Figure A - 8. Measured real-time water levels at USGS Chassahowitzka near Homosassa (read lines), near Chassahowitzka (green lines), at Dog Island (blue lines), and at Mouth (black lines) stations in the Chassahowitzka River during 12/4/2012 – 8/31/2013.

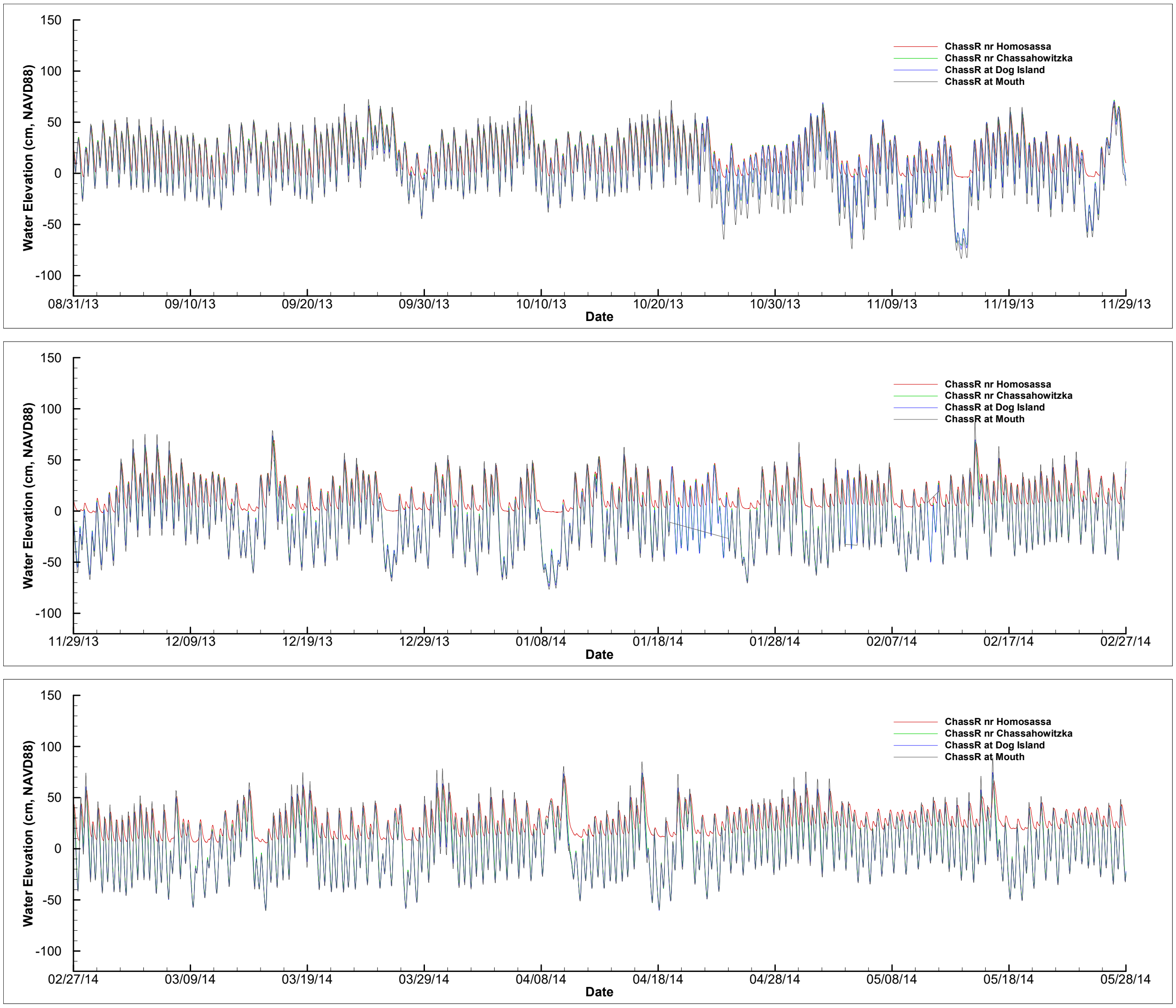

Figure A - 9. Measured real-time water levels at USGS Chassahowitzka near Homosassa (read lines), near Chassahowitzka (green lines), at Dog Island (blue lines), and at Mouth (black lines) stations in the Chassahowitzka River during 8/31/2013 – 5/28/2014.

Figure A - 10. Measured real-time water levels at USGS Chassahowitzka near Homosassa (read lines), near Chassahowitzka (green lines), at Dog Island (blue lines), and at Mouth (black lines) stations in the Chassahowitzka River during 5/28/2014 – 2/22/2015.

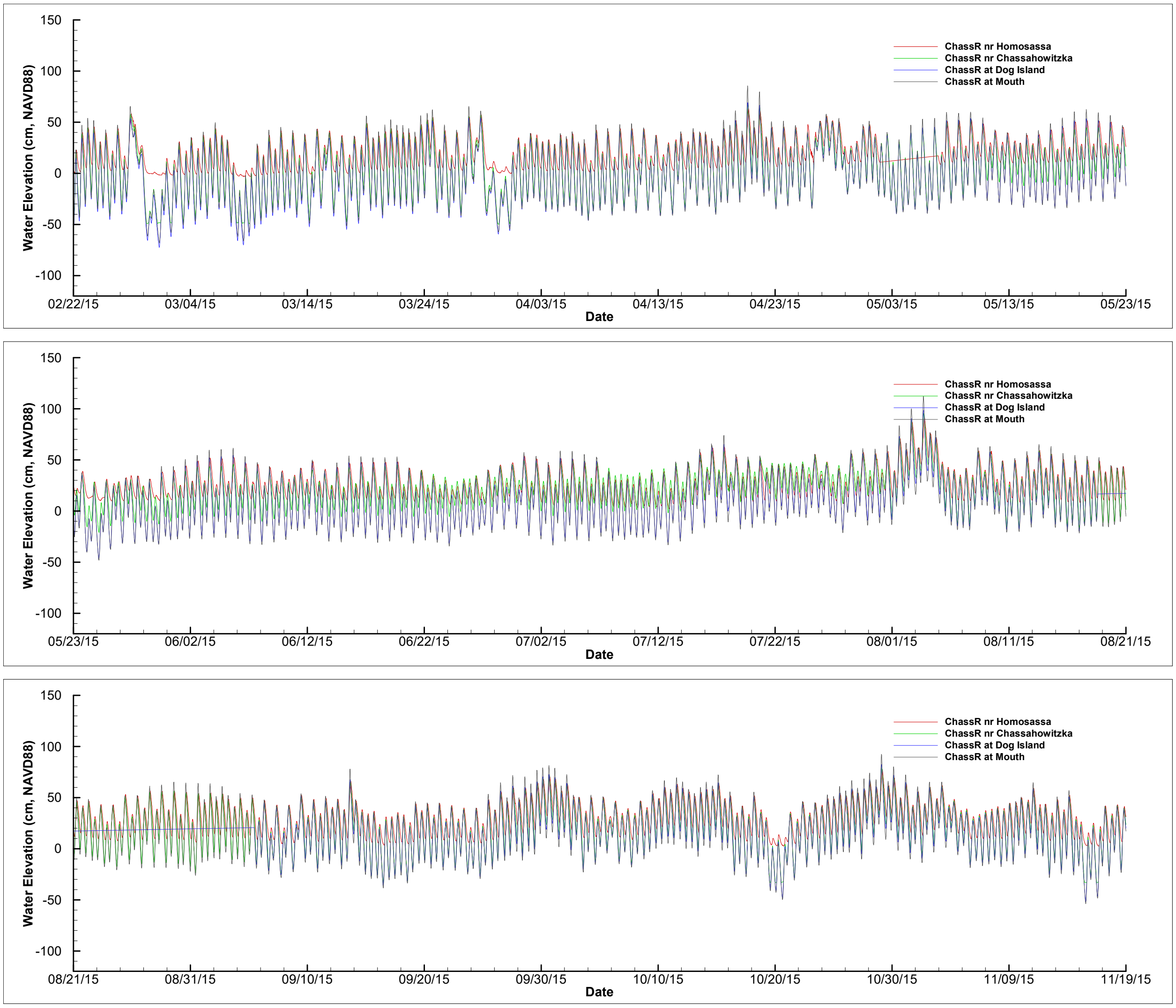

Figure A - 11. Measured real-time water levels at USGS Chassahowitzka near Homosassa (read lines), near Chassahowitzka (green lines), at Dog Island (blue lines), and at Mouth (black lines) stations in the Chassahowitzka River during 2/22/2015 – 11/19/2015.

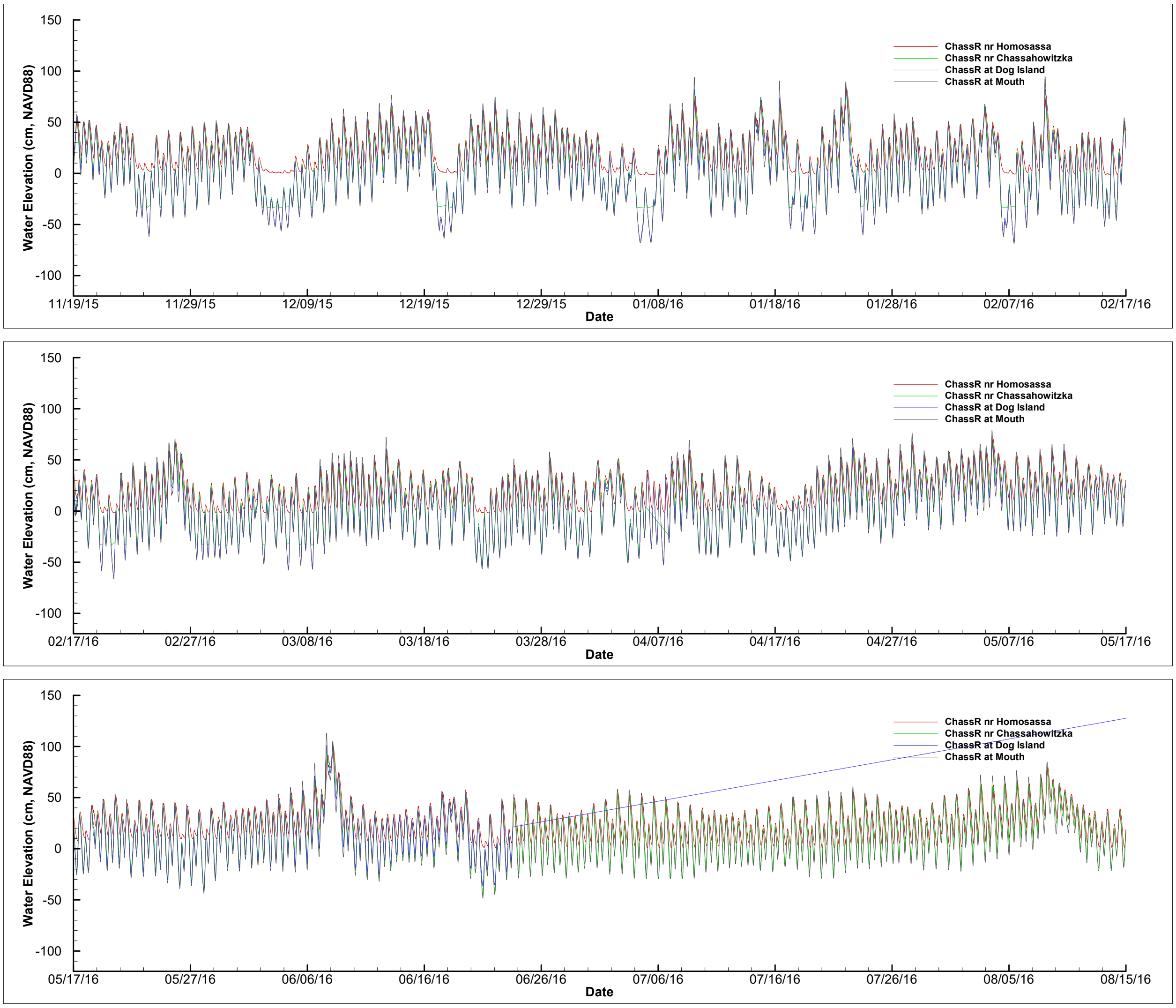

Figure A - 12. Measured real-time water levels at USGS Chassahowitzka near Homosassa (read lines), near Chassahowitzka (green lines), at Dog Island (blue lines), and at Mouth (black lines) stations in the Chassahowitzka River during 11/19/2015 – 8/15/2016.

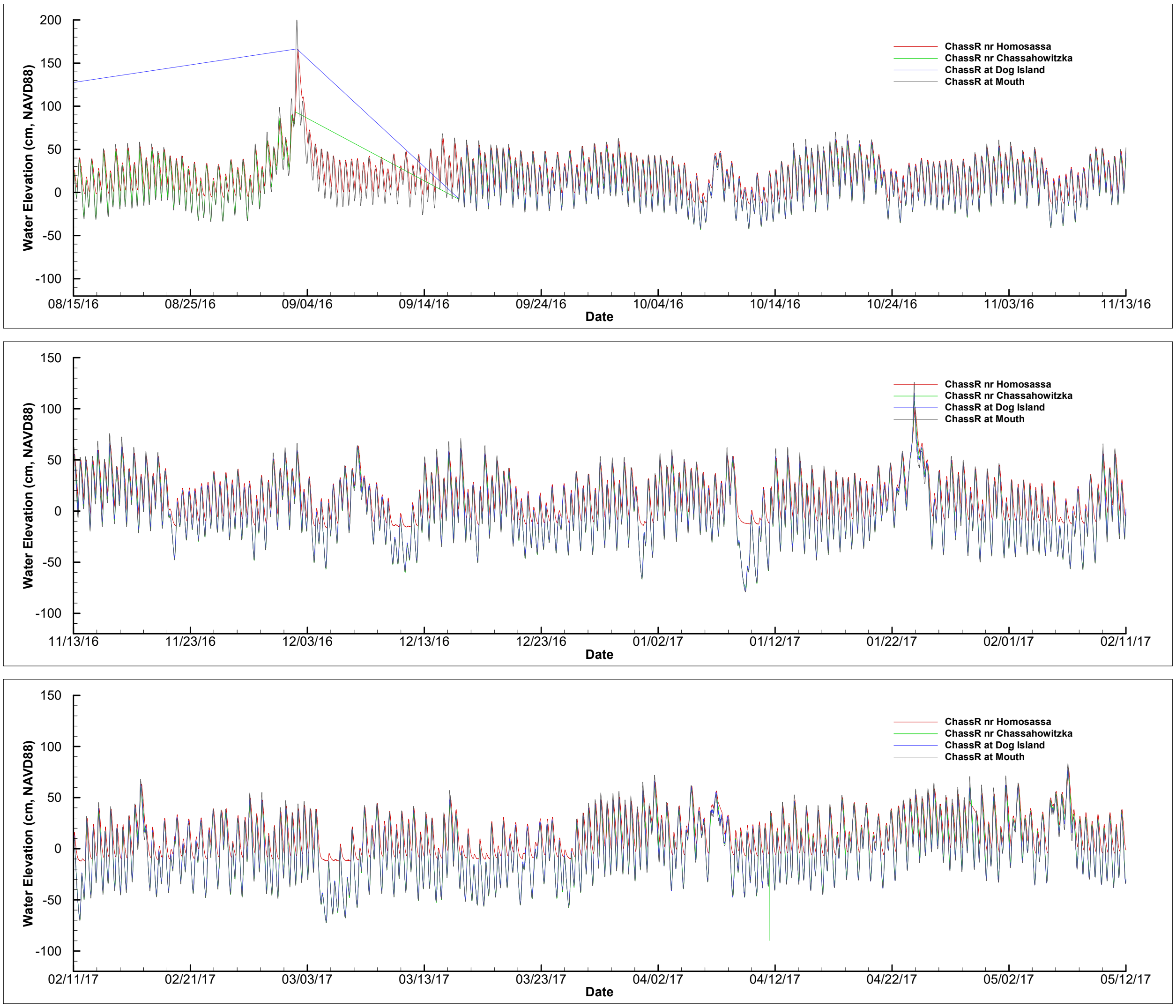

Figure A - 13. Measured real-time water levels at USGS Chassahowitzka near Homosassa (read lines), near Chassahowitzka (green lines), at Dog Island (blue lines), and at Mouth (black lines) stations in the Chassahowitzka River during 8/15/2016 – 5/12/2017.

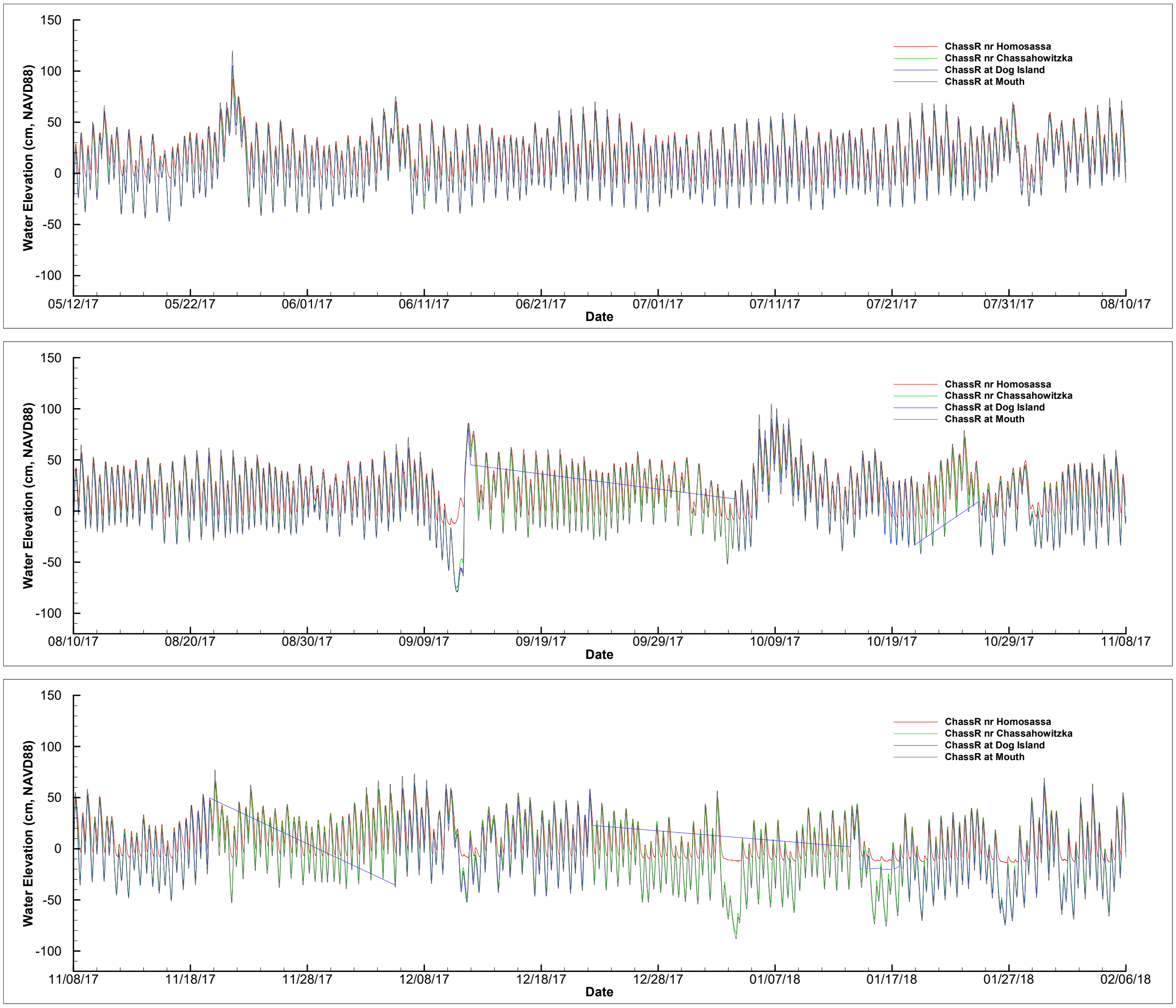

Figure A - 14. Measured real-time water levels at USGS Chassahowitzka near Homosassa (read lines), near Chassahowitzka (green lines), at Dog Island (blue lines), and at Mouth (black lines) stations in the Chassahowitzka River during 5/12/2017 – 2/6/2018.

Appendix B. Salinity Data Collected in the Chassahowitzka River

Figure B - 1. Measured real-time salinities at USGS Chassahowitzka near Homosassa (blue line, top panel), near Chassahowitzka (green line, top panel), at Dog Island (middle panel), and at Mouth (bottom panel) stations in the Chassahowitzka River during 10/2/2007 – 12/31/2007.

Figure B - 2. Measured real-time salinities at USGS Chassahowitzka near Homosassa (blue line, top panel), near Chassahowitzka (green line, top panel), at Dog Island (middle panel), and at Mouth (bottom panel) stations in the Chassahowitzka River during 12/31/2007 – 3/30/2008.

Figure B - 3. Measured real-time salinities at USGS Chassahowitzka near Homosassa (blue line, top panel), near Chassahowitzka (green line, top panel), at Dog Island (middle panel), and at Mouth (bottom panel) stations in the Chassahowitzka River during 3/30/2008 – 6/28/2008.

Figure B - 4. Measured real-time salinities at USGS Chassahowitzka near Homosassa (blue line, top panel), near Chassahowitzka (green line, top panel), at Dog Island (middle panel), and at Mouth (bottom panel) stations in the Chassahowitzka River during 6/28/2008 – 9/26/08.

Figure B - 5. Measured real-time salinities at USGS Chassahowitzka near Homosassa (blue line, top panel), near Chassahowitzka (green line, top panel), at Dog Island (middle panel), and at Mouth (bottom panel) stations in the Chassahowitzka River during 9/26/08 – 12/25/2008.

Figure B - 6. Measured real-time salinities at USGS Chassahowitzka near Homosassa (blue line, top panel), near Chassahowitzka (green line, top panel), at Dog Island (middle panel), and at Mouth (bottom panel) stations in the Chassahowitzka River during 12/25/2008 – 3/25/2009.

Figure B - 7. Measured real-time salinities at USGS Chassahowitzka near Homosassa (blue line, top panel), near Chassahowitzka (green line, top panel), at Dog Island (middle panel), and at Mouth (bottom panel) stations in the Chassahowitzka River during 3/25/2009 – 6/23/2009.

Figure B - 8. Measured real-time salinities at USGS Chassahowitzka near Homosassa (blue line, top panel), near Chassahowitzka (green line, top panel), at Dog Island (middle panel), and at Mouth (bottom panel) stations in the Chassahowitzka River during 6/23/2009 – 9/21/2009.

Figure B - 9. Measured real-time salinities at USGS Chassahowitzka near Homosassa (blue line, top panel), near Chassahowitzka (green line, top panel), at Dog Island (middle panel), and at Mouth (bottom panel) stations in the Chassahowitzka River during 9/21/2009 - 12/20/2009.

Figure B - 10. Measured real-time salinities at USGS Chassahowitzka near Homosassa (blue line, top panel), near Chassahowitzka (green line, top panel), at Dog Island (middle panel), and at Mouth (bottom panel) stations in the Chassahowitzka River during 12/20/2009 – 3/20/2010.

Figure B - 11. Measured real-time salinities at USGS Chassahowitzka near Homosassa (blue line, top panel), near Chassahowitzka (green line, top panel), at Dog Island (middle panel), and at Mouth (bottom panel) stations in the Chassahowitzka River during 3/20/2010 – 6/18/2010.

Figure B - 12. Measured real-time salinities at USGS Chassahowitzka near Homosassa (blue line, top panel), near Chassahowitzka (green line, top panel), at Dog Island (middle panel), and at Mouth (bottom panel) stations in the Chassahowitzka River during 6/18/2010 – 9/16/2010.

Figure B - 13. Measured real-time salinities at USGS Chassahowitzka near Homosassa (blue line, top panel), near Chassahowitzka (green line, top panel), at Dog Island (middle panel), and at Mouth (bottom panel) stations in the Chassahowitzka River during 9/16/2010 - 12/15/2010.

Figure B - 14. Measured real-time salinities at USGS Chassahowitzka near Homosassa (blue line, top panel), near Chassahowitzka (green line, top panel), at Dog Island (middle panel), and at Mouth (bottom panel) stations in the Chassahowitzka River during 12/15/2010 – 3/15/2011.

Figure B - 15. Measured real-time salinities at USGS Chassahowitzka near Homosassa (blue line, top panel), near Chassahowitzka (green line, top panel), at Dog Island (middle panel), and at Mouth (bottom panel) stations in the Chassahowitzka River during 3/15/2011 - 6/13/2011.

Figure B - 16. Measured real-time salinities at USGS Chassahowitzka near Homosassa (blue line, top panel), near Chassahowitzka (green line, top panel), at Dog Island (middle panel), and at Mouth (bottom panel) stations in the Chassahowitzka River during 6/13/2011 - 9/11/2011.

Figure B - 17. Measured real-time salinities at USGS Chassahowitzka near Homosassa (blue line, top panel), near Chassahowitzka (green line, top panel), at Dog Island (middle panel), and at Mouth (bottom panel) stations in the Chassahowitzka River during 9/11/2011 - 12/10/2011.

Figure B - 18. Measured real-time salinities at USGS Chassahowitzka near Homosassa (blue line, top panel), near Chassahowitzka (green line, top panel), at Dog Island (middle panel), and at Mouth (bottom panel) stations in the Chassahowitzka River during 12/10/2011 – 3/9/2012.

Figure B - 19. Measured real-time salinities at USGS Chassahowitzka near Homosassa (blue line, top panel), near Chassahowitzka (green line, top panel), at Dog Island (middle panel), and at Mouth (bottom panel) stations in the Chassahowitzka River during 3/9/2012 - 6/7/2012.

Figure B - 20. Measured real-time salinities at USGS Chassahowitzka near Homosassa (blue line, top panel), near Chassahowitzka (green line, top panel), at Dog Island (middle panel), and at Mouth (bottom panel) stations in the Chassahowitzka River during 6/7/2012 - 9/5/2012.

Figure B - 21. Measured real-time salinities at USGS Chassahowitzka near Homosassa (blue line, top panel), near Chassahowitzka (green line, top panel), at Dog Island (middle panel), and at Mouth (bottom panel) stations in the Chassahowitzka River during 9/5/2012 – 12/4/2012.

Figure B - 22. Measured real-time salinities at USGS Chassahowitzka near Homosassa (blue line, top panel), near Chassahowitzka (green line, top panel), at Dog Island (middle panel), and at Mouth (bottom panel) stations in the Chassahowitzka River during 12/4/2012 – 3/4/2013.

Figure B - 23. Measured real-time salinities at USGS Chassahowitzka near Homosassa (blue line, top panel), near Chassahowitzka (green line, top panel), at Dog Island (middle panel), and at Mouth (bottom panel) stations in the Chassahowitzka River during 3/4/2013 – 6/2/2013.

Figure B - 24. Measured real-time salinities at USGS Chassahowitzka near Homosassa (blue line, top panel), near Chassahowitzka (green line, top panel), at Dog Island (middle panel), and at Mouth (bottom panel) stations in the Chassahowitzka River during 6/2/2013 – 8/31/2013.

Figure B - 25. Measured real-time salinities at USGS Chassahowitzka near Homosassa (blue line, top panel), near Chassahowitzka (green line, top panel), at Dog Island (middle panel), and at Mouth (bottom panel) stations in the Chassahowitzka River during 8/31/2013 - 11/29/2013.

Figure B - 26. Measured real-time salinities at USGS Chassahowitzka near Homosassa (blue line, top panel), near Chassahowitzka (green line, top panel), at Dog Island (middle panel), and at Mouth (bottom panel) stations in the Chassahowitzka River during 11/29/2013 - 2/27/2014.

Figure B - 27. Measured real-time salinities at USGS Chassahowitzka near Homosassa (blue line, top panel), near Chassahowitzka (green line, top panel), at Dog Island (middle panel), and at Mouth (bottom panel) stations in the Chassahowitzka River during 2/27/2014 – 5/28/2014.

Figure B - 28. Measured real-time salinities at USGS Chassahowitzka near Homosassa (blue line, top panel), near Chassahowitzka (green line, top panel), at Dog Island (middle panel), and at Mouth (bottom panel) stations in the Chassahowitzka River during 5/28/2014 – 8/26/2014.

Figure B - 29. Measured real-time salinities at USGS Chassahowitzka near Homosassa (blue line, top panel), near Chassahowitzka (green line, top panel), at Dog Island (middle panel), and at Mouth (bottom panel) stations in the Chassahowitzka River during 8/26/2014 – 11/24/2014.

Figure B - 30. Measured real-time salinities at USGS Chassahowitzka near Homosassa (blue line, top panel), near Chassahowitzka (green line, top panel), at Dog Island (middle panel), and at Mouth (bottom panel) stations in the Chassahowitzka River during 11/24/2014 – 2/22/2015.

Figure B - 31. Measured real-time salinities at USGS Chassahowitzka near Homosassa (blue line, top panel), near Chassahowitzka (green line, top panel), at Dog Island (middle panel), and at Mouth (bottom panel) stations in the Chassahowitzka River during 2/22/2015 - 5/23/2015.

Figure B - 32. Measured real-time salinities at USGS Chassahowitzka near Homosassa (blue line, top panel), near Chassahowitzka (green line, top panel), at Dog Island (middle panel), and at Mouth (bottom panel) stations in the Chassahowitzka River during 5/23/2015 - 8/21/2015.

Figure B - 33. Measured real-time salinities at USGS Chassahowitzka near Homosassa (blue line, top panel), near Chassahowitzka (green line, top panel), at Dog Island (middle panel), and at Mouth (bottom panel) stations in the Chassahowitzka River during 8/21/2015 - 11/19/2015.

Figure B - 34. Measured real-time salinities at USGS Chassahowitzka near Homosassa (blue line, top panel), near Chassahowitzka (green line, top panel), at Dog Island (middle panel), and at Mouth (bottom panel) stations in the Chassahowitzka River during 11/19/2015 – 2/17/2016.

Figure B - 35. Measured real-time salinities at USGS Chassahowitzka near Homosassa (blue line, top panel), near Chassahowitzka (green line, top panel), at Dog Island (middle panel), and at Mouth (bottom panel) stations in the Chassahowitzka River during 2/17/2016 - 5/17/2016.

Figure B - 36. Measured real-time salinities at USGS Chassahowitzka near Homosassa (blue line, top panel), near Chassahowitzka (green line, top panel), at Dog Island (middle panel), and at Mouth (bottom panel) stations in the Chassahowitzka River during 5/17/2016 - 8/15/2016.

Figure B - 37. Measured real-time salinities at USGS Chassahowitzka near Homosassa (blue line, top panel), near Chassahowitzka (green line, top panel), at Dog Island (middle panel), and at Mouth (bottom panel) stations in the Chassahowitzka River during 8/15/2016 - 11/13/2016.

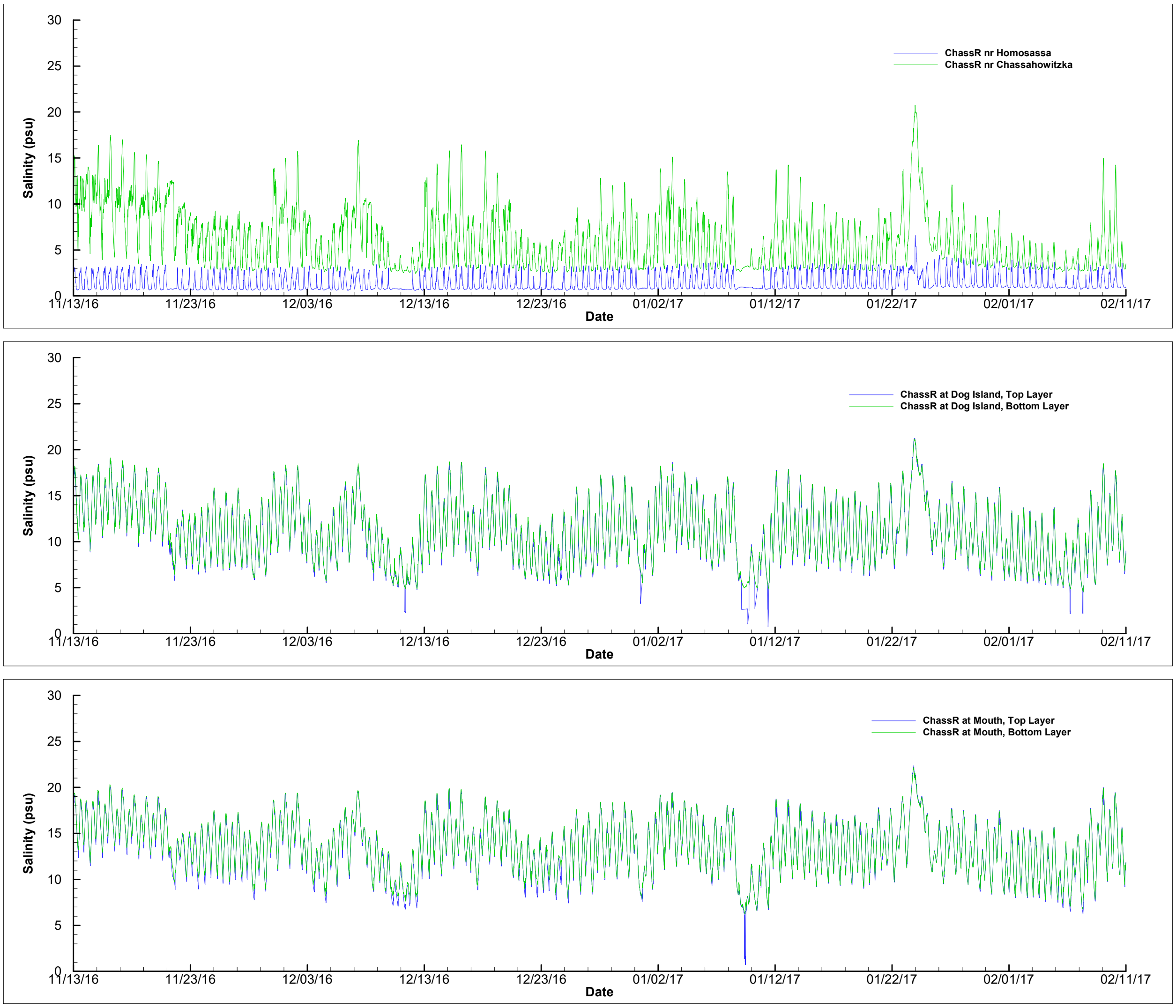

Figure B - 38. Measured real-time salinities at USGS Chassahowitzka near Homosassa (blue line, top panel), near Chassahowitzka (green line, top panel), at Dog Island (middle panel), and at Mouth (bottom panel) stations in the Chassahowitzka River during 11/13/2016 - 2/11/2017.

Figure B - 39. Measured real-time salinities at USGS Chassahowitzka near Homosassa (blue line, top panel), near Chassahowitzka (green line, top panel), at Dog Island (middle panel), and at Mouth (bottom panel) stations in the Chassahowitzka River during 2/11/2017 - 5/12/2017.

Figure B - 40. Measured real-time salinities at USGS Chassahowitzka near Homosassa (blue line, top panel), near Chassahowitzka (green line, top panel), at Dog Island (middle panel), and at Mouth (bottom panel) stations in the Chassahowitzka River during 5/12/2017 - 8/10/2017.

Figure B - 41. Measured real-time salinities at USGS Chassahowitzka near Homosassa (blue line, top panel), near Chassahowitzka (green line, top panel), at Dog Island (middle panel), and at Mouth (bottom panel) stations in the Chassahowitzka River during 8/10/2017 – 11/8/2017.

Figure B - 42. Measured real-time salinities at USGS Chassahowitzka near Homosassa (blue line, top panel), near Chassahowitzka (green line, top panel), at Dog Island (middle panel), and at Mouth (bottom panel) stations in the Chassahowitzka River during 11/8/2017 - 2/6/2018.

Figure B - 43. Measured real-time salinities at USGS Chassahowitzka near Homosassa (blue line, top panel), near Chassahowitzka (green line, top panel), at Dog Island (middle panel), and at Mouth (bottom panel) stations in the Chassahowitzka River during 2/6/2018 - 5/7/2018.

Appendix C. Temperature Data Collected in the Chassahowitzka River

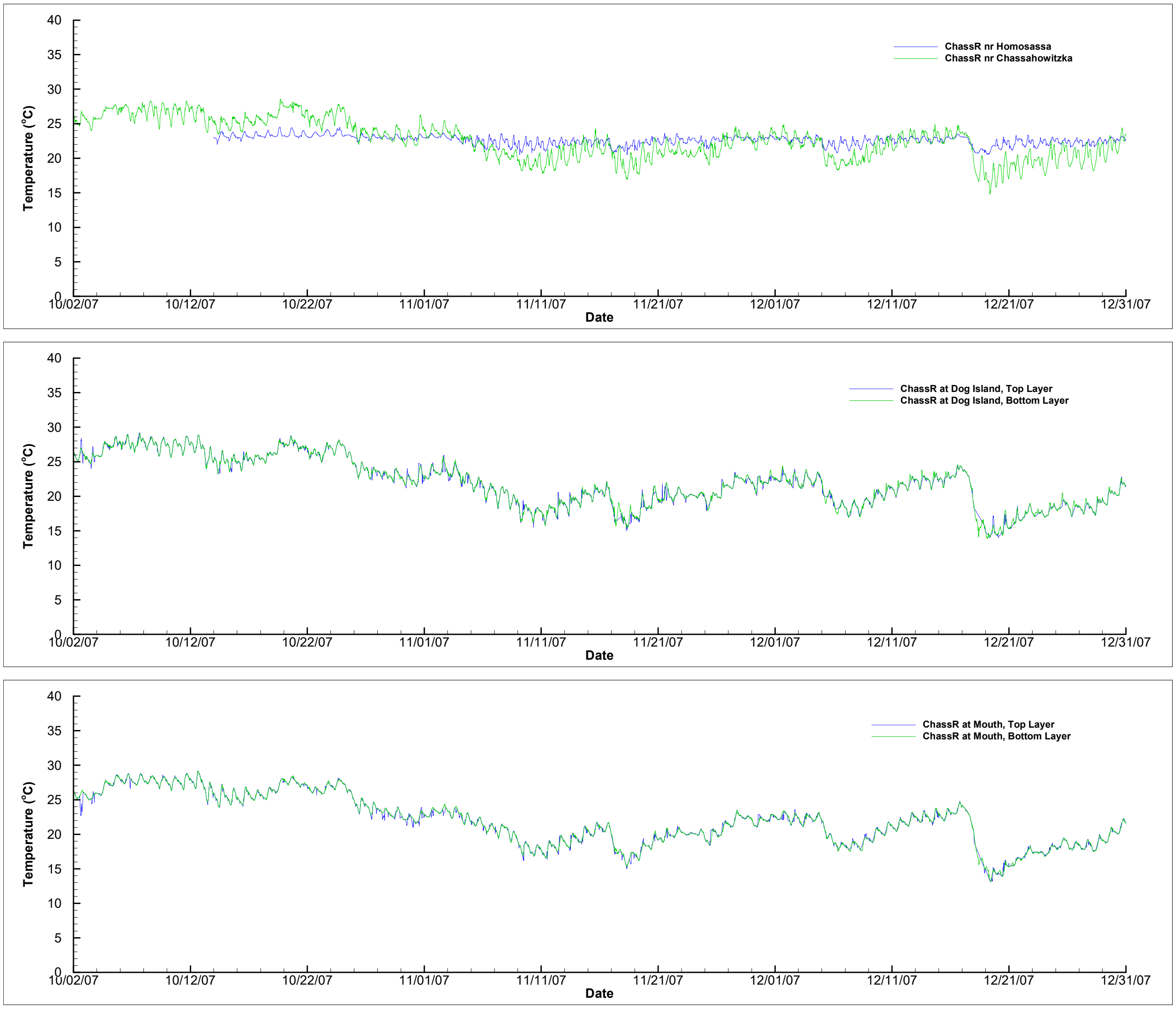

Figure C - 1. Measured real-time temperatures at USGS Chassahowitzka near Homosassa (blue line, top panel), near Chassahowitzka (green line, top panel), at Dog Island (middle panel), and at Mouth (bottom panel) stations in the Chassahowitzka River during 10/2/2007 – 12/31/2007.

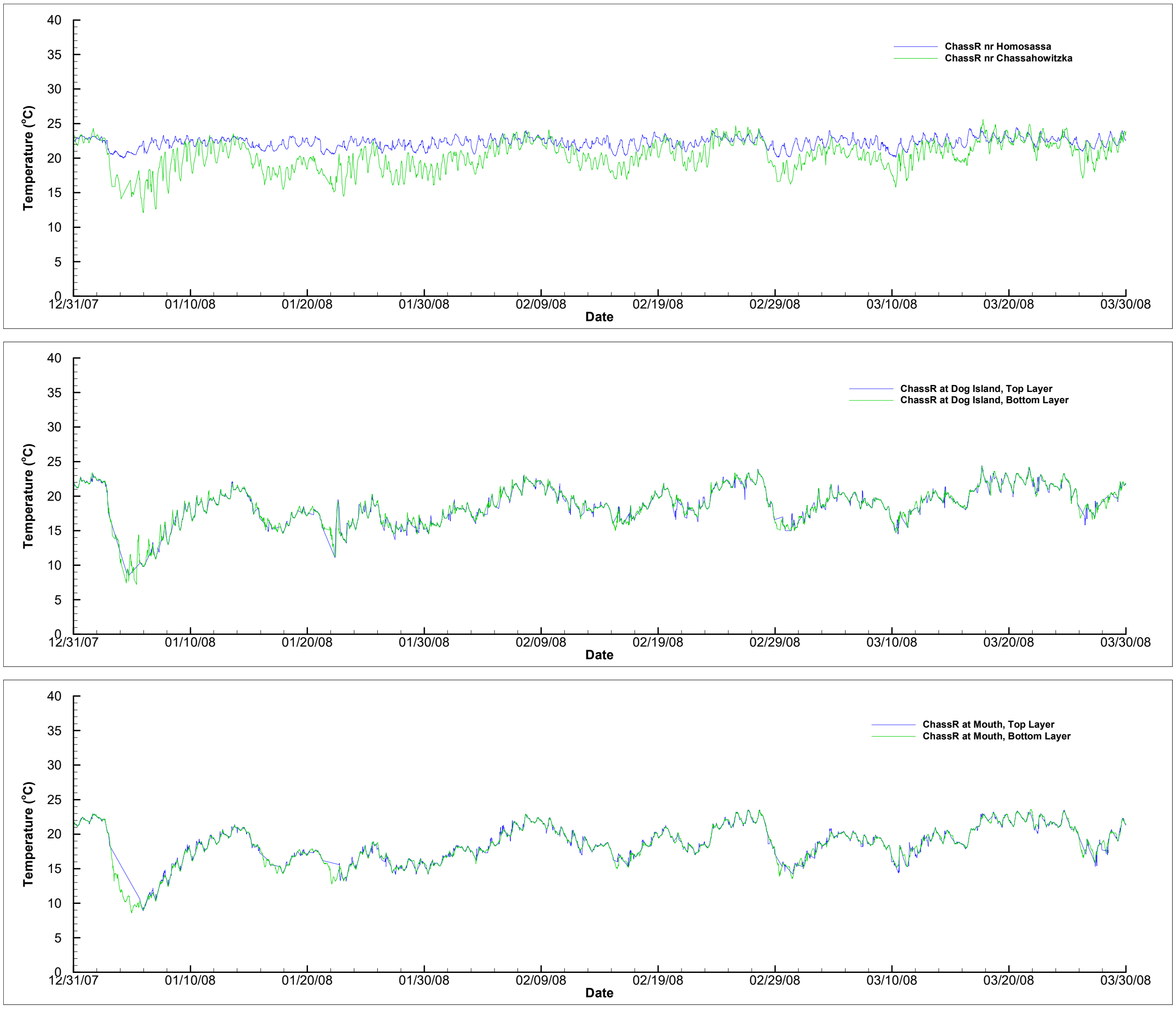

Figure C - 2. Measured real-time salinities at USGS Chassahowitzka near Homosassa (blue line, top panel), near Chassahowitzka (green line, top panel), at Dog Island (middle panel), and at Mouth (bottom panel) stations in the Chassahowitzka River during 12/31/2007 – 3/30/2008.

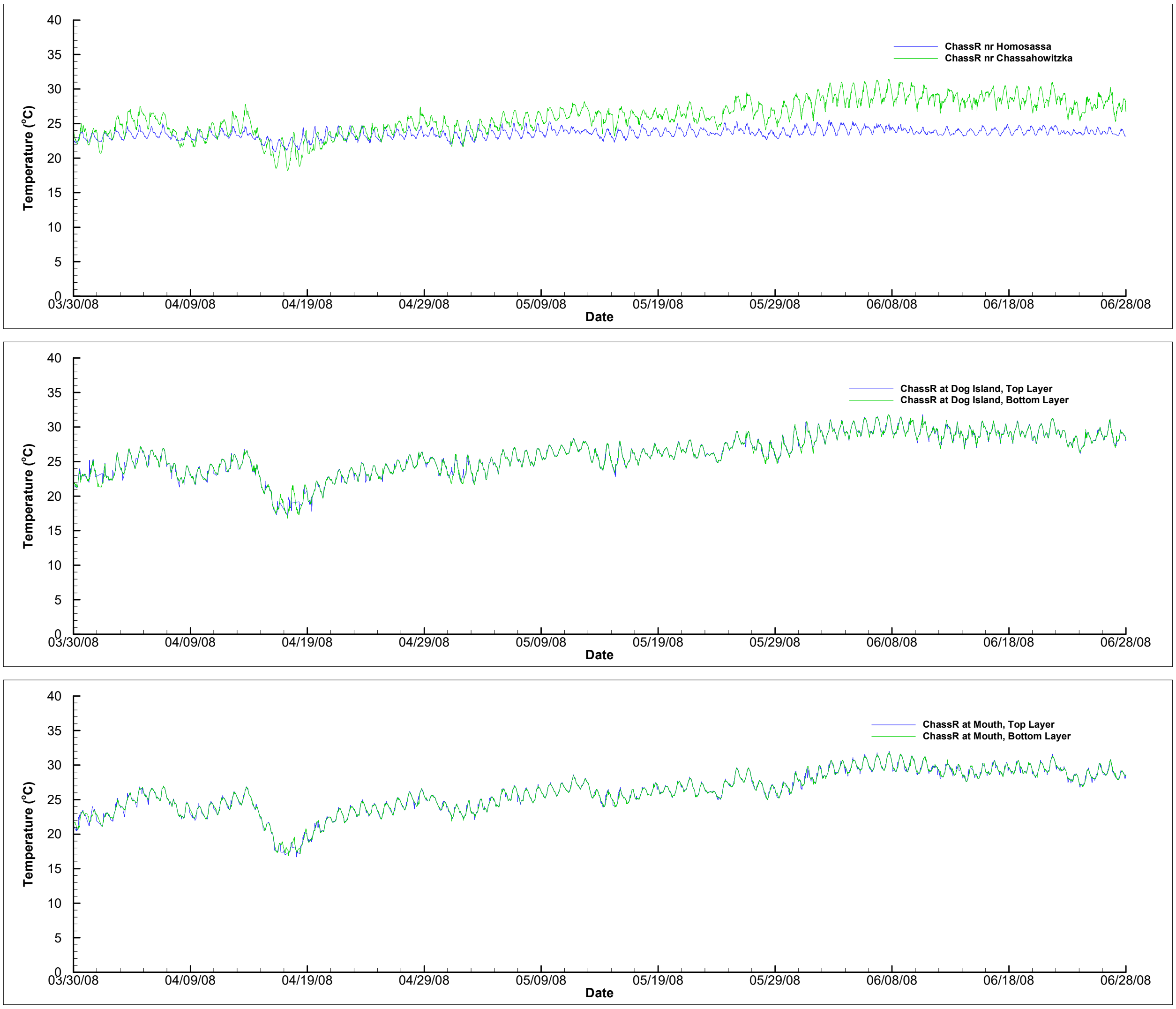

Figure C - 3. Measured real-time temperatures at USGS Chassahowitzka near Homosassa (blue line, top panel), near Chassahowitzka (green line, top panel), at Dog Island (middle panel), and at Mouth (bottom panel) stations in the Chassahowitzka River during 3/30/2008 – 6/28/2008.

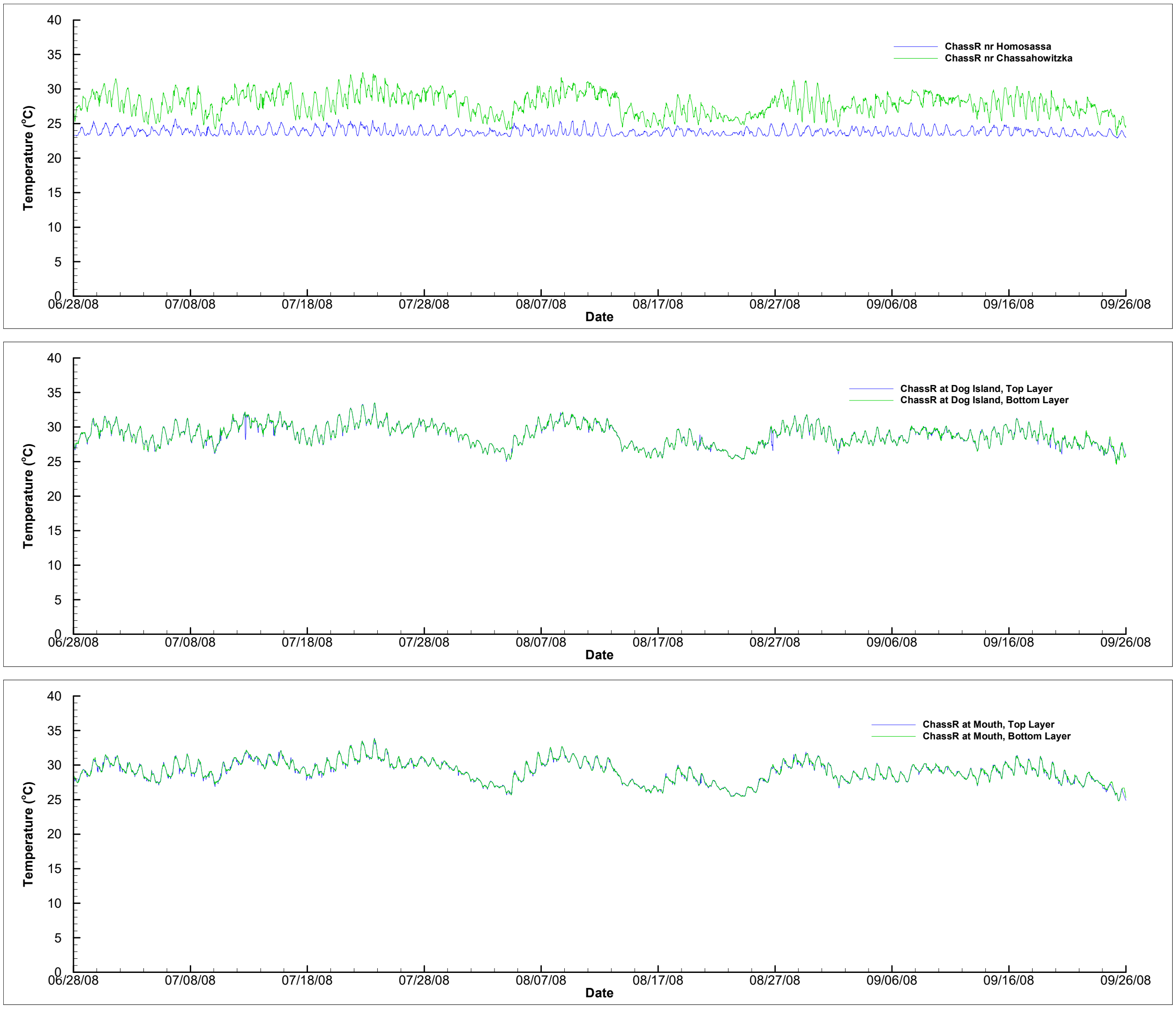

Figure C - 4. Measured real-time temperatures at USGS Chassahowitzka near Homosassa (blue line, top panel), near Chassahowitzka (green line, top panel), at Dog Island (middle panel), and at Mouth (bottom panel) stations in the Chassahowitzka River during 6/28/2008 – 9/26/08.

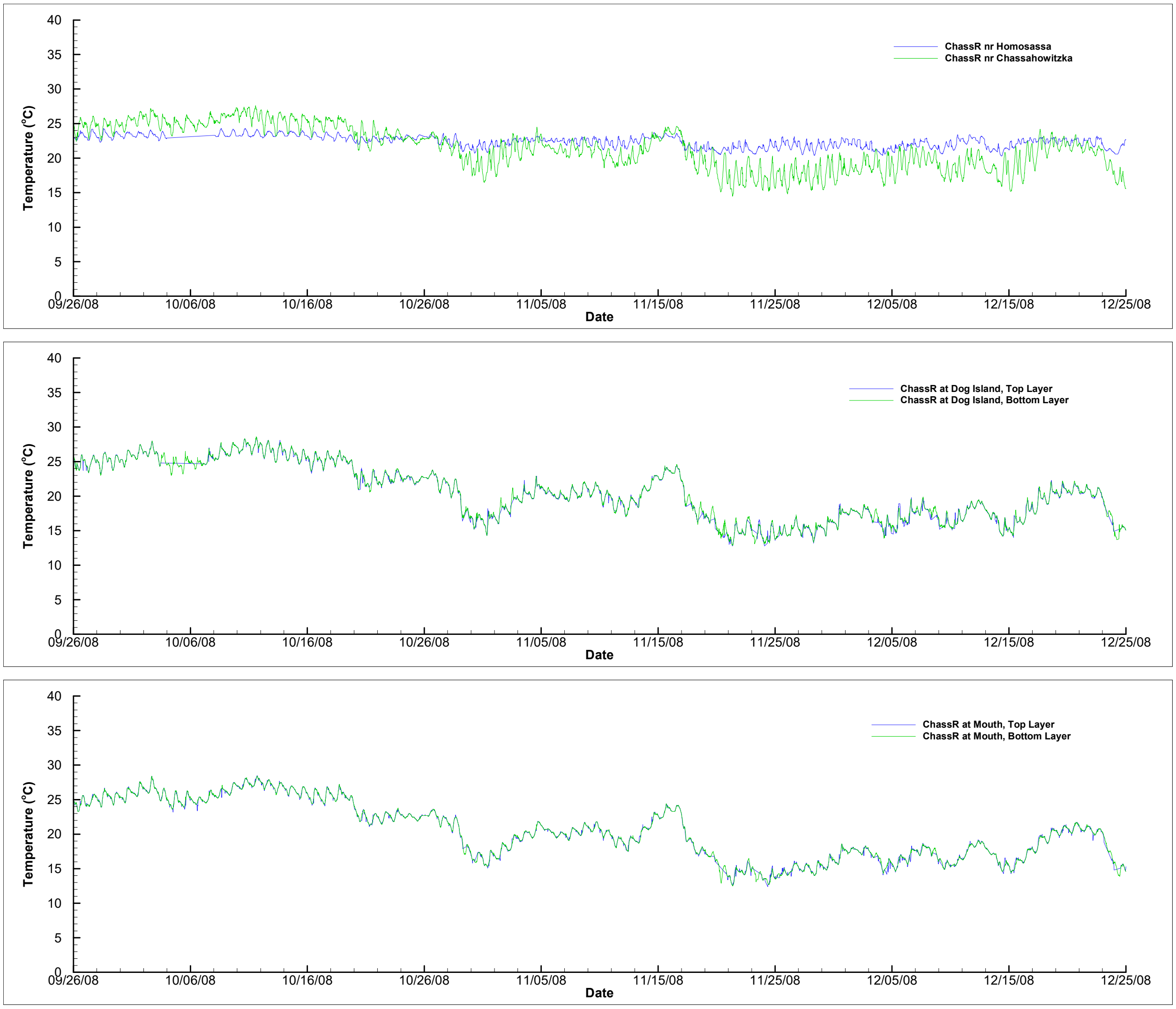

Figure C - 5. Measured real-time temperatures at USGS Chassahowitzka near Homosassa (blue line, top panel), near Chassahowitzka (green line, top panel), at Dog Island (middle panel), and at Mouth (bottom panel) stations in the Chassahowitzka River during 9/26/08 – 12/25/2008.

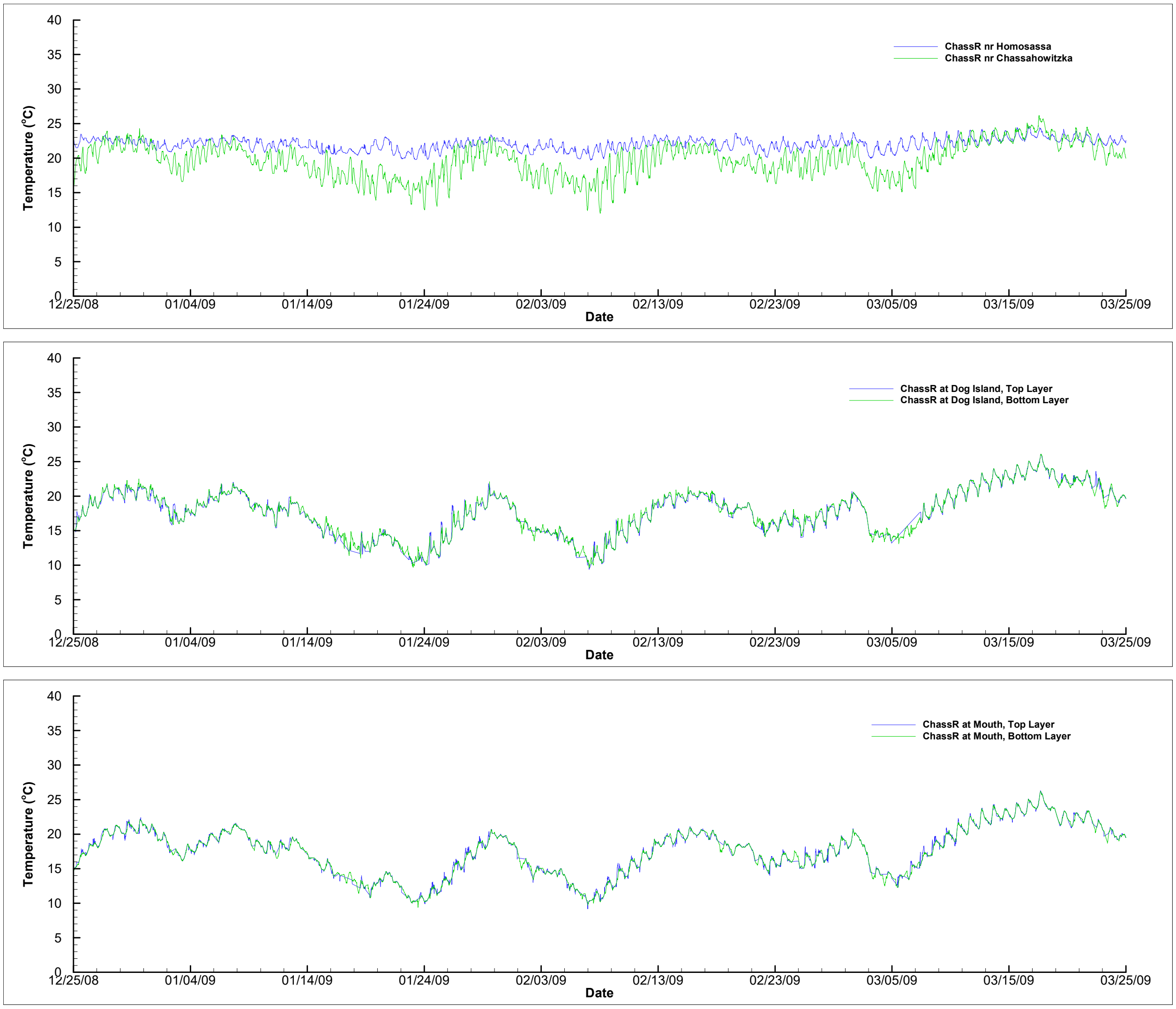

Figure C - 6. Measured real-time temperatures at USGS Chassahowitzka near Homosassa (blue line, top panel), near Chassahowitzka (green line, top panel), at Dog Island (middle panel), and at Mouth (bottom panel) stations in the Chassahowitzka River during 12/25/2008 – 3/25/2009.

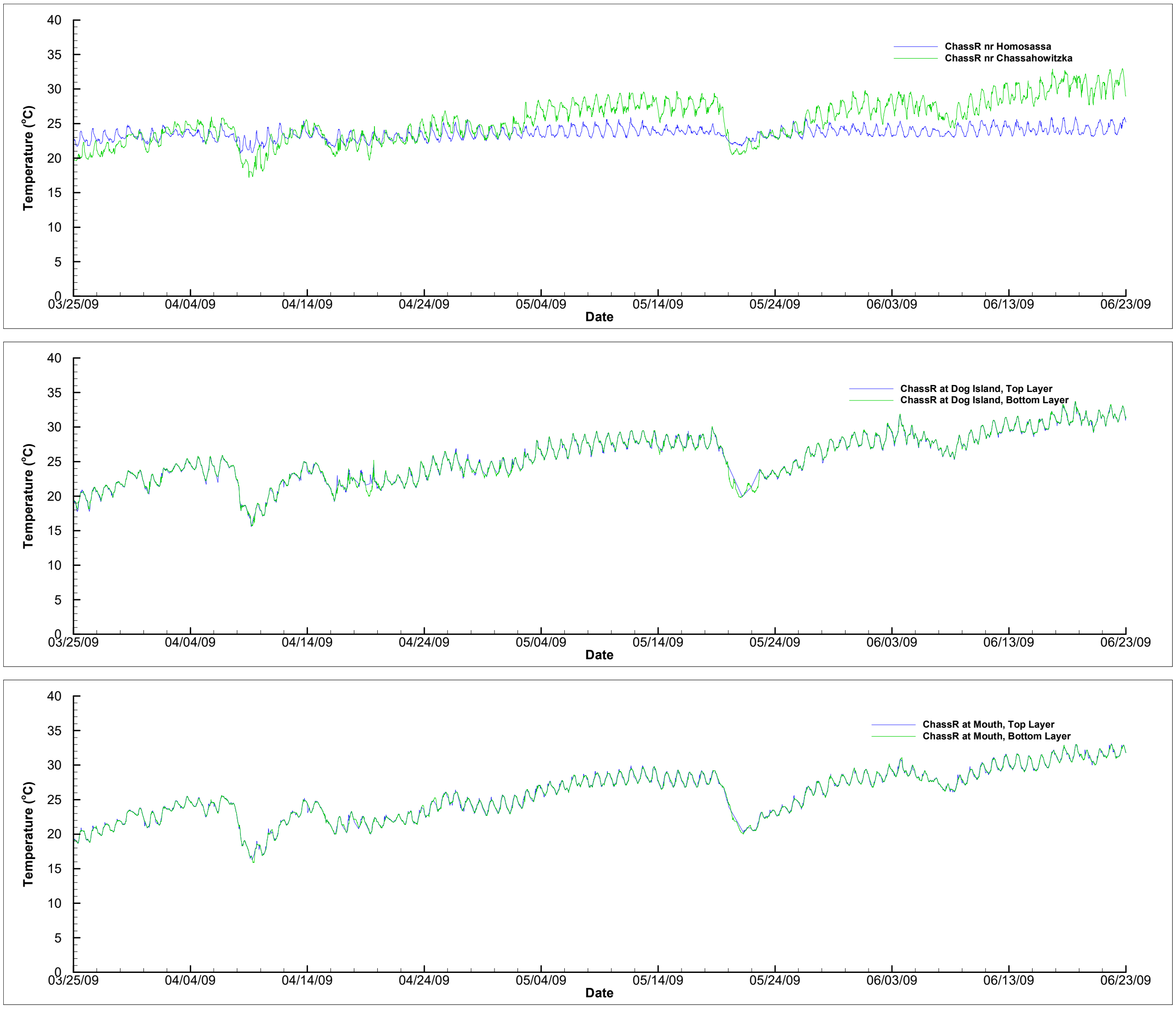

Figure C - 7. Measured real-time temperatures at USGS Chassahowitzka near Homosassa (blue line, top panel), near Chassahowitzka (green line, top panel), at Dog Island (middle panel), and at Mouth (bottom panel) stations in the Chassahowitzka River during 3/25/2009 – 6/23/2009.

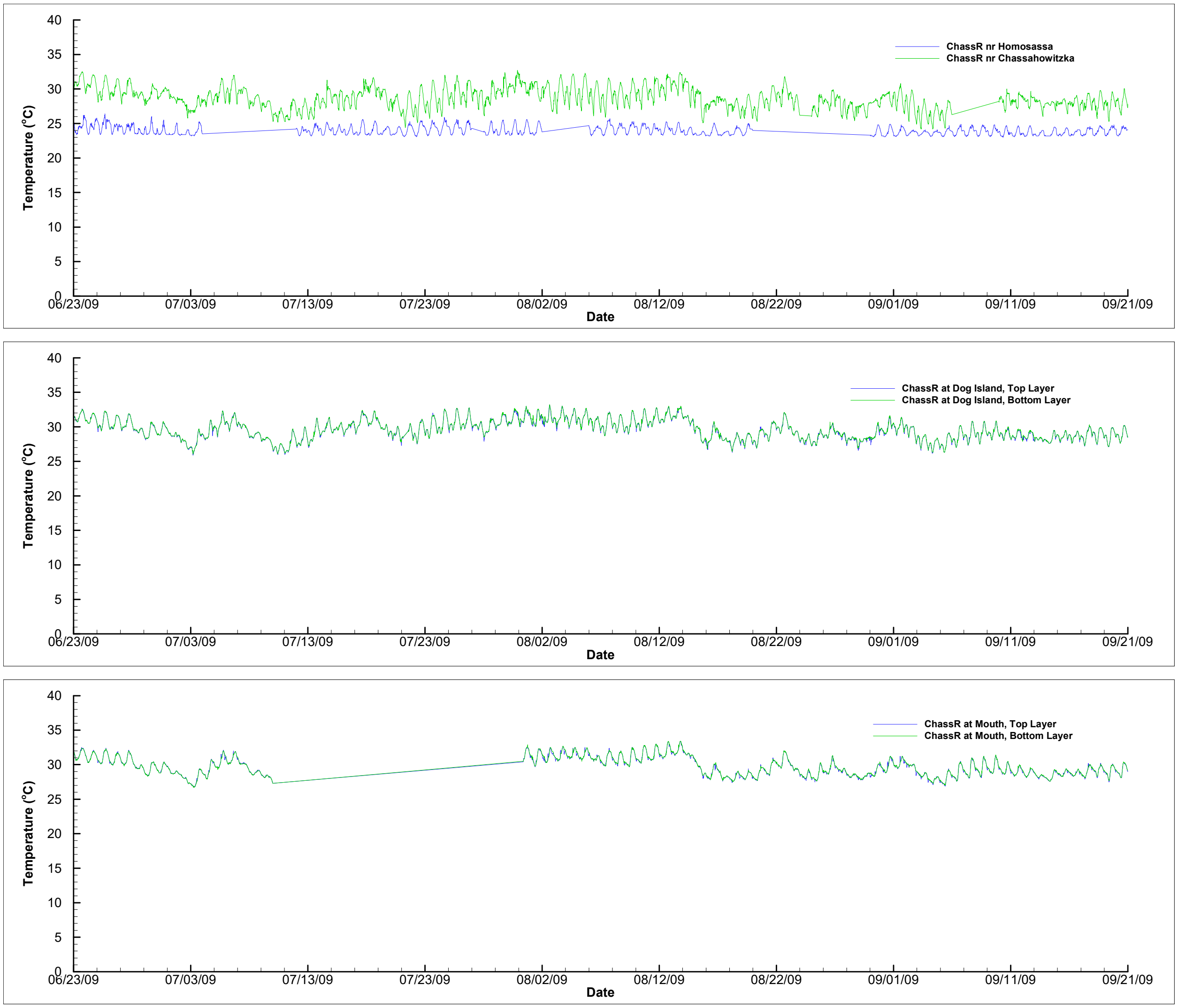

Figure C - 8. Measured real-time temperatures at USGS Chassahowitzka near Homosassa (blue line, top panel), near Chassahowitzka (green line, top panel), at Dog Island (middle panel), and at Mouth (bottom panel) stations in the Chassahowitzka River during 6/23/2009 – 9/21/2009.

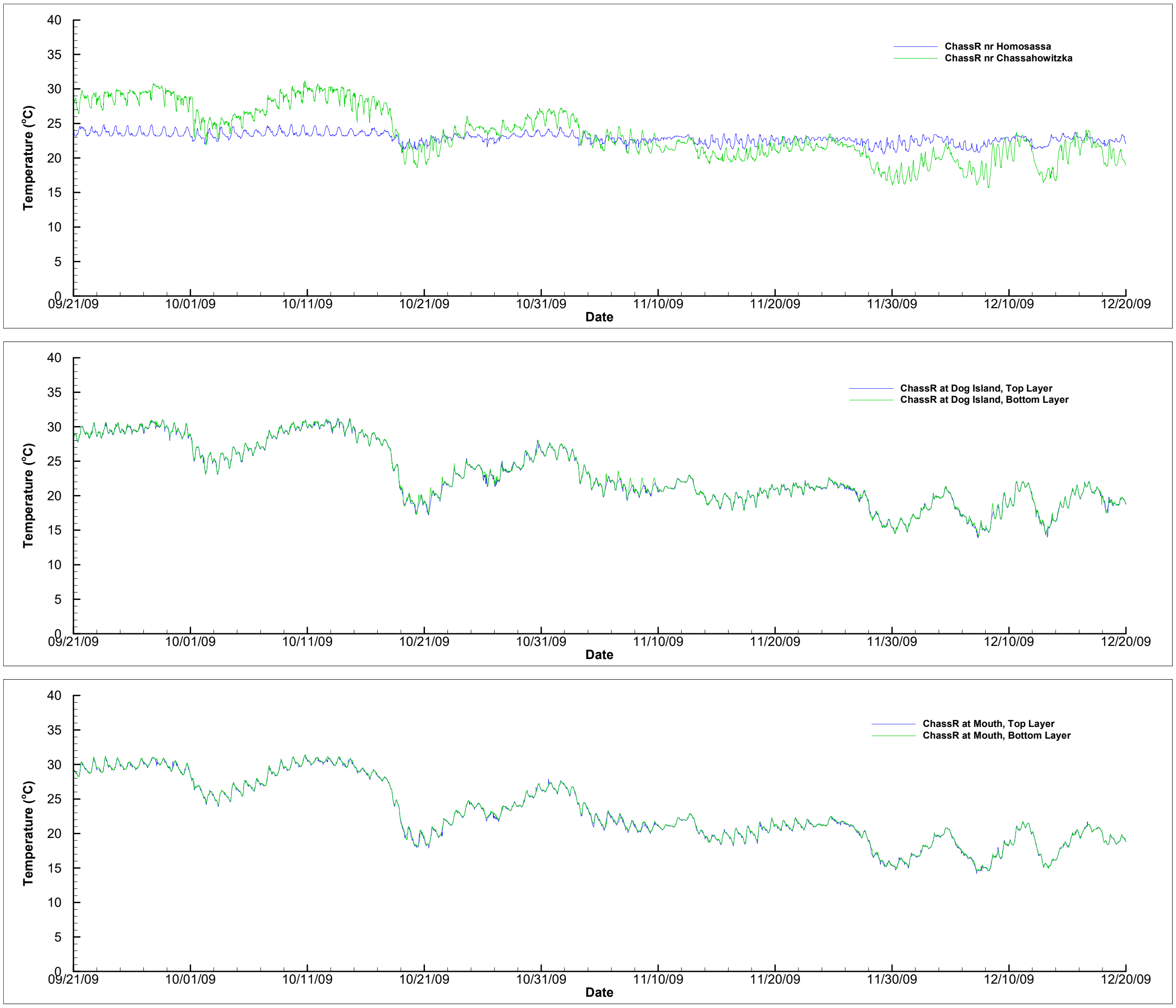

Figure C - 9. Measured real-time temperatures at USGS Chassahowitzka near Homosassa (blue line, top panel), near Chassahowitzka (green line, top panel), at Dog Island (middle panel), and at Mouth (bottom panel) stations in the Chassahowitzka River during 9/21/2009 - 12/20/2009.

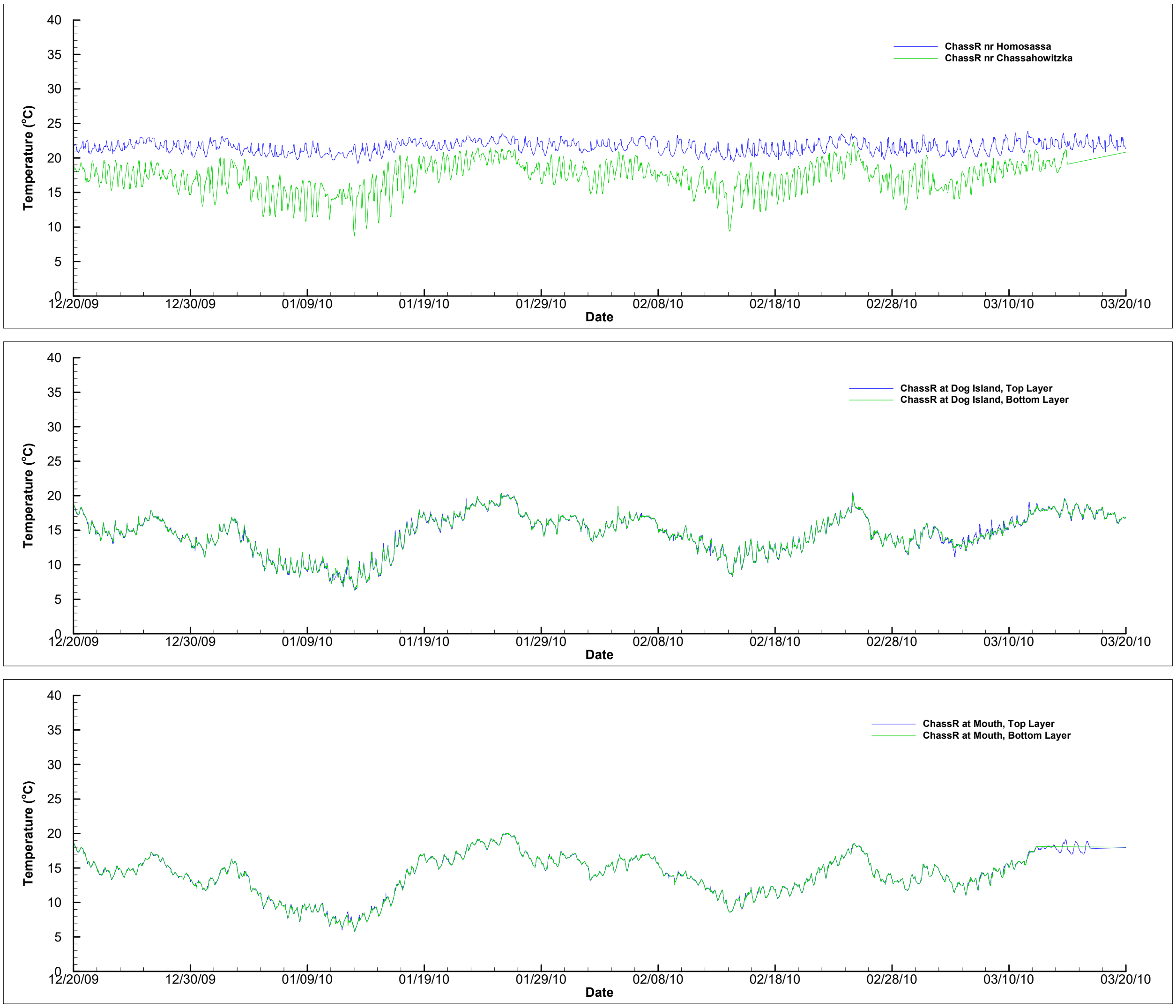

Figure C - 10. Measured real-time temperatures at USGS Chassahowitzka near Homosassa (blue line, top panel), near Chassahowitzka (green line, top panel), at Dog Island (middle panel), and at Mouth (bottom panel) stations in the Chassahowitzka River during 12/20/2009 – 3/20/2010.

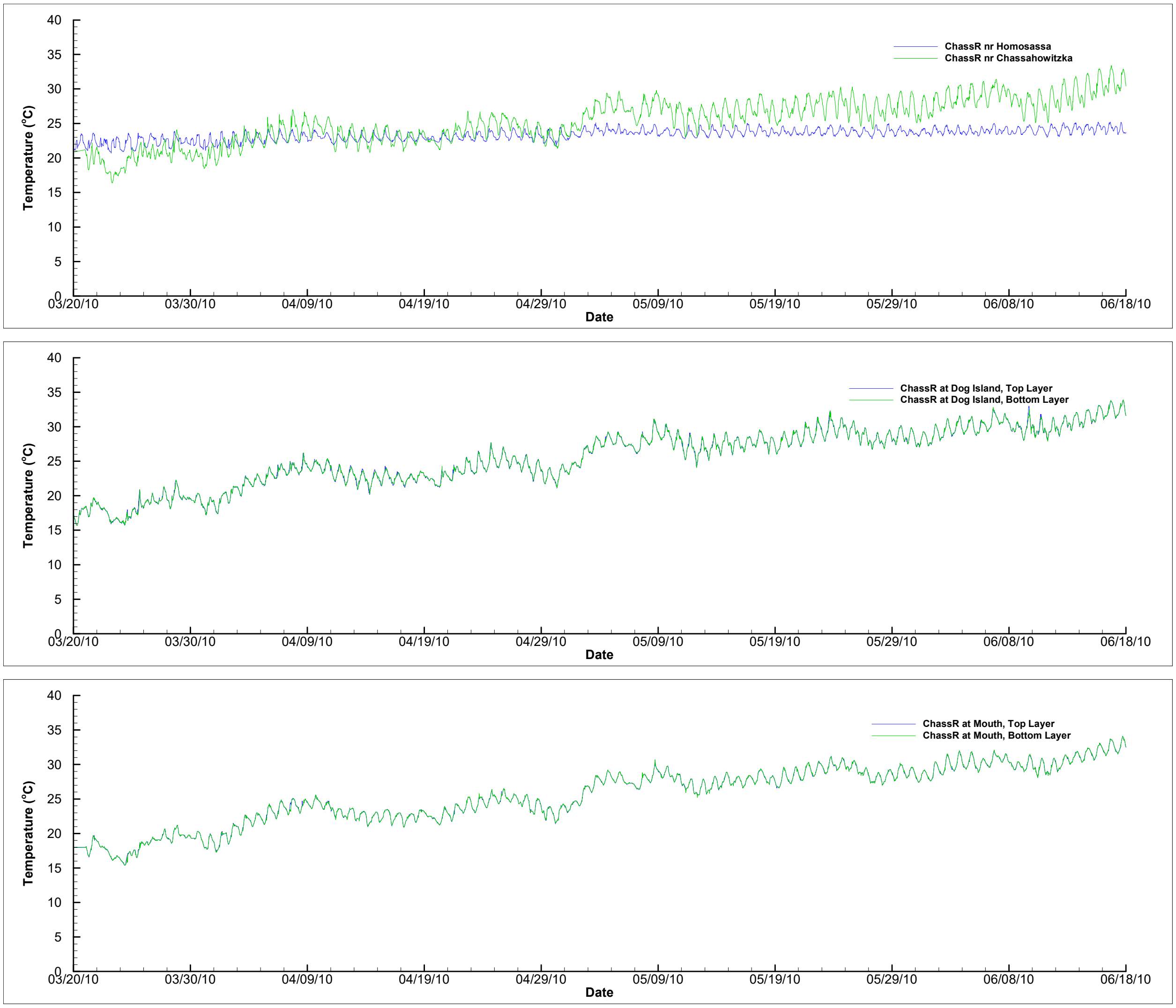

Figure C - 11. Measured real-time temperatures at USGS Chassahowitzka near Homosassa (blue line, top panel), near Chassahowitzka (green line, top panel), at Dog Island (middle panel), and at Mouth (bottom panel) stations in the Chassahowitzka River during 3/20/2010 – 6/18/2010.

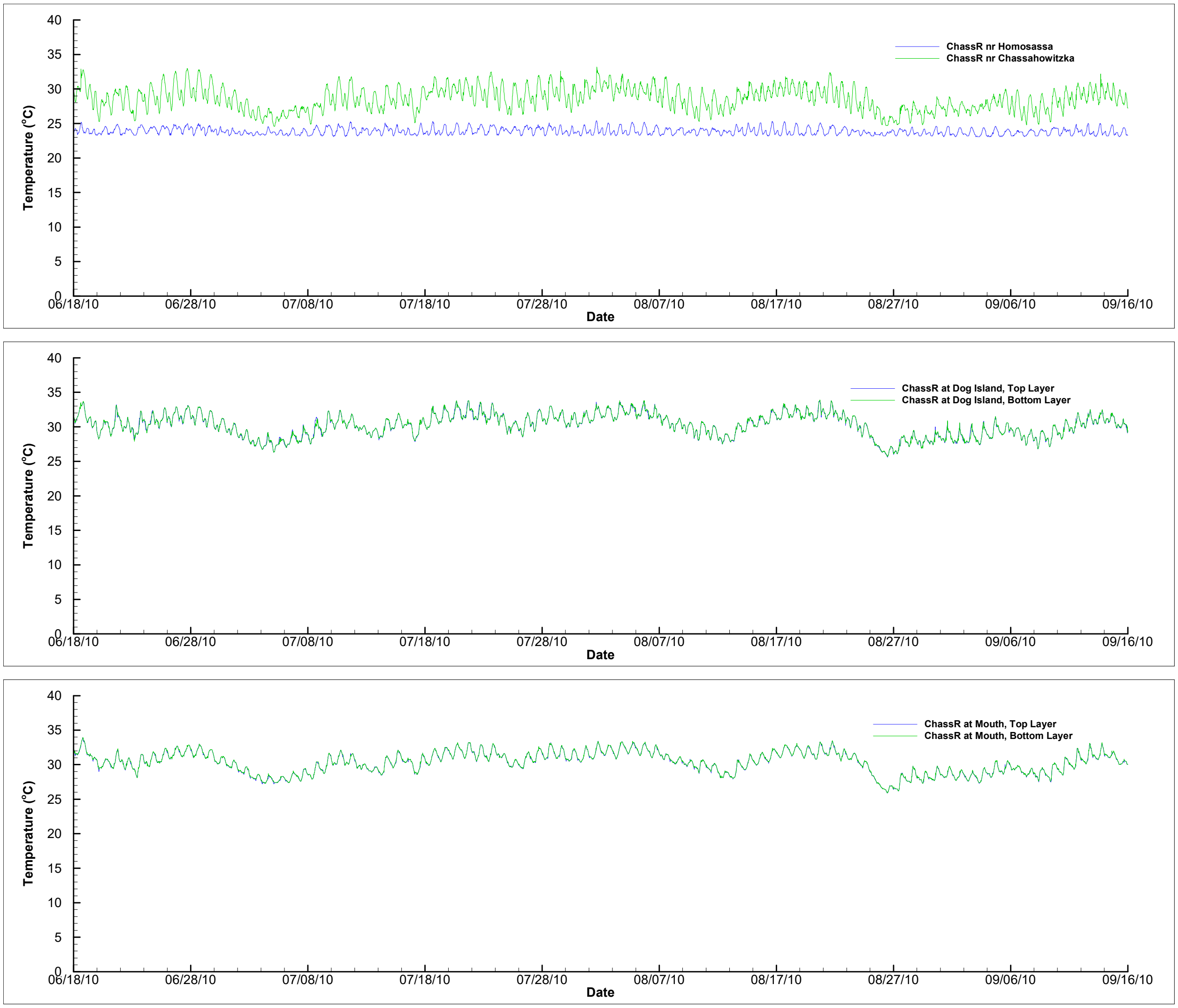

Figure C - 12. Measured real-time temperatures at USGS Chassahowitzka near Homosassa (blue line, top panel), near Chassahowitzka (green line, top panel), at Dog Island (middle panel), and at Mouth (bottom panel) stations in the Chassahowitzka River during 6/18/2010 – 9/16/2010.

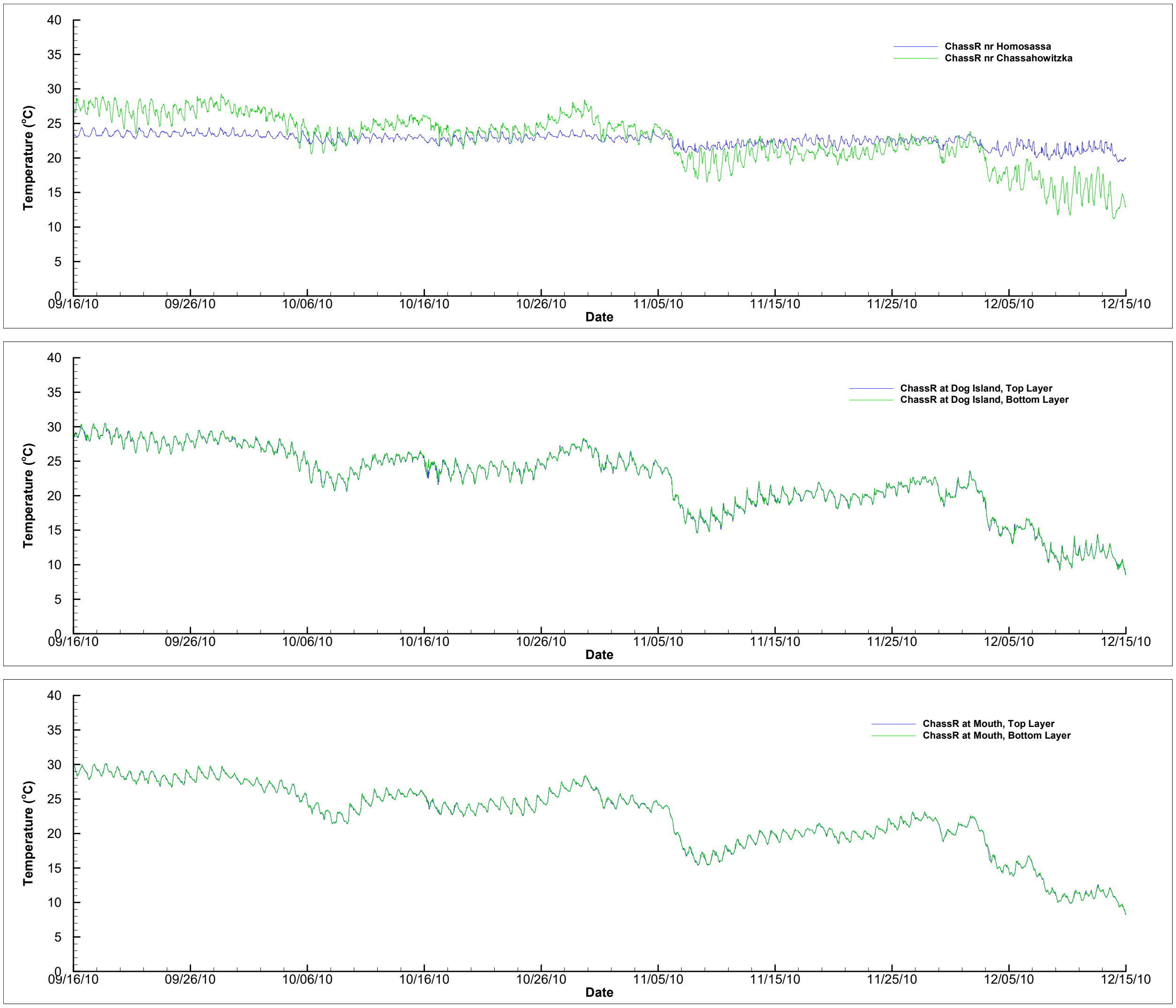

Figure C - 13. Measured real-time temperatures at USGS Chassahowitzka near Homosassa (blue line, top panel), near Chassahowitzka (green line, top panel), at Dog Island (middle panel), and at Mouth (bottom panel) stations in the Chassahowitzka River during 9/16/2010 - 12/15/2010.

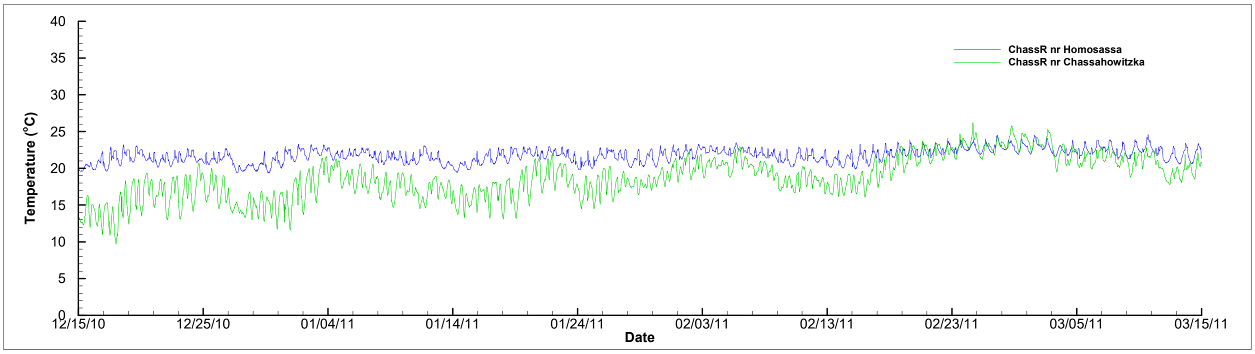

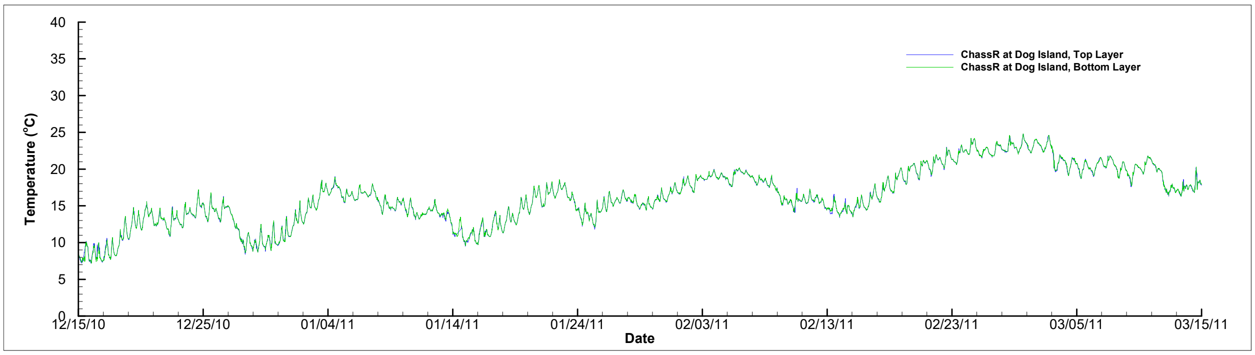

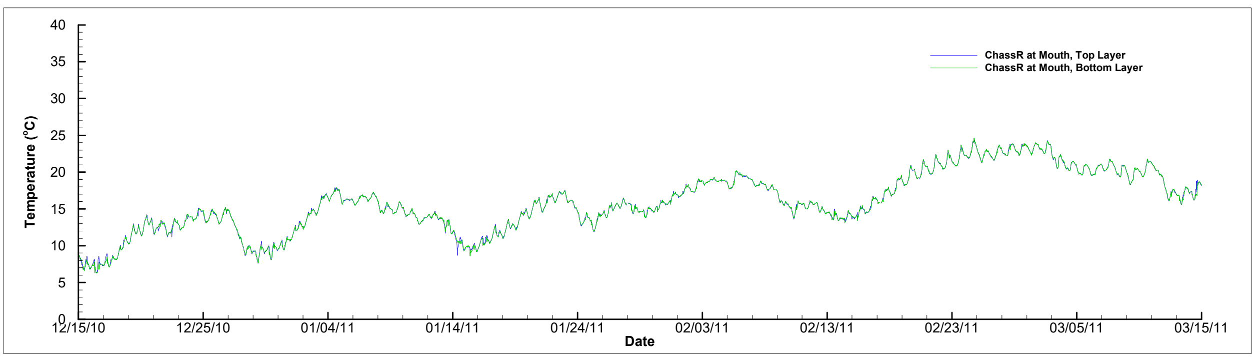

Figure C - 14. Measured real-time temperatures at USGS Chassahowitzka near Homosassa (blue line, top panel), near Chassahowitzka (green line, top panel), at Dog Island (middle panel), and at Mouth (bottom panel) stations in the Chassahowitzka River during 12/15/2010 – 3/15/2011.

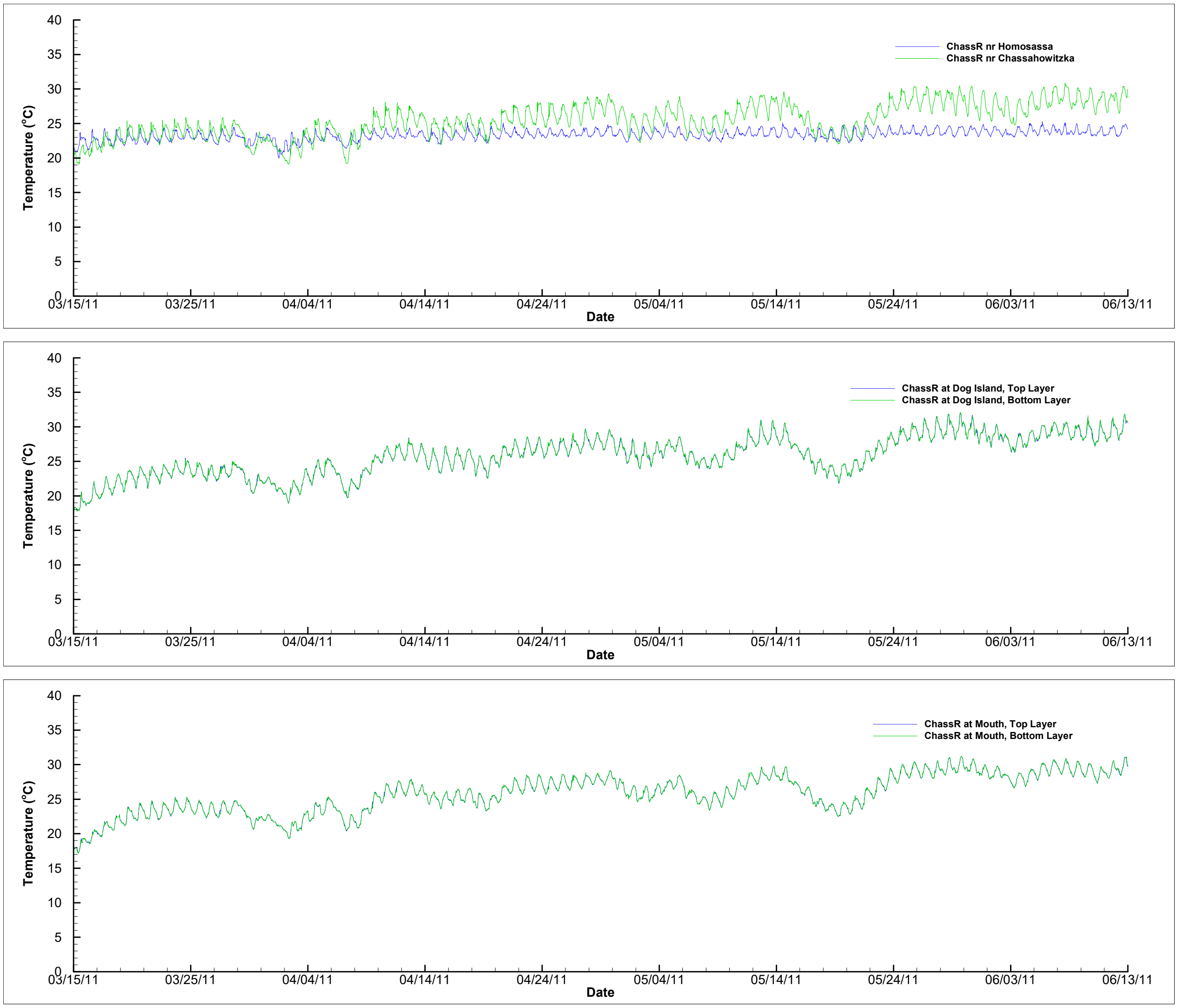

Figure C - 15. Measured real-time temperatures at USGS Chassahowitzka near Homosassa (blue line, top panel), near Chassahowitzka (green line, top panel), at Dog Island (middle panel), and at Mouth (bottom panel) stations in the Chassahowitzka River during 3/15/2011 - 6/13/2011.

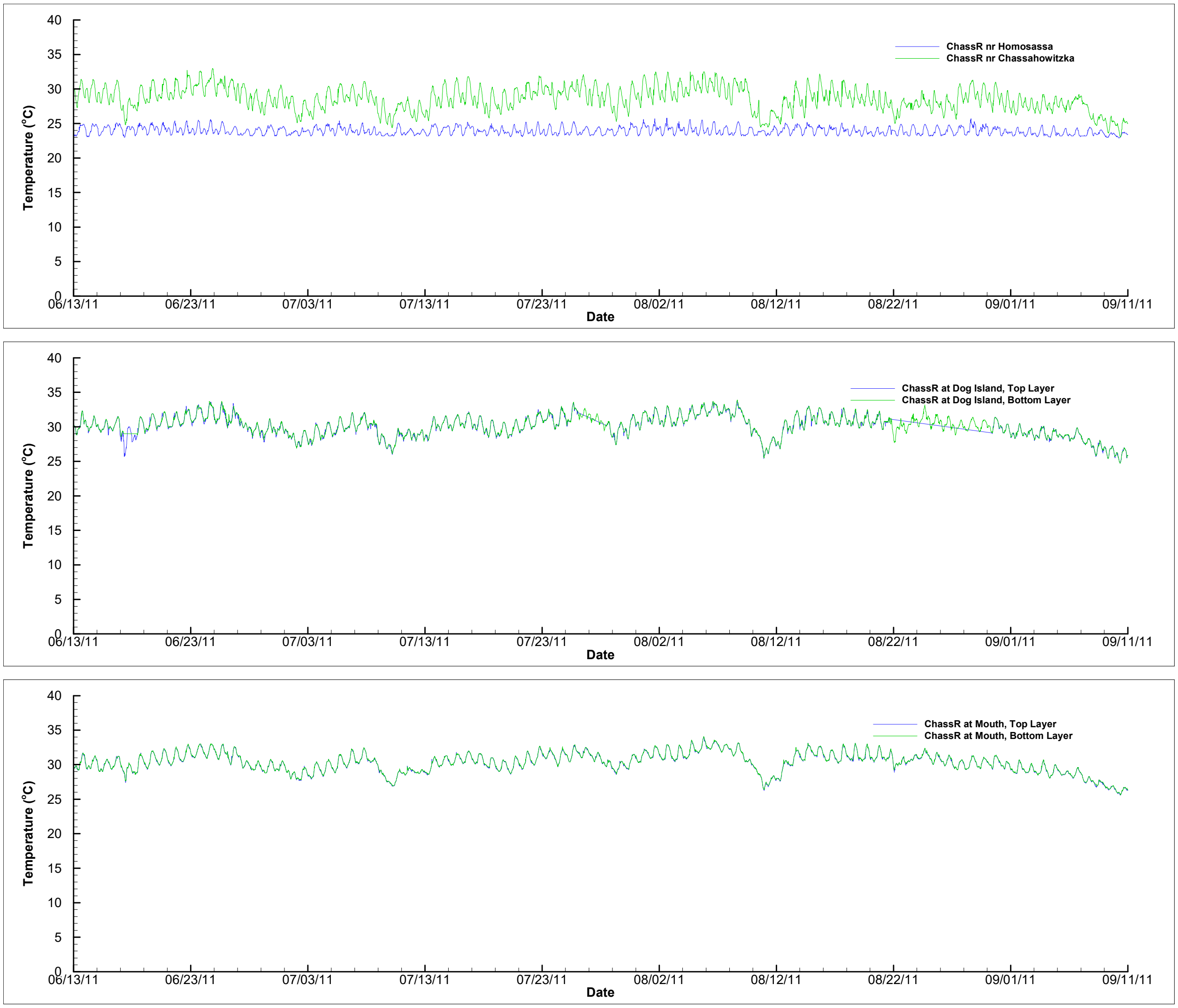

Figure C - 16. Measured real-time temperatures at USGS Chassahowitzka near Homosassa (blue line, top panel), near Chassahowitzka (green line, top panel), at Dog Island (middle panel), and at Mouth (bottom panel) stations in the Chassahowitzka River during 6/13/2011 - 9/11/2011.

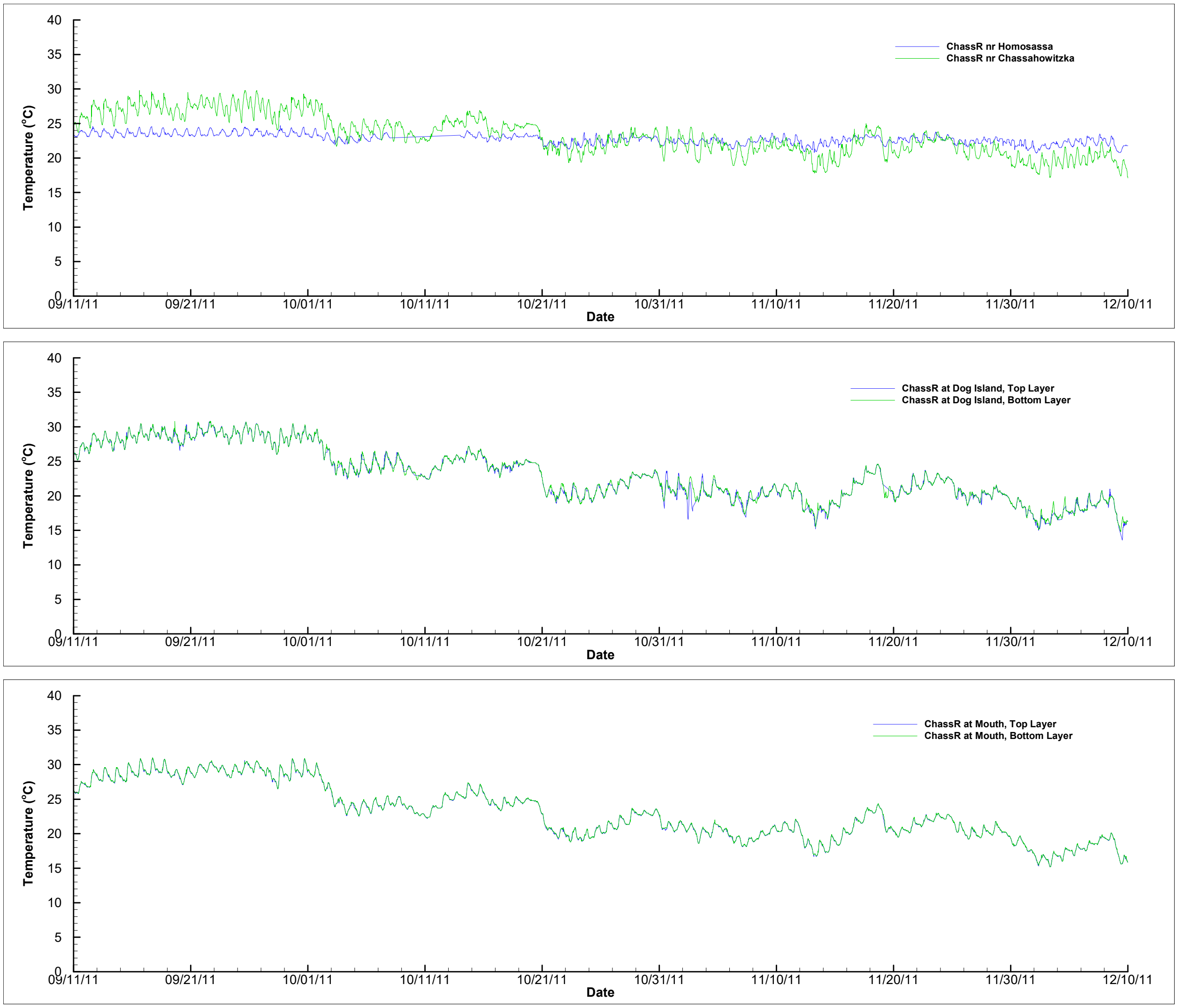

Figure C - 17. Measured real-time temperatures at USGS Chassahowitzka near Homosassa (blue line, top panel), near Chassahowitzka (green line, top panel), at Dog Island (middle panel), and at Mouth (bottom panel) stations in the Chassahowitzka River during 9/11/2011 - 12/10/2011.

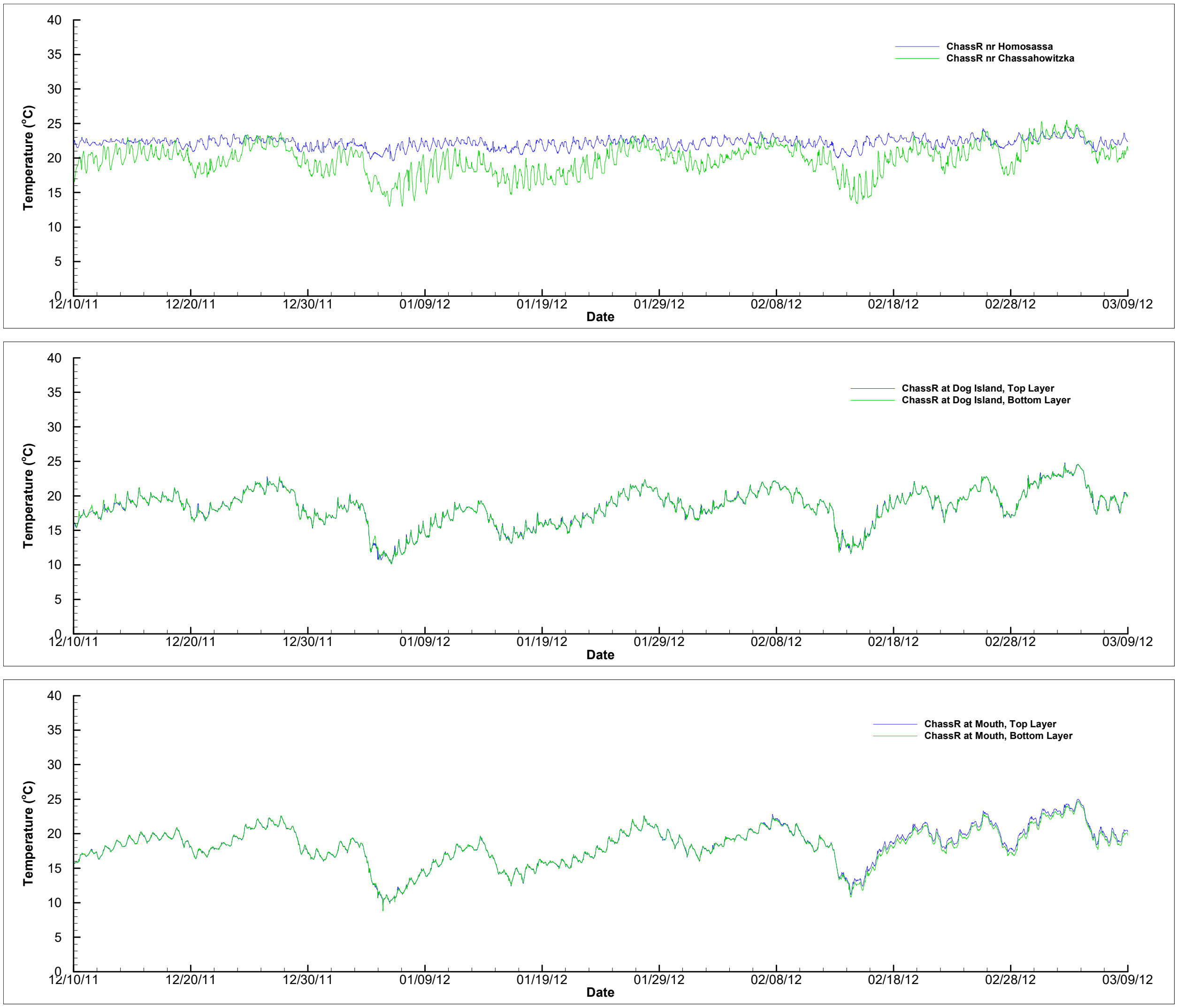

Figure C - 18. Measured real-time temperatures at USGS Chassahowitzka near Homosassa (blue line, top panel), near Chassahowitzka (green line, top panel), at Dog Island (middle panel), and at Mouth (bottom panel) stations in the Chassahowitzka River during 12/10/2011 – 3/9/2012.

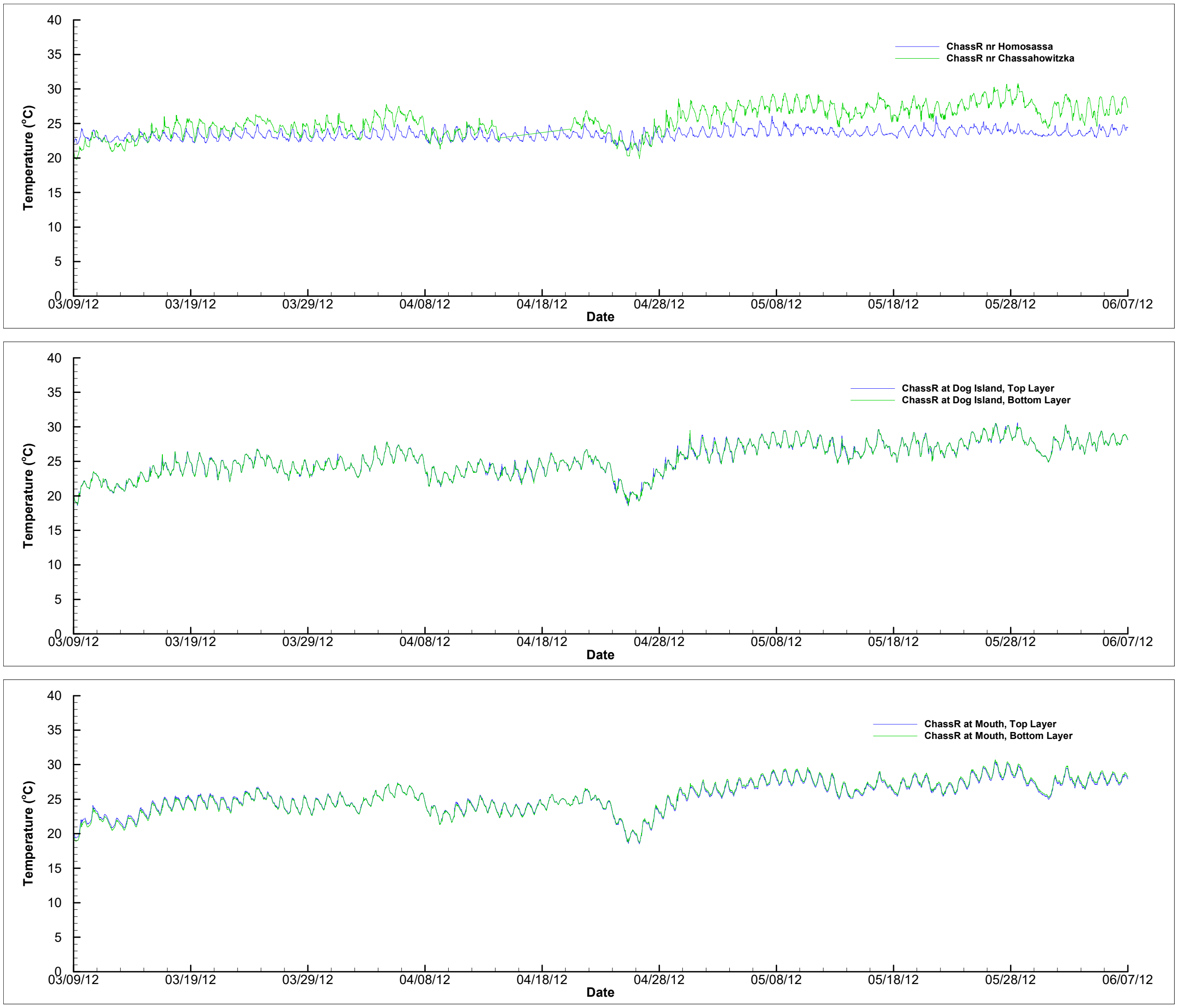

Figure C - 19. Measured real-time temperatures at USGS Chassahowitzka near Homosassa (blue line, top panel), near Chassahowitzka (green line, top panel), at Dog Island (middle panel), and at Mouth (bottom panel) stations in the Chassahowitzka River during 3/9/2012 - 6/7/2012.

Figure C - 20. Measured real-time temperatures at USGS Chassahowitzka near Homosassa (blue line, top panel), near Chassahowitzka (green line, top panel), at Dog Island (middle panel), and at Mouth (bottom panel) stations in the Chassahowitzka River during 6/7/2012 - 9/5/2012.

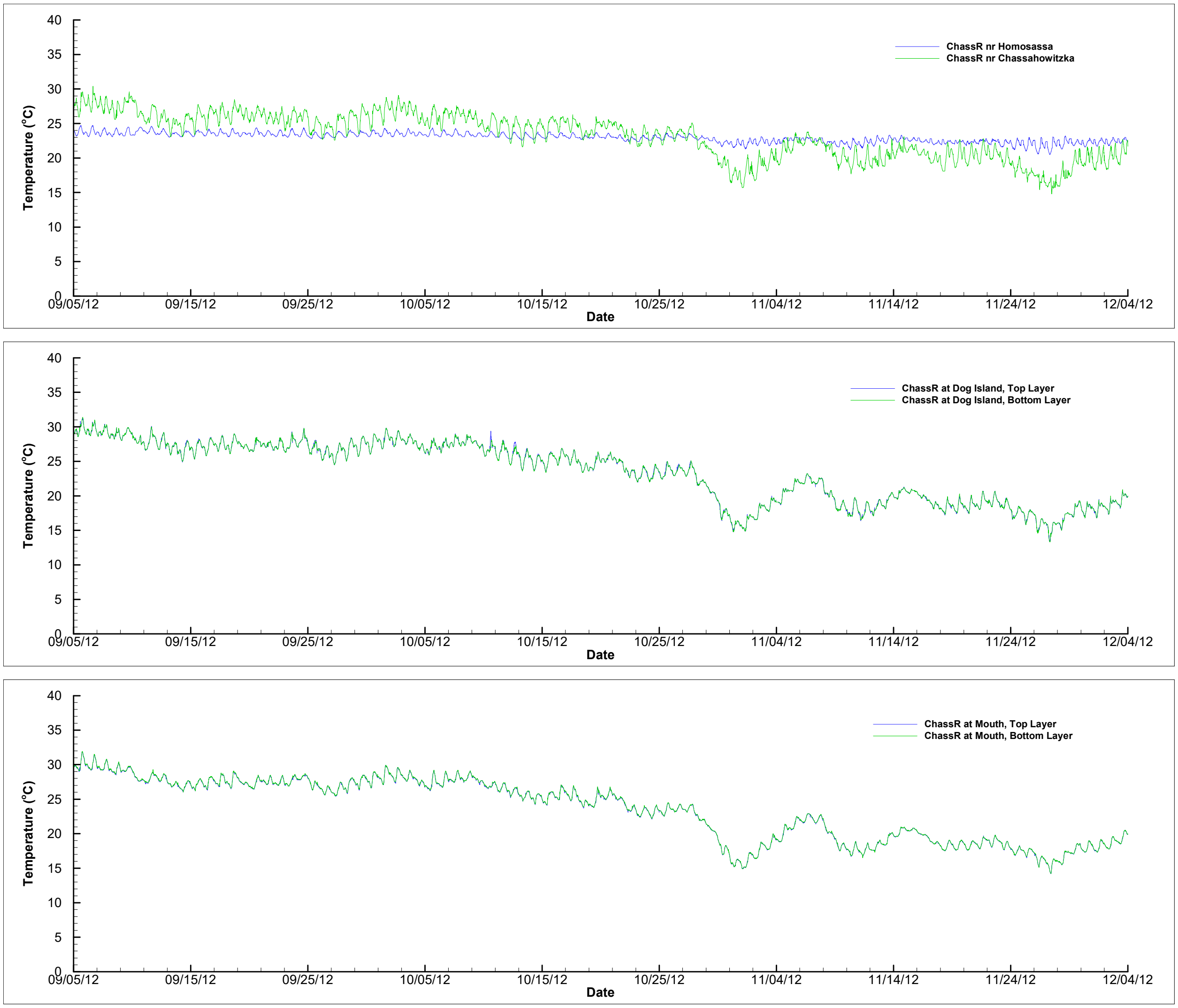

Figure C - 21. Measured real-time temperatures at USGS Chassahowitzka near Homosassa (blue line, top panel), near Chassahowitzka (green line, top panel), at Dog Island (middle panel), and at Mouth (bottom panel) stations in the Chassahowitzka River during 9/5/2012 – 12/4/2012.

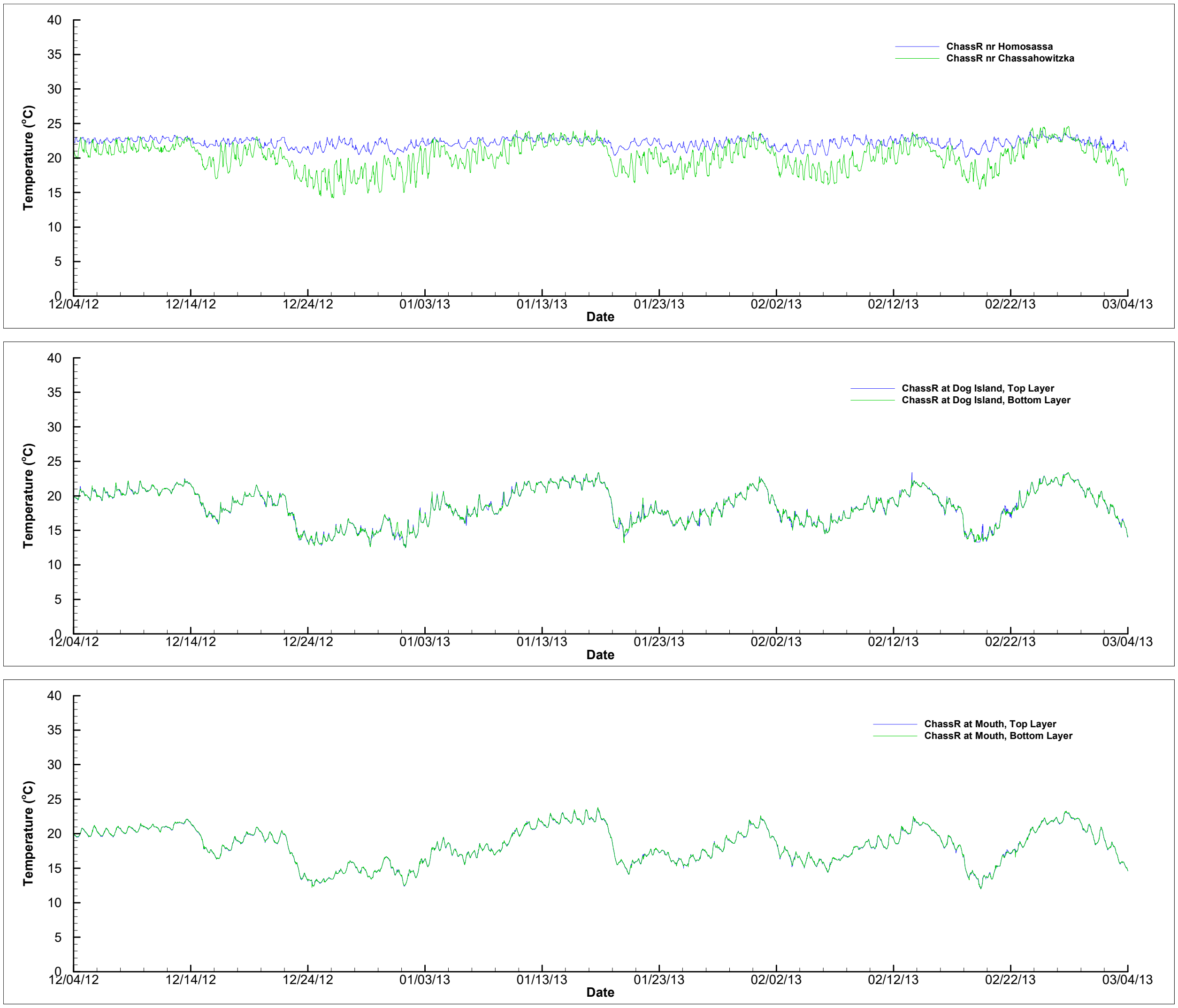

Figure C - 22. Measured real-time temperatures at USGS Chassahowitzka near Homosassa (blue line, top panel), near Chassahowitzka (green line, top panel), at Dog Island (middle panel), and at Mouth (bottom panel) stations in the Chassahowitzka River during 12/4/2012 – 3/4/2013.

Figure C - 23. Measured real-time temperatures at USGS Chassahowitzka near Homosassa (blue line, top panel), near Chassahowitzka (green line, top panel), at Dog Island (middle panel), and at Mouth (bottom panel) stations in the Chassahowitzka River during 3/4/2013 – 6/2/2013.

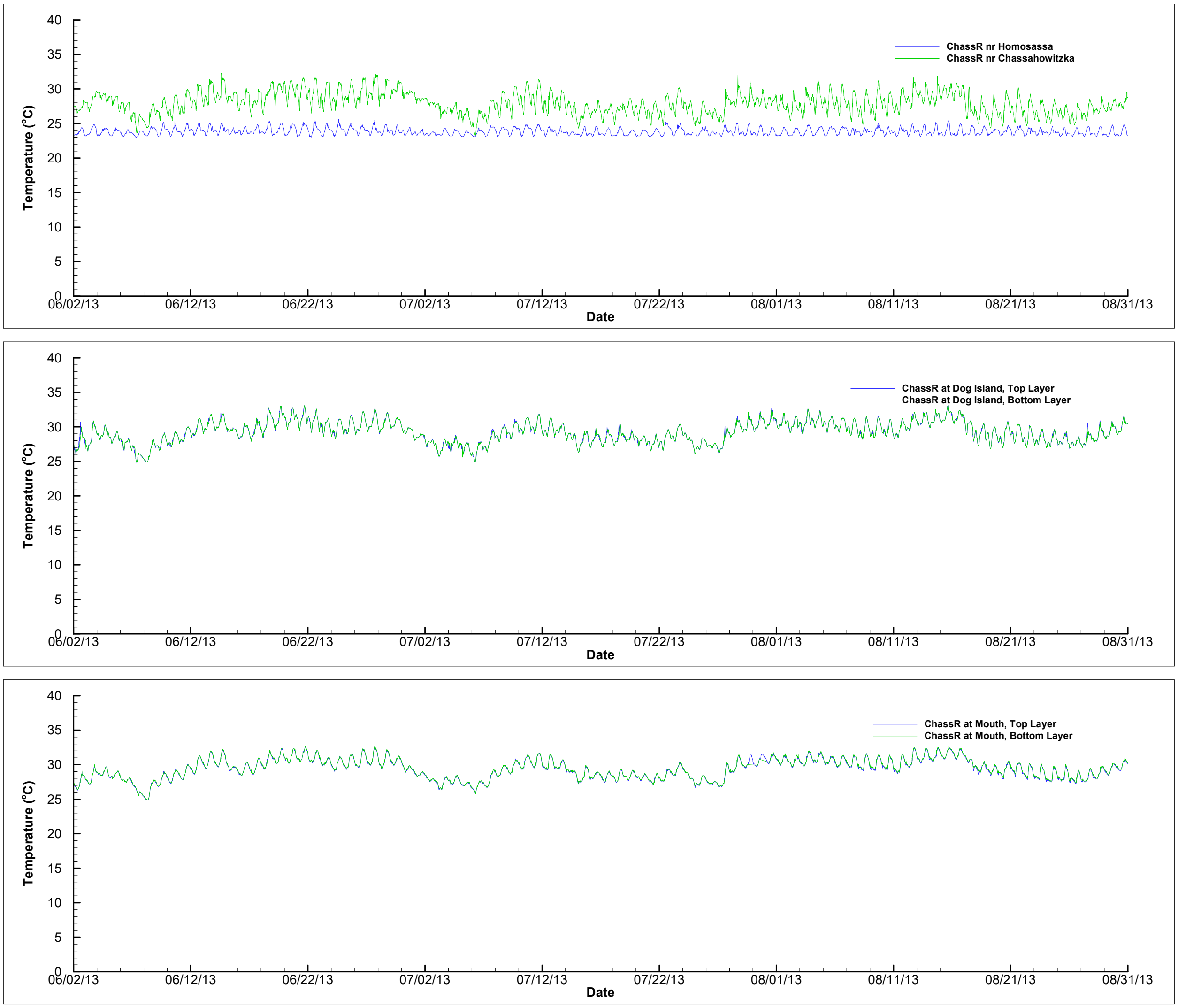

Figure C - 24. Measured real-time temperatures at USGS Chassahowitzka near Homosassa (blue line, top panel), near Chassahowitzka (green line, top panel), at Dog Island (middle panel), and at Mouth (bottom panel) stations in the Chassahowitzka River during 6/2/2013 – 8/31/2013.

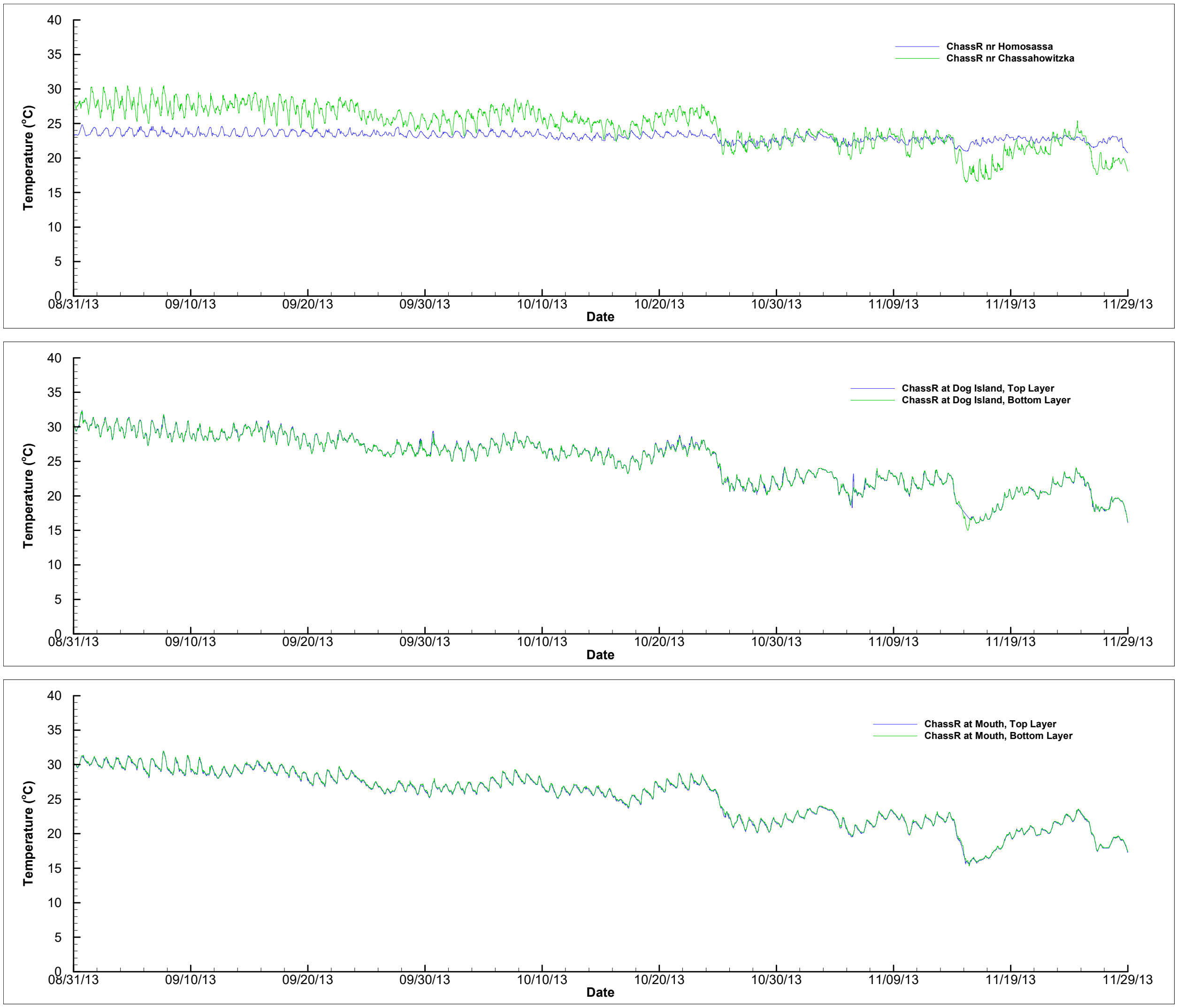

Figure C - 25. Measured real-time temperatures at USGS Chassahowitzka near Homosassa (blue line, top panel), near Chassahowitzka (green line, top panel), at Dog Island (middle panel), and at Mouth (bottom panel) stations in the Chassahowitzka River during 8/31/2013 - 11/29/2013.

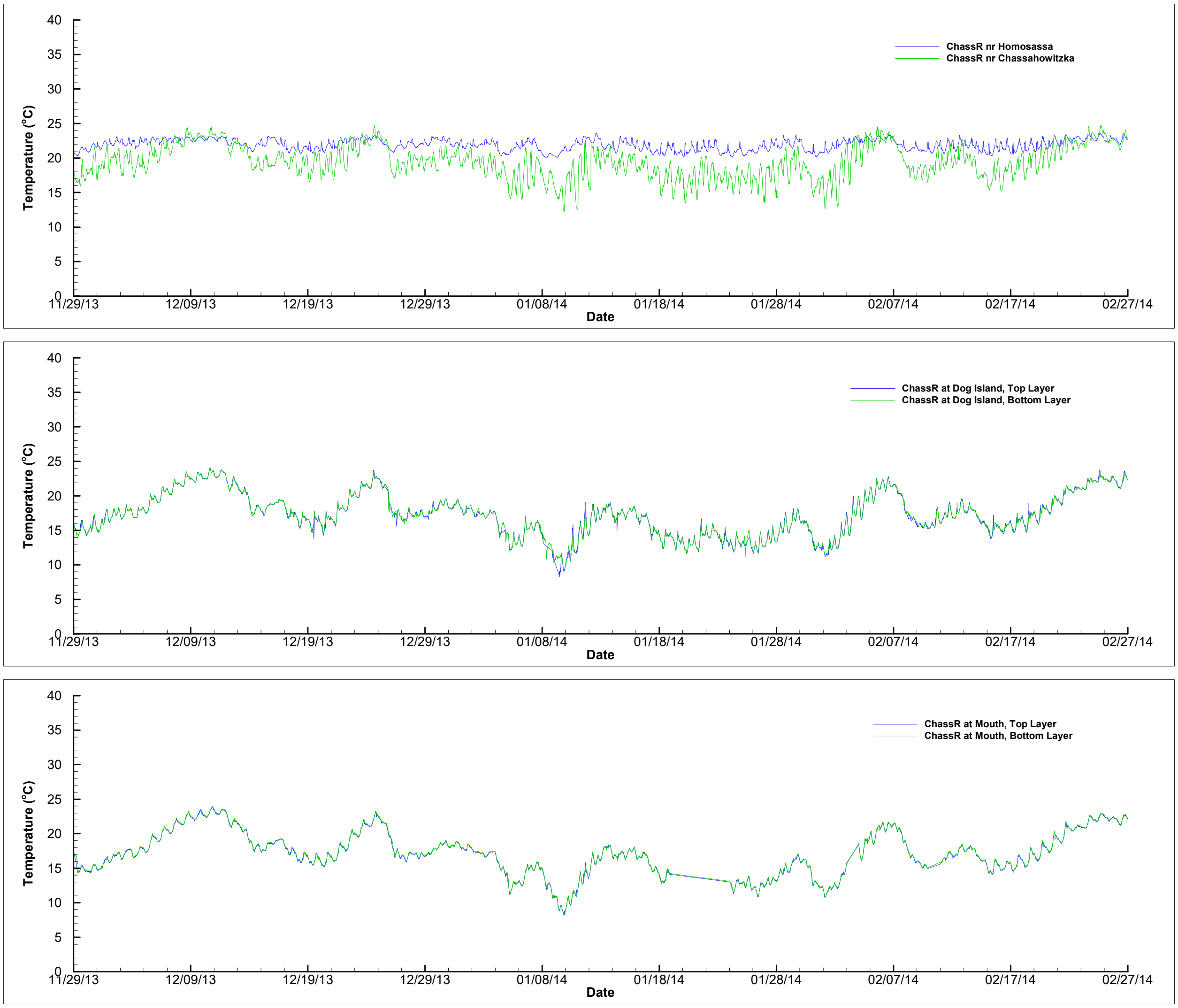

Figure C - 26. Measured real-time temperatures at USGS Chassahowitzka near Homosassa (blue line, top panel), near Chassahowitzka (green line, top panel), at Dog Island (middle panel), and at Mouth (bottom panel) stations in the Chassahowitzka River during 11/29/2013 - 2/27/2014.

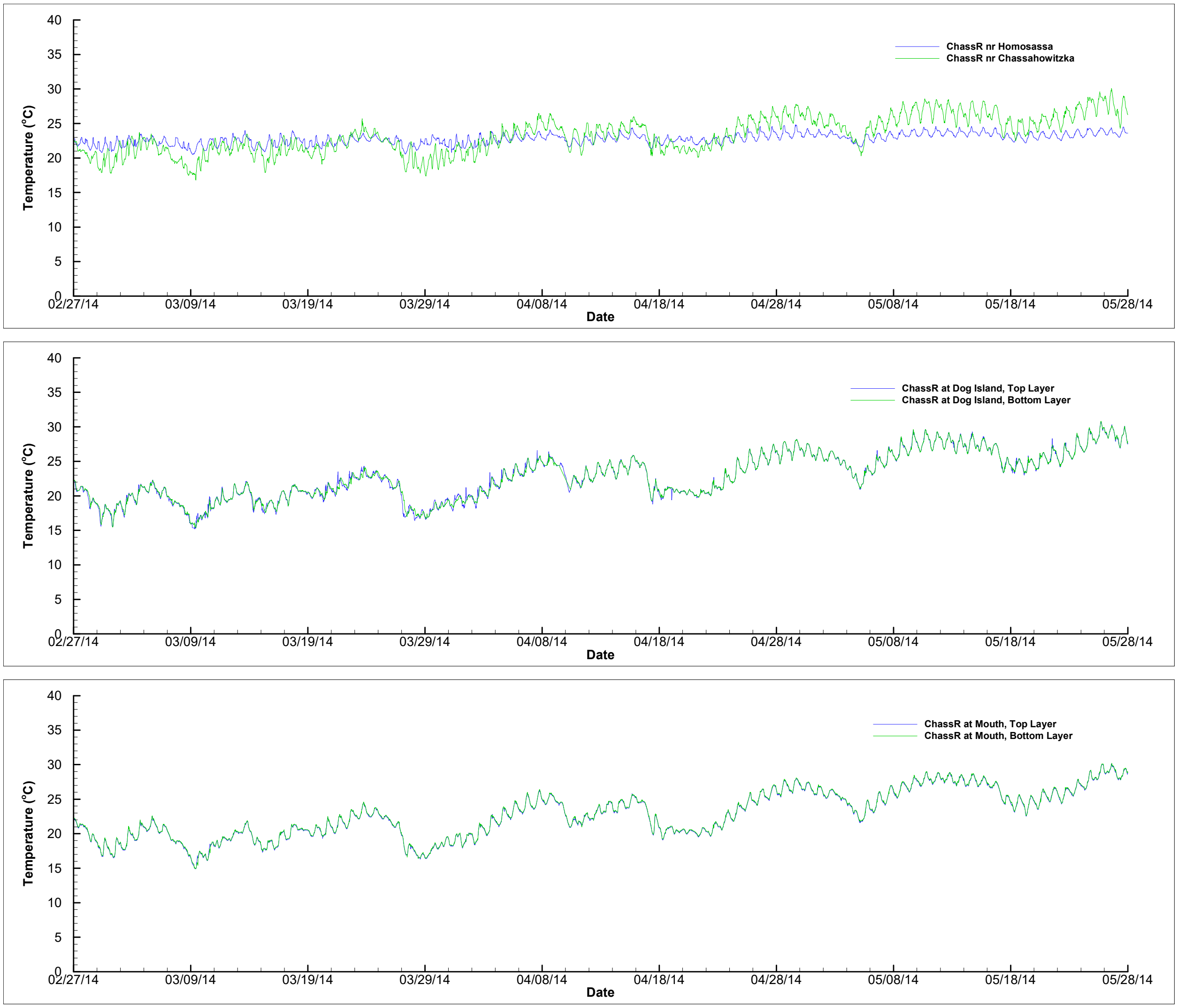

Figure C - 27. Measured real-time temperatures at USGS Chassahowitzka near Homosassa (blue line, top panel), near Chassahowitzka (green line, top panel), at Dog Island (middle panel), and at Mouth (bottom panel) stations in the Chassahowitzka River during 2/27/2014 – 5/28/2014.

Figure C - 28. Measured real-time temperatures at USGS Chassahowitzka near Homosassa (blue line, top panel), near Chassahowitzka (green line, top panel), at Dog Island (middle panel), and at Mouth (bottom panel) stations in the Chassahowitzka River during 5/28/2014 – 8/26/2014.

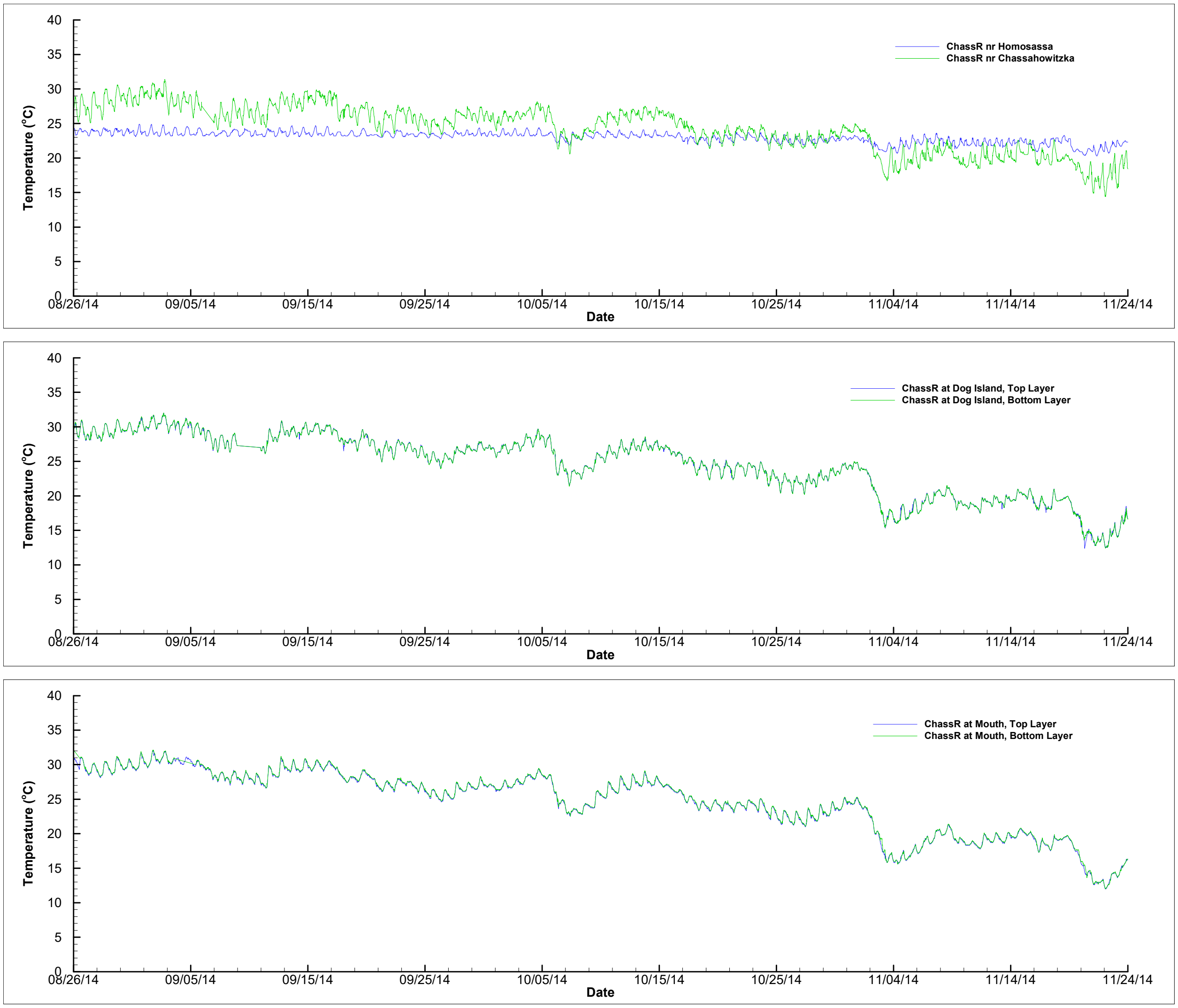

Figure C - 29. Measured real-time temperatures at USGS Chassahowitzka near Homosassa (blue line, top panel), near Chassahowitzka (green line, top panel), at Dog Island (middle panel), and at Mouth (bottom panel) stations in the Chassahowitzka River during 8/26/2014 – 11/24/2014.

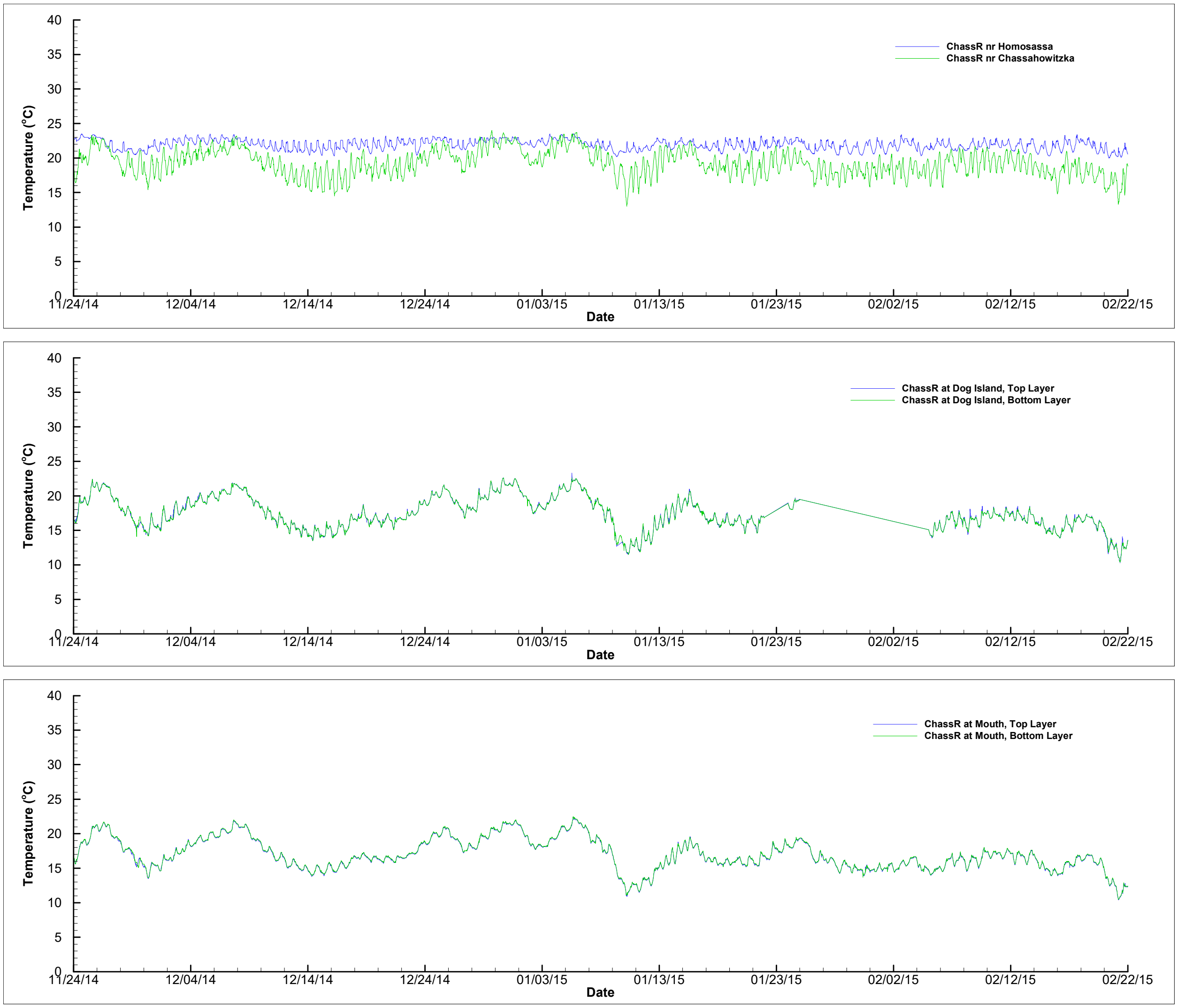

Figure C - 30. Measured real-time temperatures at USGS Chassahowitzka near Homosassa (blue line, top panel), near Chassahowitzka (green line, top panel), at Dog Island (middle panel), and at Mouth (bottom panel) stations in the Chassahowitzka River during 11/24/2014 – 2/22/2015.

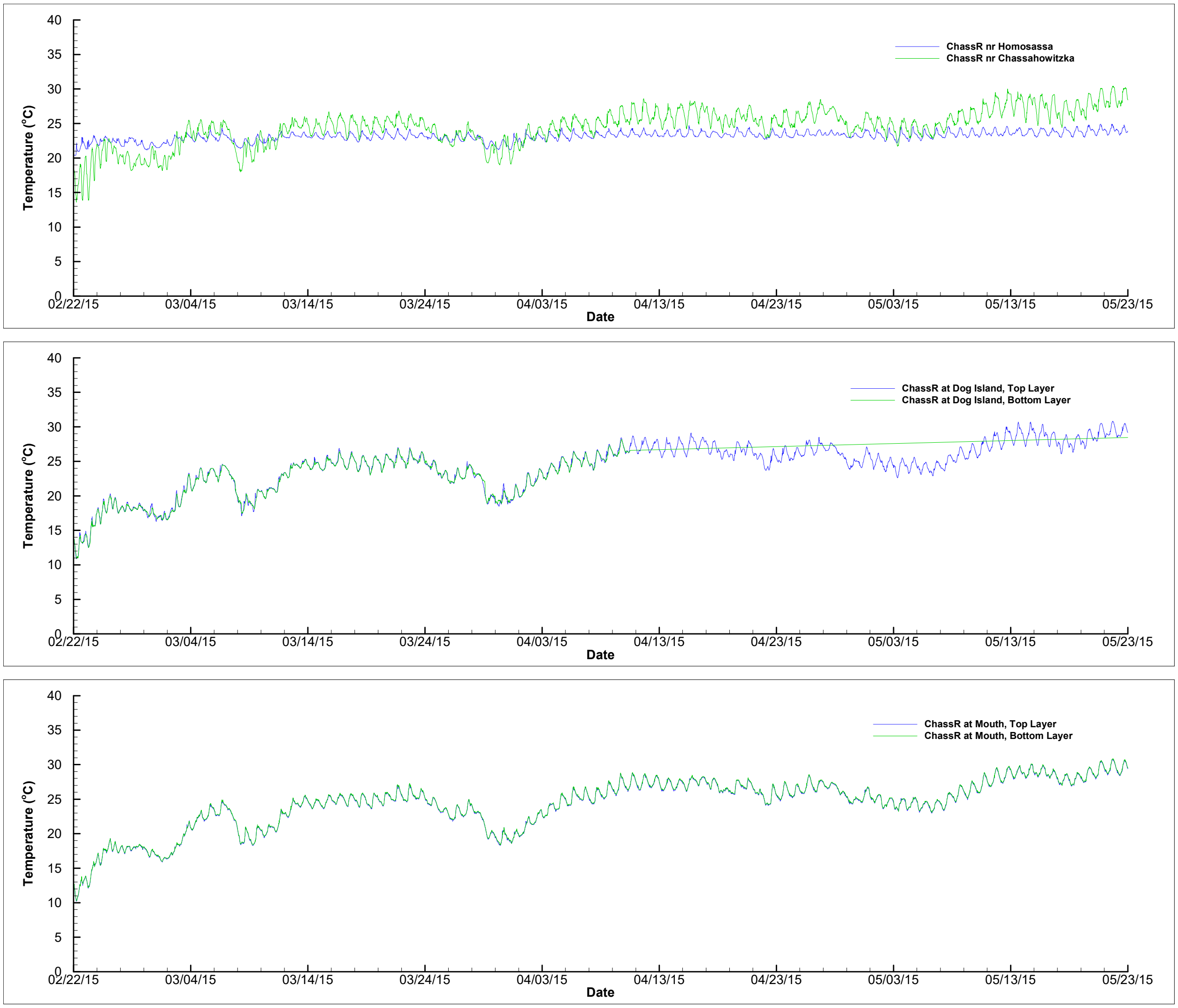

Figure C - 31. Measured real-time temperatures at USGS Chassahowitzka near Homosassa (blue line, top panel), near Chassahowitzka (green line, top panel), at Dog Island (middle panel), and at Mouth (bottom panel) stations in the Chassahowitzka River during 2/22/2015 - 5/23/2015.

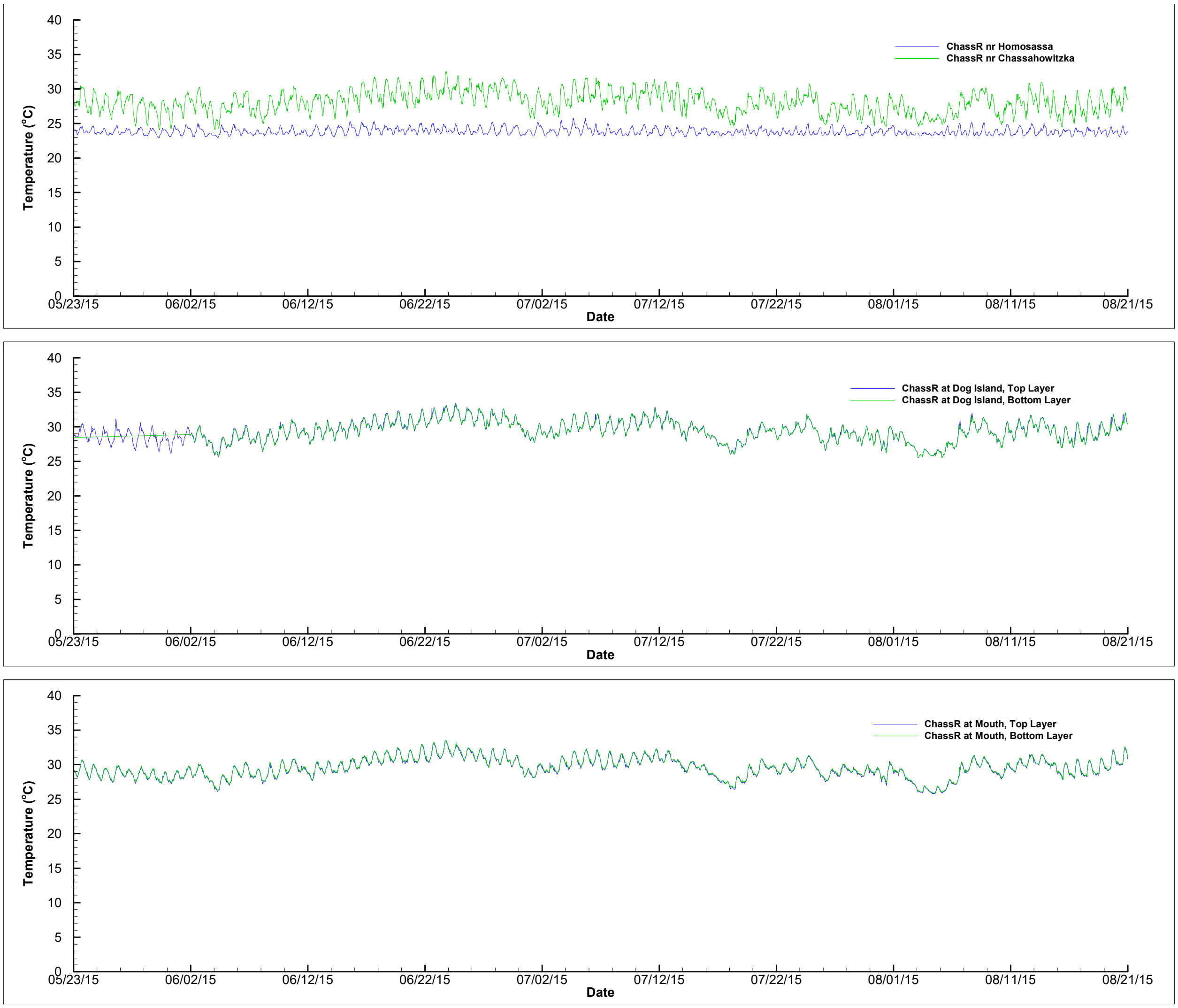

Figure C - 32. Measured real-time temperatures at USGS Chassahowitzka near Homosassa (blue line, top panel), near Chassahowitzka (green line, top panel), at Dog Island (middle panel), and at Mouth (bottom panel) stations in the Chassahowitzka River during 5/23/2015 - 8/21/2015.

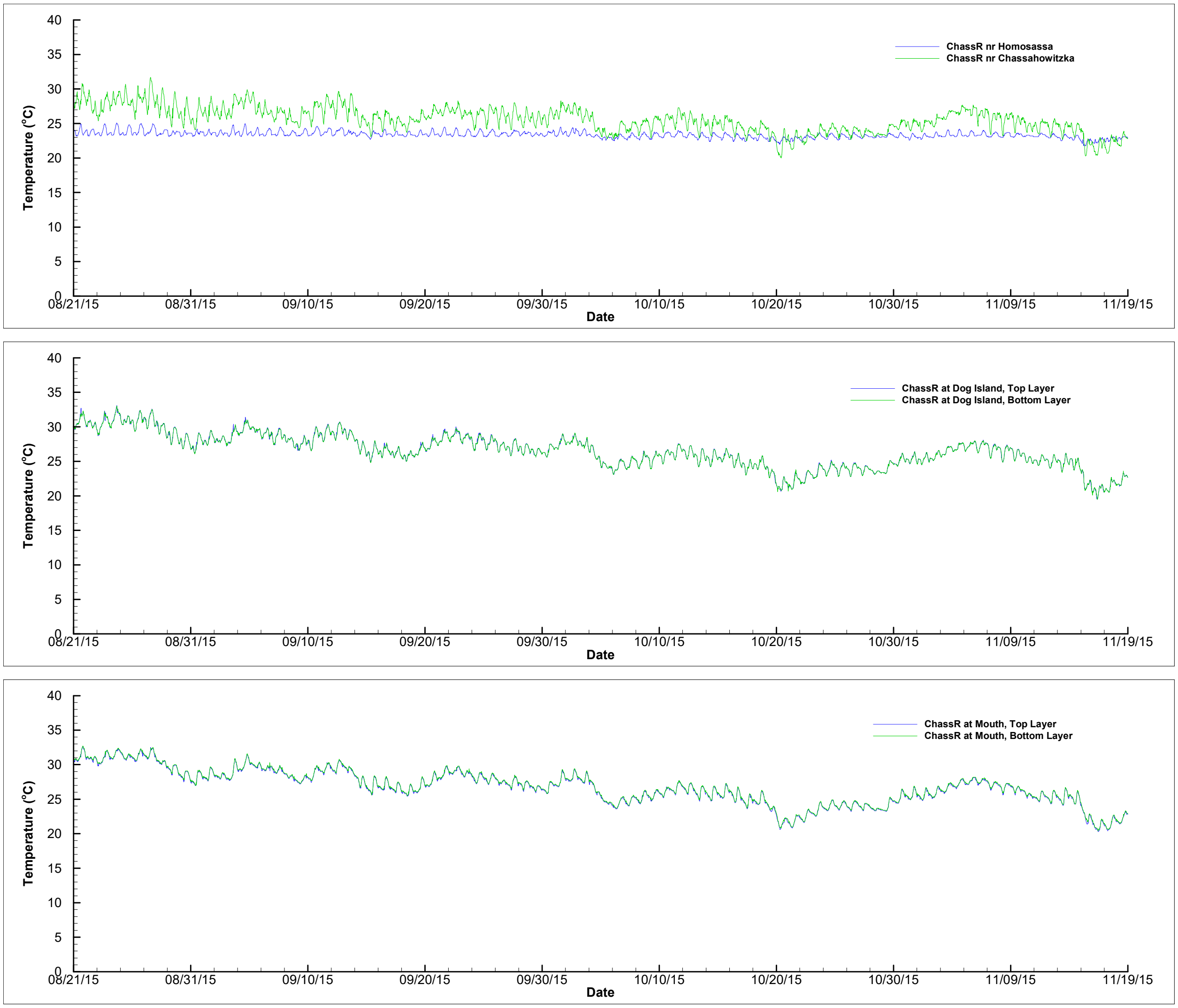

Figure C - 33. Measured real-time temperatures at USGS Chassahowitzka near Homosassa (blue line, top panel), near Chassahowitzka (green line, top panel), at Dog Island (middle panel), and at Mouth (bottom panel) stations in the Chassahowitzka River during 8/21/2015 - 11/19/2015.

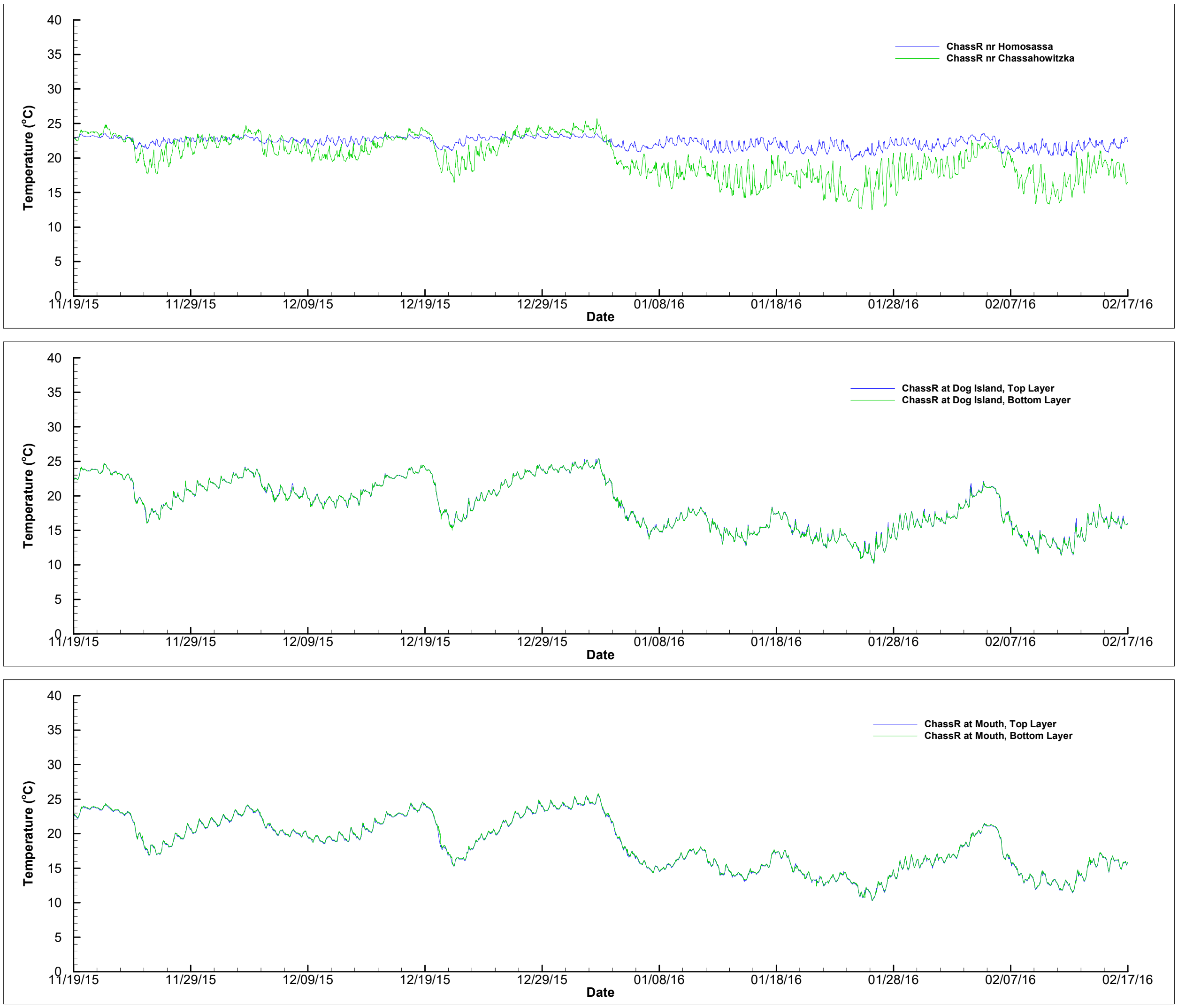

Figure C - 34. Measured real-time temperatures at USGS Chassahowitzka near Homosassa (blue line, top panel), near Chassahowitzka (green line, top panel), at Dog Island (middle panel), and at Mouth (bottom panel) stations in the Chassahowitzka River during 11/19/2015 – 2/17/2016.

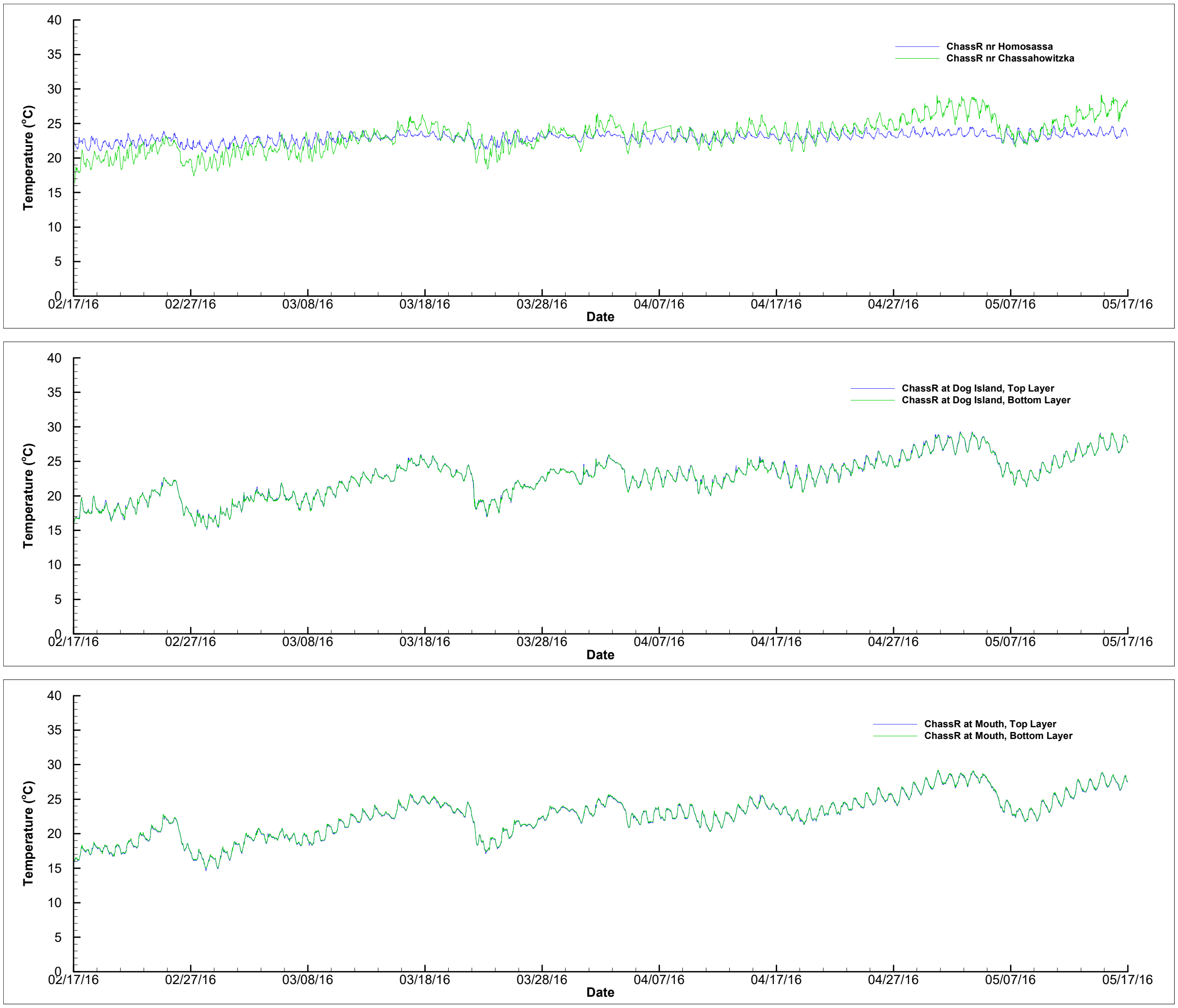

Figure C - 35. Measured real-time temperatures at USGS Chassahowitzka near Homosassa (blue line, top panel), near Chassahowitzka (green line, top panel), at Dog Island (middle panel), and at Mouth (bottom panel) stations in the Chassahowitzka River during 2/17/2016 - 5/17/2016.

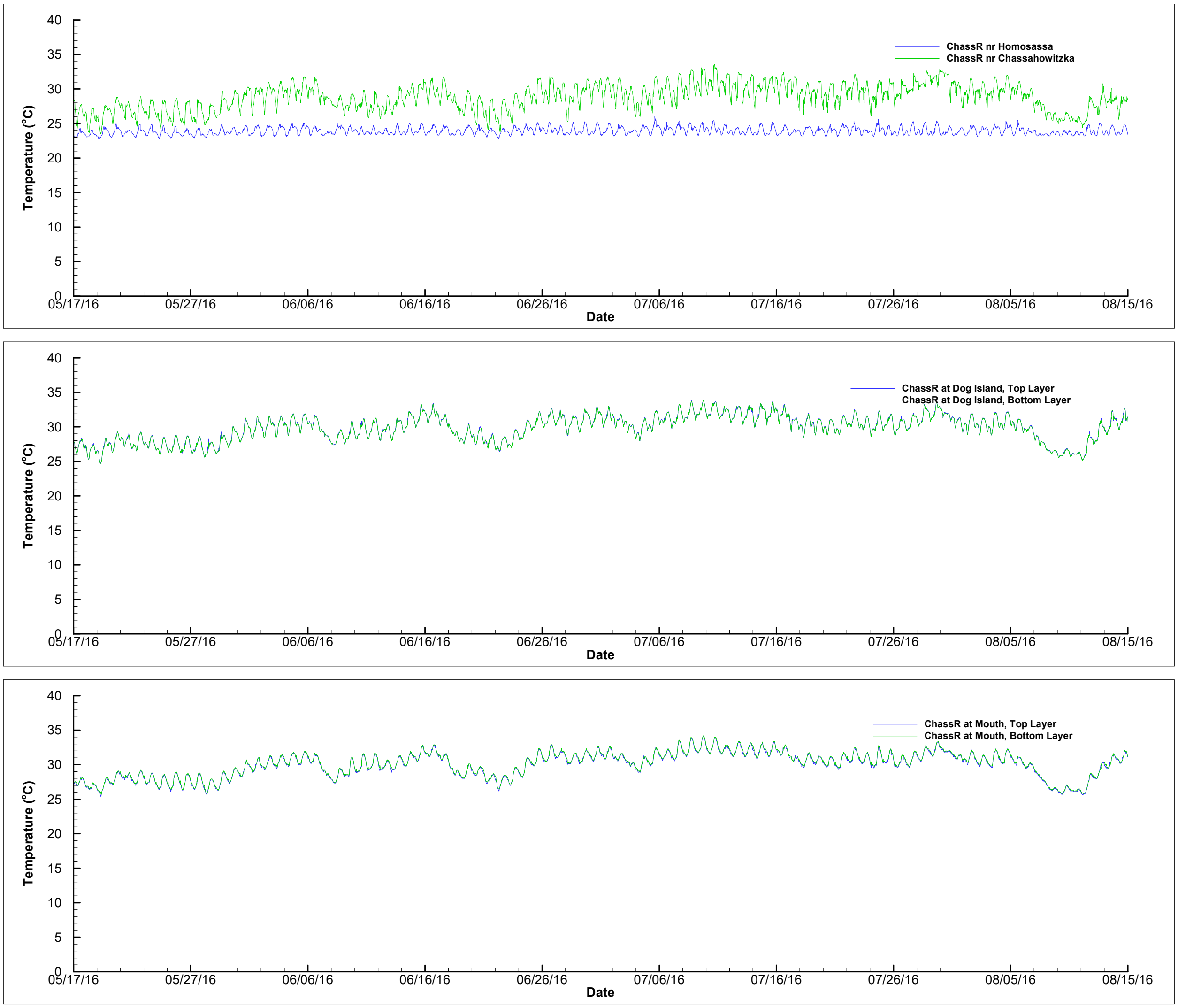

Figure C - 36. Measured real-time temperatures at USGS Chassahowitzka near Homosassa (blue line, top panel), near Chassahowitzka (green line, top panel), at Dog Island (middle panel), and at Mouth (bottom panel) stations in the Chassahowitzka River during 5/17/2016 - 8/15/2016.

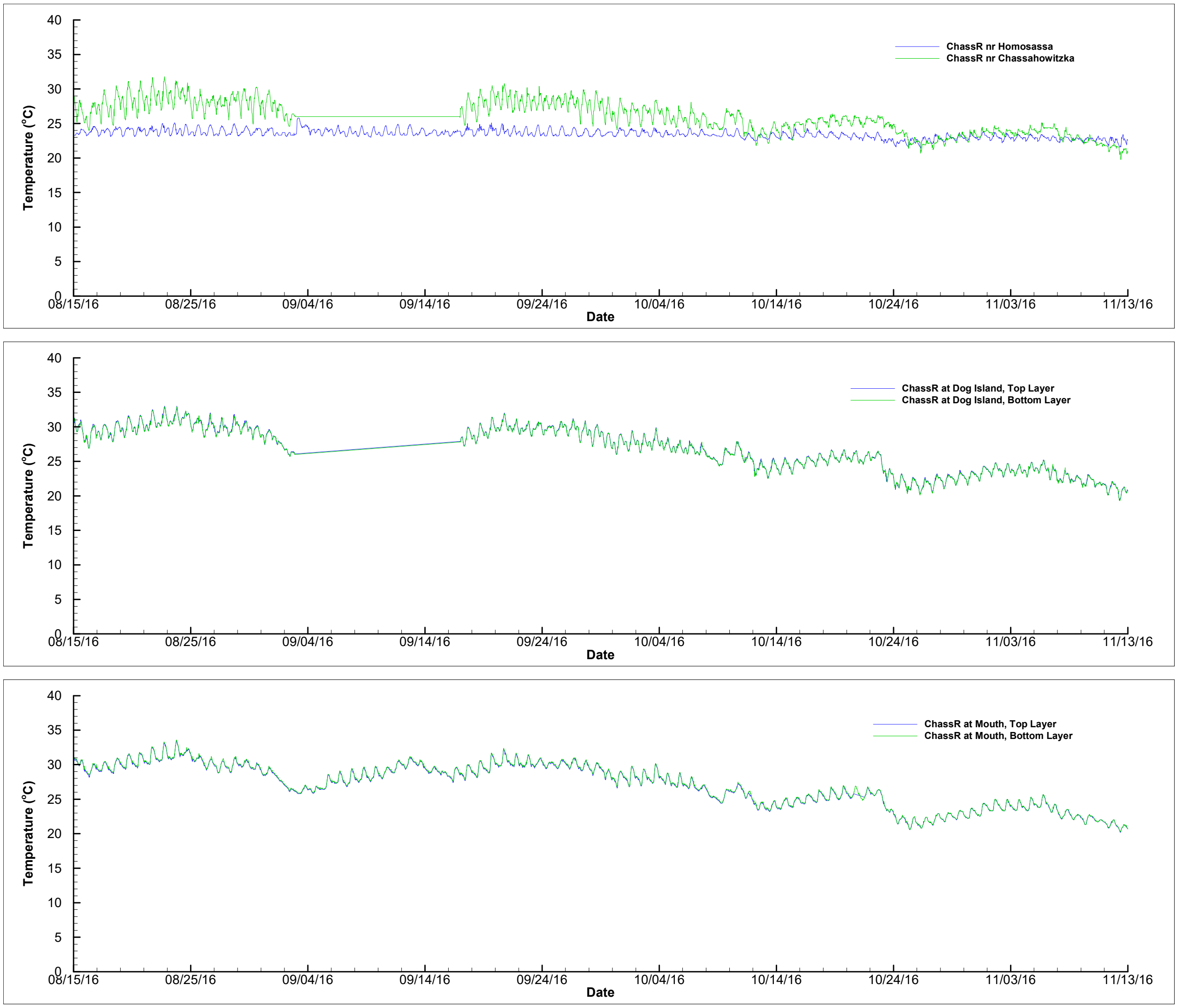

Figure C - 37. Measured real-time temperatures at USGS Chassahowitzka near Homosassa (blue line, top panel), near Chassahowitzka (green line, top panel), at Dog Island (middle panel), and at Mouth (bottom panel) stations in the Chassahowitzka River during 8/15/2016 - 11/13/2016.

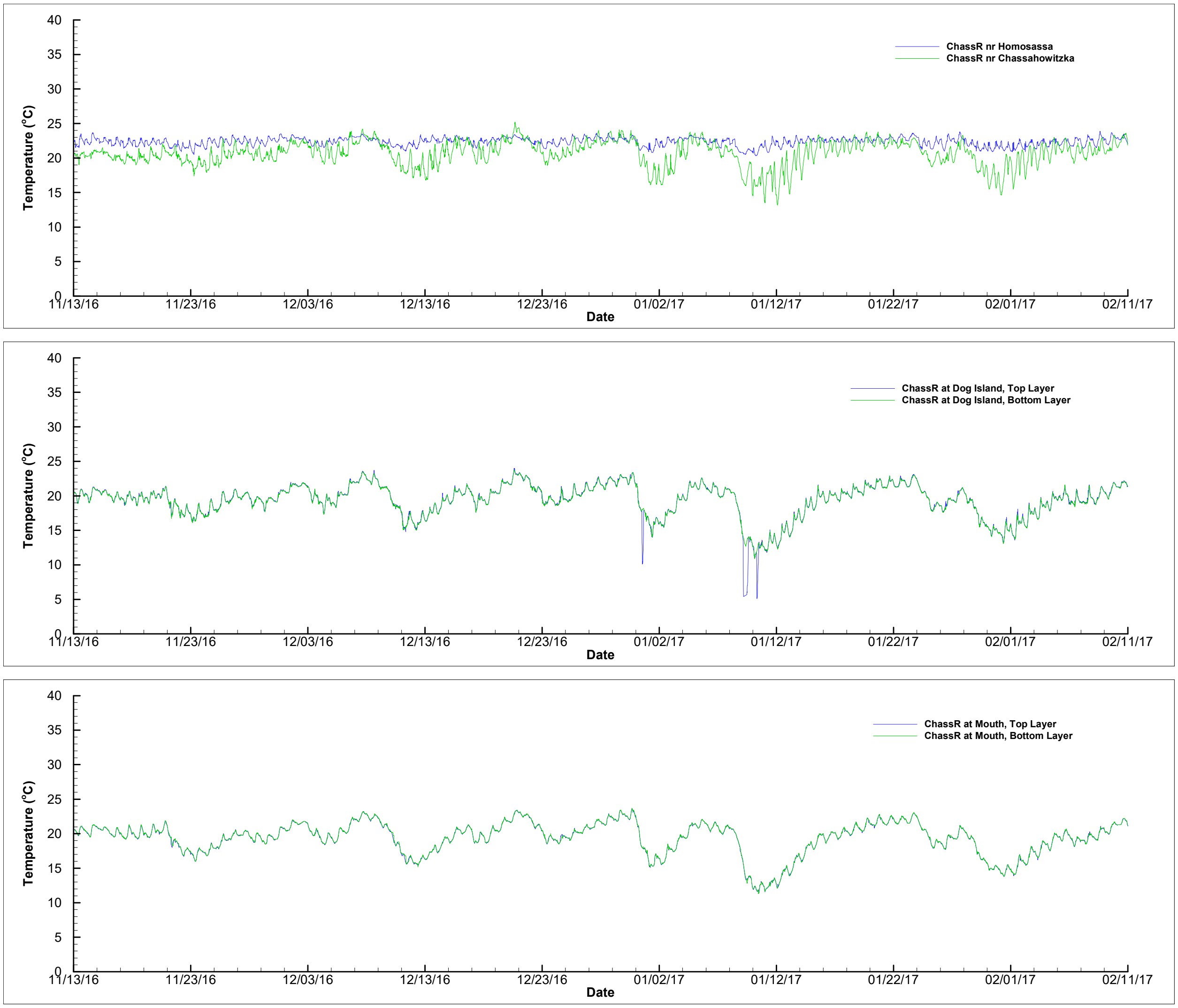

Figure C - 38. Measured real-time temperatures at USGS Chassahowitzka near Homosassa (blue line, top panel), near Chassahowitzka (green line, top panel), at Dog Island (middle panel), and at Mouth (bottom panel) stations in the Chassahowitzka River during 11/13/2016 - 2/11/2017.

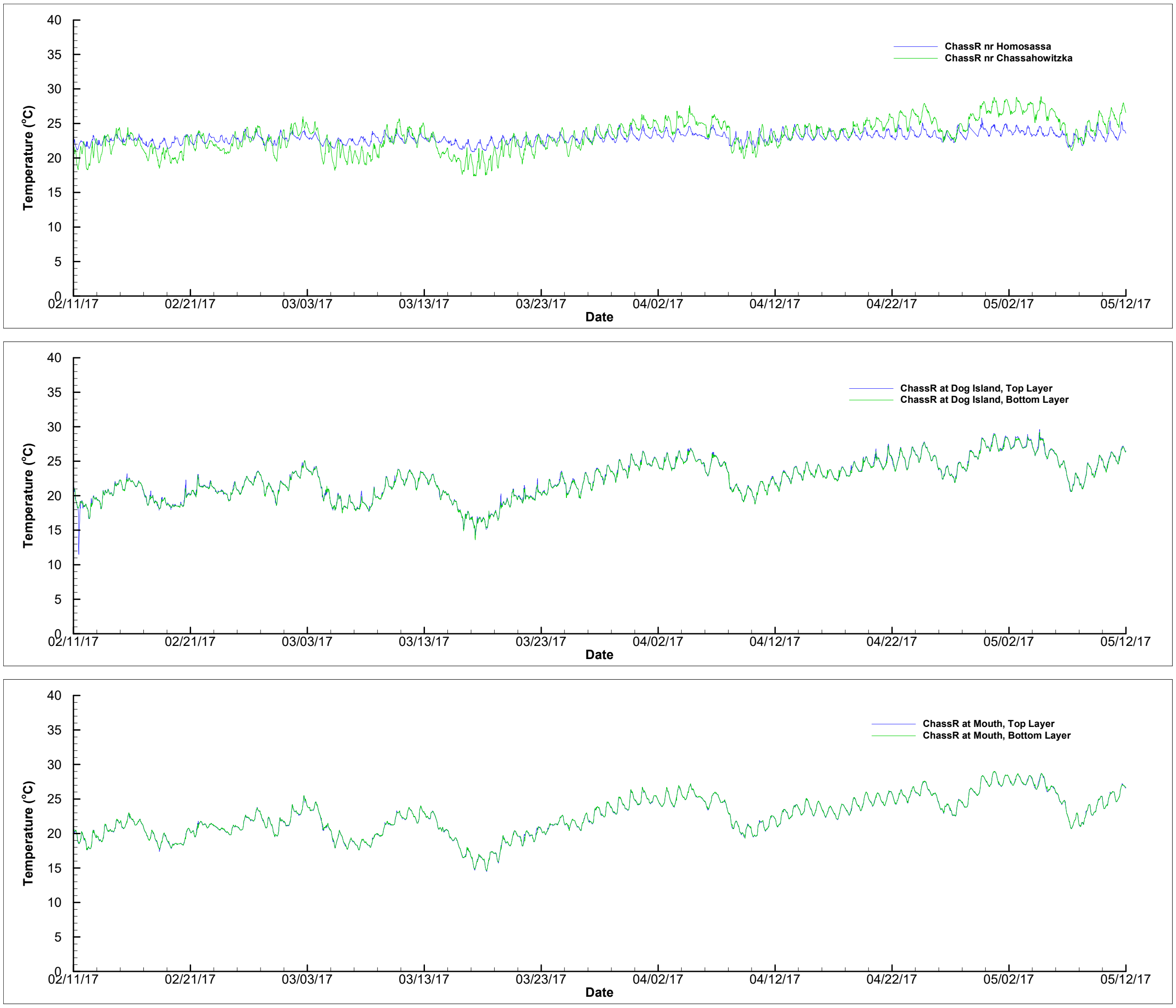

Figure C - 39. Measured real-time temperatures at USGS Chassahowitzka near Homosassa (blue line, top panel), near Chassahowitzka (green line, top panel), at Dog Island (middle panel), and at Mouth (bottom panel) stations in the Chassahowitzka River during 2/11/2017 - 5/12/2017.

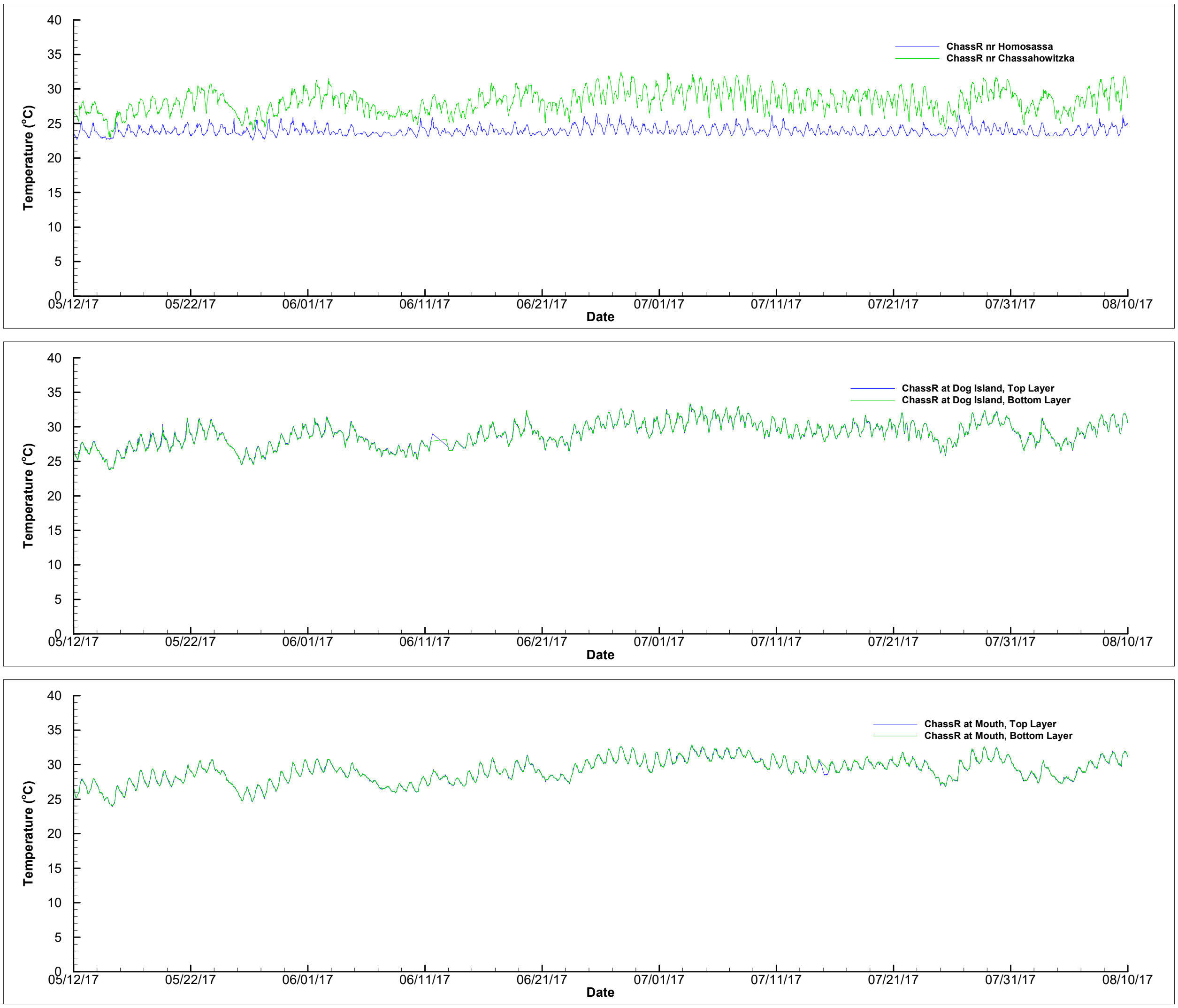

Figure C - 40. Measured real-time temperatures at USGS Chassahowitzka near Homosassa (blue line, top panel), near Chassahowitzka (green line, top panel), at Dog Island (middle panel), and at Mouth (bottom panel) stations in the Chassahowitzka River during 5/12/2017 - 8/10/2017.

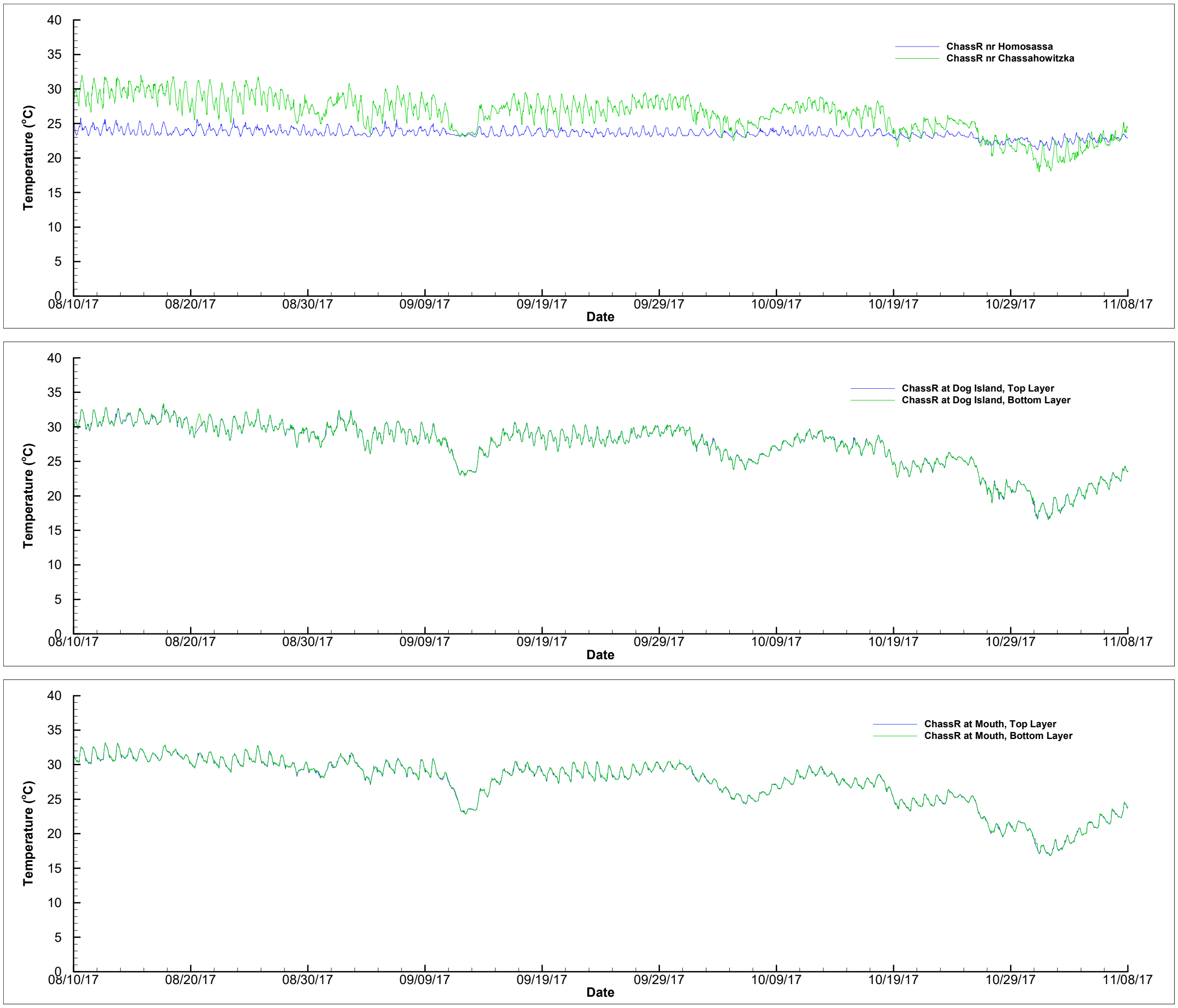

Figure C - 41. Measured real-time temperatures at USGS Chassahowitzka near Homosassa (blue line, top panel), near Chassahowitzka (green line, top panel), at Dog Island (middle panel), and at Mouth (bottom panel) stations in the Chassahowitzka River during 8/10/2017 – 11/8/2017.

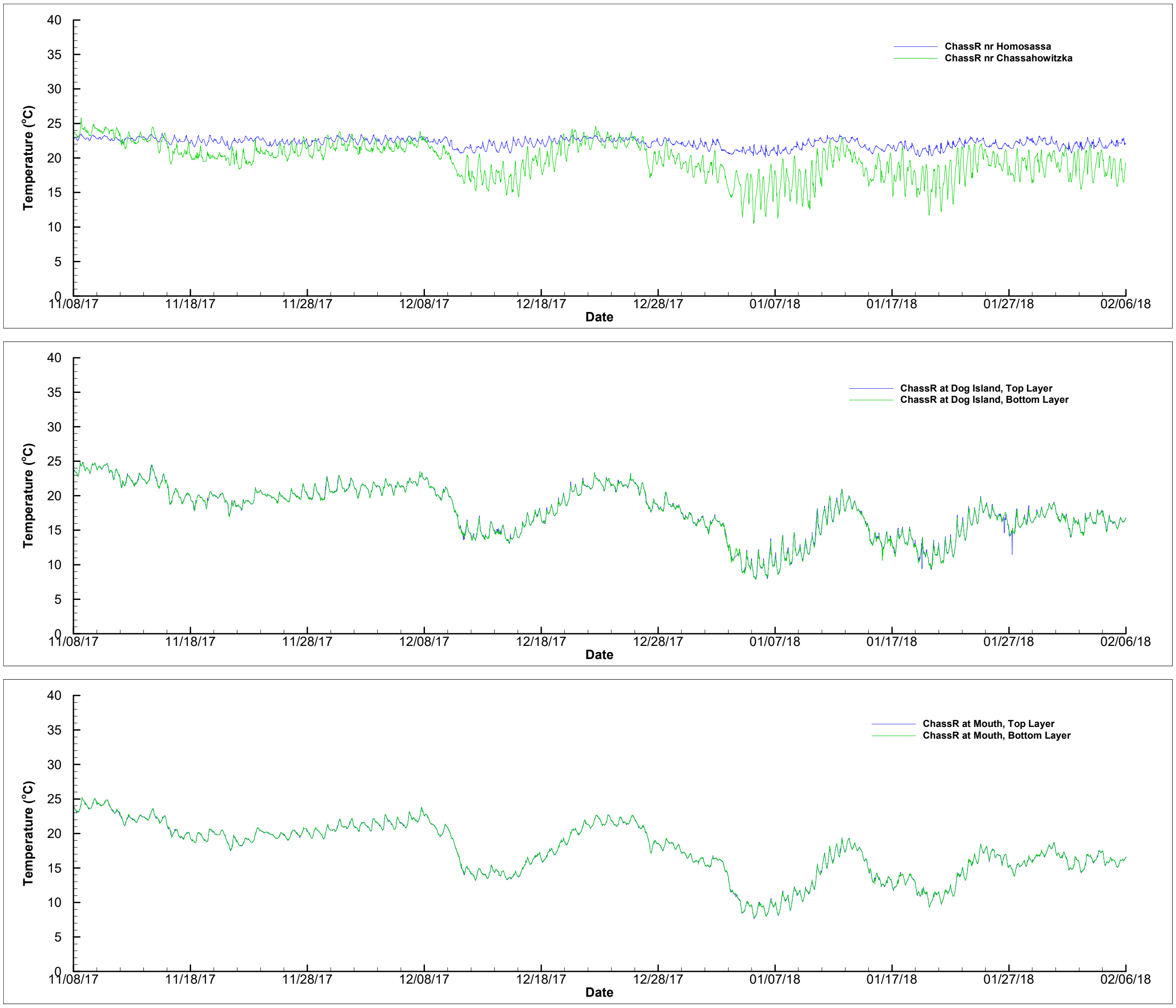

Figure C - 42. Measured real-time temperatures at USGS Chassahowitzka near Homosassa (blue line, top panel), near Chassahowitzka (green line, top panel), at Dog Island (middle panel), and at Mouth (bottom panel) stations in the Chassahowitzka River during 11/8/2017 - 2/6/2018.

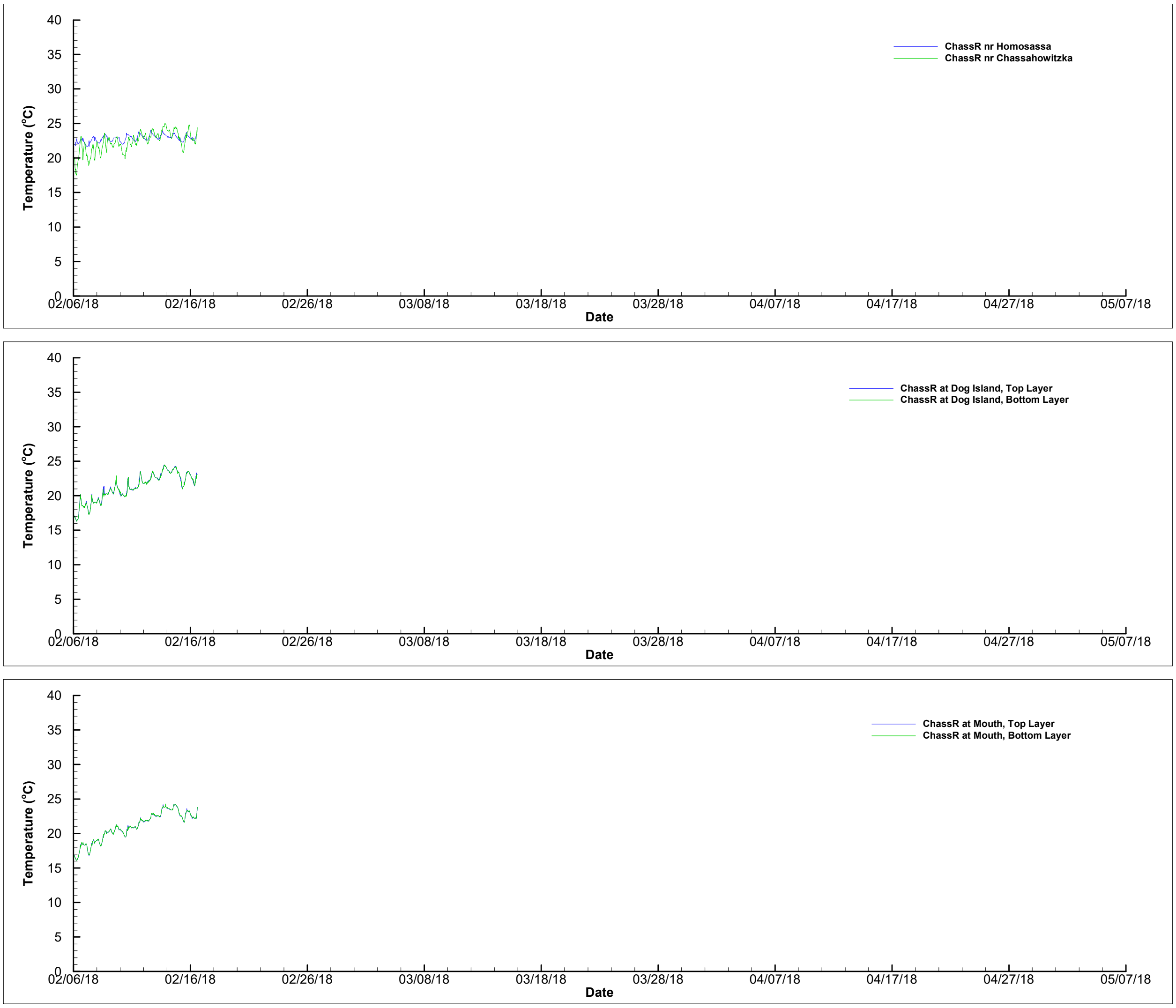

Figure C - 43. Measured real-time temperatures at USGS Chassahowitzka near Homosassa (blue line, top panel), near Chassahowitzka (green line, top panel), at Dog Island (middle panel), and at Mouth (bottom panel) stations in the Chassahowitzka River during 2/6/2018 - 5/7/2018.

Appendix D. Simulated and Measured Water Levels

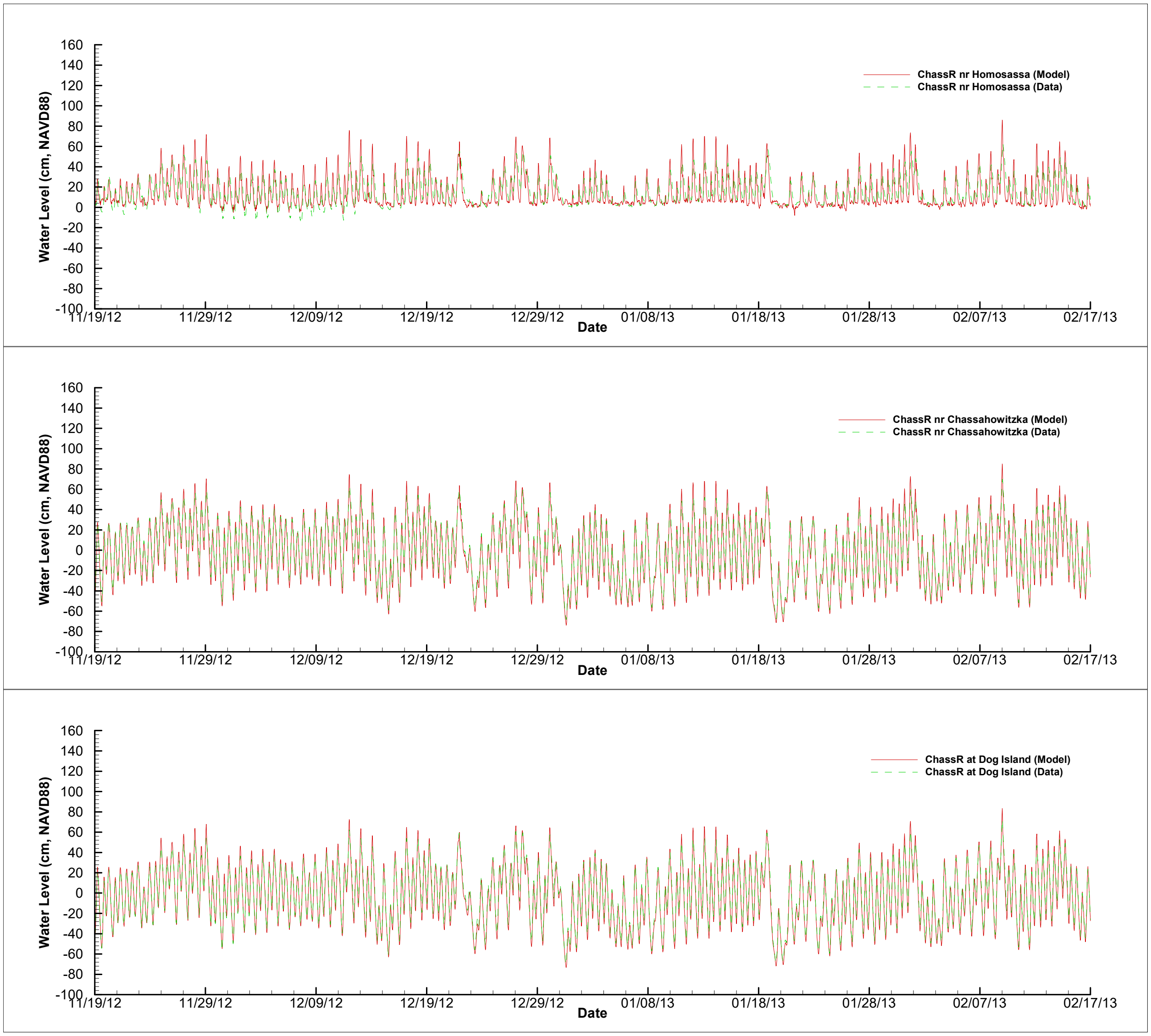

Figure D - 1. Comparisons of simulated (red lines) and measured (dashed green lines) water levels at the Chassahowitzka River near Homosassa (top panel), near Chassahowitzka, and at Dog Island stations during 11/19/2012 – 2/17/2013.

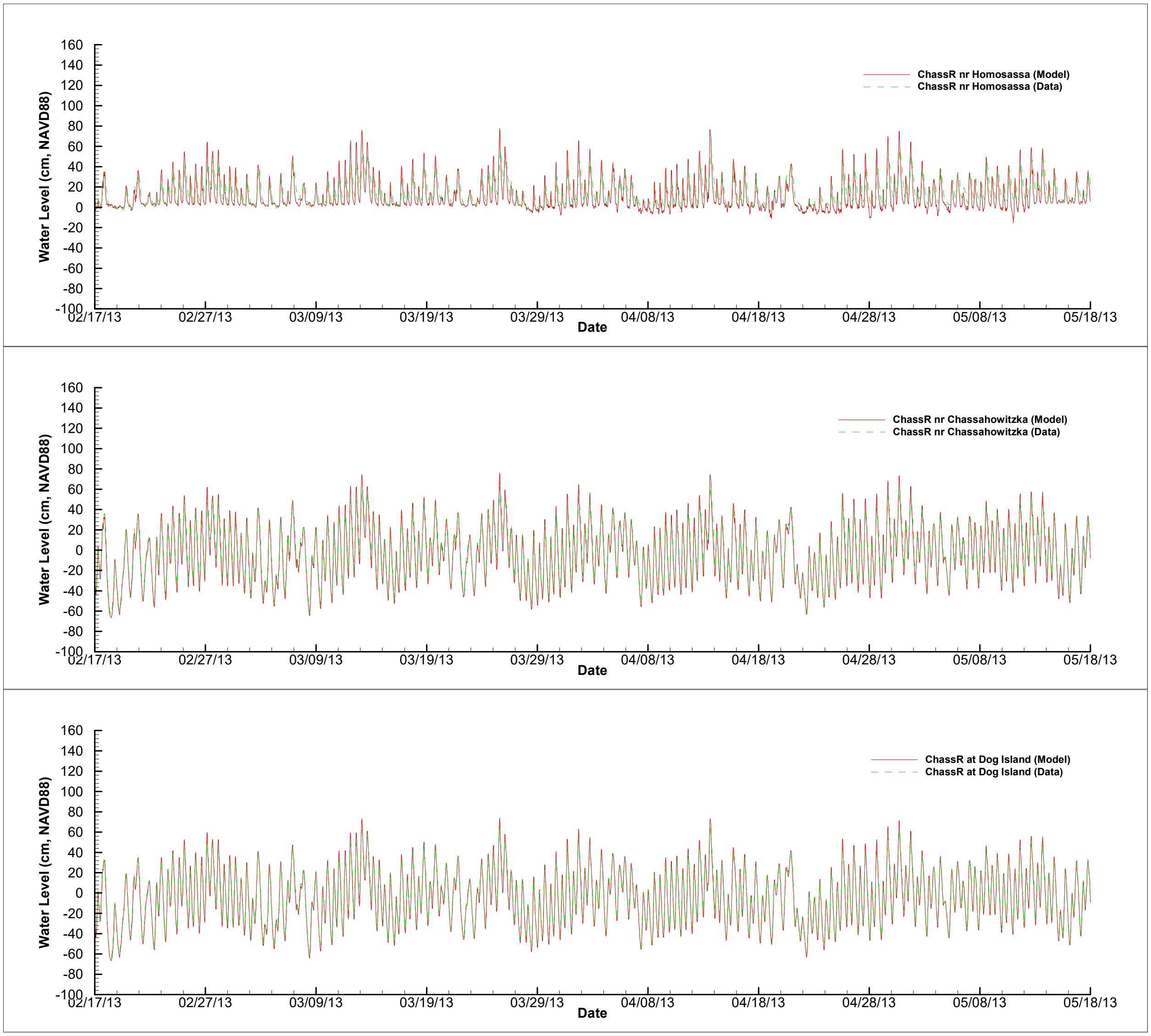

Figure D - 2. Comparisons of simulated (red lines) and measured (dashed green lines) water levels at the Chassahowitzka River near Homosassa (top panel), near Chassahowitzka, and at Dog Island stations during 2/17/2013 – 5/18/2013.

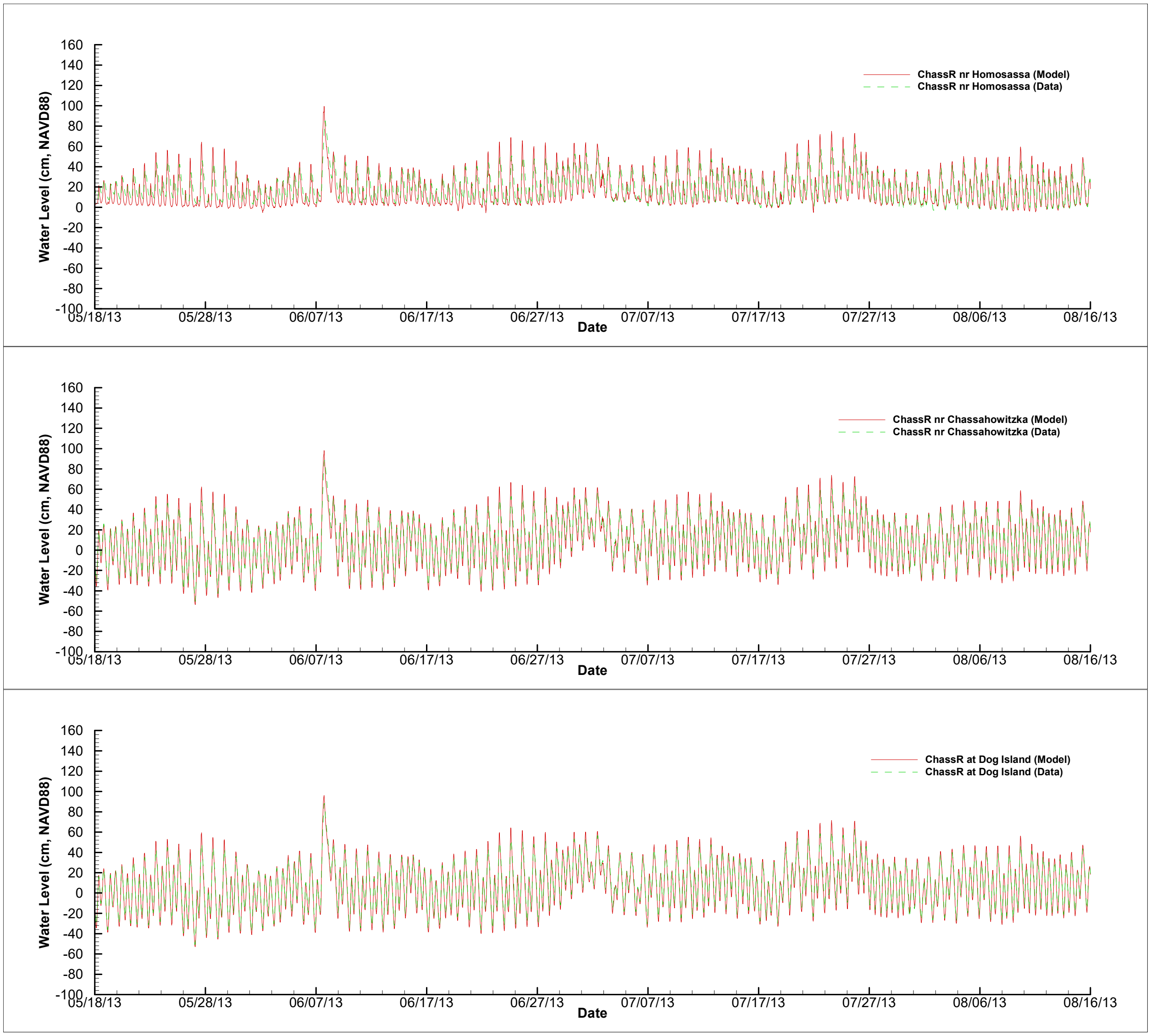

Figure D - 3. Comparisons of simulated (red lines) and measured (dashed green lines) water levels at the Chassahowitzka River near Homosassa (top panel), near Chassahowitzka, and at Dog Island stations during 5/18/2013 – 8/16/2013.

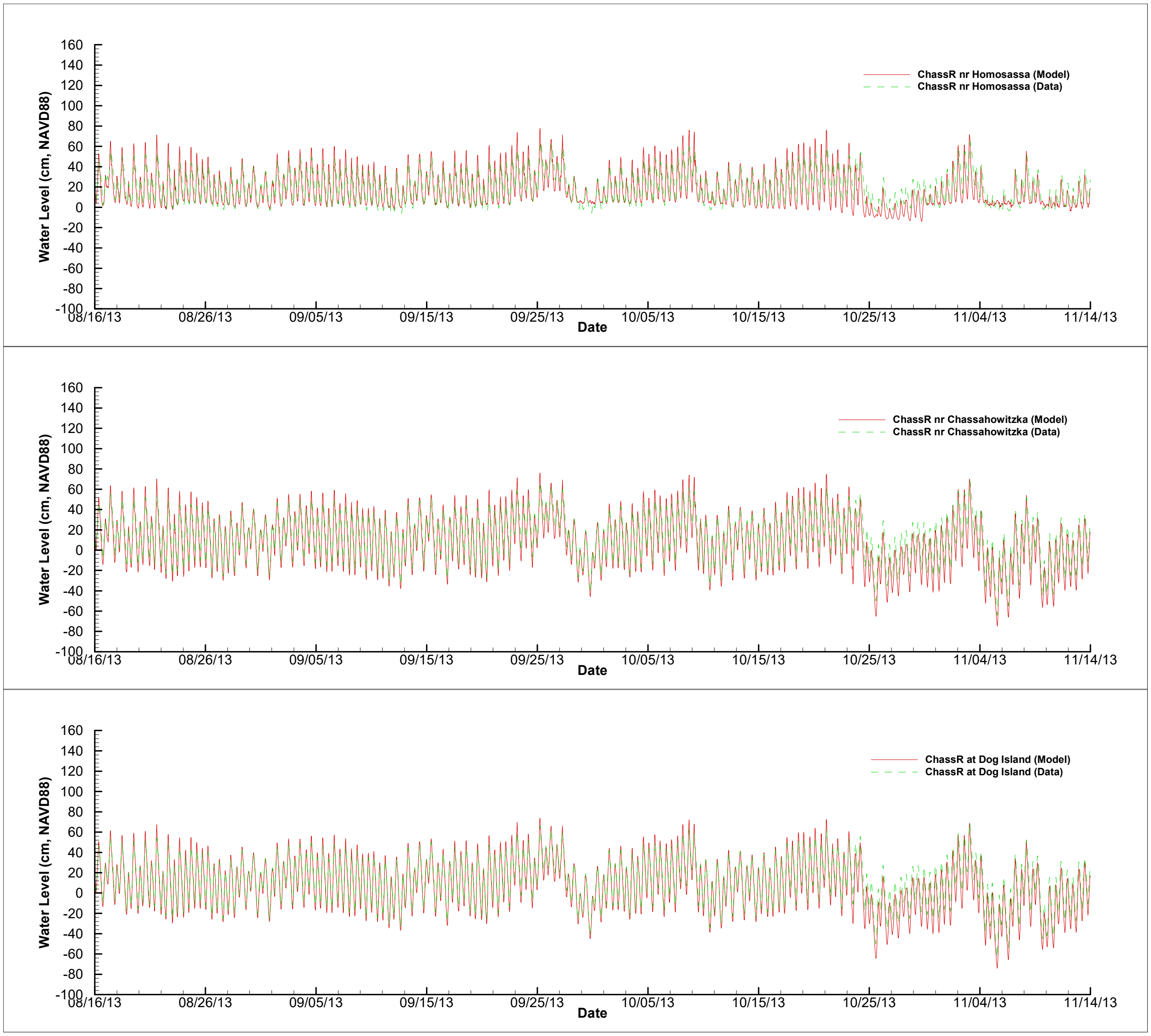

Figure D - 4. Comparisons of simulated (red lines) and measured (dashed green lines) water levels at the Chassahowitzka River near Homosassa (top panel), near Chassahowitzka, and at Dog Island stations during 8/16/2013 – 11/14/2013.

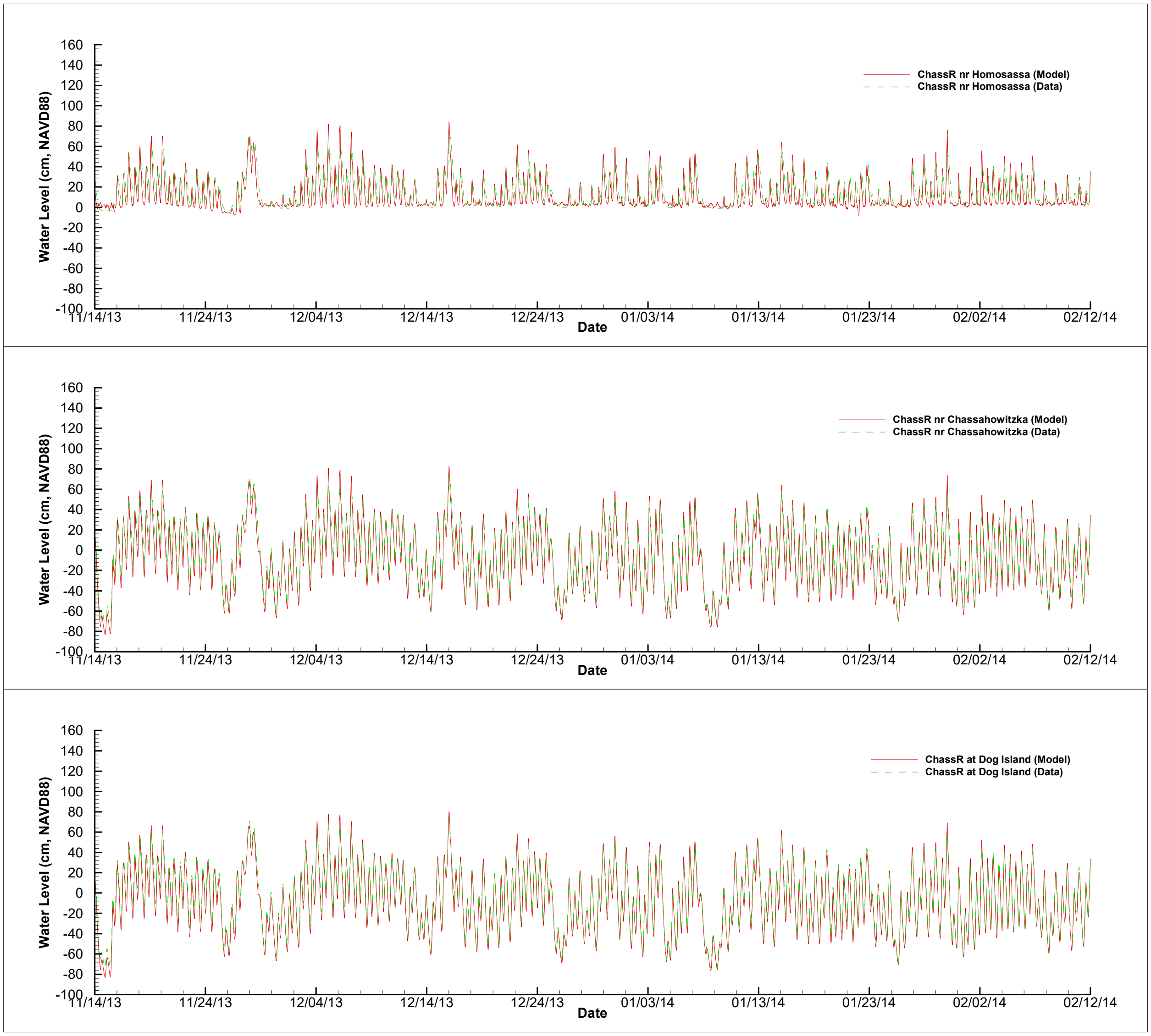

Figure D - 5. Comparisons of simulated (red lines) and measured (dashed green lines) water levels at the Chassahowitzka River near Homosassa (top panel), near Chassahowitzka, and at Dog Island stations during 11/14/2013 – 2/12/2014.

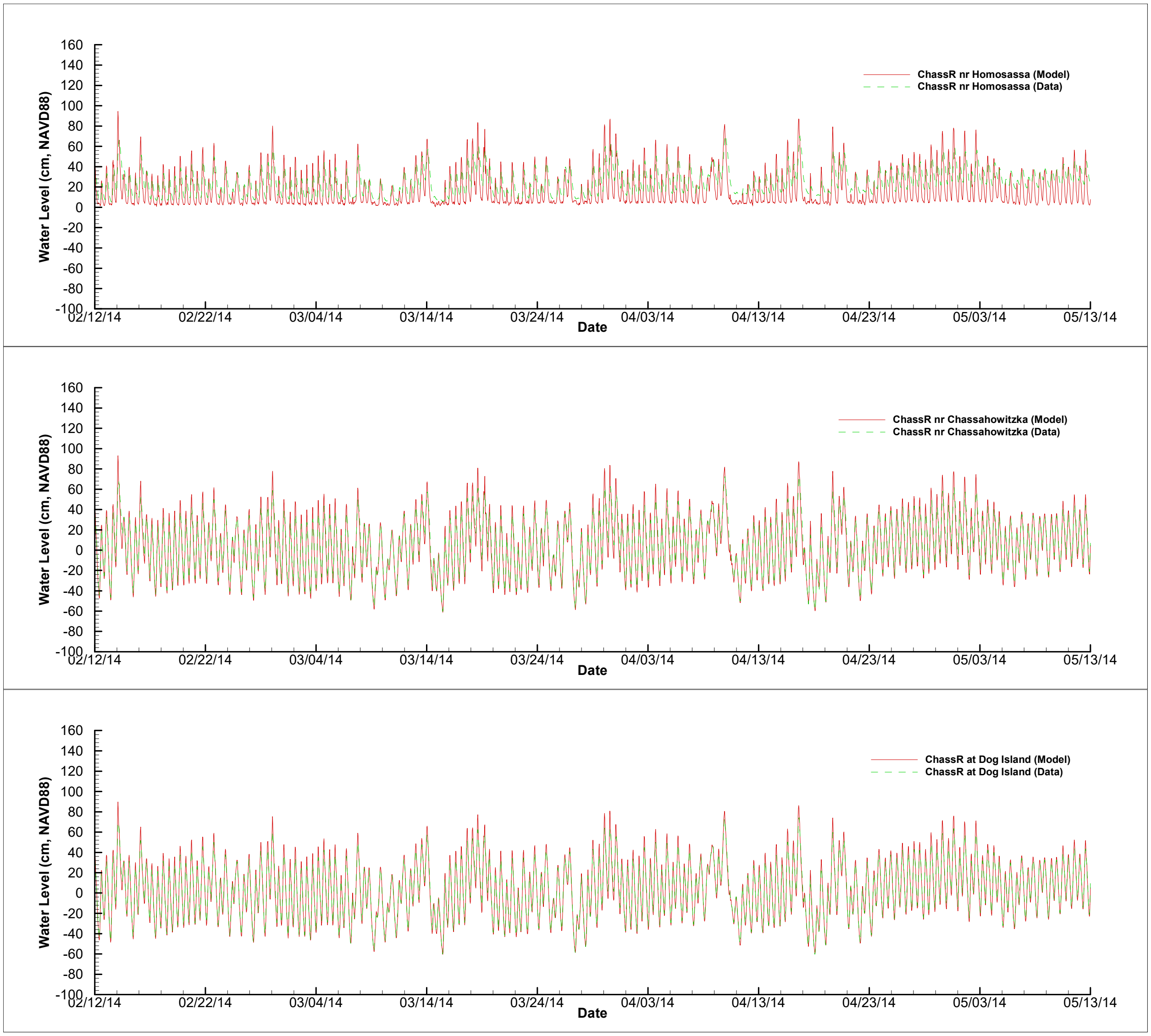

Figure D - 6. Comparisons of simulated (red lines) and measured (dashed green lines) water levels at the Chassahowitzka River near Homosassa (top panel), near Chassahowitzka, and at Dog Island stations during 2/12/2014 – 5/13/2014.

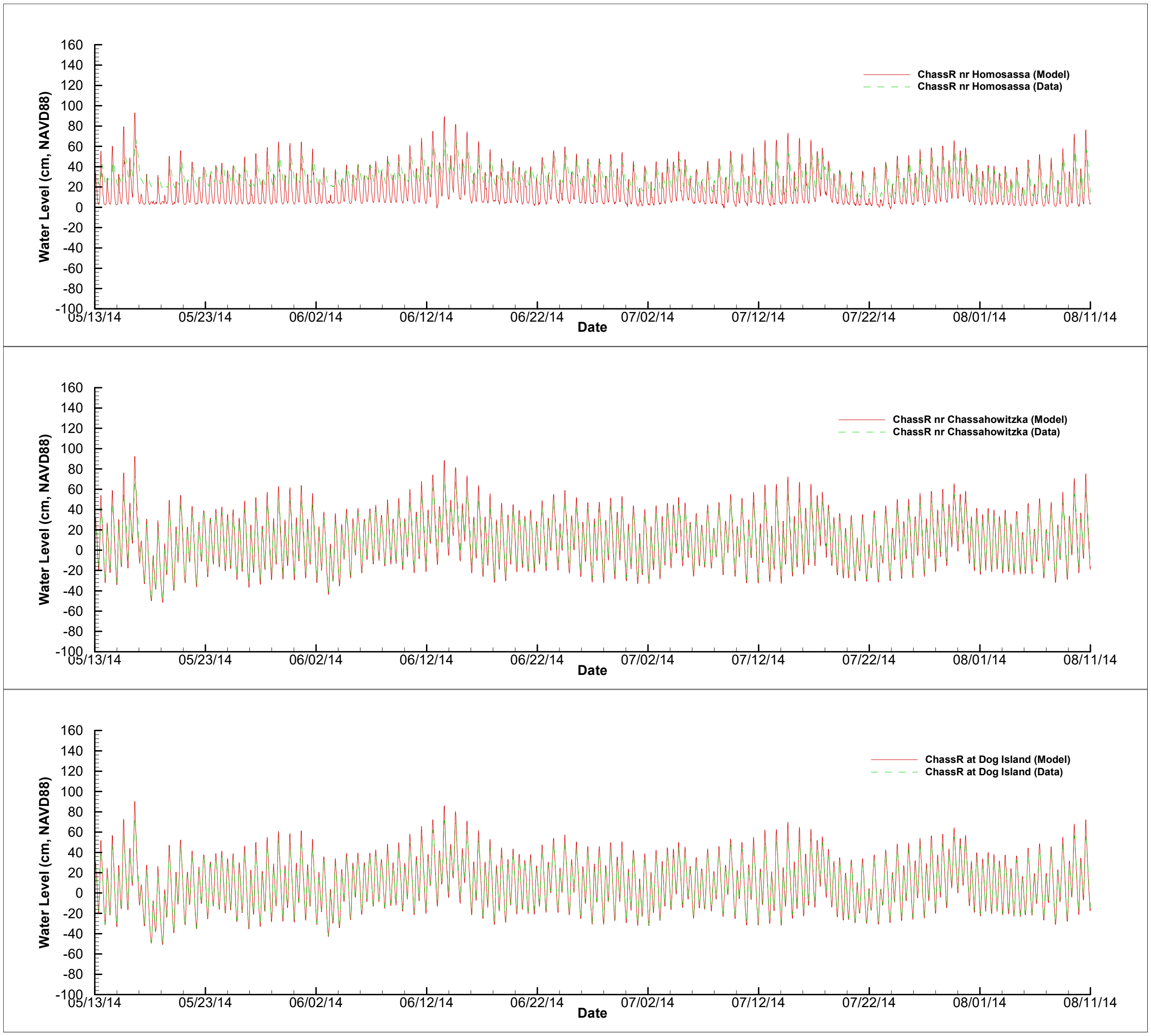

Figure D - 7. Comparisons of simulated (red lines) and measured (dashed green lines) water levels at the Chassahowitzka River near Homosassa (top panel), near Chassahowitzka, and at Dog Island stations during 5/13/2014 – 8/11/2014.

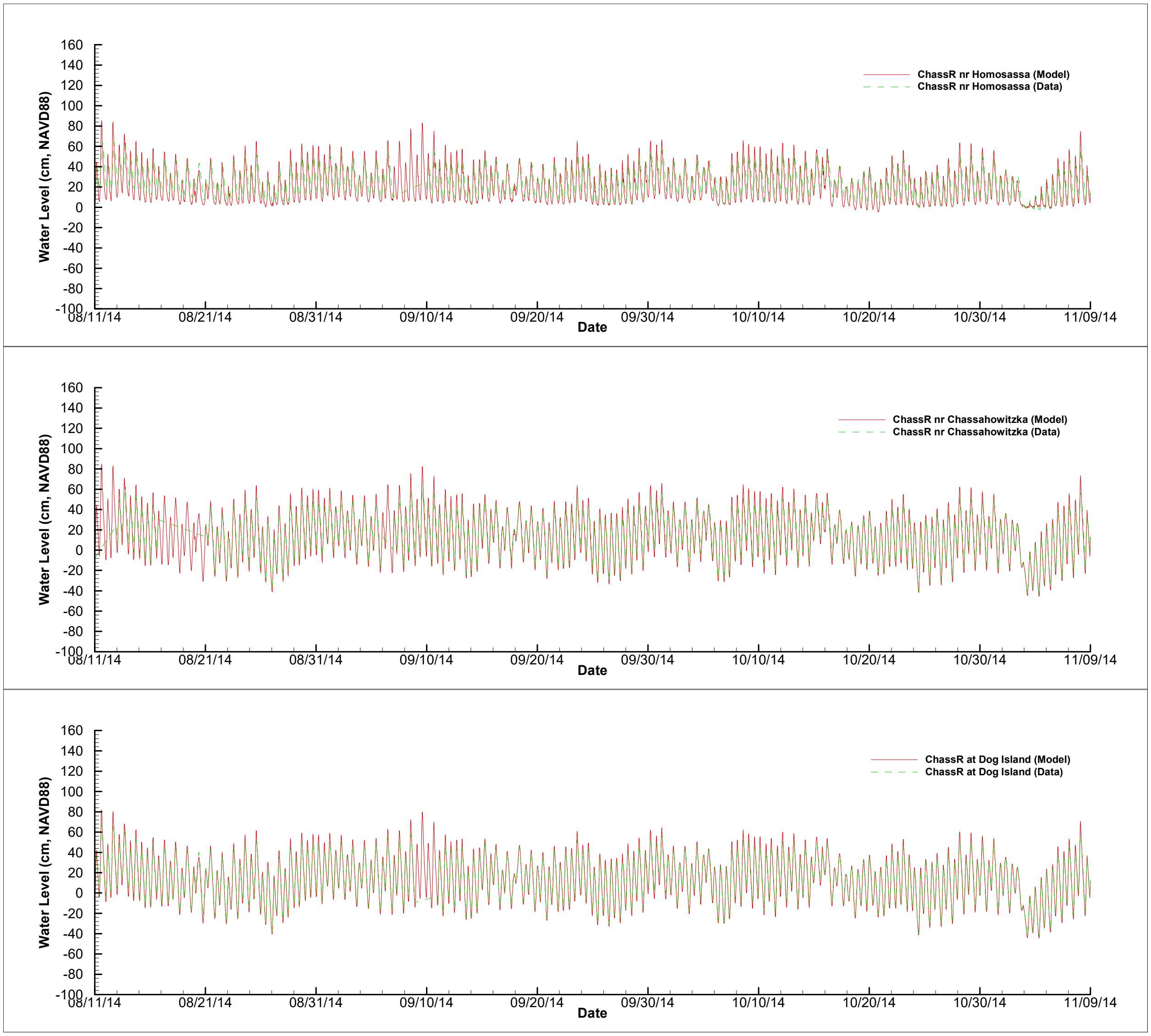

Figure D - 8. Comparisons of simulated (red lines) and measured (dashed green lines) water levels at the Chassahowitzka River near Homosassa (top panel), near Chassahowitzka, and at Dog Island stations during 8/11/2014 – 11/9/2014.

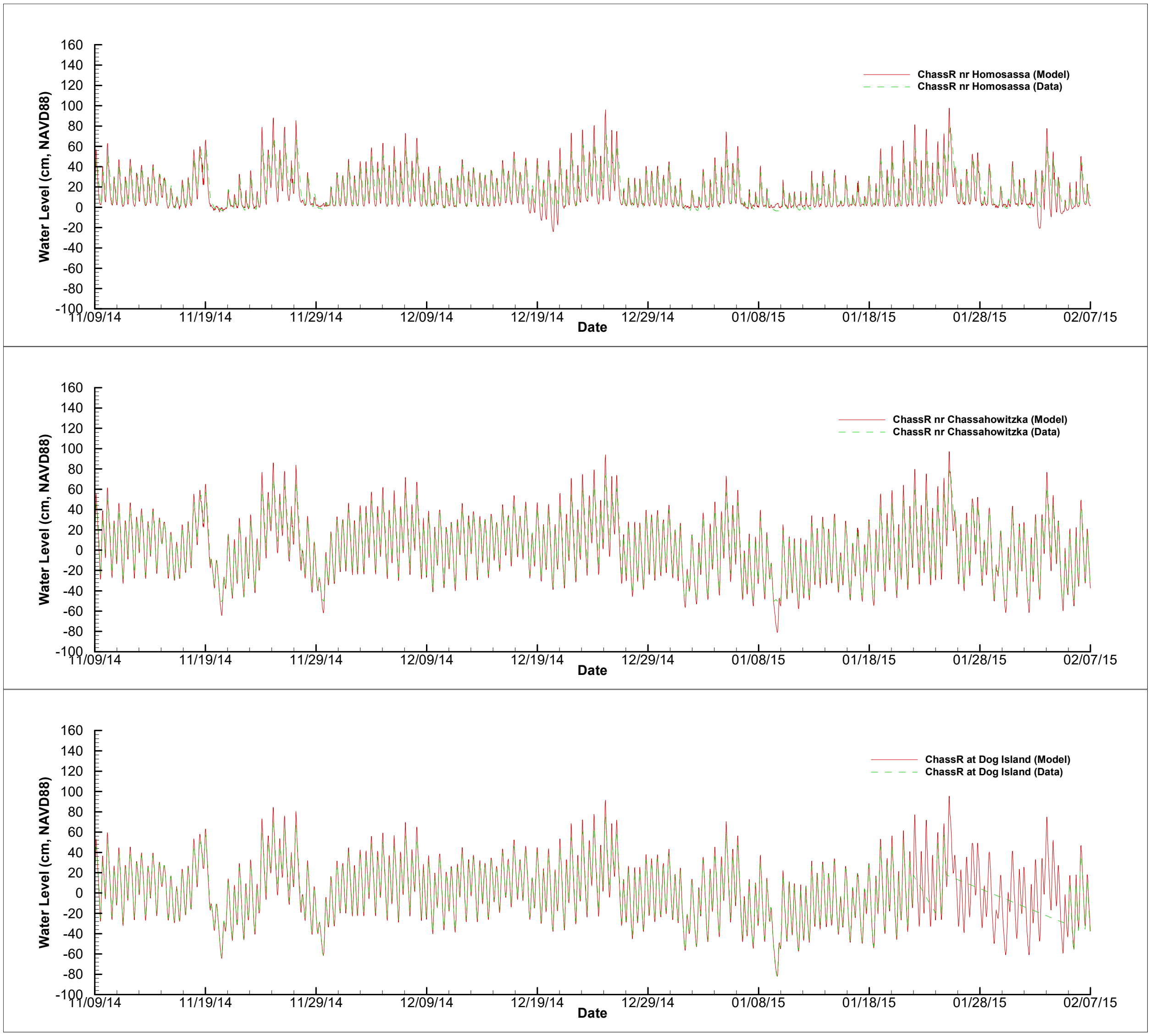

Figure D - 9. Comparisons of simulated (red lines) and measured (dashed green lines) water levels at the Chassahowitzka River near Homosassa (top panel), near Chassahowitzka, and at Dog Island stations during 11/9/2014 – 2/7/2015.

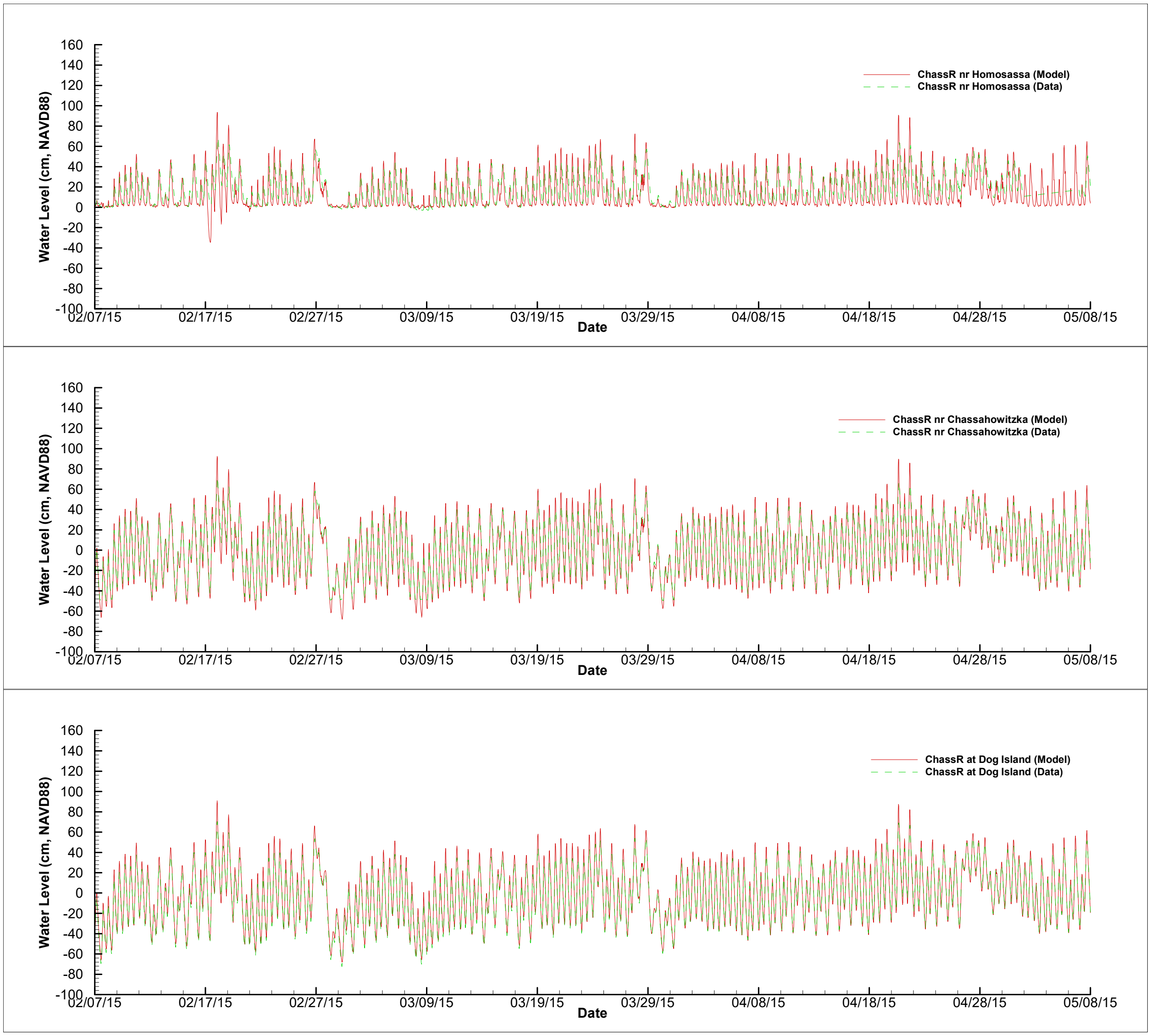

Figure D - 10. Comparisons of simulated (red lines) and measured (dashed green lines) water levels at the Chassahowitzka River near Homosassa (top panel), near Chassahowitzka, and at Dog Island stations during 2/7/2015 – 5/8/2015.

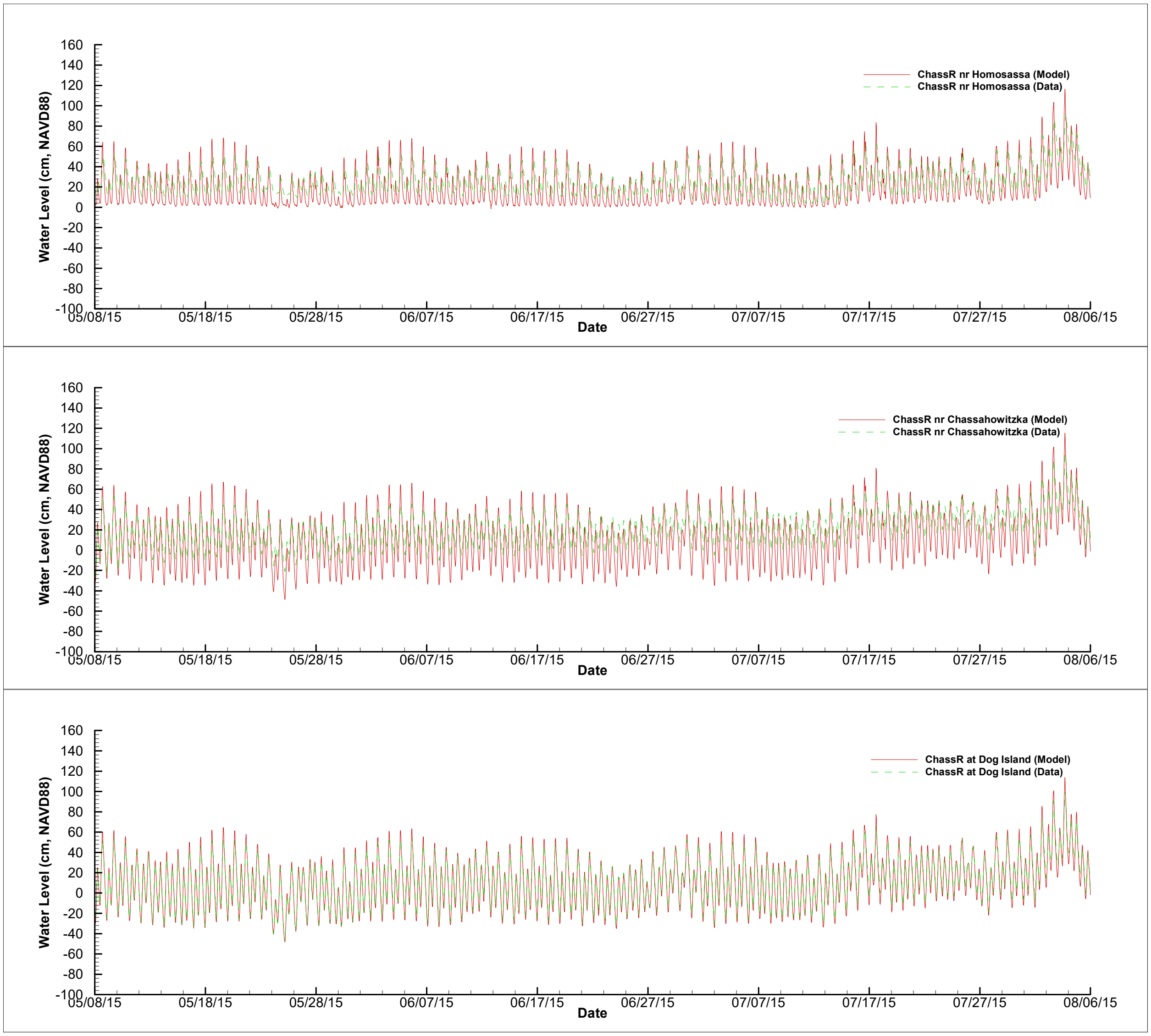

Figure D - 11. Comparisons of simulated (red lines) and measured (dashed green lines) water levels at the Chassahowitzka River near Homosassa (top panel), near Chassahowitzka, and at Dog Island stations during 5/8/2015 – 8/6/2015.

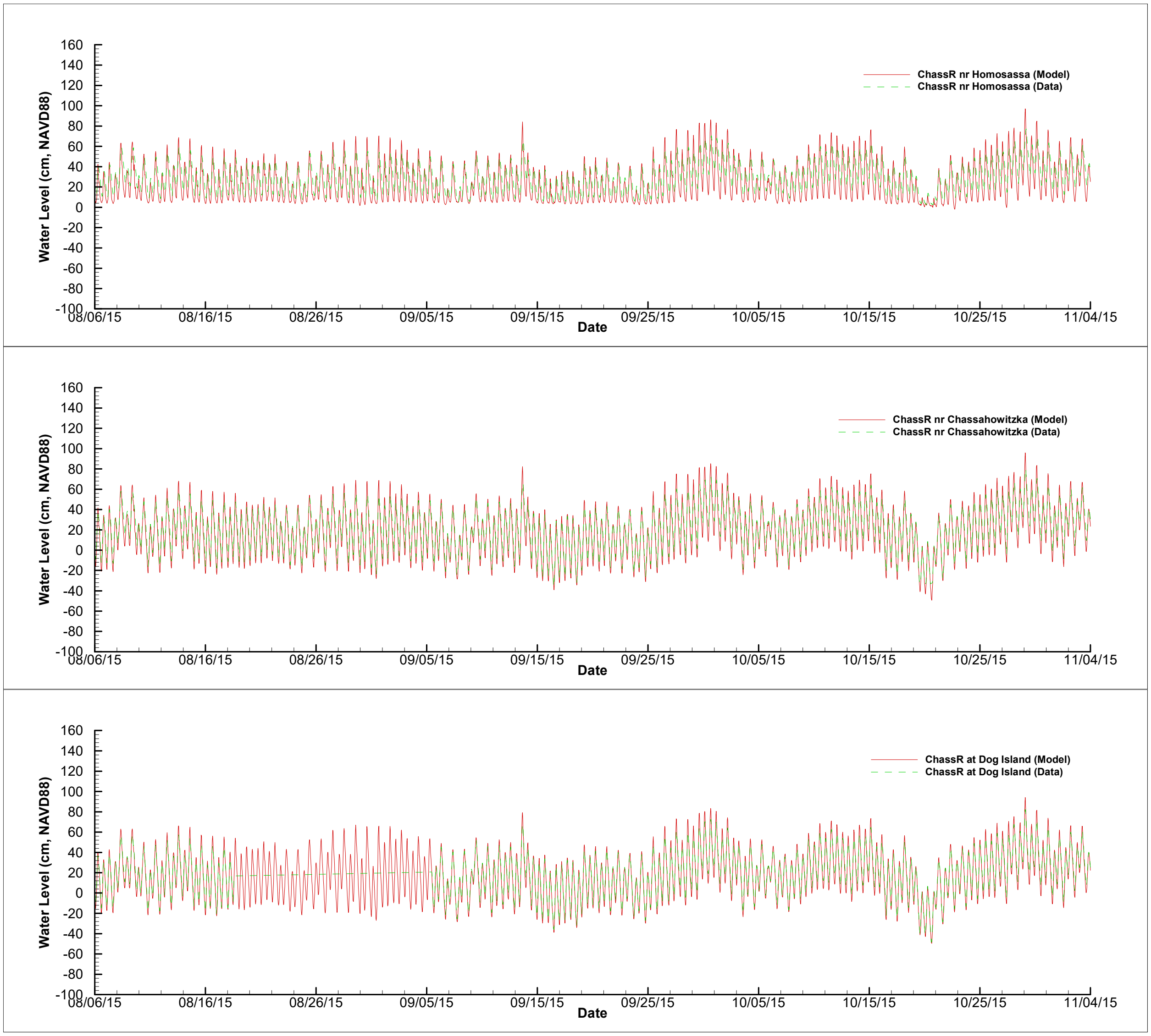

Figure D - 12. Comparisons of simulated (red lines) and measured (dashed green lines) water levels at the Chassahowitzka River near Homosassa (top panel), near Chassahowitzka, and at Dog Island stations during 8/6/2015 – 11/4/2015.

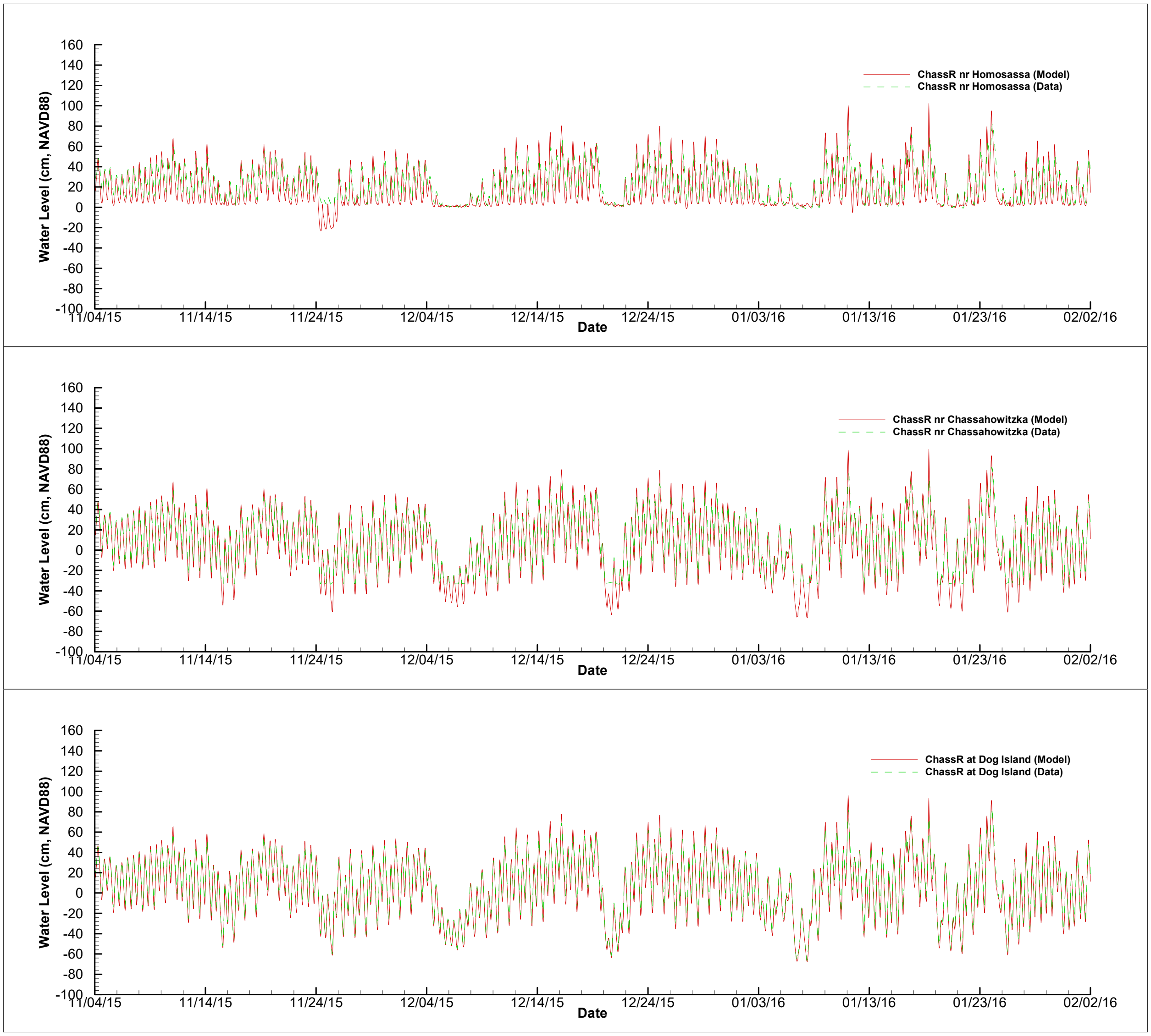

Figure D - 13. Comparisons of simulated (red lines) and measured (dashed green lines) water levels at the Chassahowitzka River near Homosassa (top panel), near Chassahowitzka, and at Dog Island stations during 11/4/2015 – 2/2/2016.

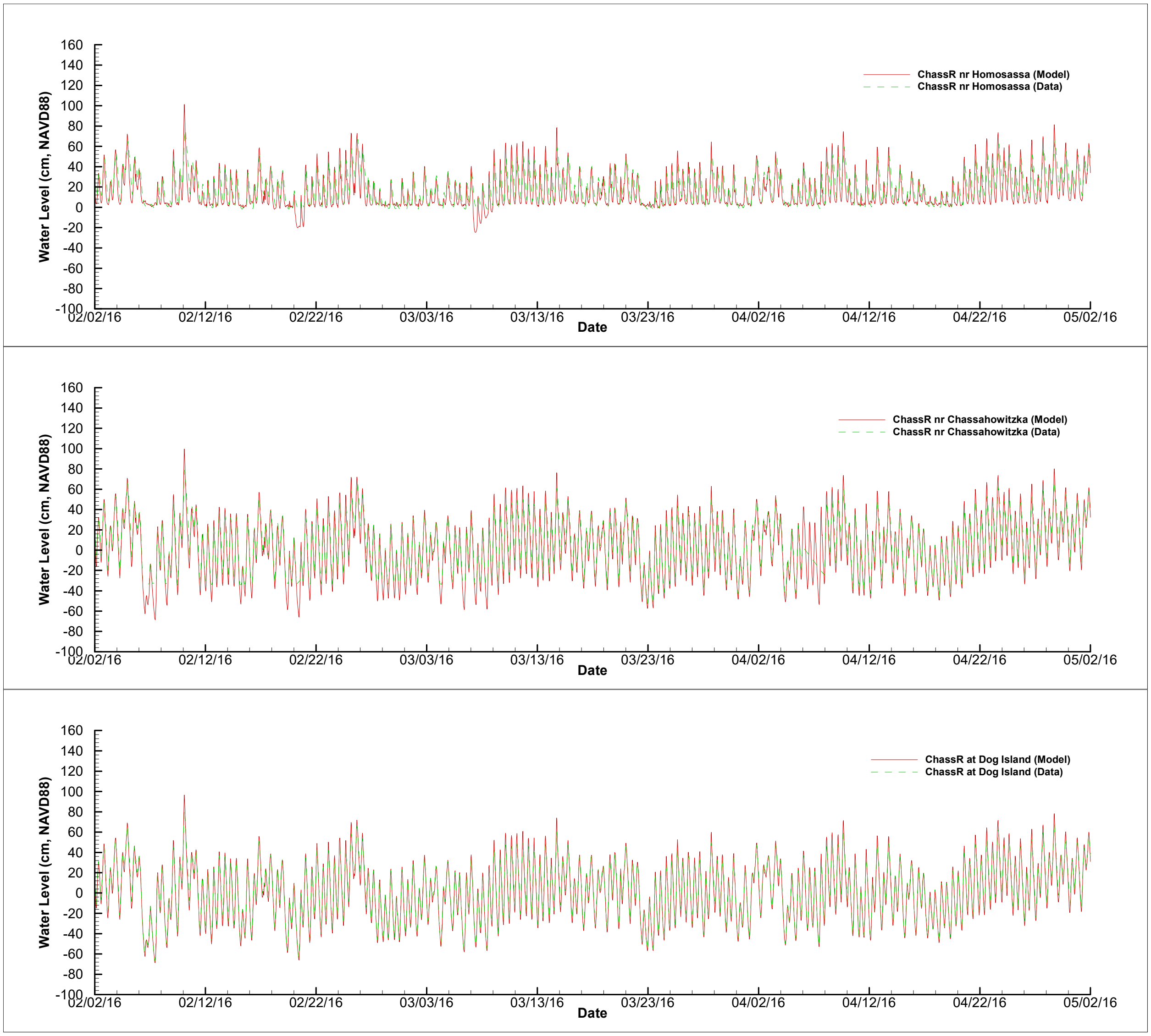

Figure D - 14. Comparisons of simulated (red lines) and measured (dashed green lines) water levels at the Chassahowitzka River near Homosassa (top panel), near Chassahowitzka, and at Dog Island stations during 2/2/2016 – 5/2/2016.

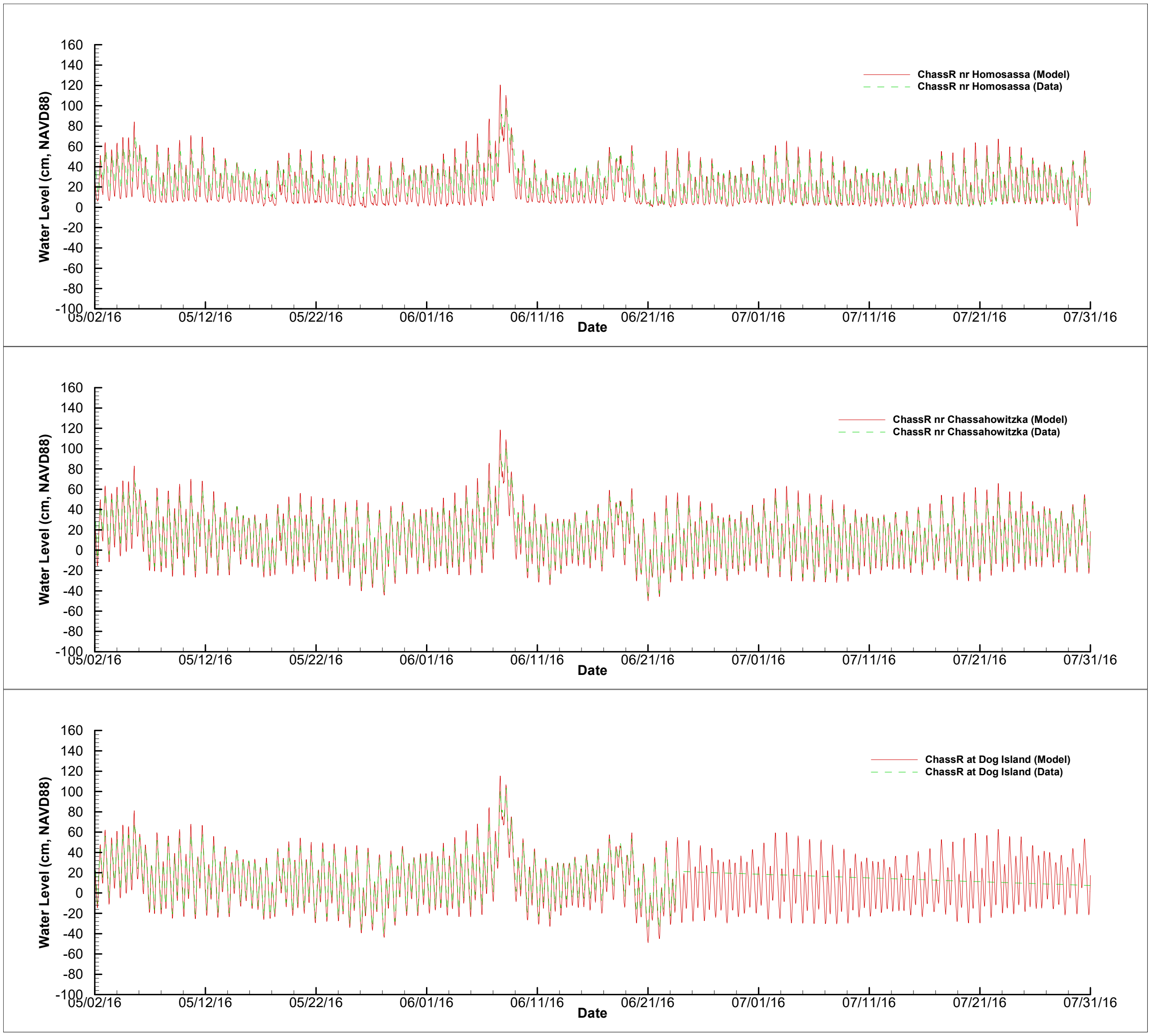

Figure D - 15. Comparisons of simulated (red lines) and measured (dashed green lines) water levels at the Chassahowitzka River near Homosassa (top panel), near Chassahowitzka, and at Dog Island stations during 5/2/2016 - 7/31/2016.

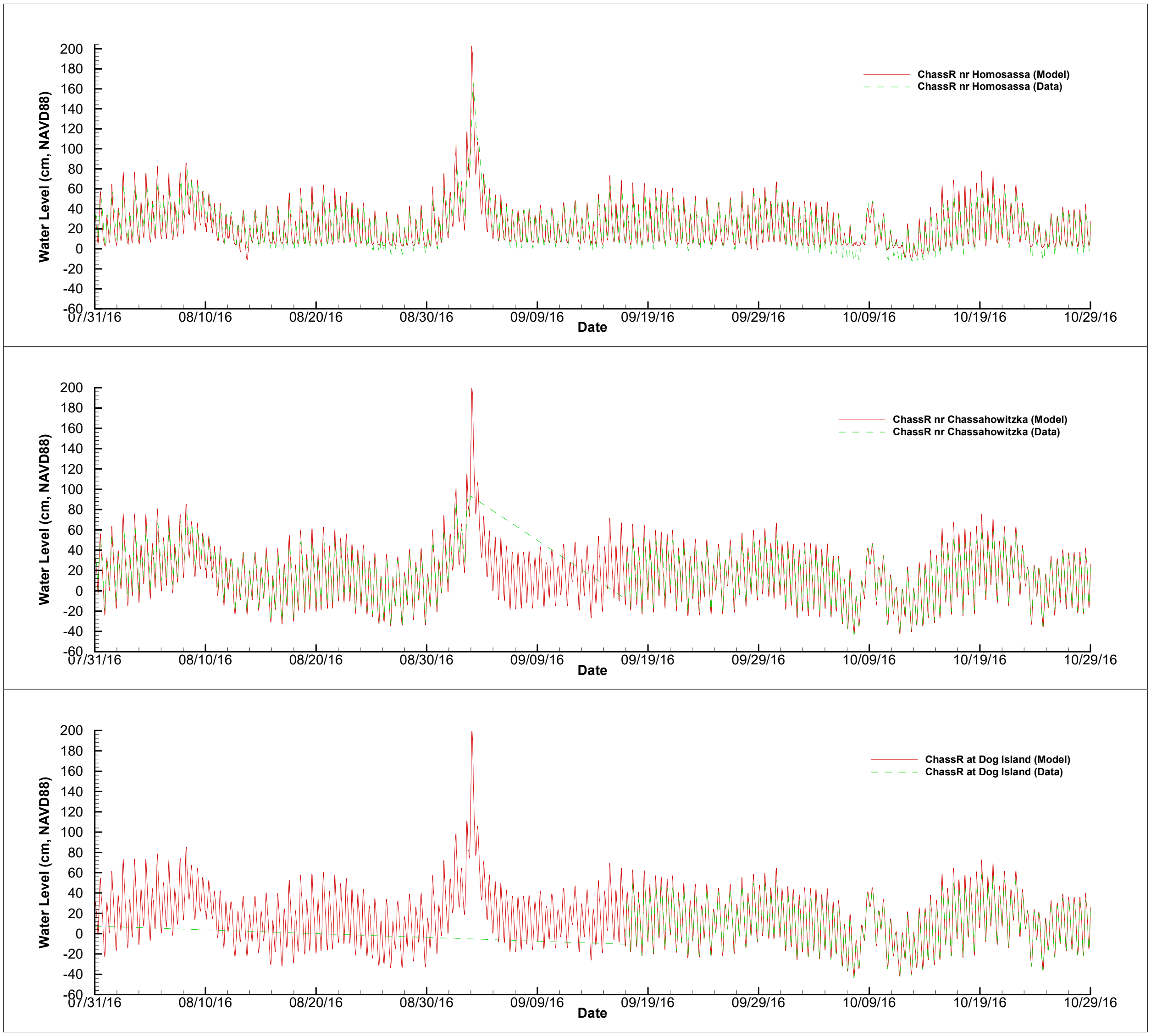

Figure D - 16. Comparisons of simulated (red lines) and measured (dashed green lines) water levels at the Chassahowitzka River near Homosassa (top panel), near Chassahowitzka, and at Dog Island stations during 7/31/2016 – 10/29/2016.

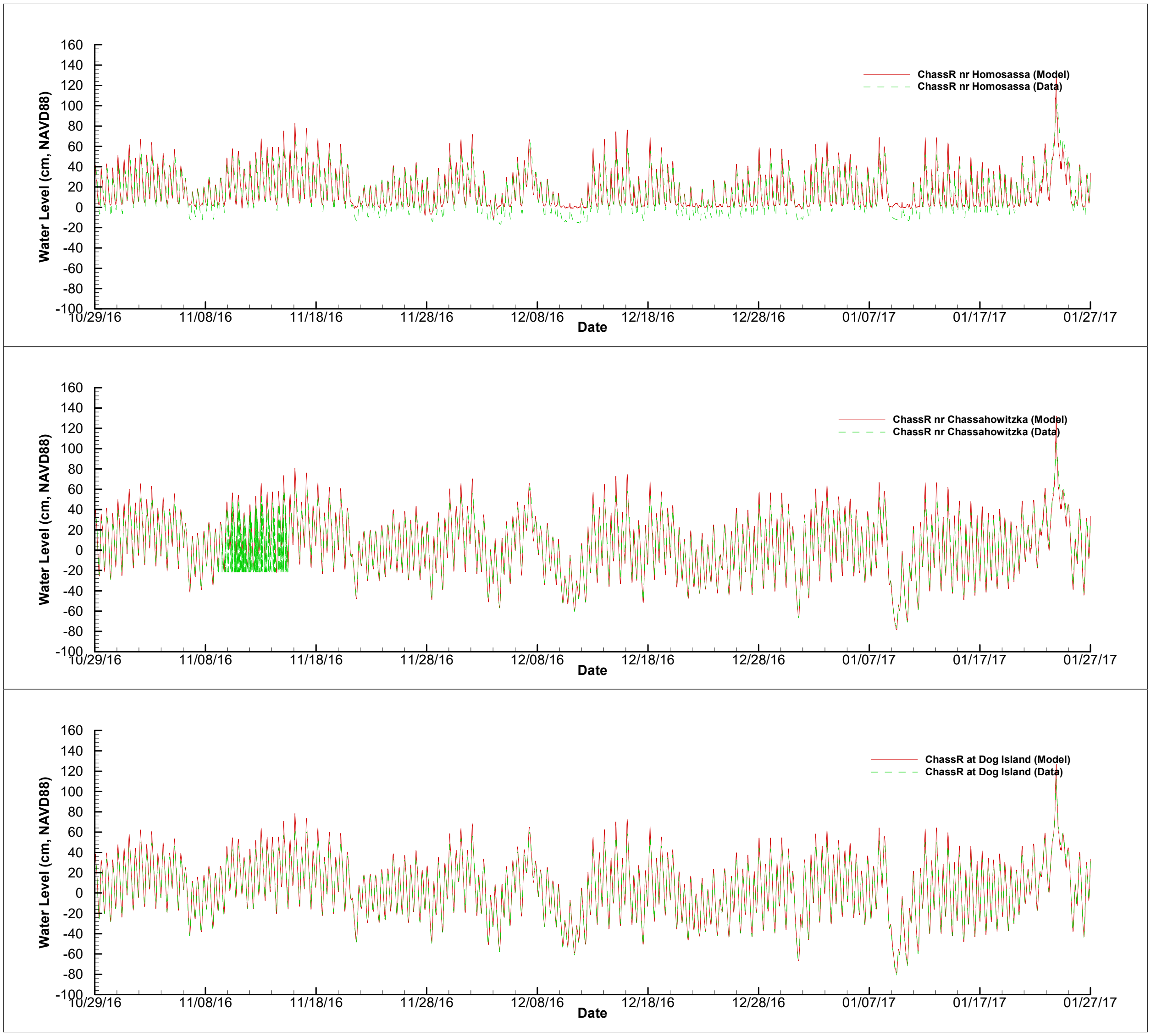

Figure D - 17. Comparisons of simulated (red lines) and measured (dashed green lines) water levels at the Chassahowitzka River near Homosassa (top panel), near Chassahowitzka, and at Dog Island stations during 10/29/2016 – 1/27/2017.

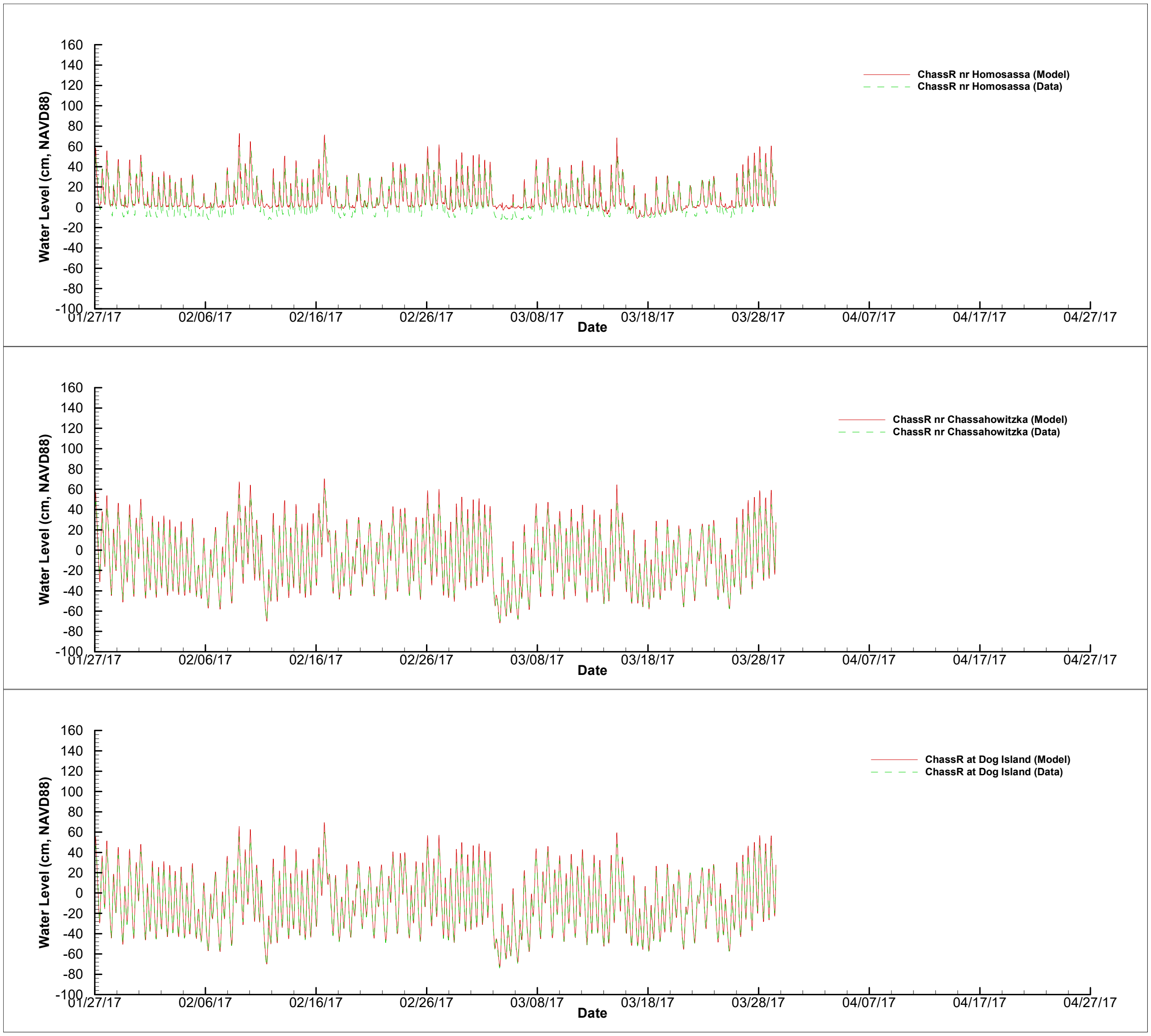

Figure D - 18. Comparisons of simulated (red lines) and measured (dashed green lines) water levels at the Chassahowitzka River near Homosassa (top panel), near Chassahowitzka, and at Dog Island stations during 1/27/2017 – 4/27/2017.

Appendix E. Simulated and Measured Salinities

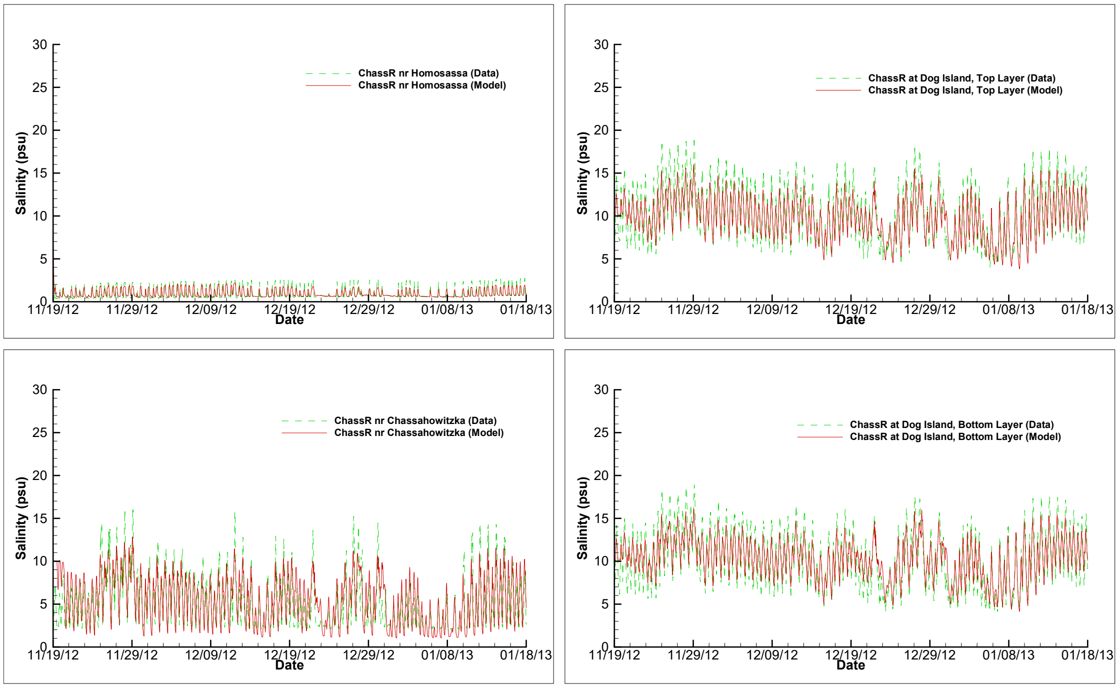

Figure E - 1. Simulated (red lines) and measured (dashed green lines) salinities at the Chassahowitzka River near Homosassa (top left panel), near Chassahowitzka (bottom left), and at Dog Island (right panels) stations during 11/19/2012 – 1/18/2013.

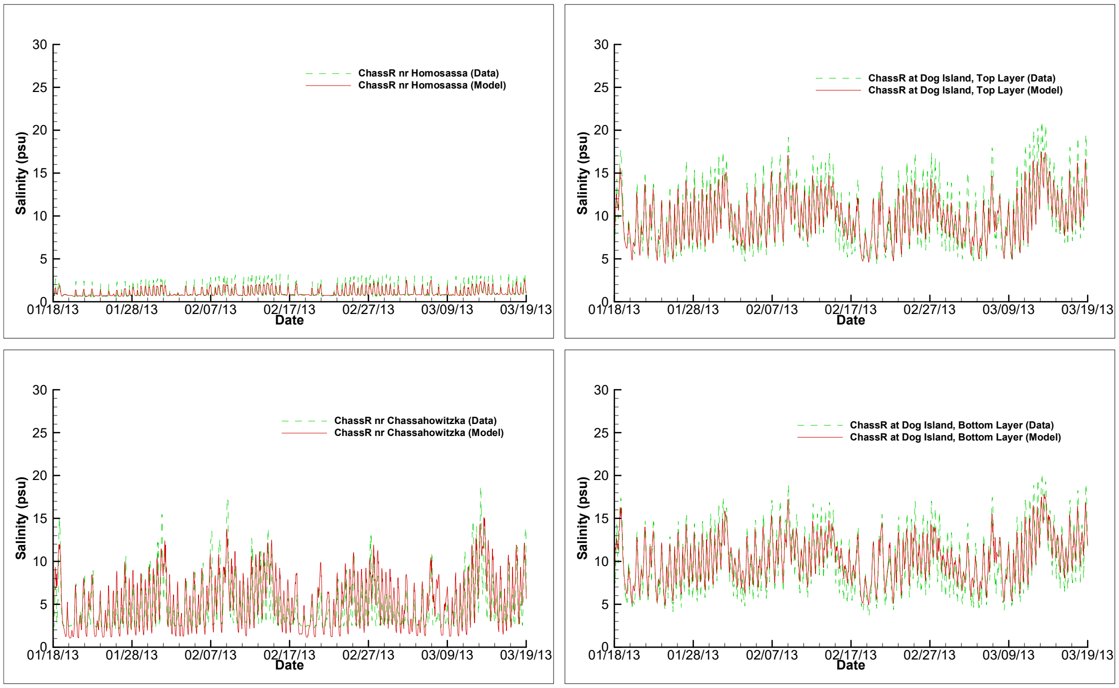

Figure E - 2. Simulated (red lines) and measured (dashed green lines) salinities at the Chassahowitzka River near Homosassa (top left panel), near Chassahowitzka (bottom left), and at Dog Island (right panels) stations during 1/18/2013 – 3/19/2013.

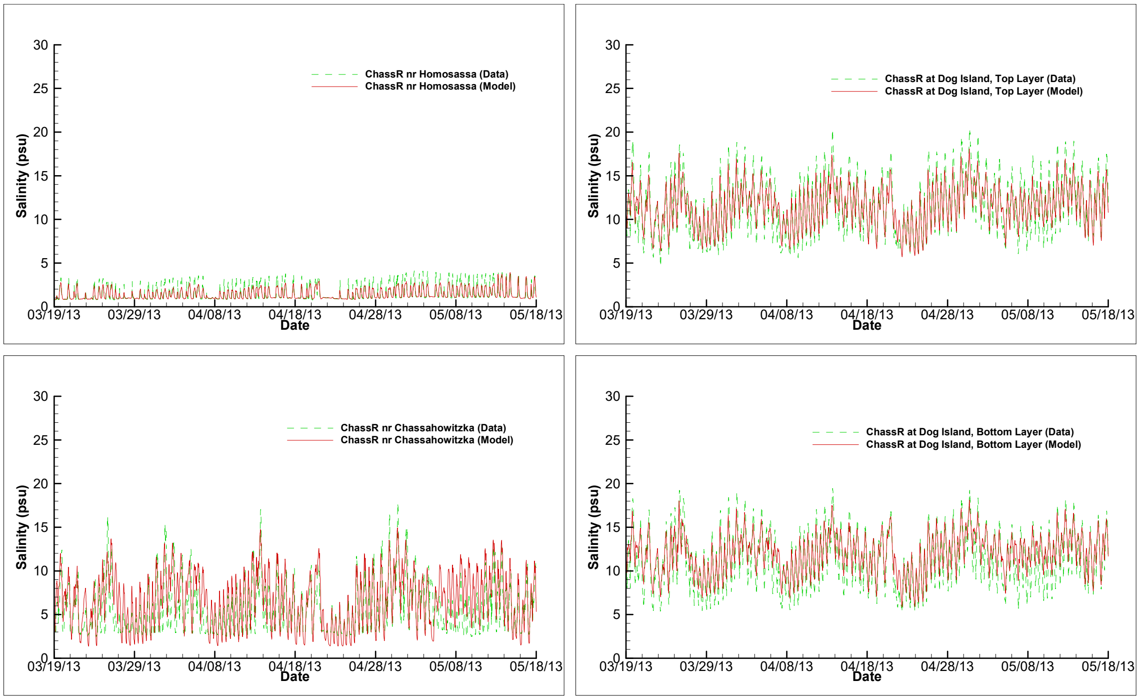

Figure E - 3. Simulated (red lines) and measured (dashed green lines) salinities at the Chassahowitzka River near Homosassa (top left panel), near Chassahowitzka (bottom left), and at Dog Island (right panels) stations during 3/19/2013 – 5/18/2013.

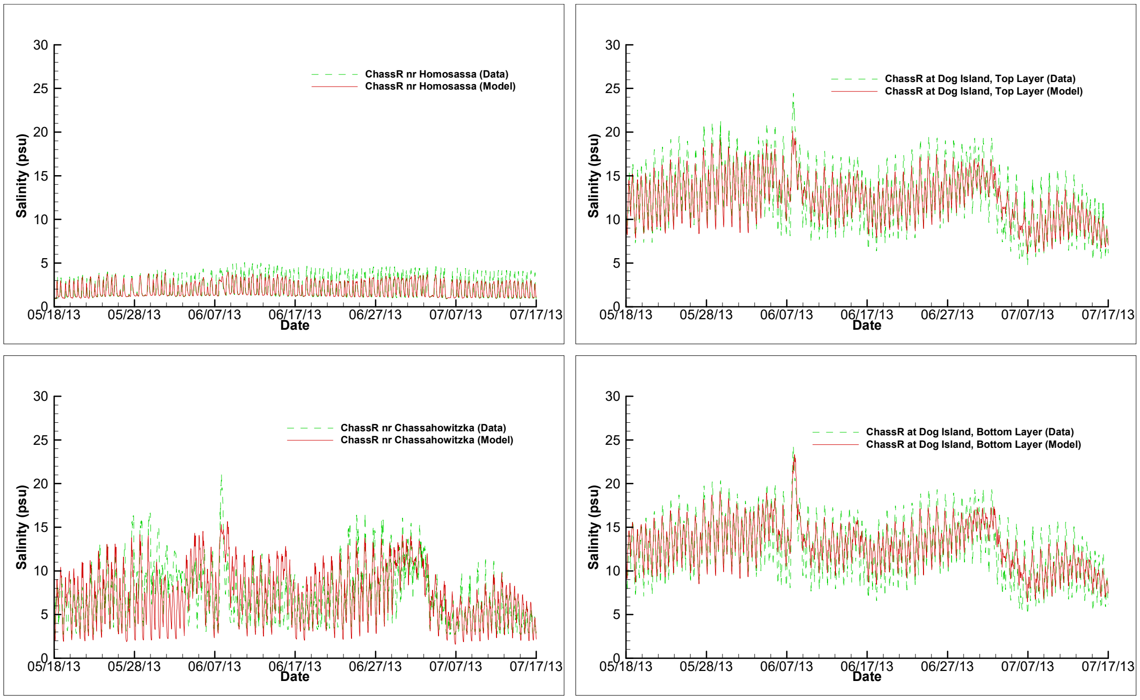

Figure E - 4. Simulated (red lines) and measured (dashed green lines) salinities at the Chassahowitzka River near Homosassa (top left panel), near Chassahowitzka (bottom left), and at Dog Island (right panels) stations during 5/18/2013 – 7/17/2013.

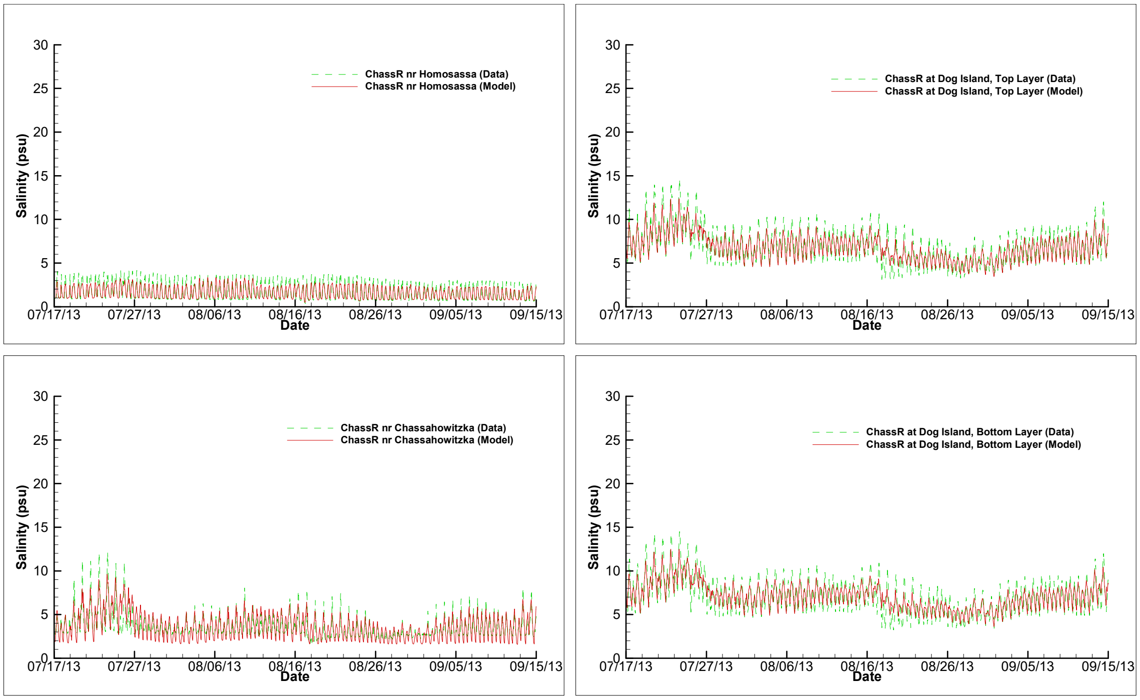

Figure E - 5. Simulated (red lines) and measured (dashed green lines) salinities at the Chassahowitzka River near Homosassa (top left panel), near Chassahowitzka (bottom left), and at Dog Island (right panels) stations during 7/17/2013 – 9/15/2013.

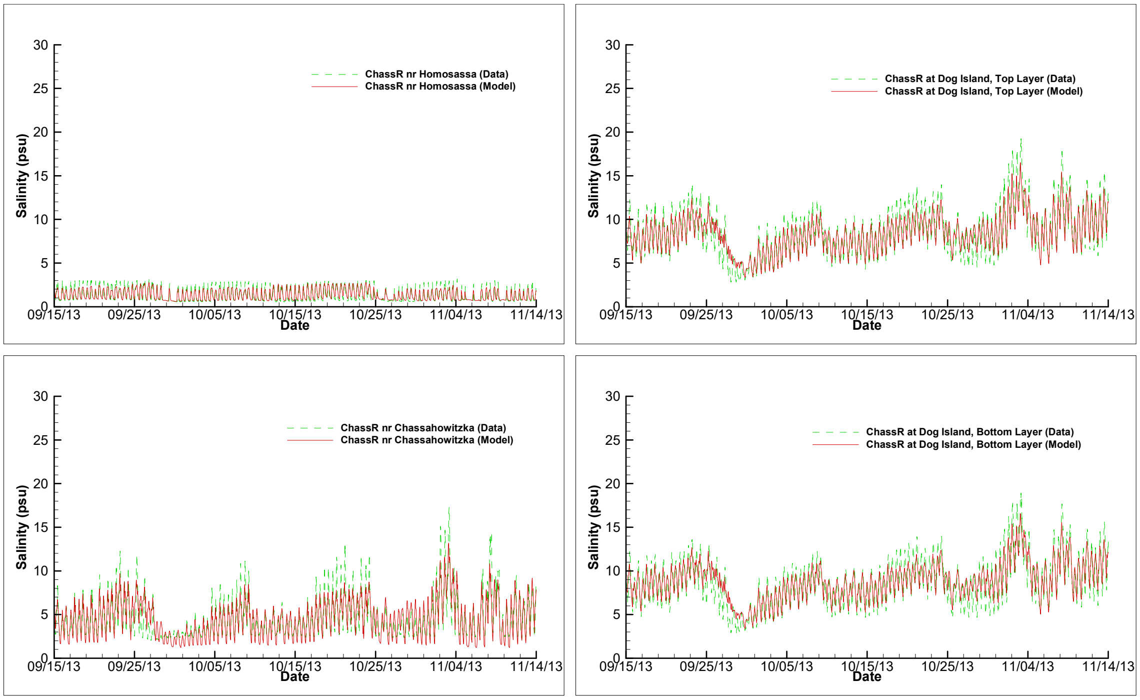

Figure E - 6. Simulated (red lines) and measured (dashed green lines) salinities at the Chassahowitzka River near Homosassa (top left panel), near Chassahowitzka (bottom left), and at Dog Island (right panels) stations during 9/15/2013 – 11/14/2013.

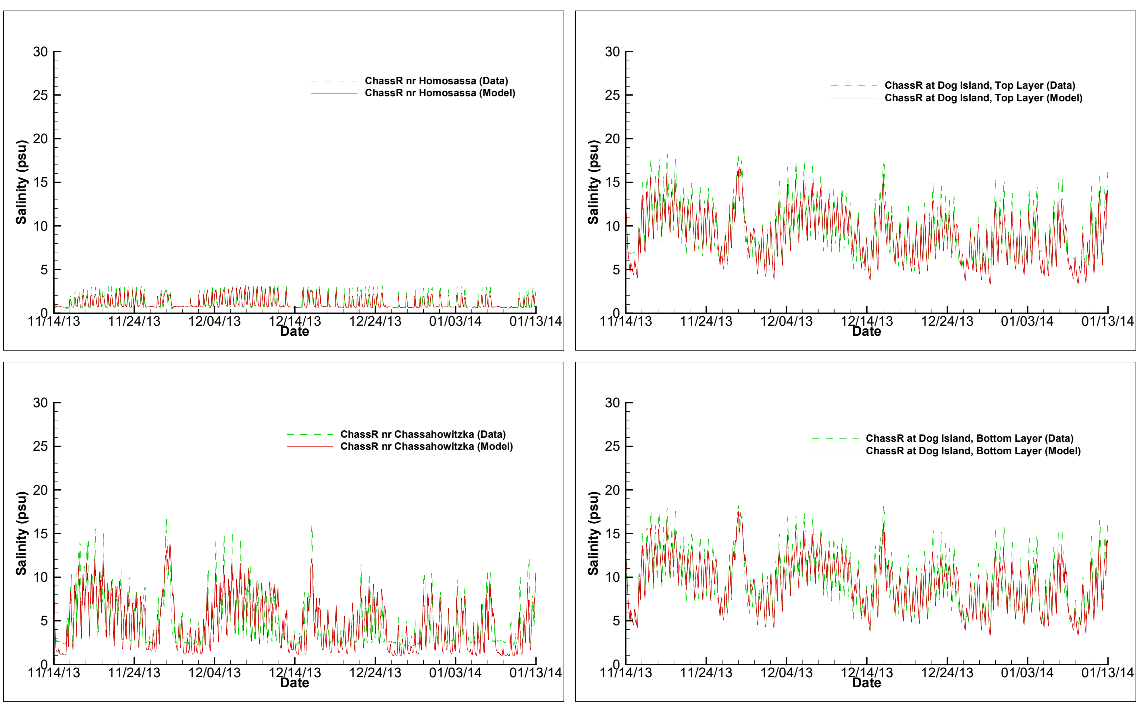

Figure E - 7. Simulated (red lines) and measured (dashed green lines) salinities at the Chassahowitzka River near Homosassa (top left panel), near Chassahowitzka (bottom left), and at Dog Island (right panels) stations during 11/14/2013 – 1/13/2014.

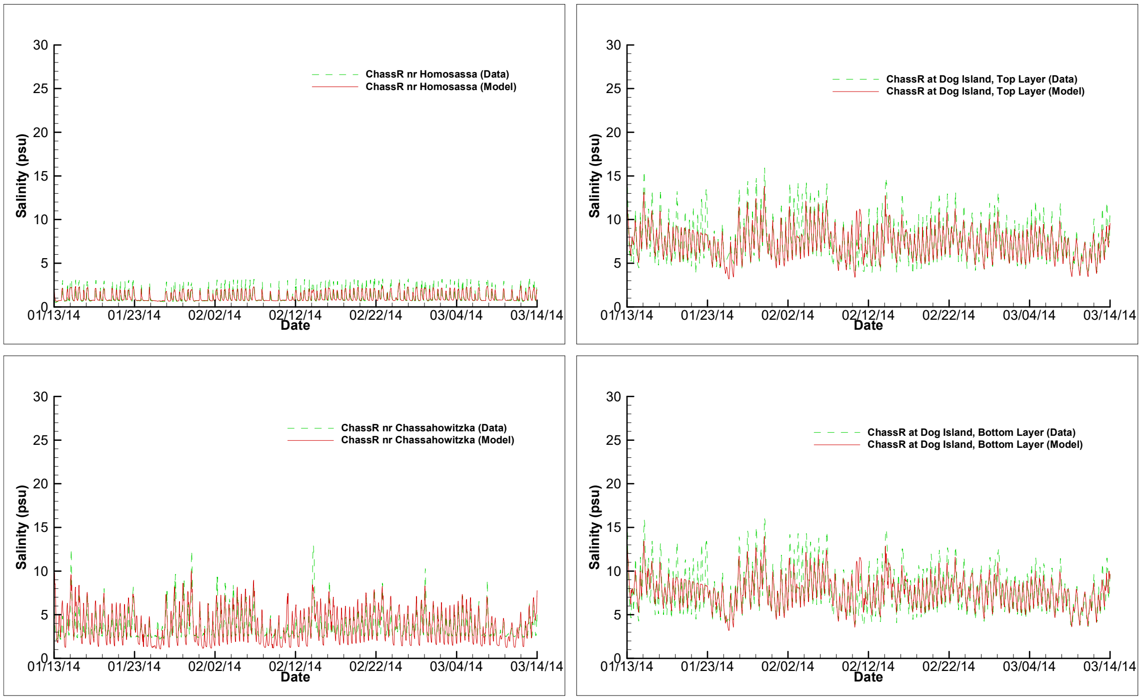

Figure E - 8. Simulated (red lines) and measured (dashed green lines) salinities at the Chassahowitzka River near Homosassa (top left panel), near Chassahowitzka (bottom left), and at Dog Island (right panels) stations during 1/13/2014 – 3/14/2014.

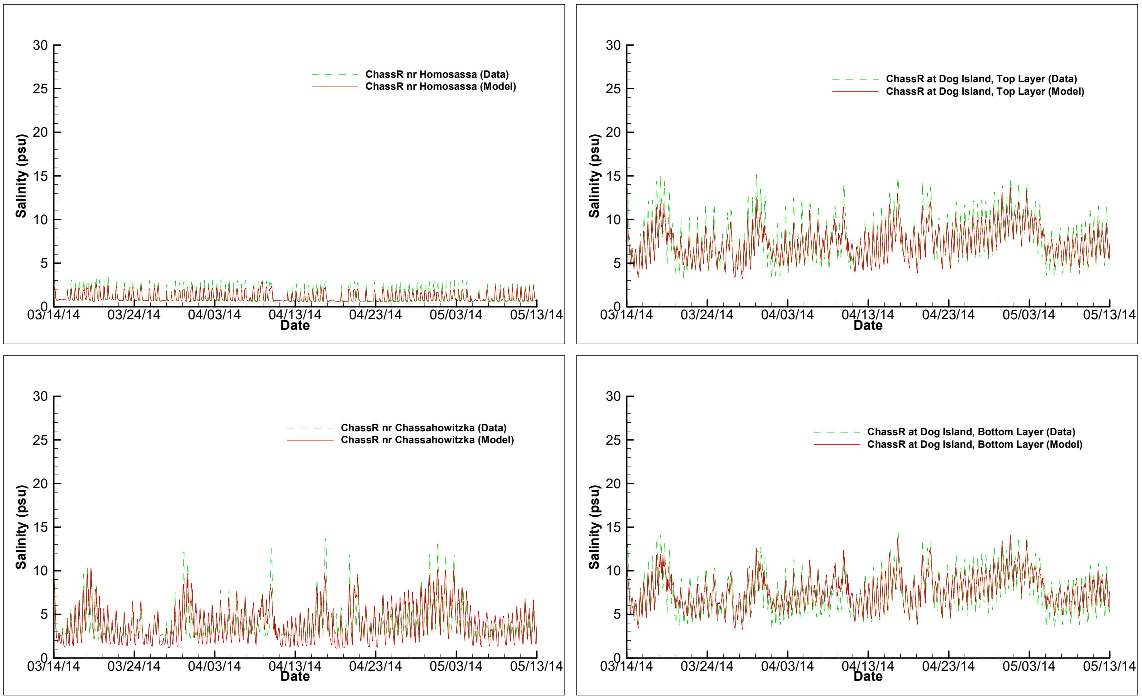

Figure E - 9. Simulated (red lines) and measured (dashed green lines) salinities at the Chassahowitzka River near Homosassa (top left panel), near Chassahowitzka (bottom left), and at Dog Island (right panels) stations during 3/14/2014 – 5/1/3/2014.

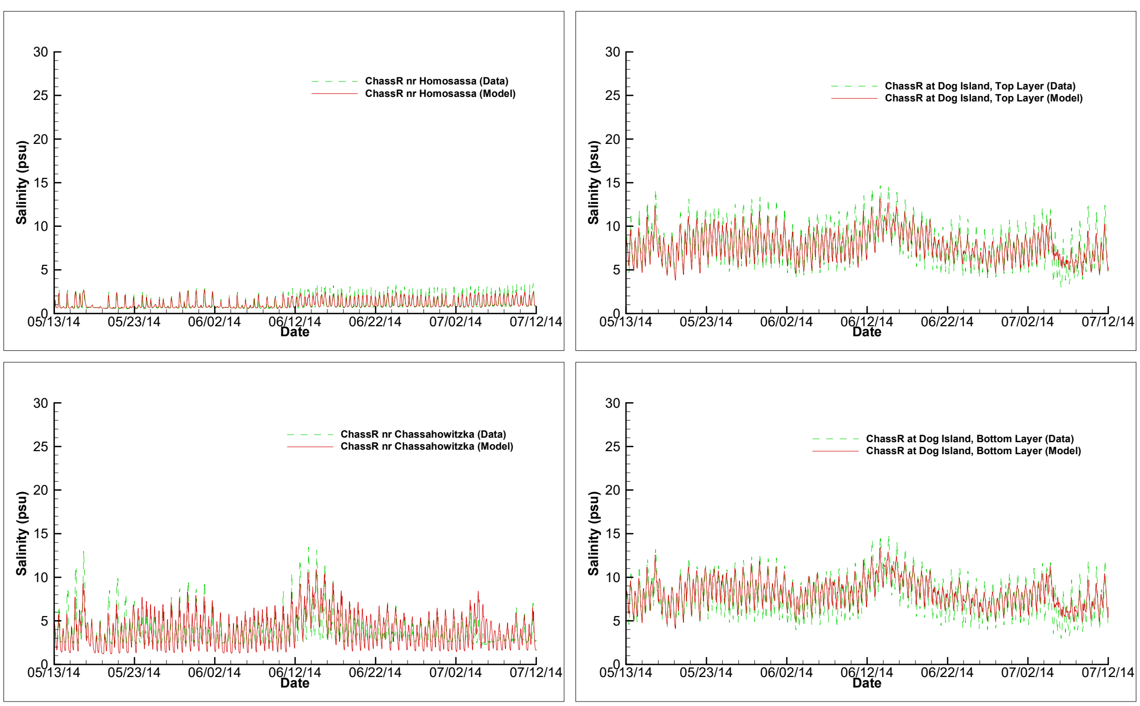

Figure E - 10. Simulated (red lines) and measured (dashed green lines) salinities at the Chassahowitzka River near Homosassa (top left panel), near Chassahowitzka (bottom left), and at Dog Island (right panels) stations during 5/13/2014 – 7/12/2014.

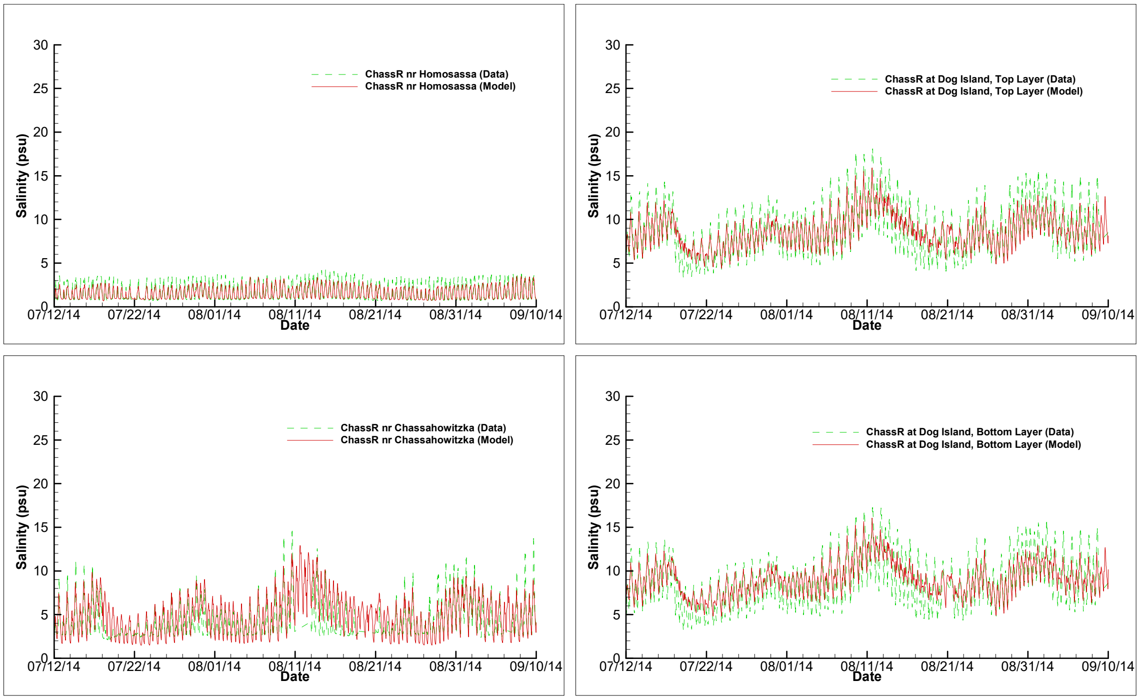

Figure E - 11. Simulated (red lines) and measured (dashed green lines) salinities at the Chassahowitzka River near Homosassa (top left panel), near Chassahowitzka (bottom left), and at Dog Island (right panels) stations during 7/12/2014 – 9/10/2014.

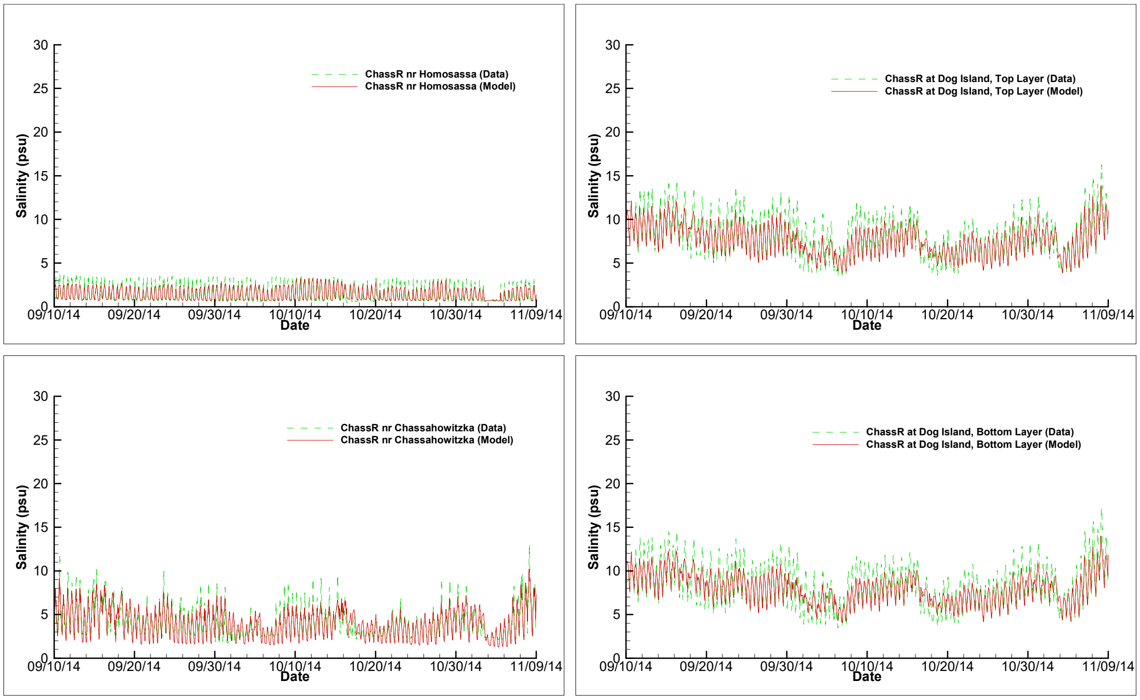

Figure E - 12. Simulated (red lines) and measured (dashed green lines) salinities at the Chassahowitzka River near Homosassa (top left panel), near Chassahowitzka (bottom left), and at Dog Island (right panels) stations during 9/10/2014 – 11/9/2014.

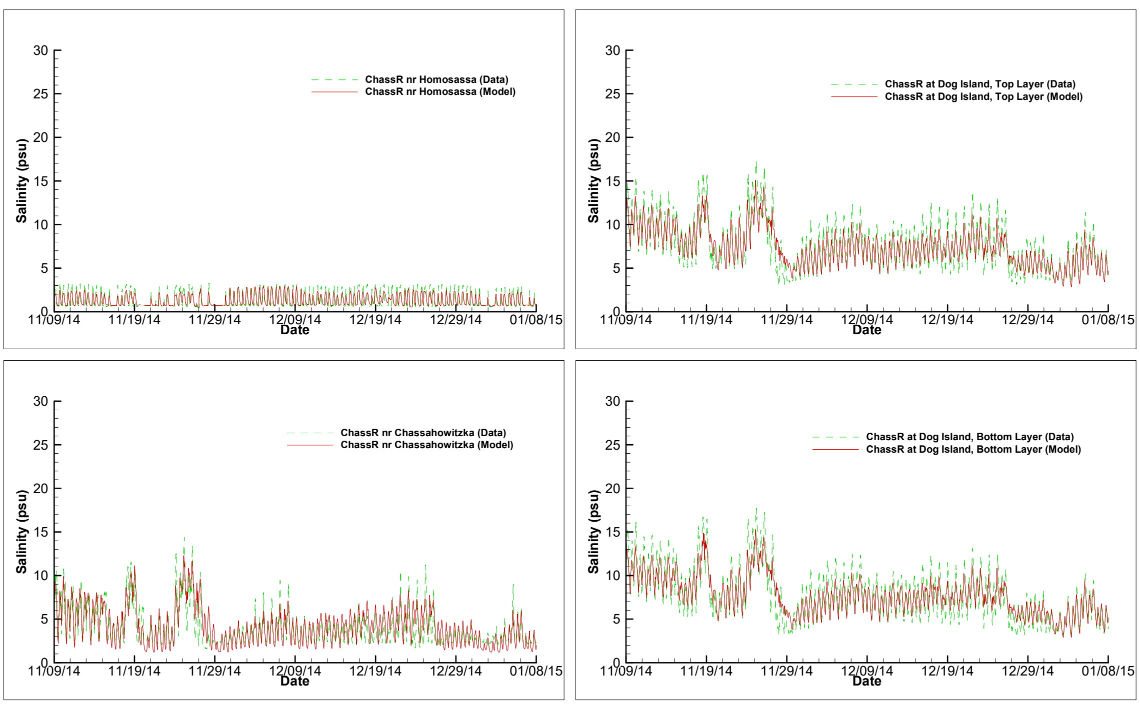

Figure E - 13. Simulated (red lines) and measured (dashed green lines) salinities at the Chassahowitzka River near Homosassa (top left panel), near Chassahowitzka (bottom left), and at Dog Island (right panels) stations during 11/9/2014 – 1/8/2015.

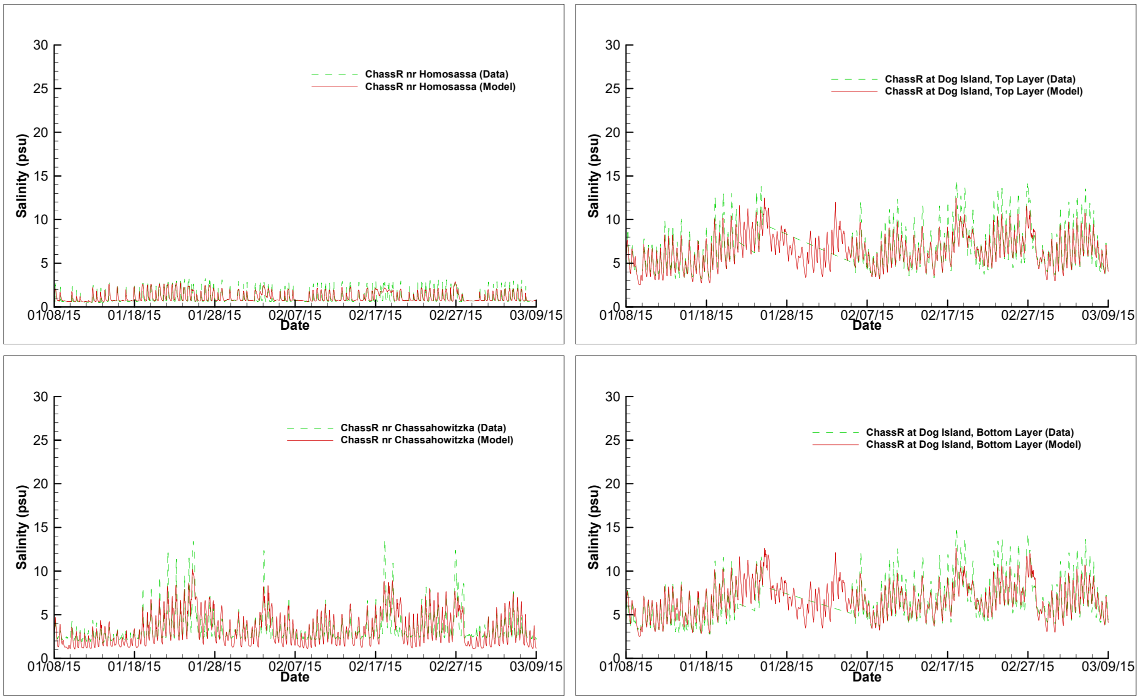

Figure E - 14. Simulated (red lines) and measured (dashed green lines) salinities at the Chassahowitzka River near Homosassa (top left panel), near Chassahowitzka (bottom left), and at Dog Island (right panels) stations during 1/8/2015 – 3/9/2015.

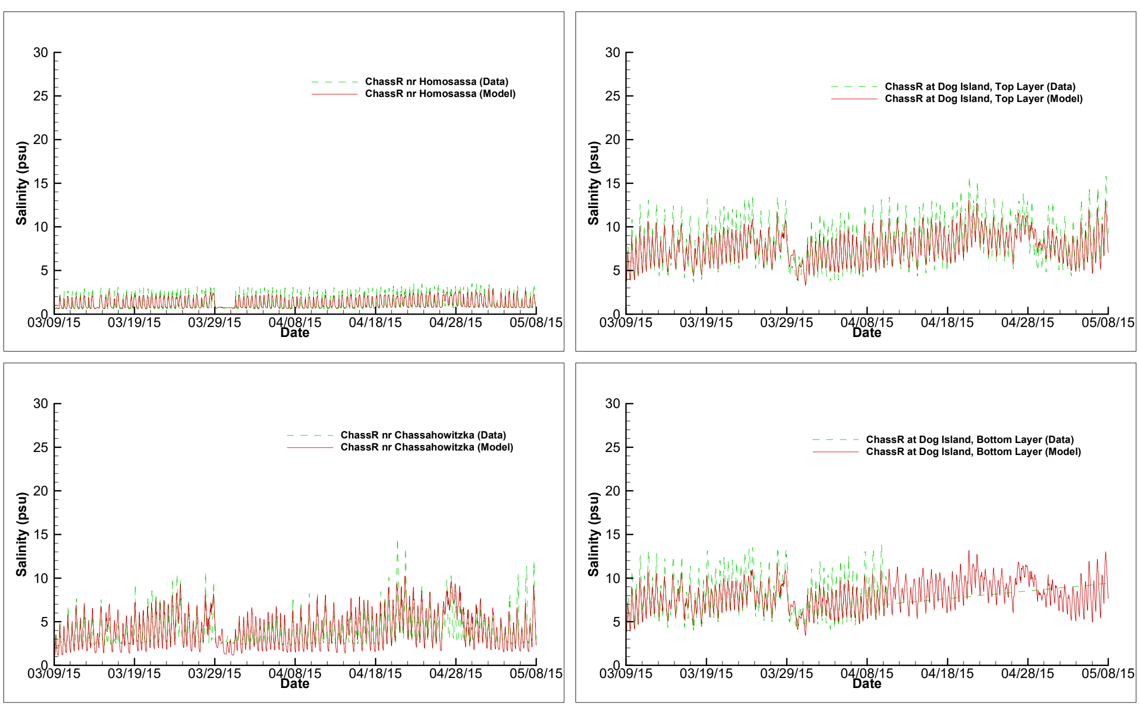

Figure E - 15. Simulated (red lines) and measured (dashed green lines) salinities at the Chassahowitzka River near Homosassa (top left panel), near Chassahowitzka (bottom left), and at Dog Island (right panels) stations during 3/9/2015 – 5/8/2015.

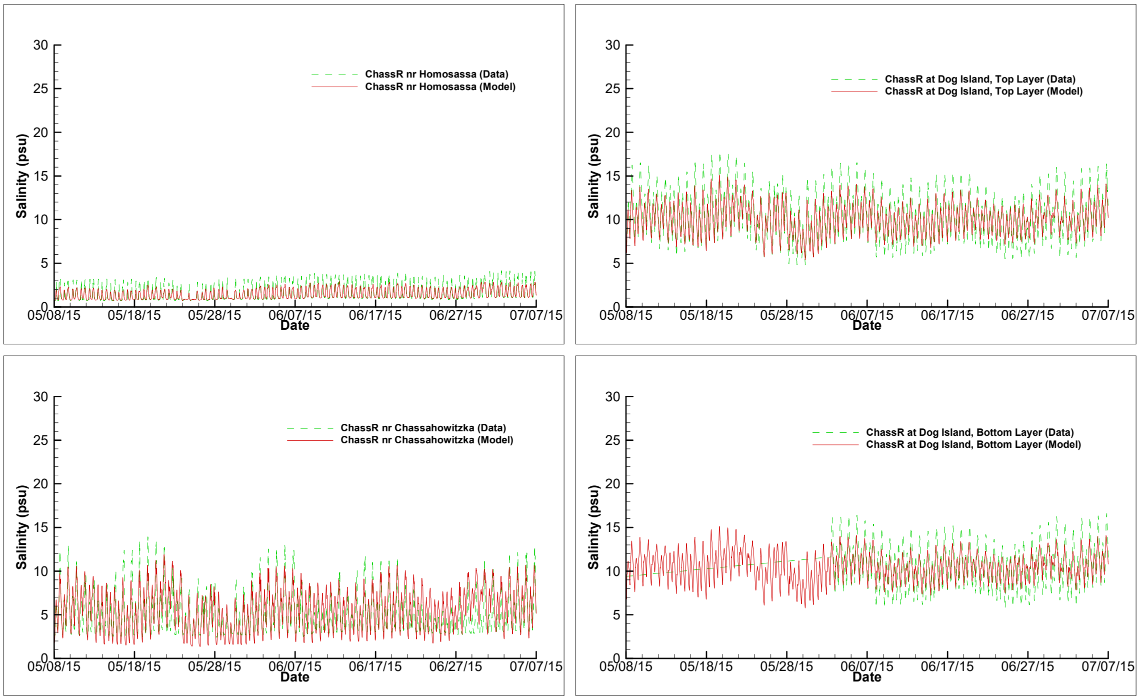

Figure E - 16. Simulated (red lines) and measured (dashed green lines) salinities at the Chassahowitzka River near Homosassa (top left panel), near Chassahowitzka (bottom left), and at Dog Island (right panels) stations during 5/8/2015 – 7/7/2015.

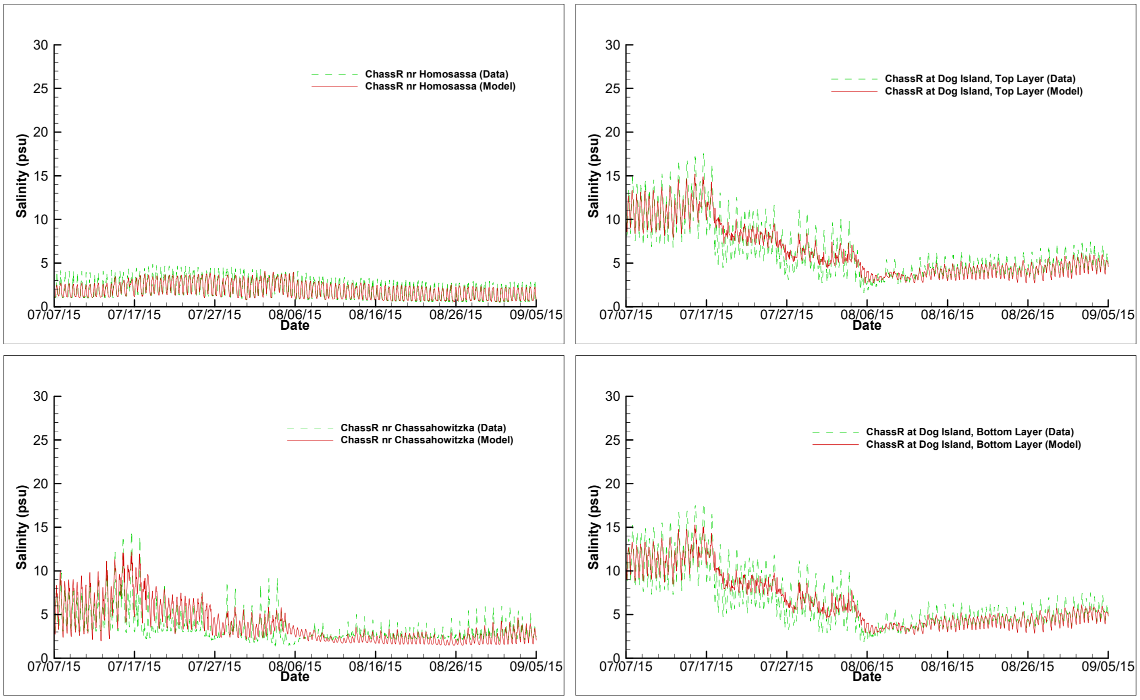

Figure E - 17. Simulated (red lines) and measured (dashed green lines) salinities at the Chassahowitzka River near Homosassa (top left panel), near Chassahowitzka (bottom left), and at Dog Island (right panels) stations during 7/7/2015 -9/5/2015.

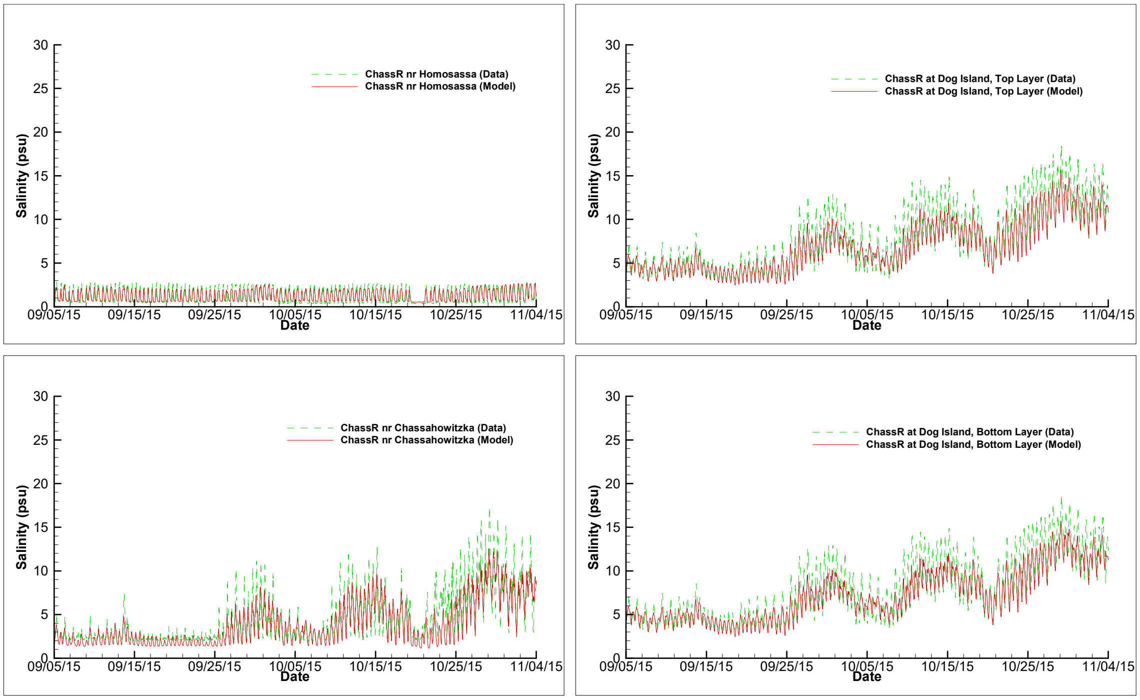

Figure E - 18. Simulated (red lines) and measured (dashed green lines) salinities at the Chassahowitzka River near Homosassa (top left panel), near Chassahowitzka (bottom left), and at Dog Island (right panels) stations during 9/5/2015 – 11/4/2015.

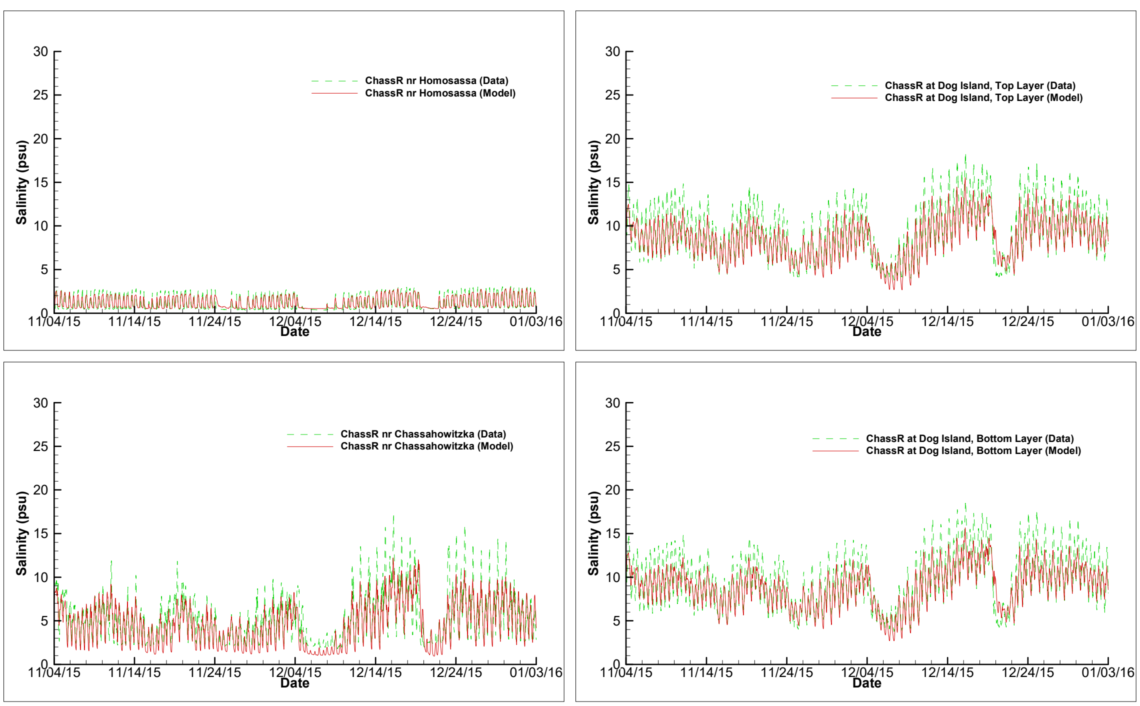

Figure E - 19. Simulated (red lines) and measured (dashed green lines) salinities at the Chassahowitzka River near Homosassa (top left panel), near Chassahowitzka (bottom left), and at Dog Island (right panels) stations during 11/4/2015 – 1/3/2016.

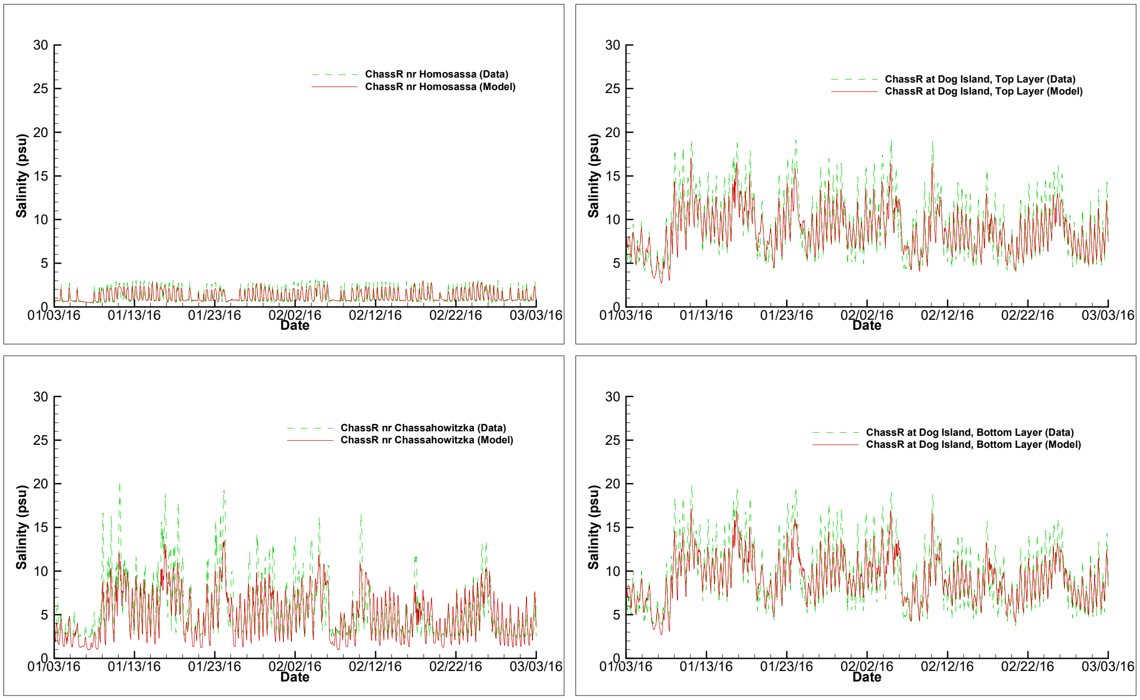

Figure E - 20. Simulated (red lines) and measured (dashed green lines) salinities at the Chassahowitzka River near Homosassa (top left panel), near Chassahowitzka (bottom left), and at Dog Island (right panels) stations during 1/3/2016 – 3/3/2016.

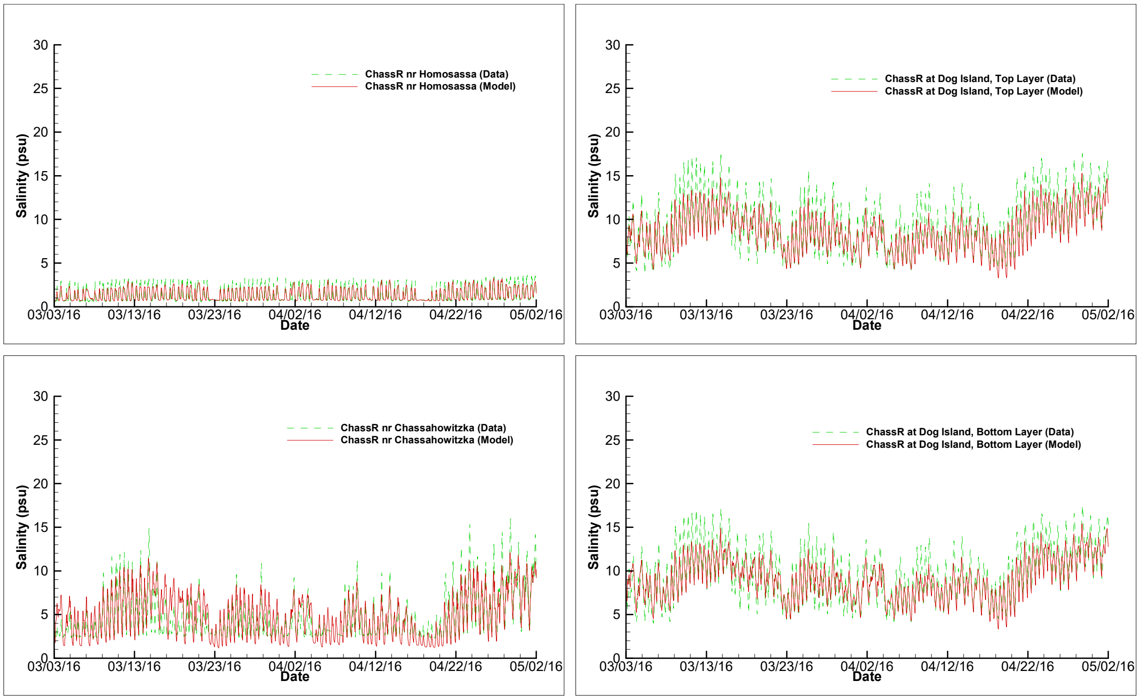

Figure E - 21. Simulated (red lines) and measured (dashed green lines) salinities at the Chassahowitzka River near Homosassa (top left panel), near Chassahowitzka (bottom left), and at Dog Island (right panels) stations during 3/3/2016 – 5/2/2016.

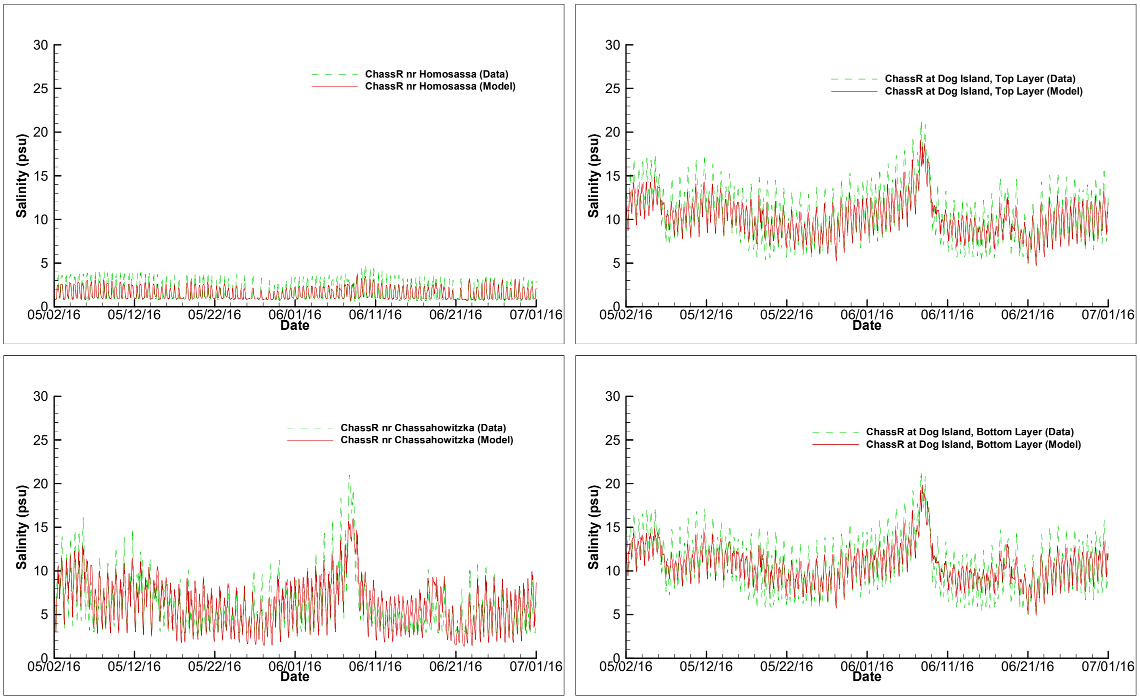

Figure E - 22. Simulated (red lines) and measured (dashed green lines) salinities at the Chassahowitzka River near Homosassa (top left panel), near Chassahowitzka (bottom left), and at Dog Island (right panels) stations during 5/2/2016 – 7/1/2016.

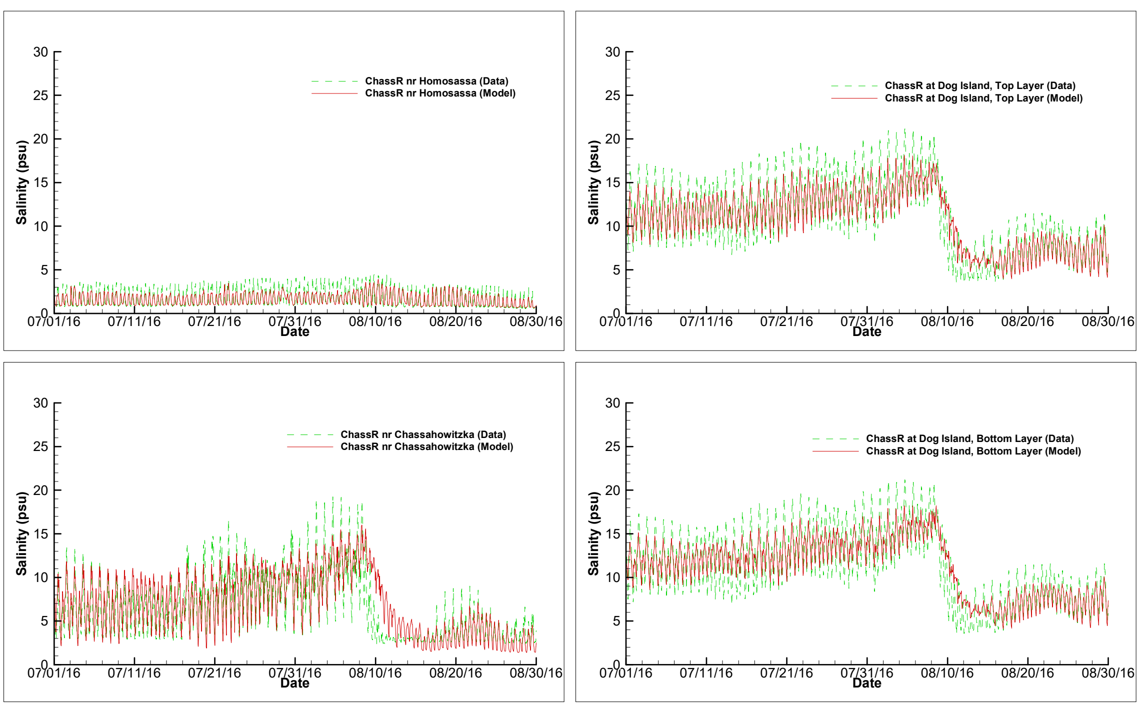

Figure E - 23. Simulated (red lines) and measured (dashed green lines) salinities at the Chassahowitzka River near Homosassa (top left panel), near Chassahowitzka (bottom left), and at Dog Island (right panels) stations during 7/1/2016 – 8/30/2016.

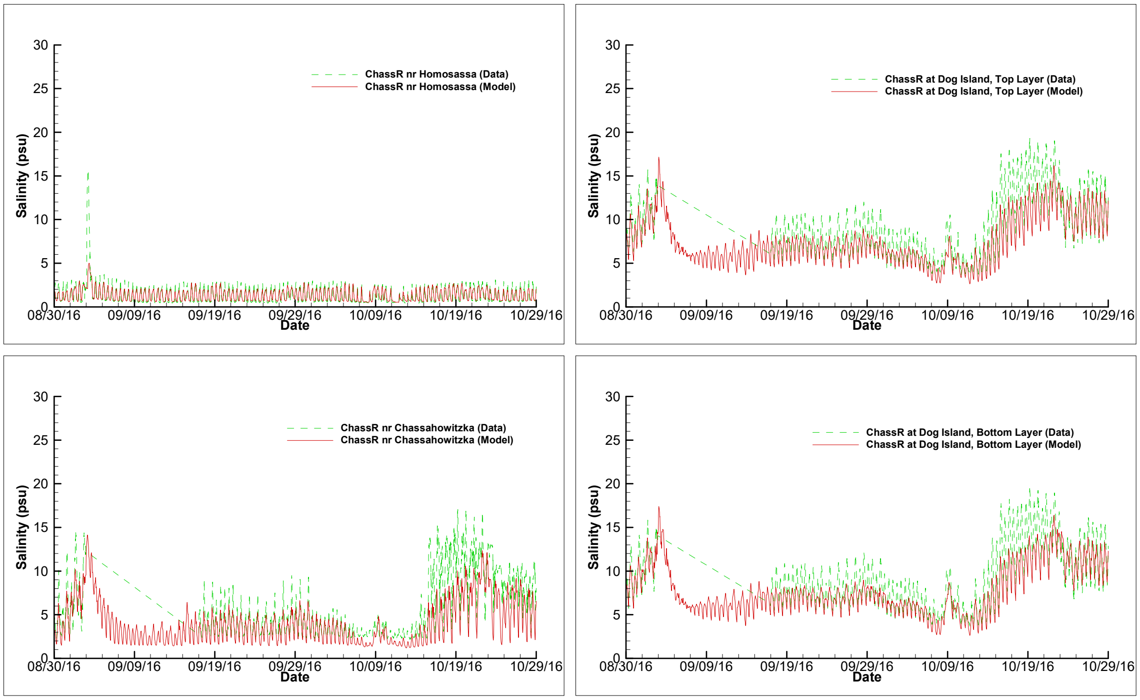

Figure E - 24. Simulated (red lines) and measured (dashed green lines) salinities at the Chassahowitzka River near Homosassa (top left panel), near Chassahowitzka (bottom left), and at Dog Island (right panels) stations during 8/30/2016 – 10/29/2016.

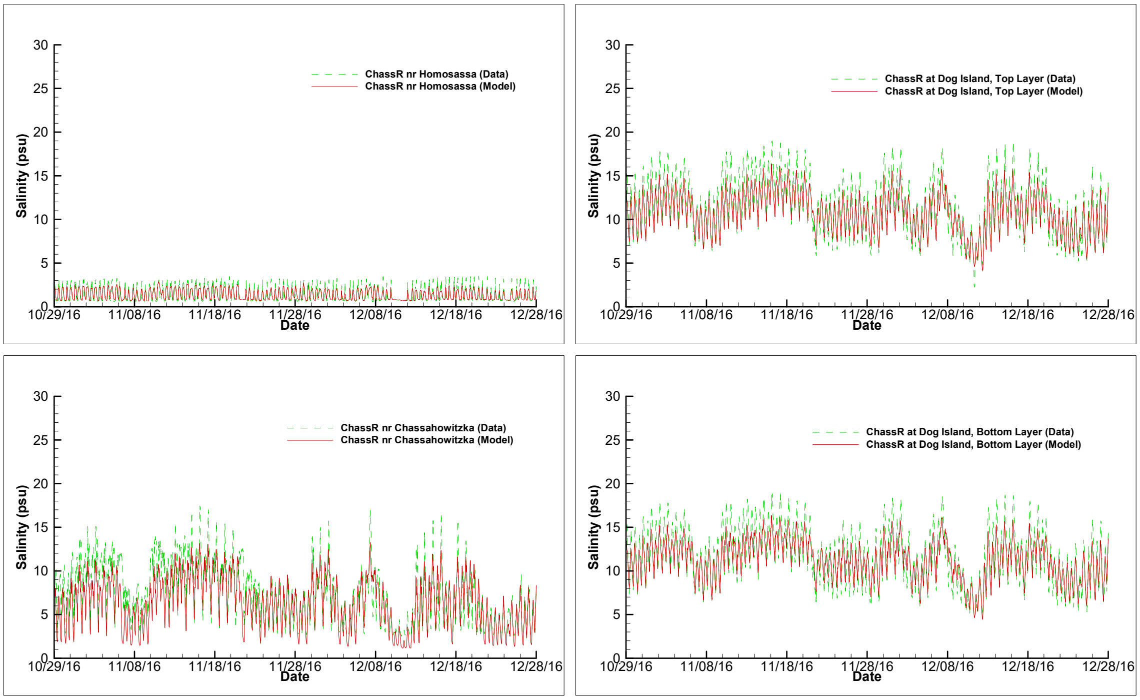

Figure E - 25. Simulated (red lines) and measured (dashed green lines) salinities at the Chassahowitzka River near Homosassa (top left panel), near Chassahowitzka (bottom left), and at Dog Island (right panels) stations during 10/29/2016 – 12/28/2016.

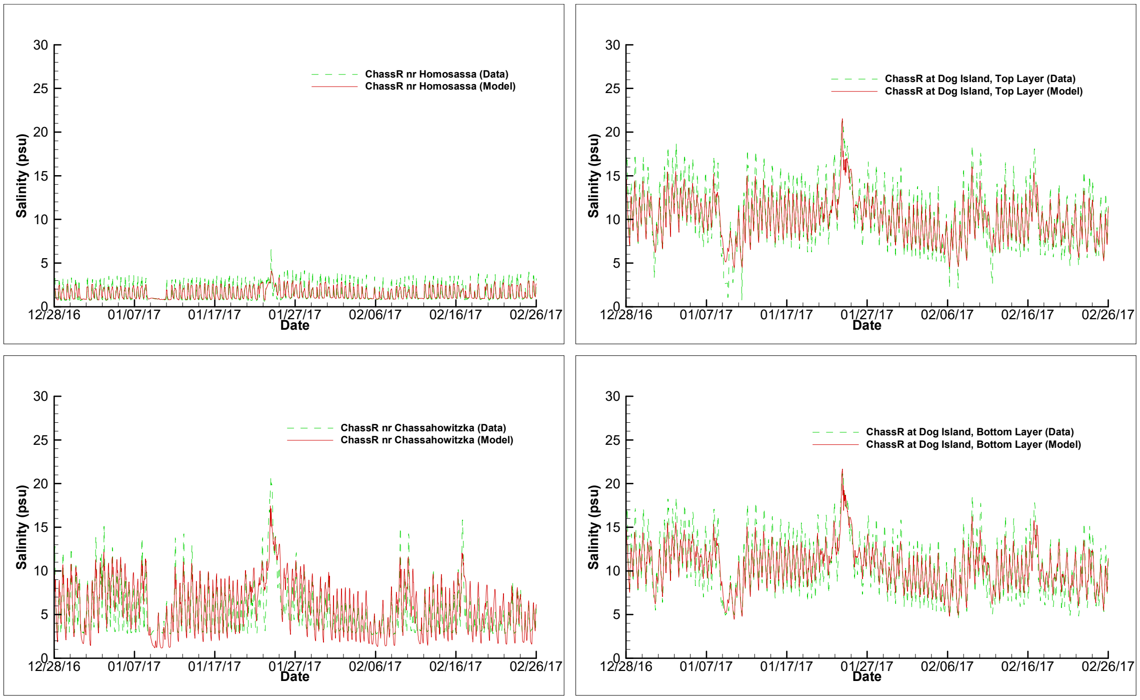

Figure E - 26. Simulated (red lines) and measured (dashed green lines) salinities at the Chassahowitzka River near Homosassa (top left panel), near Chassahowitzka (bottom left), and at Dog Island (right panels) stations during 12/28/2016 – 2/26/2017.

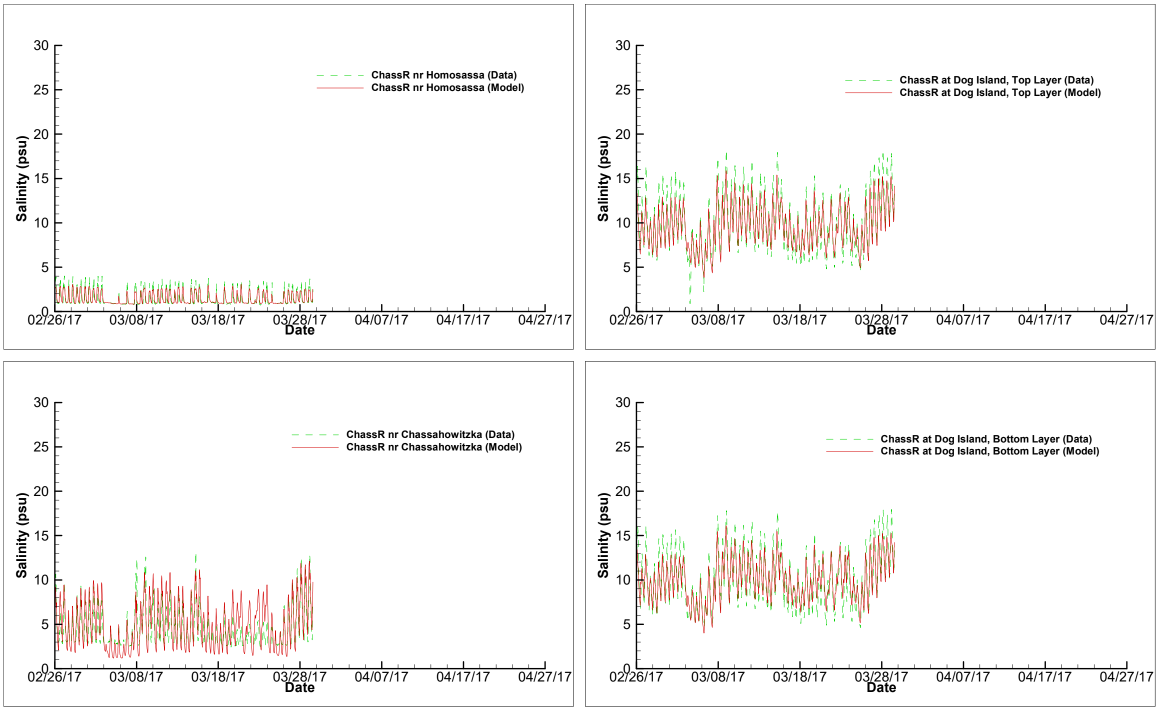

Figure E - 27. Simulated (red lines) and measured (dashed green lines) salinities at the Chassahowitzka River near Homosassa (top left panel), near Chassahowitzka (bottom left), and at Dog Island (right panels) stations during 2/26/2017 – 4/27/2017.

Appendix F. Simulated and Measured Temperatures

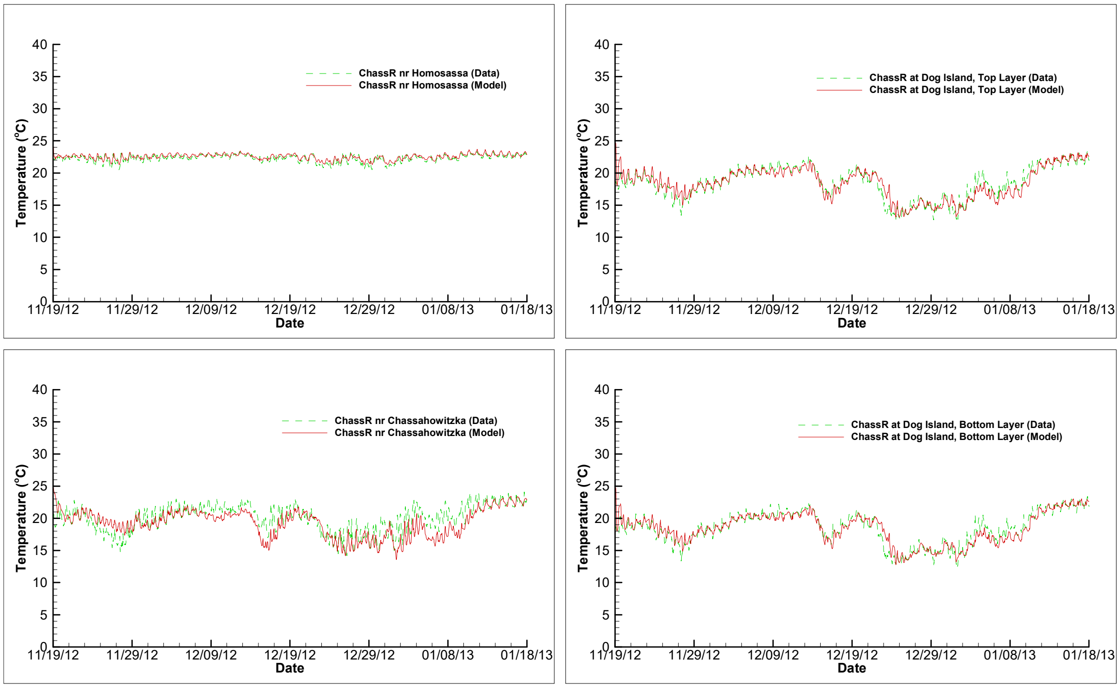

Figure F - 1. Comparisons of simulated (red lines) and measured (dashed green lines) temperatures at the Chassahowitzka River near Homosassa (top left panel), near Chassahowitzka (bottom left), and at Dog Island (right panels) stations during 11/19/2012 – 1/18/2013.

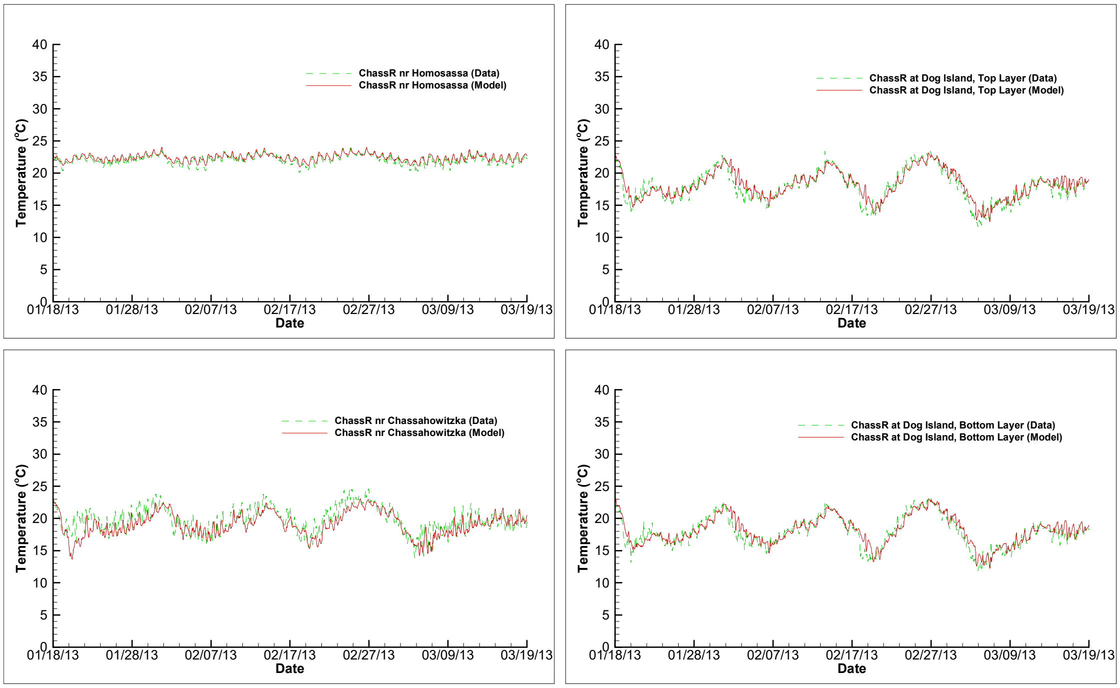

Figure F - 2. Comparisons of simulated (red lines) and measured (dashed green lines) temperatures at the Chassahowitzka River near Homosassa (top left panel), near Chassahowitzka (bottom left), and at Dog Island (right panels) stations during 1/18/2013 – 3/19/2013.

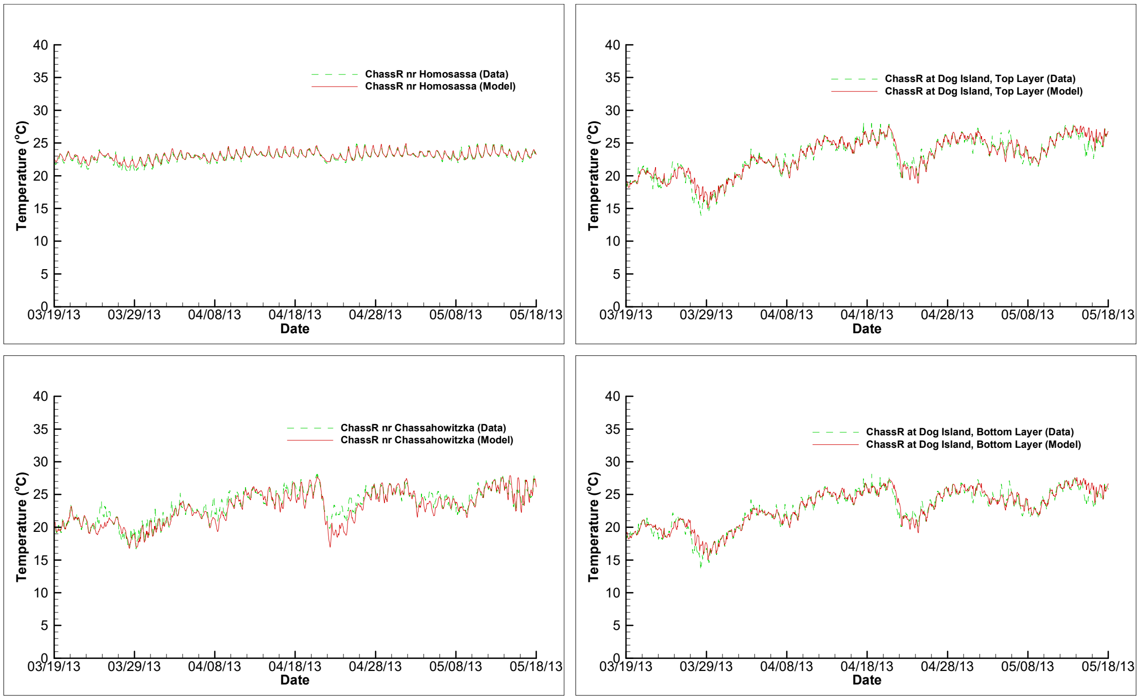

Figure F - 3. Comparisons of simulated (red lines) and measured (dashed green lines) temperatures at the Chassahowitzka River near Homosassa (top left panel), near Chassahowitzka (bottom left), and at Dog Island (right panels) stations during 3/19/2013 – 5/18/2013.

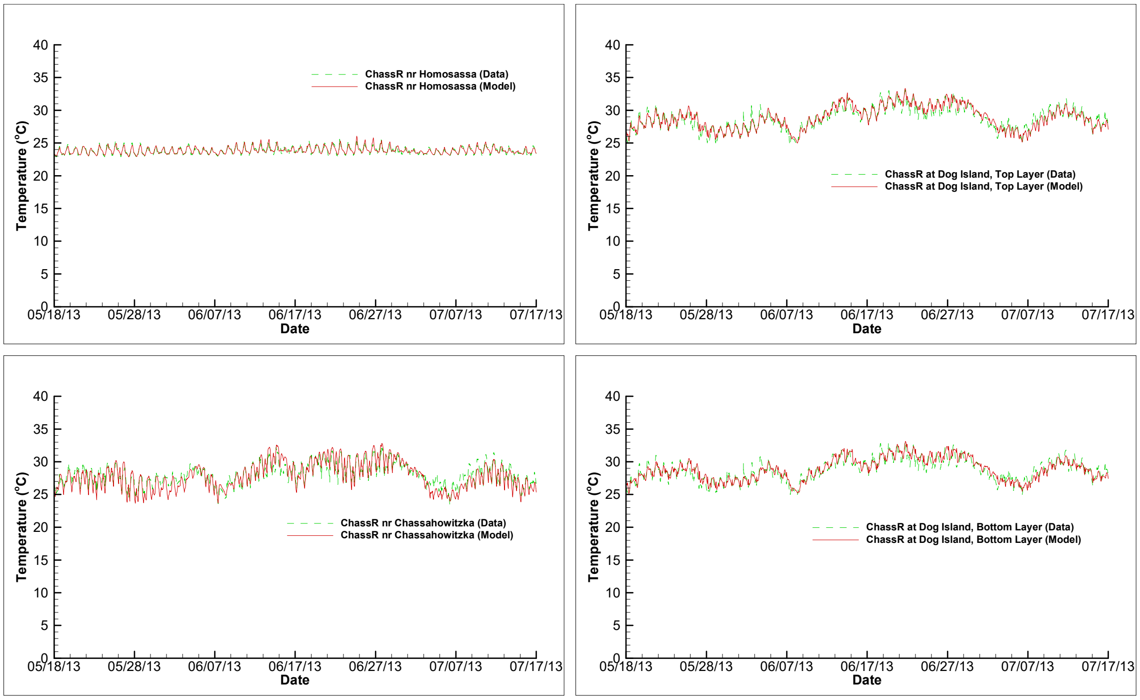

Figure F - 4. Comparisons of simulated (red lines) and measured (dashed green lines) temperatures at the Chassahowitzka River near Homosassa (top left panel), near Chassahowitzka (bottom left), and at Dog Island (right panels) stations during 5/18/2013 – 7/17/2013.

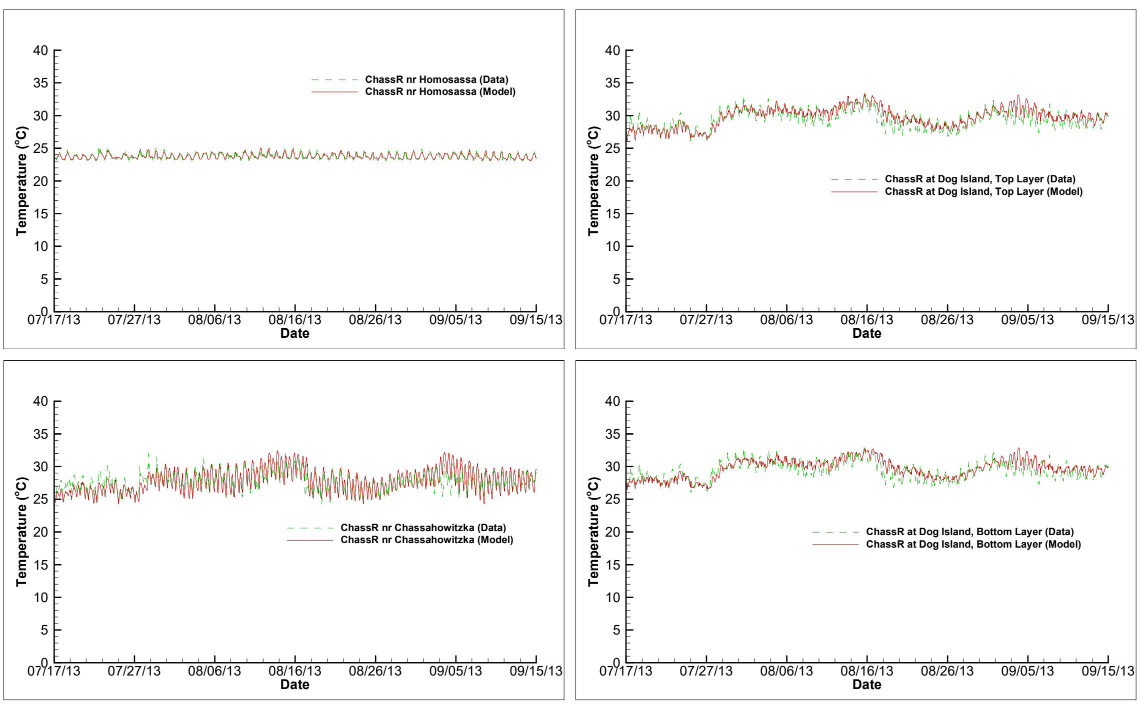

Figure F - 5. Comparisons of simulated (red lines) and measured (dashed green lines) temperatures at the Chassahowitzka River near Homosassa (top left panel), near Chassahowitzka (bottom left), and at Dog Island (right panels) stations during 7/17/2013 – 9/15/2013.

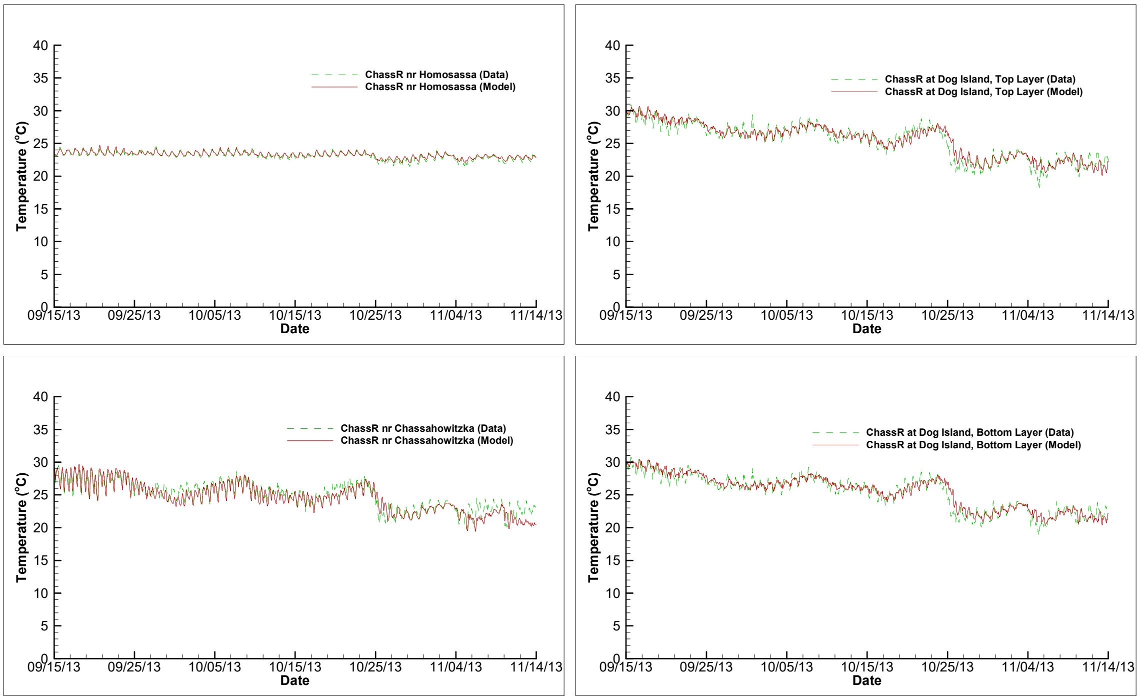

Figure F - 6. Comparisons of simulated (red lines) and measured (dashed green lines) temperatures at the Chassahowitzka River near Homosassa (top left panel), near Chassahowitzka (bottom left), and at Dog Island (right panels) stations during 9/15/2013 – 11/14/2013.

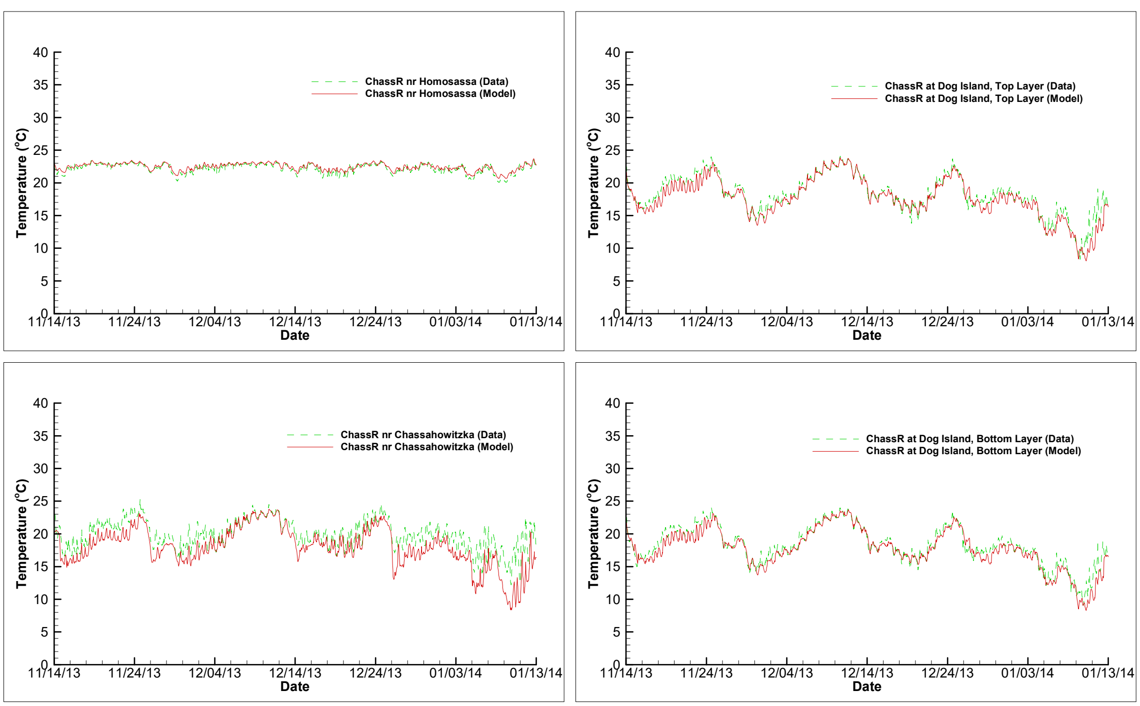

Figure F - 7. Comparisons of simulated (red lines) and measured (dashed green lines) temperatures at the Chassahowitzka River near Homosassa (top left panel), near Chassahowitzka (bottom left), and at Dog Island (right panels) stations during 11/14/2013 – 1/13/2014.

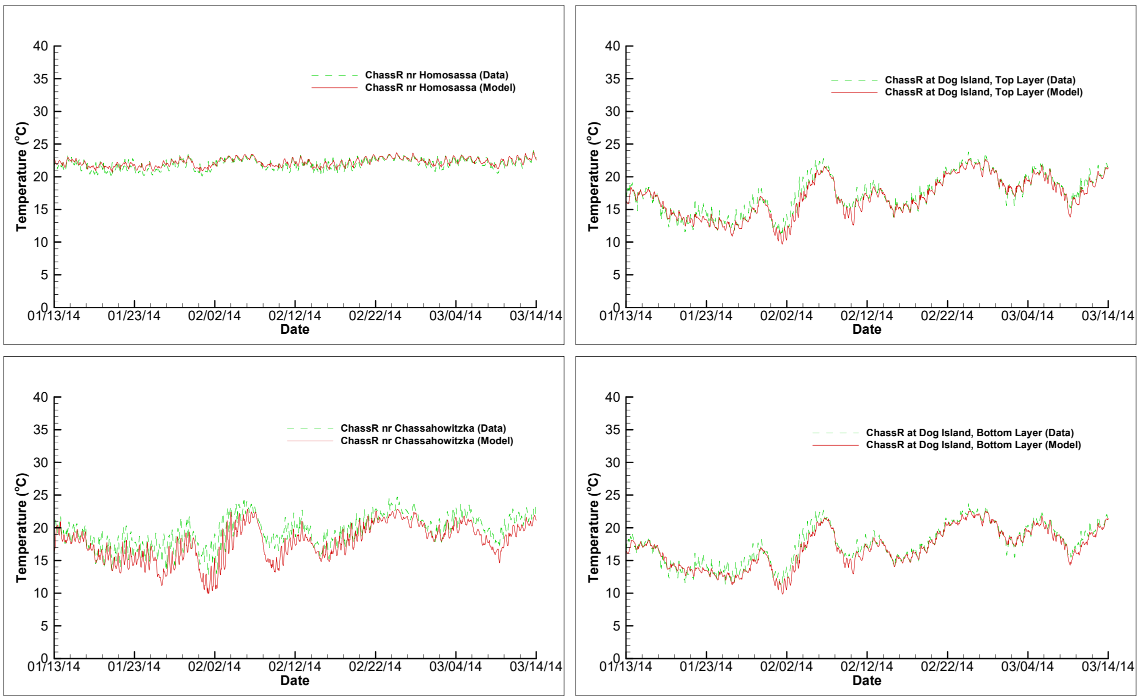

Figure F - 8. Comparisons of simulated (red lines) and measured (dashed green lines) temperatures at the Chassahowitzka River near Homosassa (top left panel), near Chassahowitzka (bottom left), and at Dog Island (right panels) stations during 1/13/2014 – 3/14/2014.

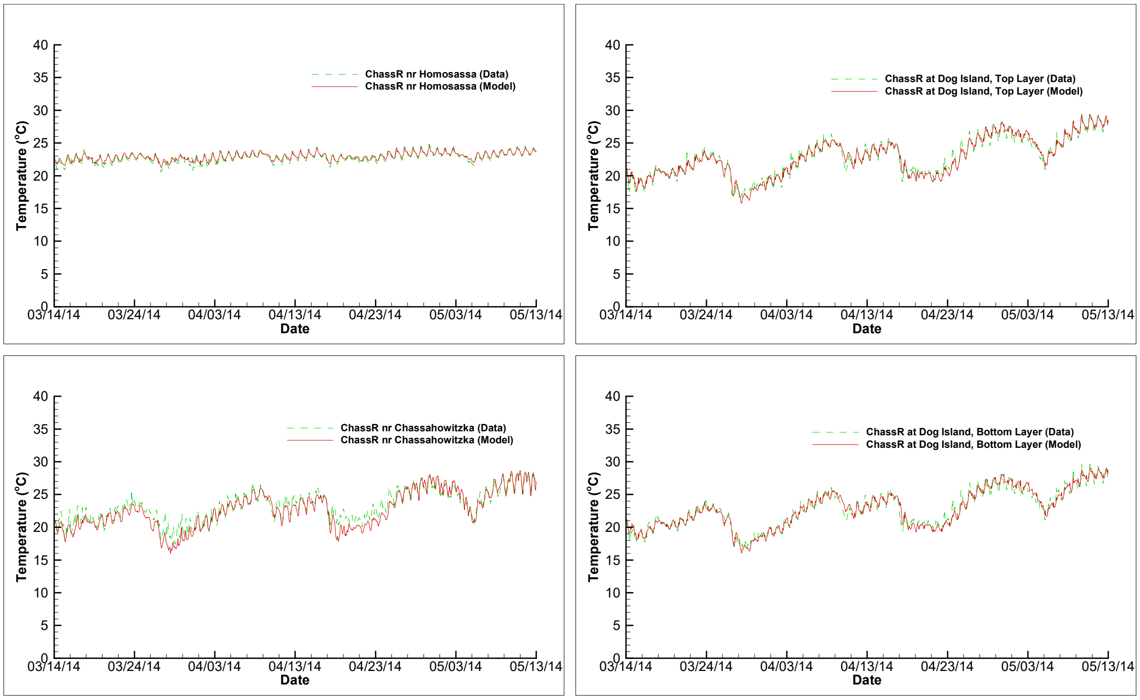

Figure F - 9. Comparisons of simulated (red lines) and measured (dashed green lines) temperatures at the Chassahowitzka River near Homosassa (top left panel), near Chassahowitzka (bottom left), and at Dog Island (right panels) stations during 3/14/2014 – 5/13/2014.

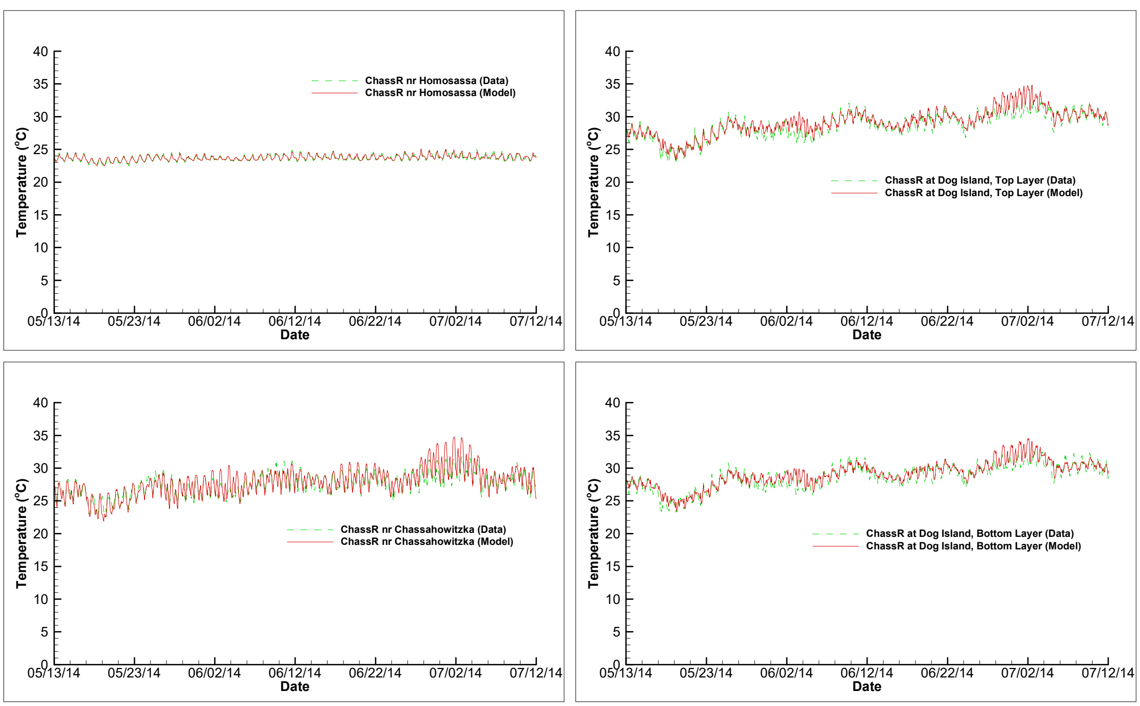

Figure F - 10. Comparisons of simulated (red lines) and measured (dashed green lines) temperatures at the Chassahowitzka River near Homosassa (top left panel), near Chassahowitzka (bottom left), and at Dog Island (right panels) stations during 5/13/2014 – 7/12/2014.

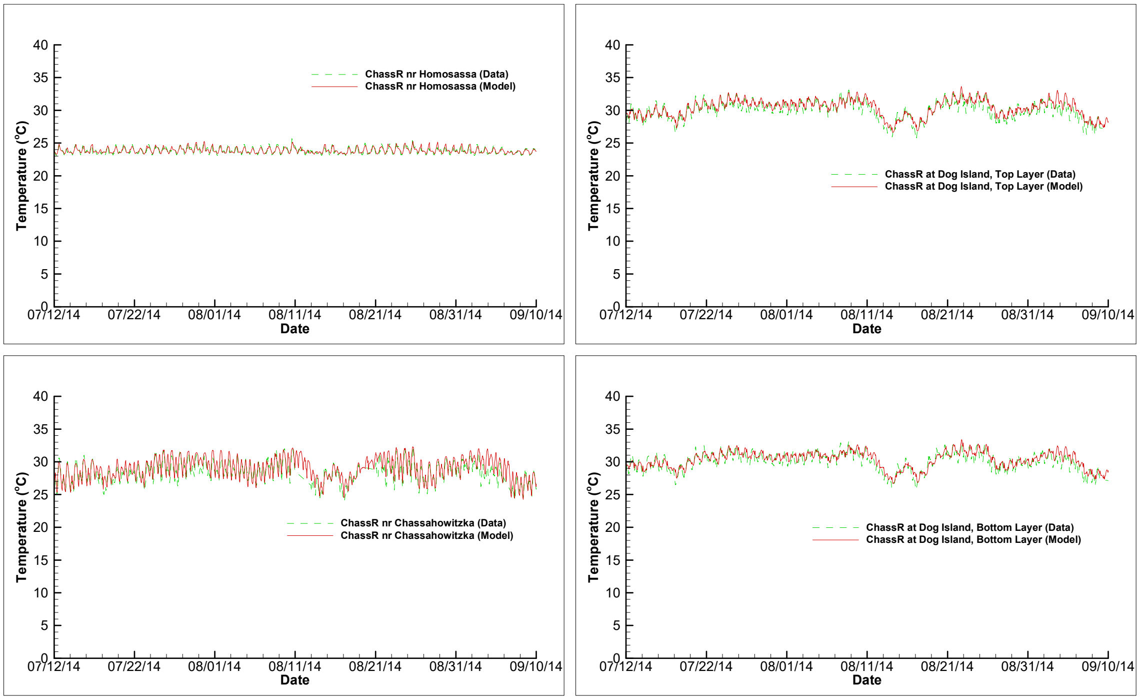

Figure F - 11. Comparisons of simulated (red lines) and measured (dashed green lines) temperatures at the Chassahowitzka River near Homosassa (top left panel), near Chassahowitzka (bottom left), and at Dog Island (right panels) stations during 7/12/2014 – 9/10/2014.

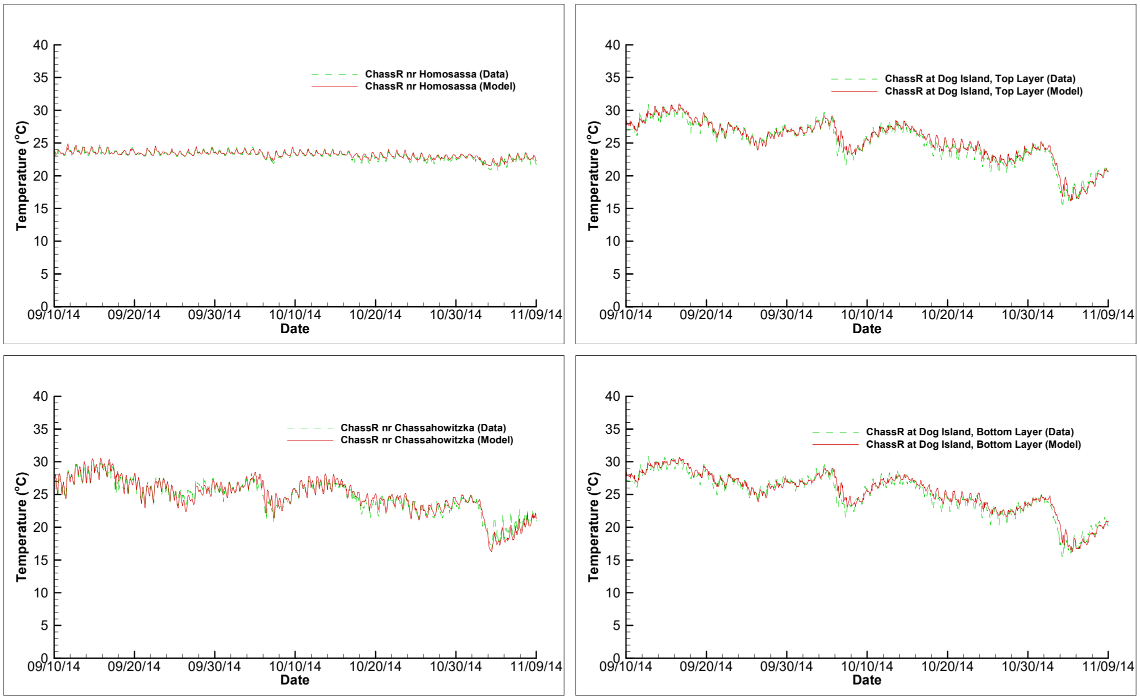

Figure F - 12. Comparisons of simulated (red lines) and measured (dashed green lines) temperatures at the Chassahowitzka River near Homosassa (top left panel), near Chassahowitzka (bottom left), and at Dog Island (right panels) stations during 9/10/2014 – 11/9/2014.

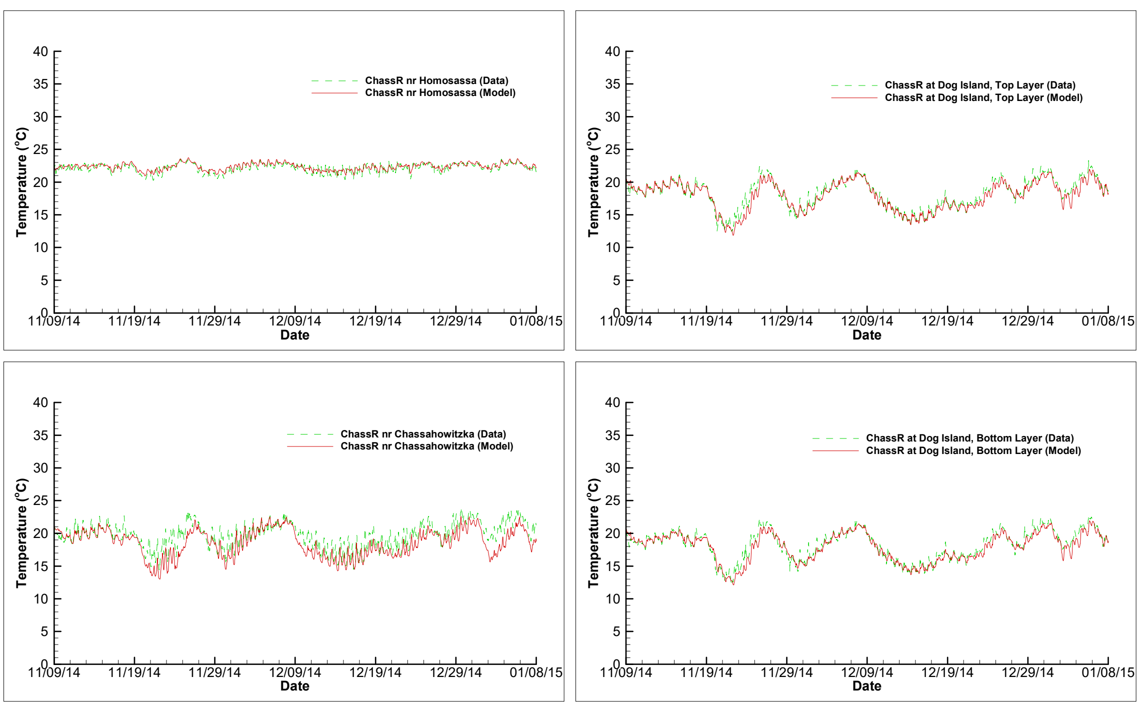

Figure F - 13. Comparisons of simulated (red lines) and measured (dashed green lines) temperatures at the Chassahowitzka River near Homosassa (top left panel), near Chassahowitzka (bottom left), and at Dog Island (right panels) stations during 11/9/2014 – 1/8/2015.

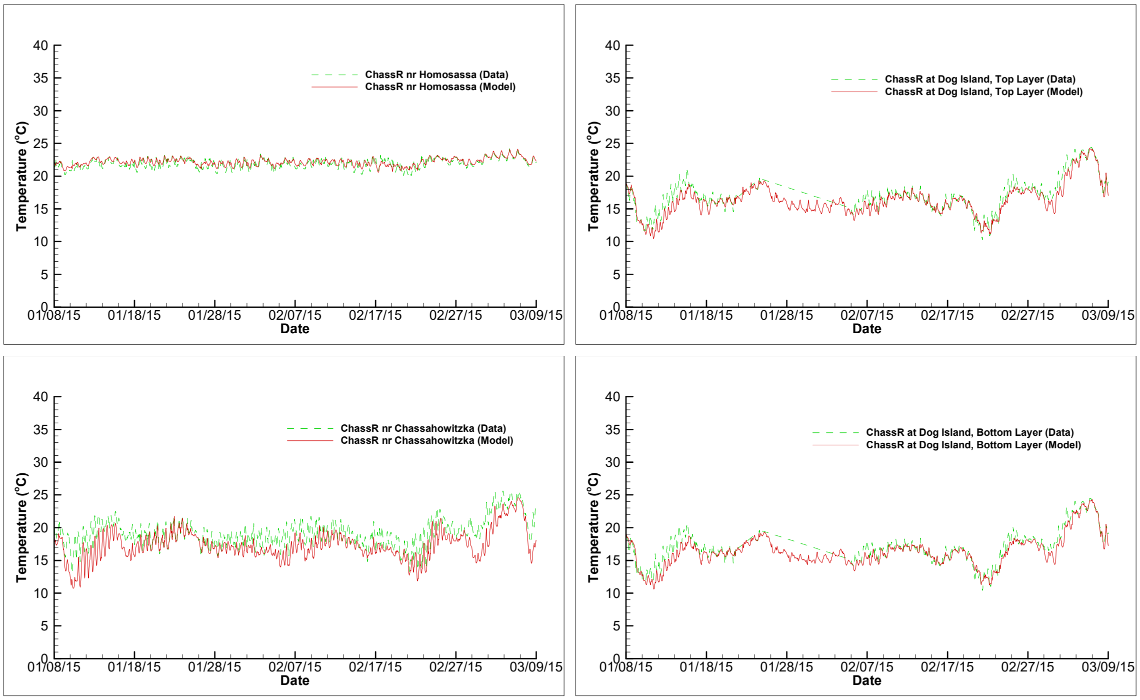

Figure F - 14. Comparisons of simulated (red lines) and measured (dashed green lines) temperatures at the Chassahowitzka River near Homosassa (top left panel), near Chassahowitzka (bottom left), and at Dog Island (right panels) stations during 1/8/2015 – 3/9/2015.

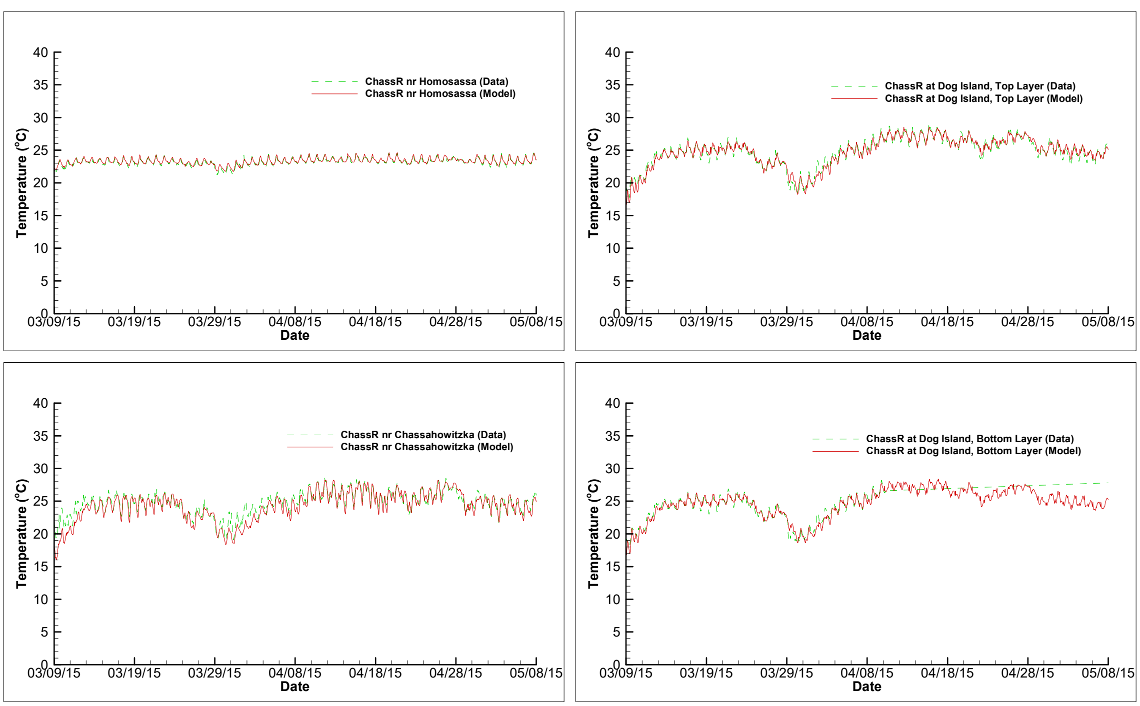

Figure F - 15. Comparisons of simulated (red lines) and measured (dashed green lines) temperatures at the Chassahowitzka River near Homosassa (top left panel), near Chassahowitzka (bottom left), and at Dog Island (right panels) stations during 3/9/2015 – 5/8/2015.

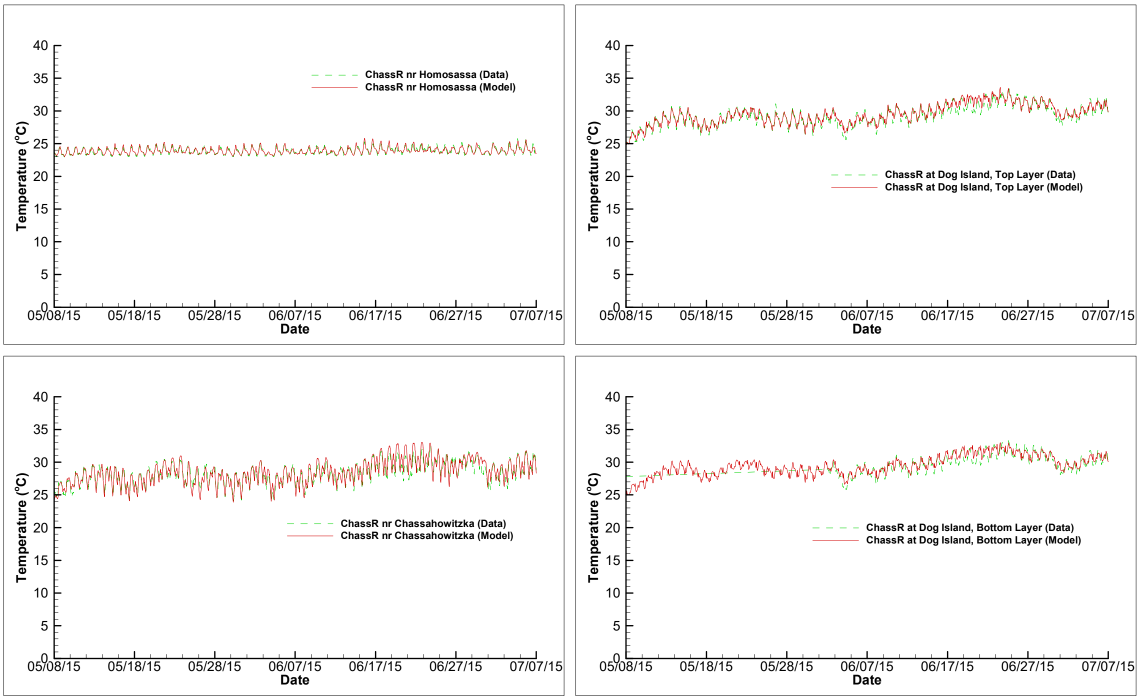

Figure F - 16. Comparisons of simulated (red lines) and measured (dashed green lines) temperatures at the Chassahowitzka River near Homosassa (top left panel), near Chassahowitzka (bottom left), and at Dog Island (right panels) stations during 5/8/2015 – 7/7/2015.

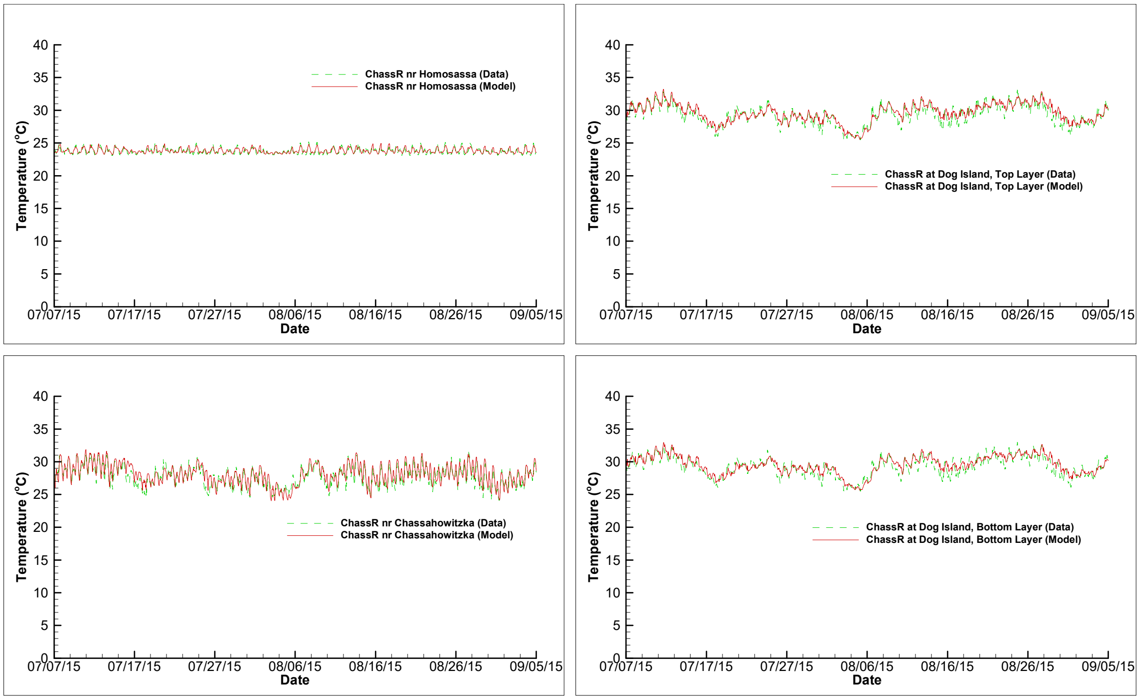

Figure F - 17. Comparisons of simulated (red lines) and measured (dashed green lines) temperatures at the Chassahowitzka River near Homosassa (top left panel), near Chassahowitzka (bottom left), and at Dog Island (right panels) stations during 7/7/2015 – 9/5/2015.

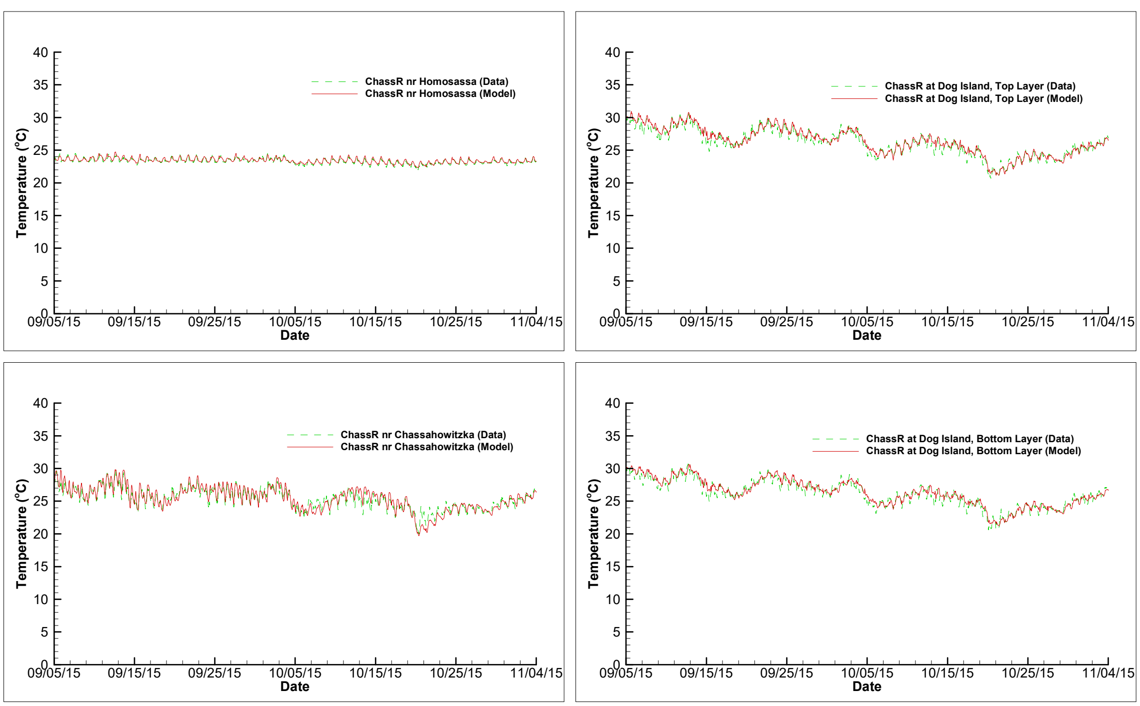

Figure F - 18. Comparisons of simulated (red lines) and measured (dashed green lines) temperatures at the Chassahowitzka River near Homosassa (top left panel), near Chassahowitzka (bottom left), and at Dog Island (right panels) stations during 9/5/2015 – 11/4/2015.

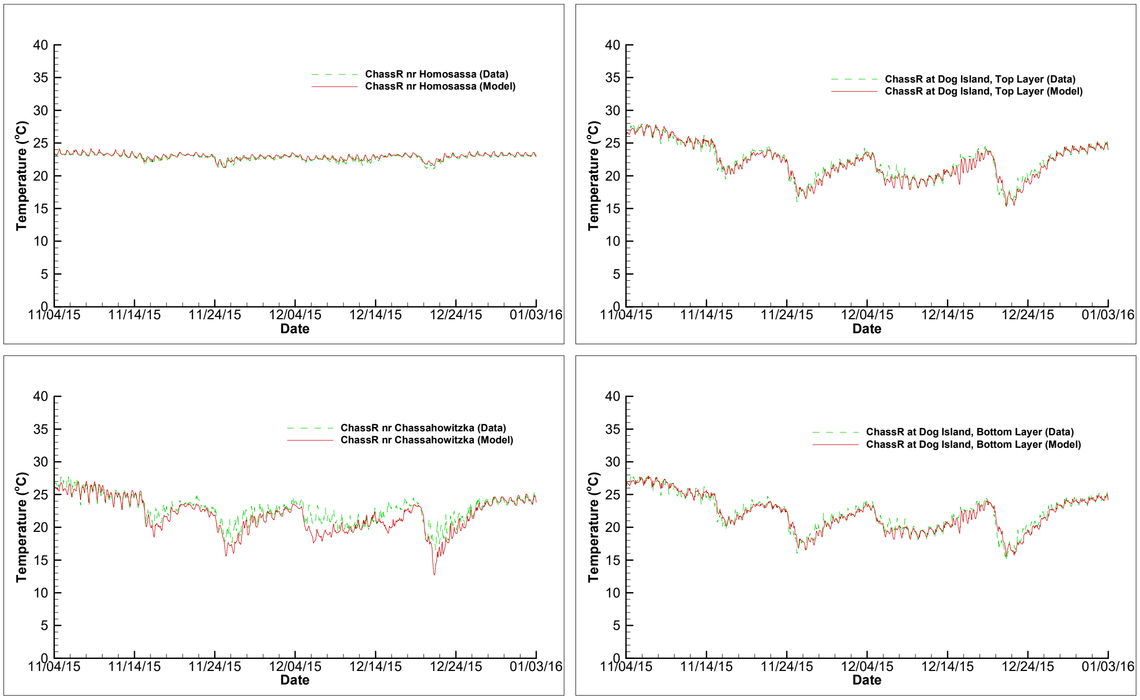

Figure F - 19. Comparisons of simulated (red lines) and measured (dashed green lines) temperatures at the Chassahowitzka River near Homosassa (top left panel), near Chassahowitzka (bottom left), and at Dog Island (right panels) stations during 11/4/2015 – 1/3/2016.

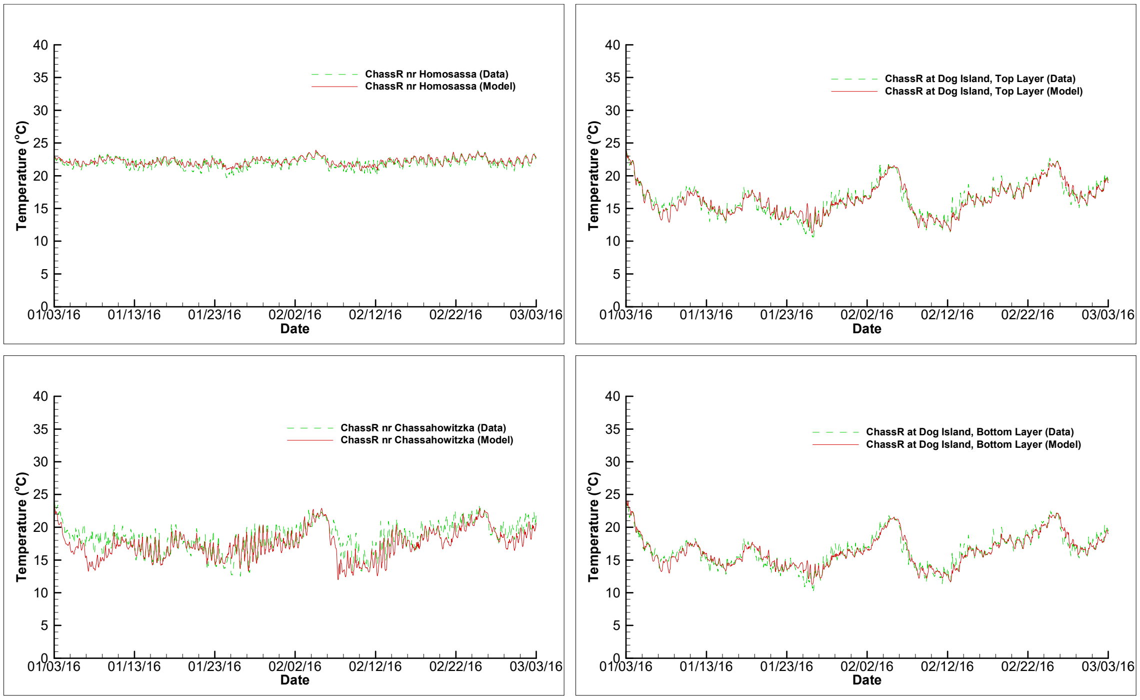

Figure F - 20. Comparisons of simulated (red lines) and measured (dashed green lines) temperatures at the Chassahowitzka River near Homosassa (top left panel), near Chassahowitzka (bottom left), and at Dog Island (right panels) stations during 1/3/2016 – 3/3/2016.

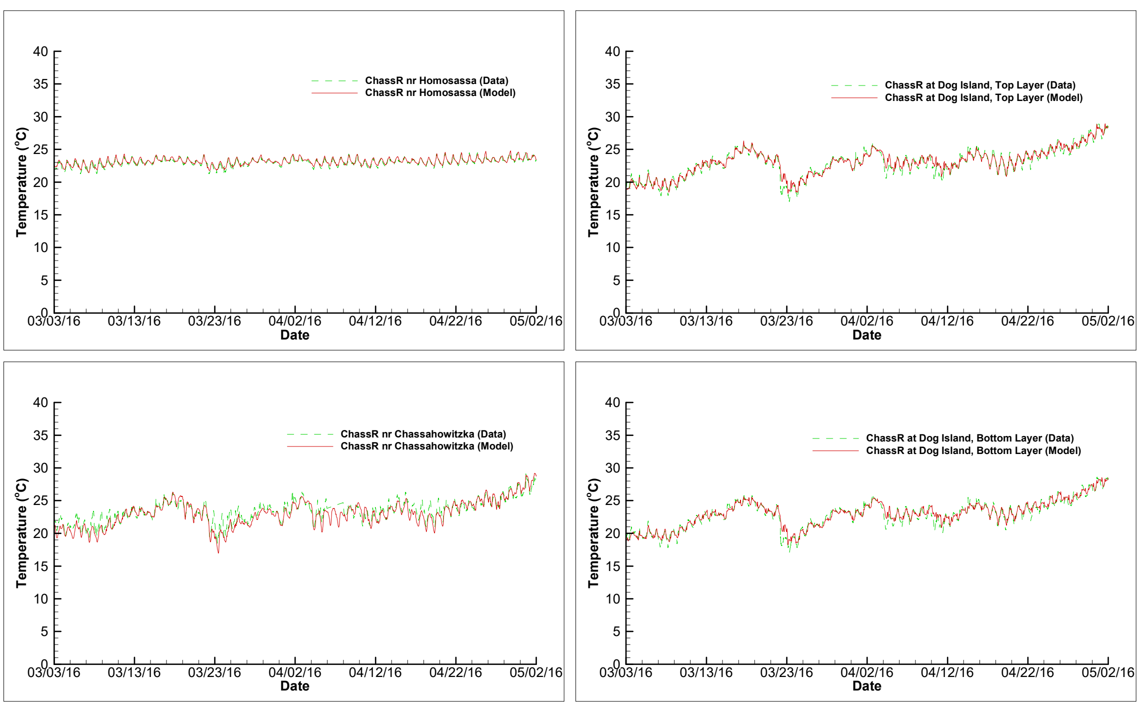

Figure F - 21. Comparisons of simulated (red lines) and measured (dashed green lines) temperatures at the Chassahowitzka River near Homosassa (top left panel), near Chassahowitzka (bottom left), and at Dog Island (right panels) stations during 3/3/2016 – 5/2/2016.

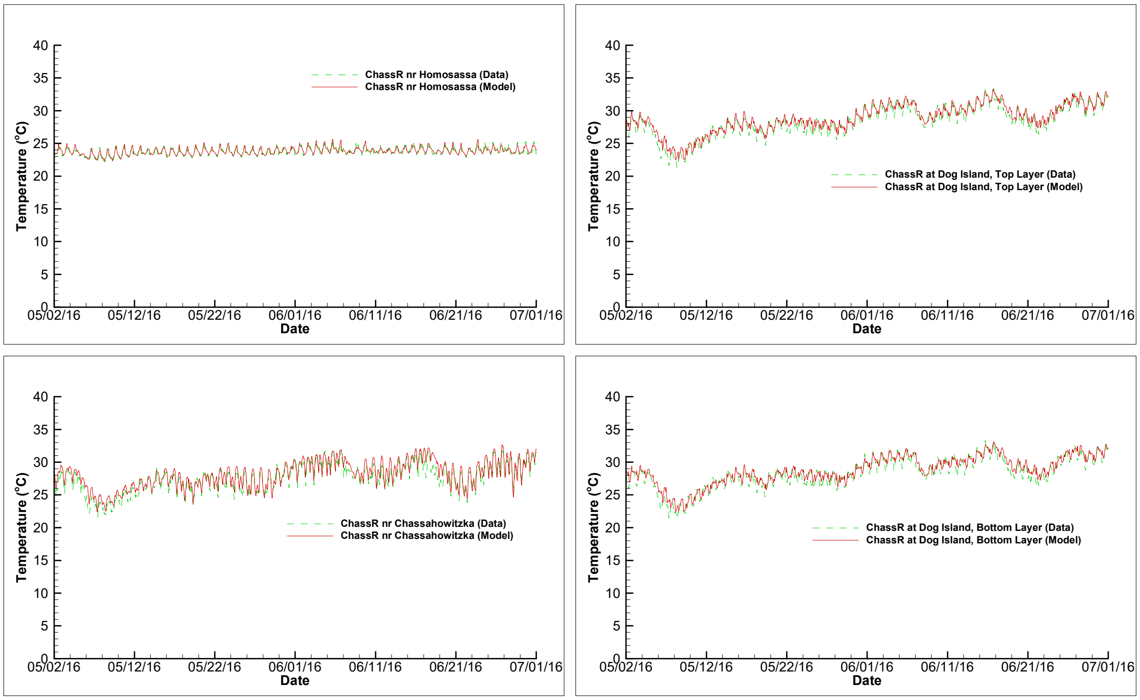

Figure F - 22. Comparisons of simulated (red lines) and measured (dashed green lines) temperatures at the Chassahowitzka River near Homosassa (top left panel), near Chassahowitzka (bottom left), and at Dog Island (right panels) stations during 5/2/2016 – 7/1/2016.

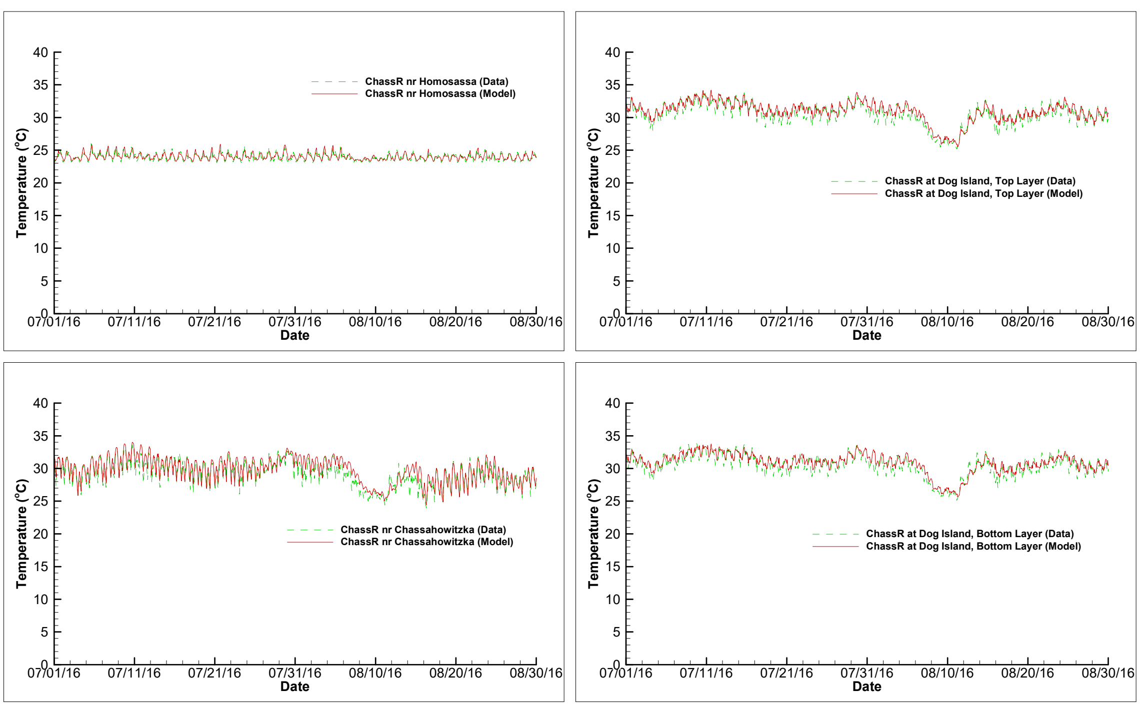

Figure F - 23. Comparisons of simulated (red lines) and measured (dashed green lines) temperatures at the Chassahowitzka River near Homosassa (top left panel), near Chassahowitzka (bottom left), and at Dog Island (right panels) stations during 7/1/2016 – 8/30/2016.

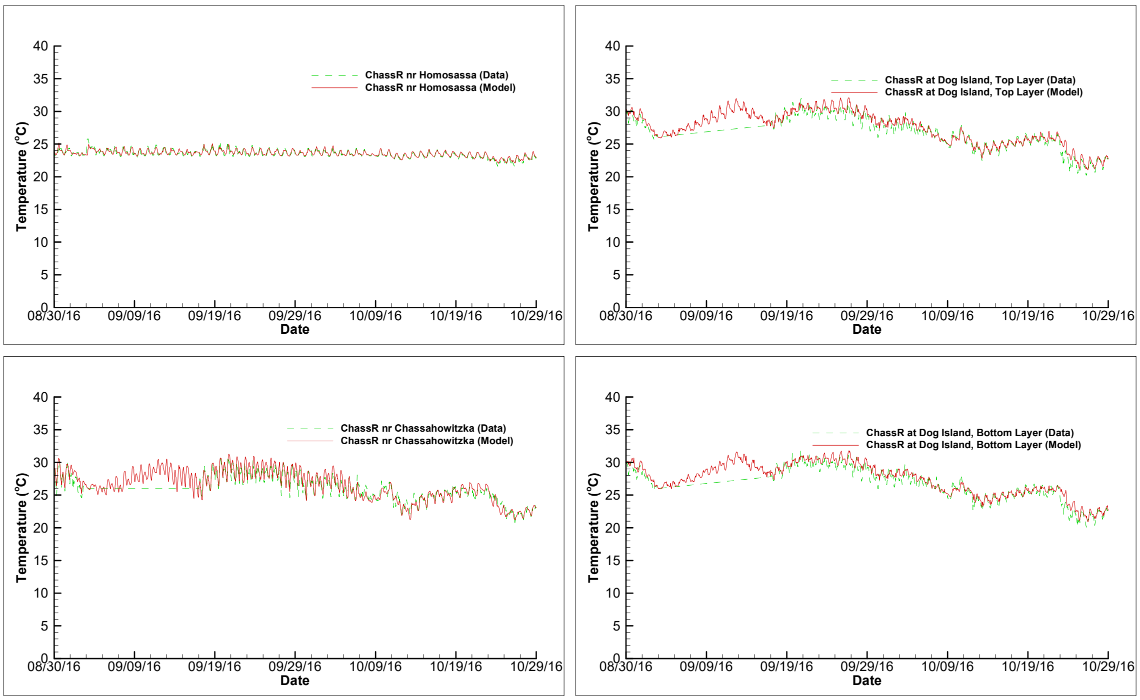

Figure F - 24. Comparisons of simulated (red lines) and measured (dashed green lines) temperatures at the Chassahowitzka River near Homosassa (top left panel), near Chassahowitzka (bottom left), and at Dog Island (right panels) stations during 8/30/2016 – 10/29/2016.

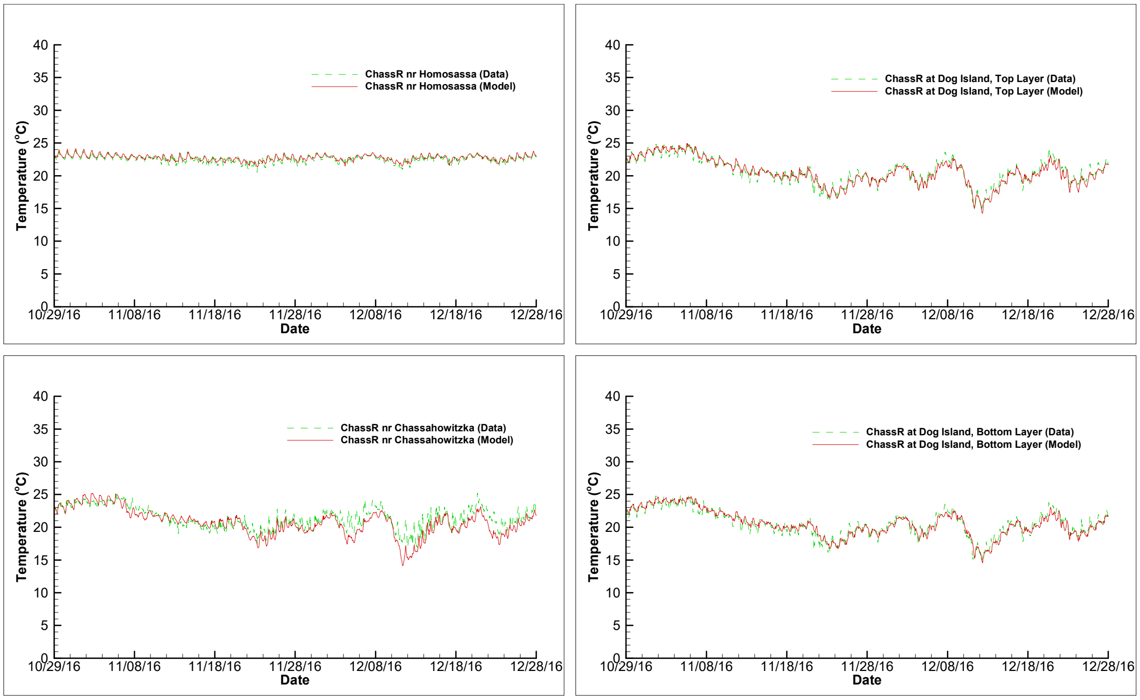

Figure F - 25. Comparisons of simulated (red lines) and measured (dashed green lines) temperatures at the Chassahowitzka River near Homosassa (top left panel), near Chassahowitzka (bottom left), and at Dog Island (right panels) stations during 10/29/2016 – 12/28/2016.

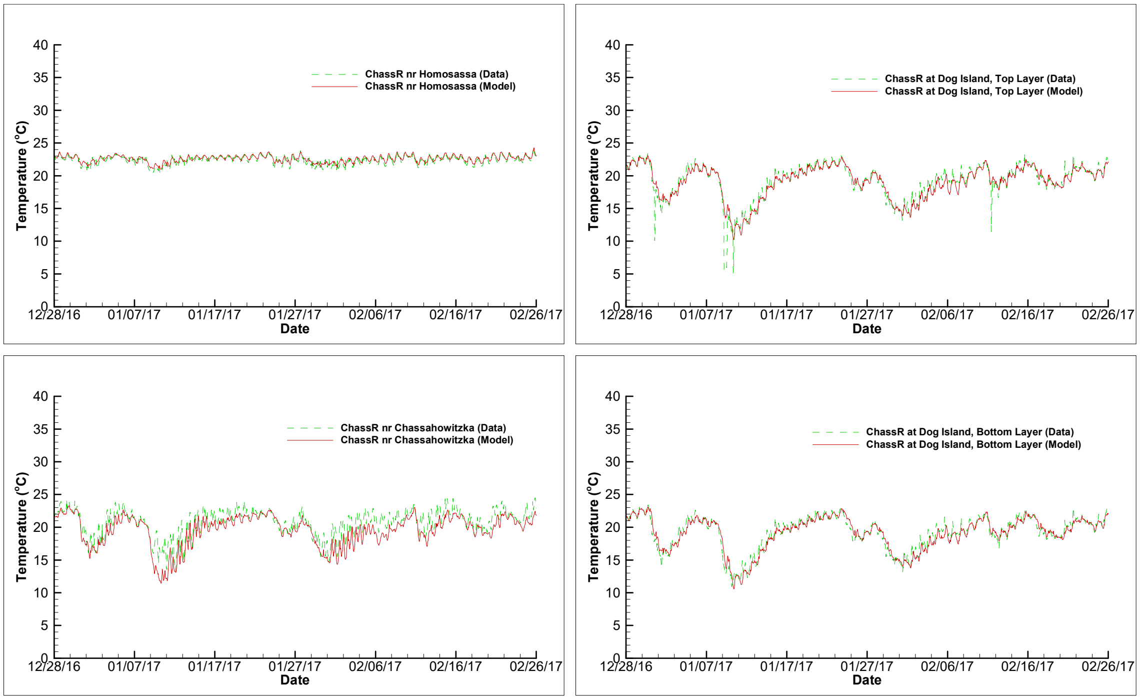

Figure F - 26. Comparisons of simulated (red lines) and measured (dashed green lines) temperatures at the Chassahowitzka River near Homosassa (top left panel), near Chassahowitzka (bottom left), and at Dog Island (right panels) stations during 12/28/2016 – 2/26/2017.

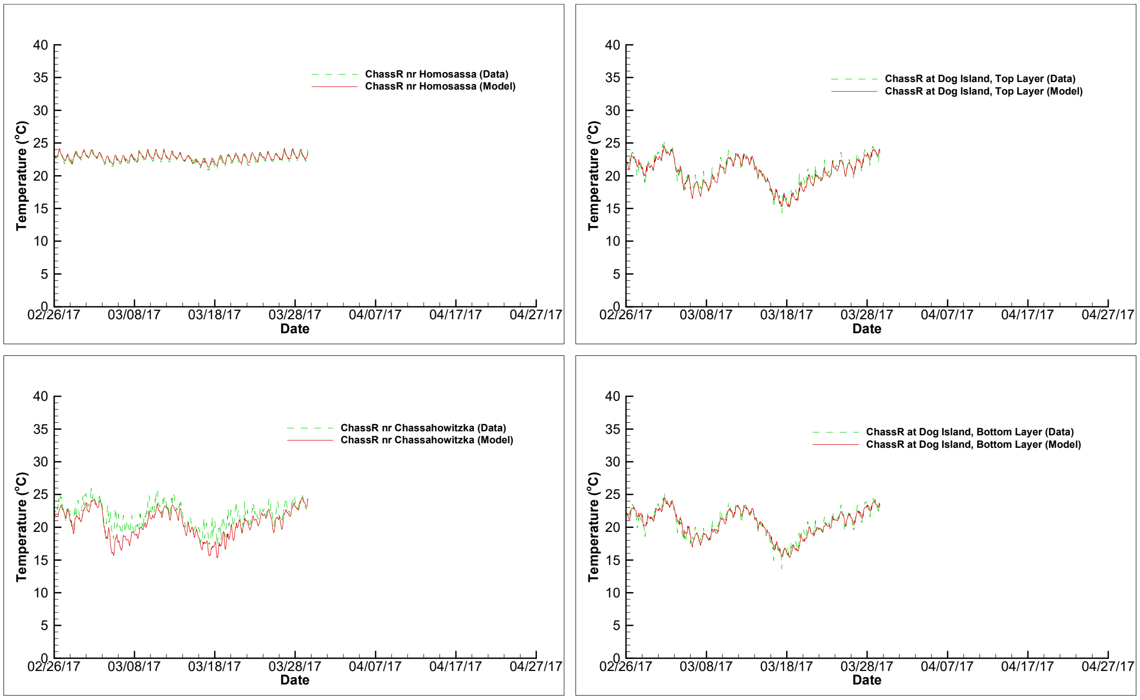

Figure F - 27. Comparisons of simulated (red lines) and measured (dashed green lines) temperatures at the Chassahowitzka River near Homosassa (top left panel), near Chassahowitzka (bottom left), and at Dog Island (right panels) stations during 2/26/2017 – 4/27/2017.

Appendix G. Simulated and Measured Discharges

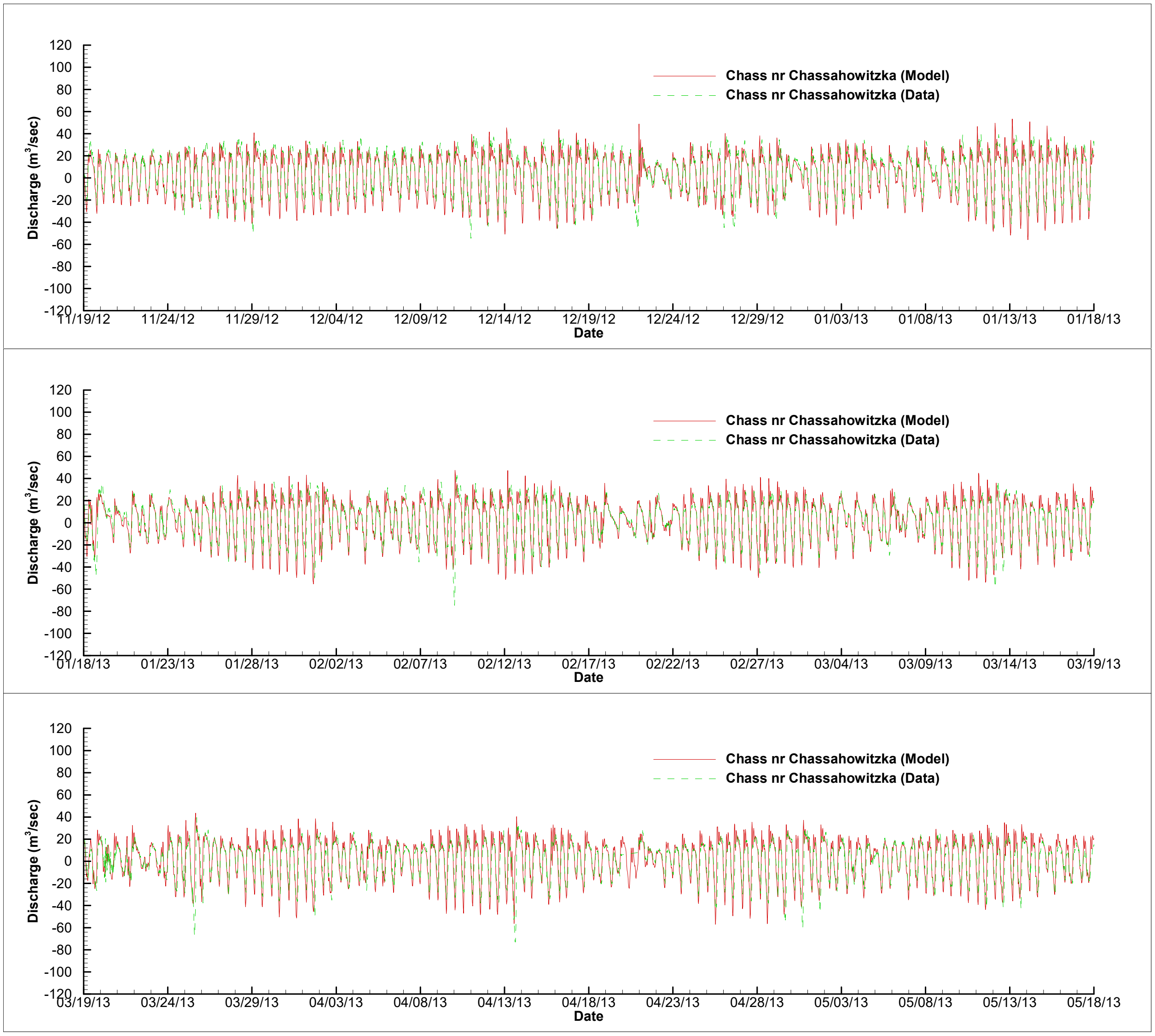

Figure G - 1. Comparisons of simulated (red lines) and measured (dashed green lines) discharges at the Chassahowitzka River near Chassahowitzka station 11/19/2012 – 5/18/2013.

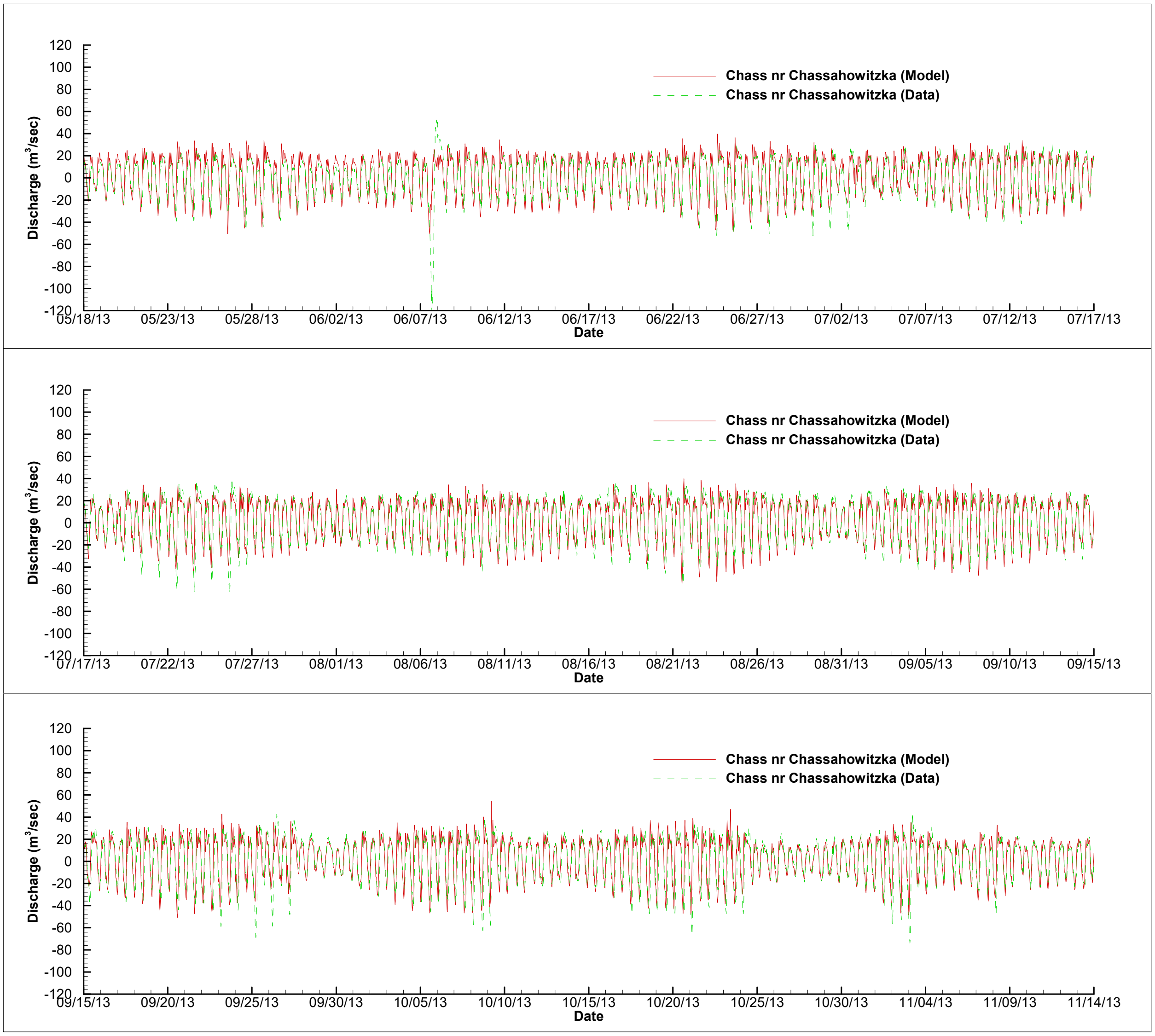

Figure G - 2. Comparisons of simulated (red lines) and measured (dashed green lines) discharges at the Chassahowitzka River near Chassahowitzka station 5/18/2013 - 11/14/2013.

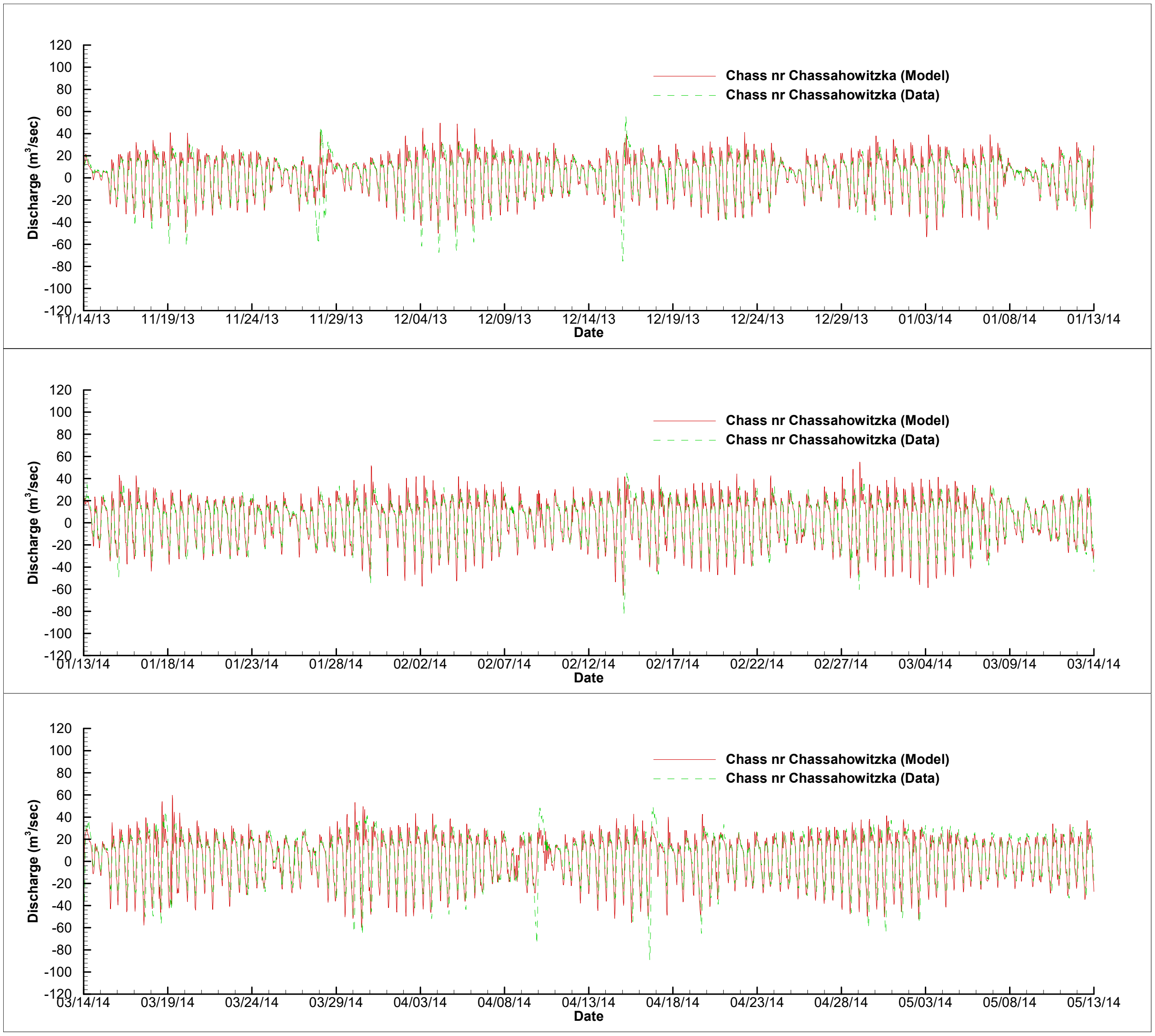

Figure G - 3. Comparisons of simulated (red lines) and measured (dashed green lines) discharges at the Chassahowitzka River near Chassahowitzka station 11/14/2013 – 5/13/2014.

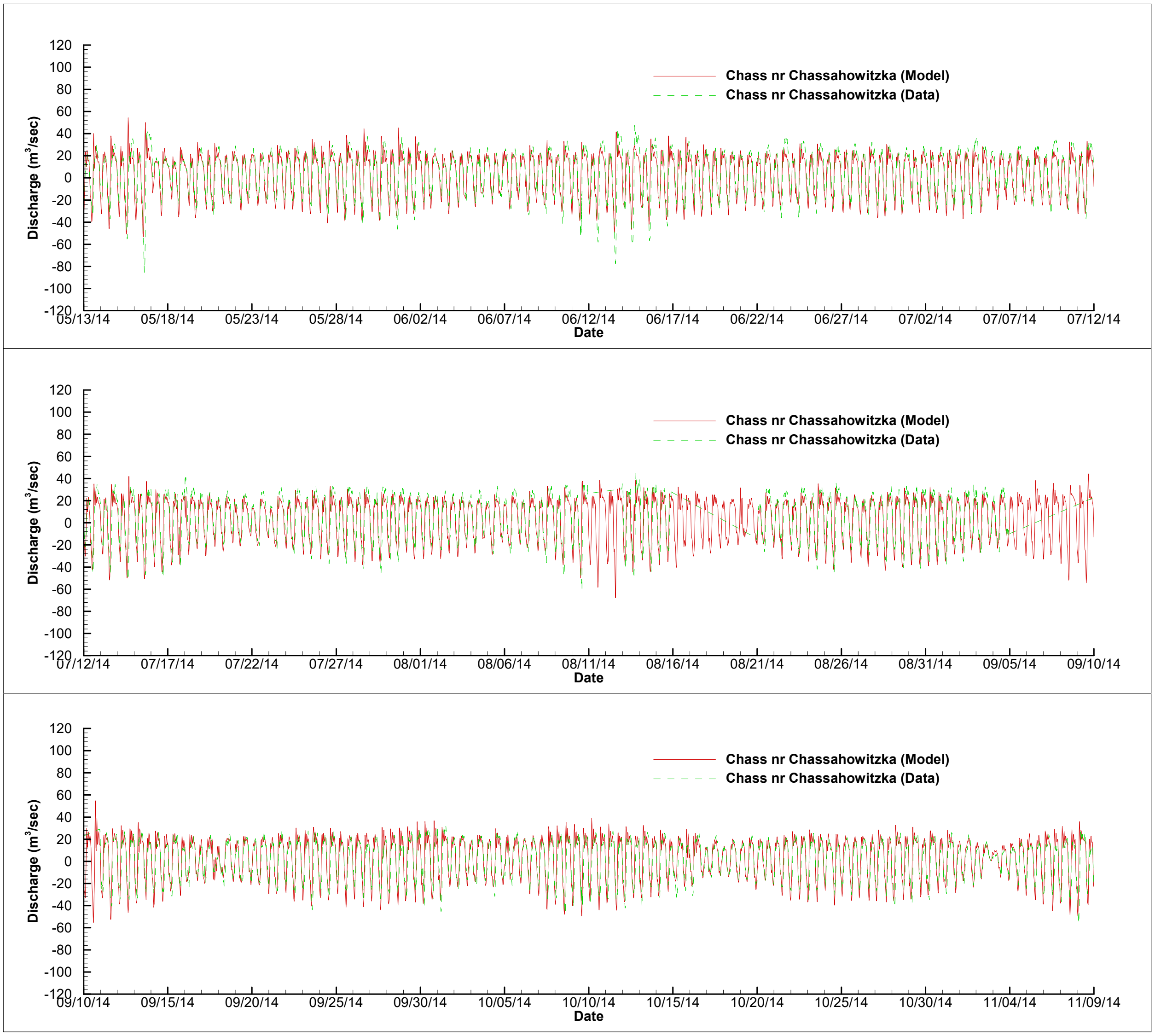

Figure G - 4. Comparisons of simulated (red lines) and measured (dashed green lines) discharges at the Chassahowitzka River near Chassahowitzka station 5/13/2014 – 11/9/2014.

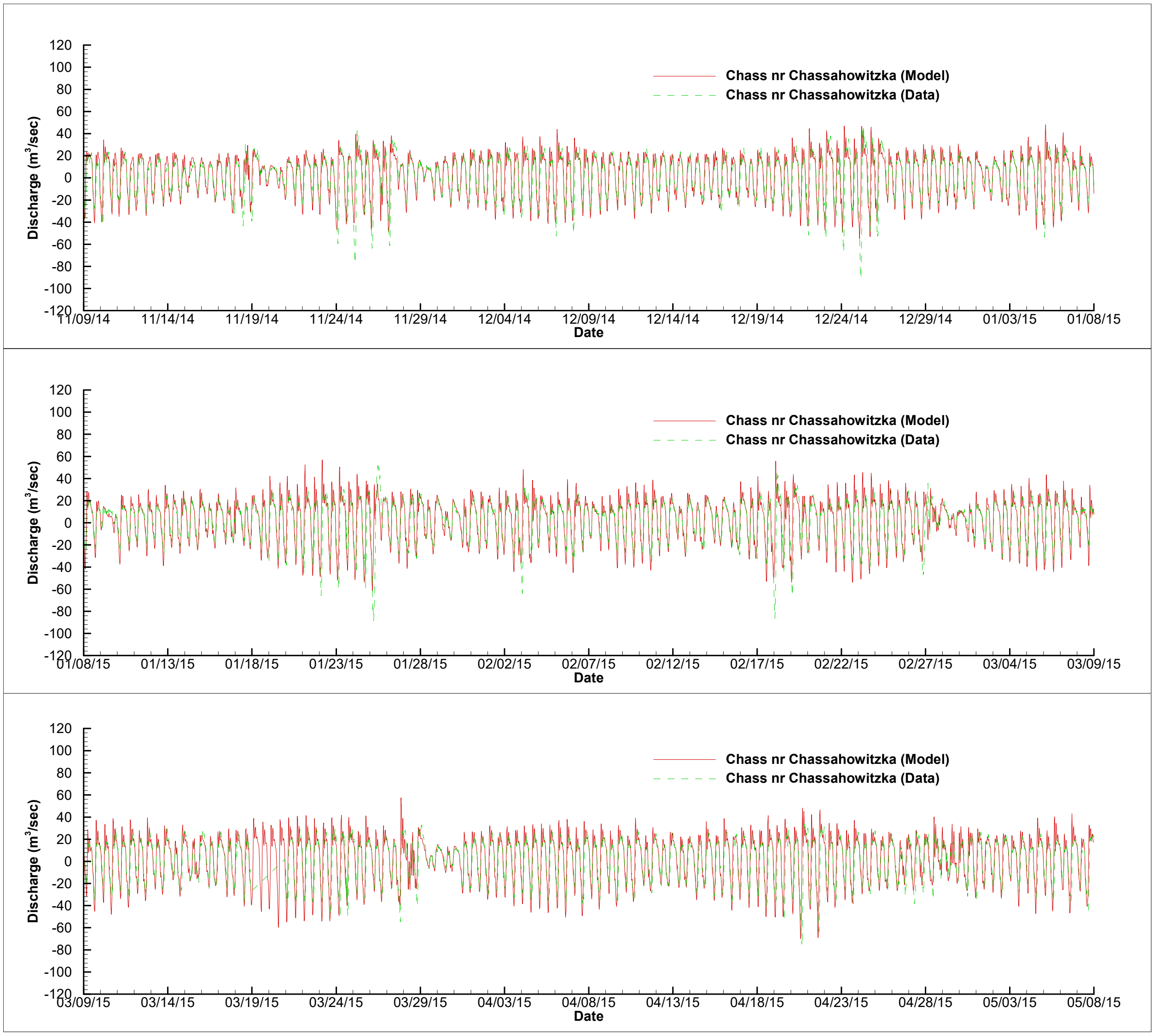

Figure G - 5. Comparisons of simulated (red lines) and measured (dashed green lines) discharges at the Chassahowitzka River near Chassahowitzka station 11/9/2014 – 5/8/2015.

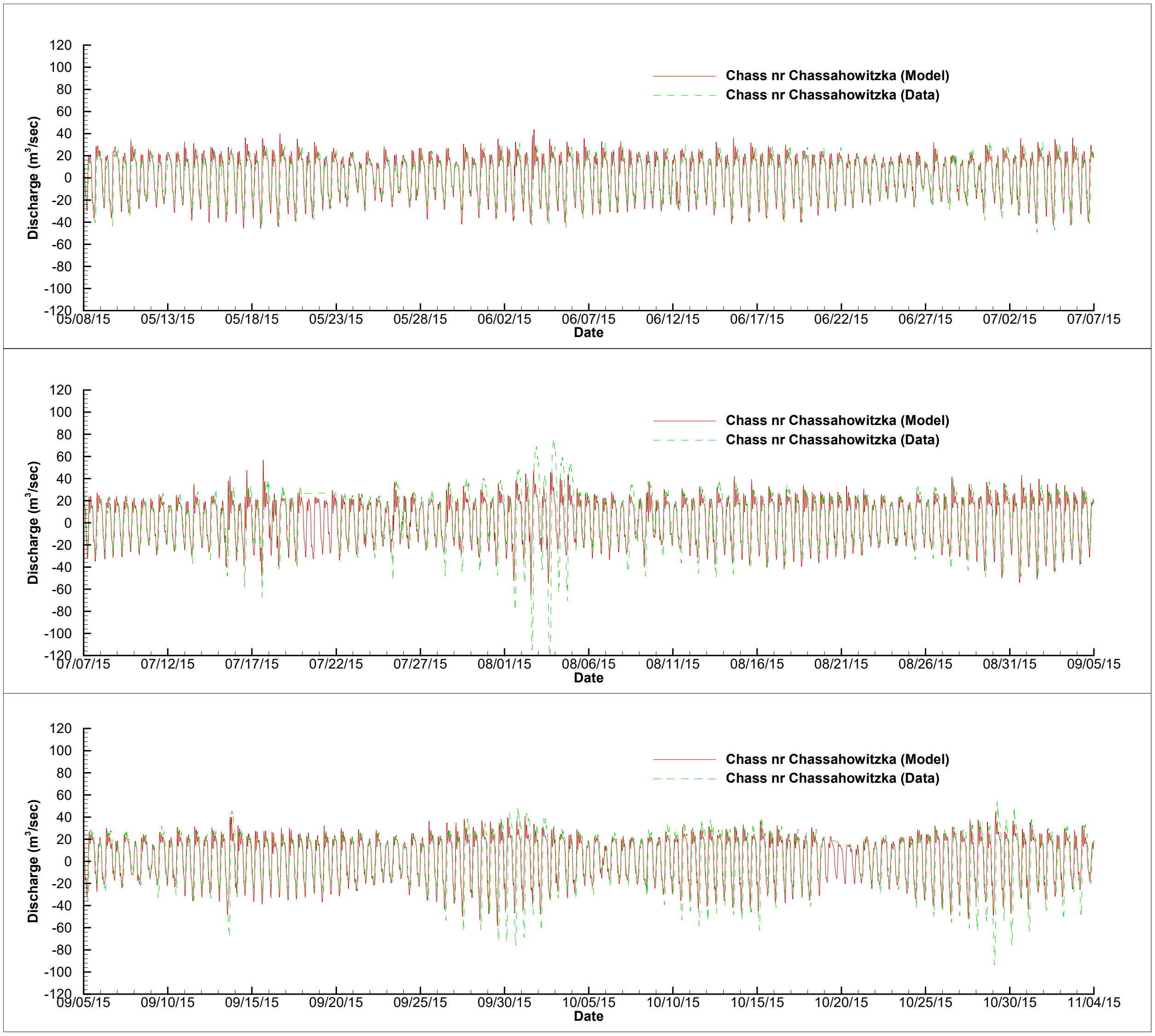

Figure G - 6. Comparisons of simulated (red lines) and measured (dashed green lines) discharges at the Chassahowitzka River near Chassahowitzka station 5/8/2015 - 11/4/2015.

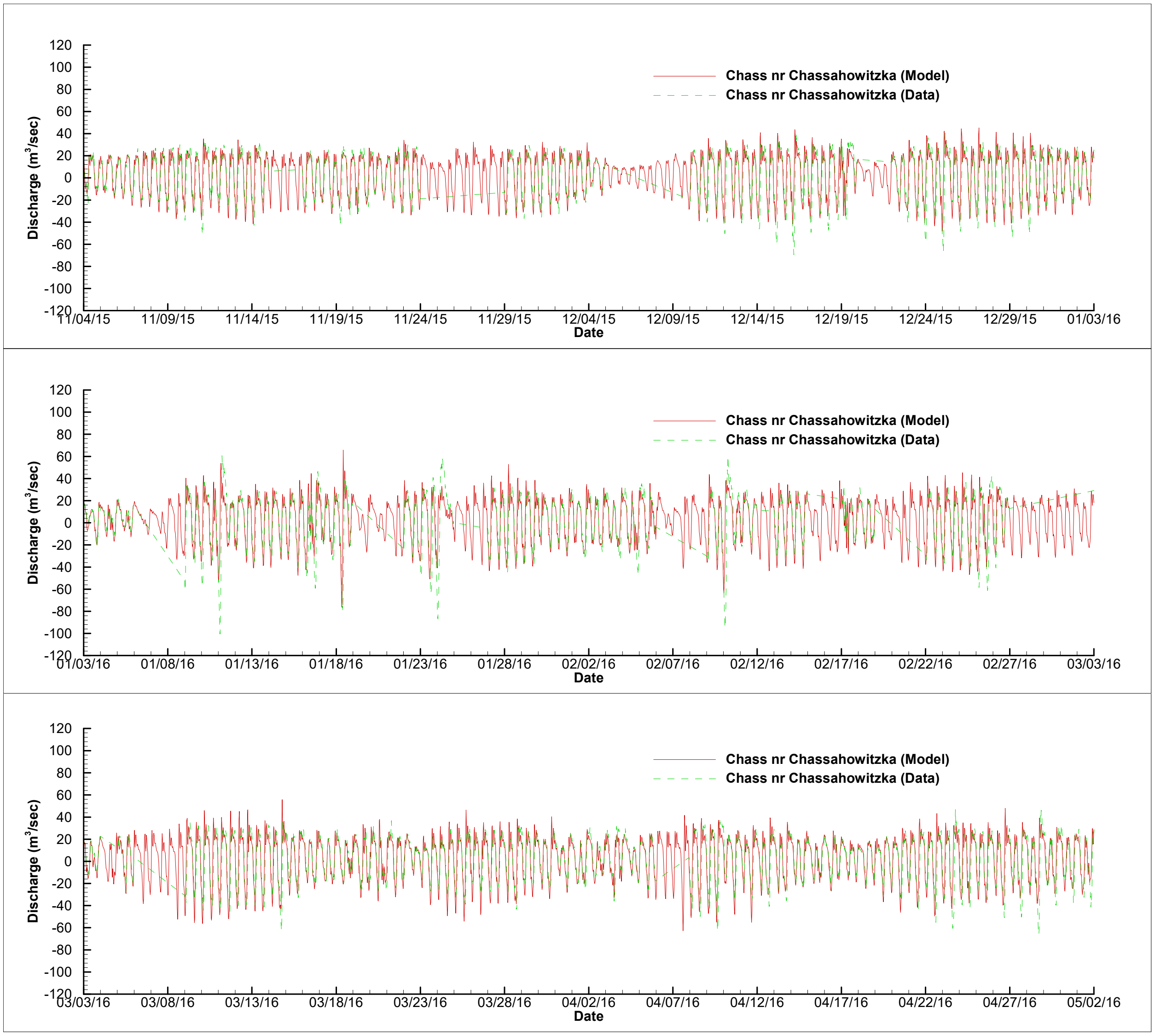

Figure G - 7. Comparisons of simulated (red lines) and measured (dashed green lines) discharges at the Chassahowitzka River near Chassahowitzka station 11/4/2015 – 5/2/2016.

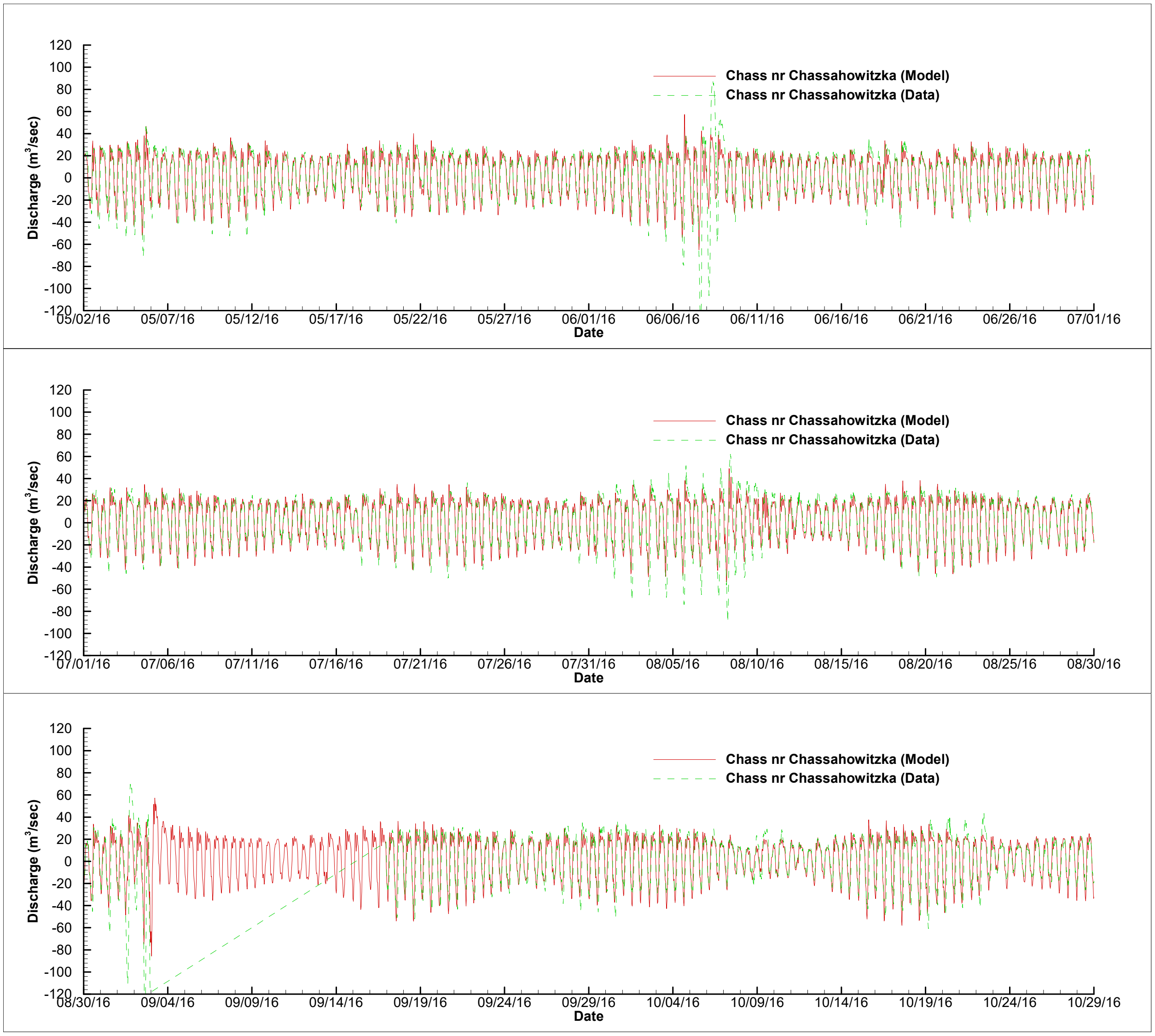

Figure G - 8. Comparisons of simulated (red lines) and measured (dashed green lines) discharges at the Chassahowitzka River near Chassahowitzka station 5/2/2016 - 10/29/2016.

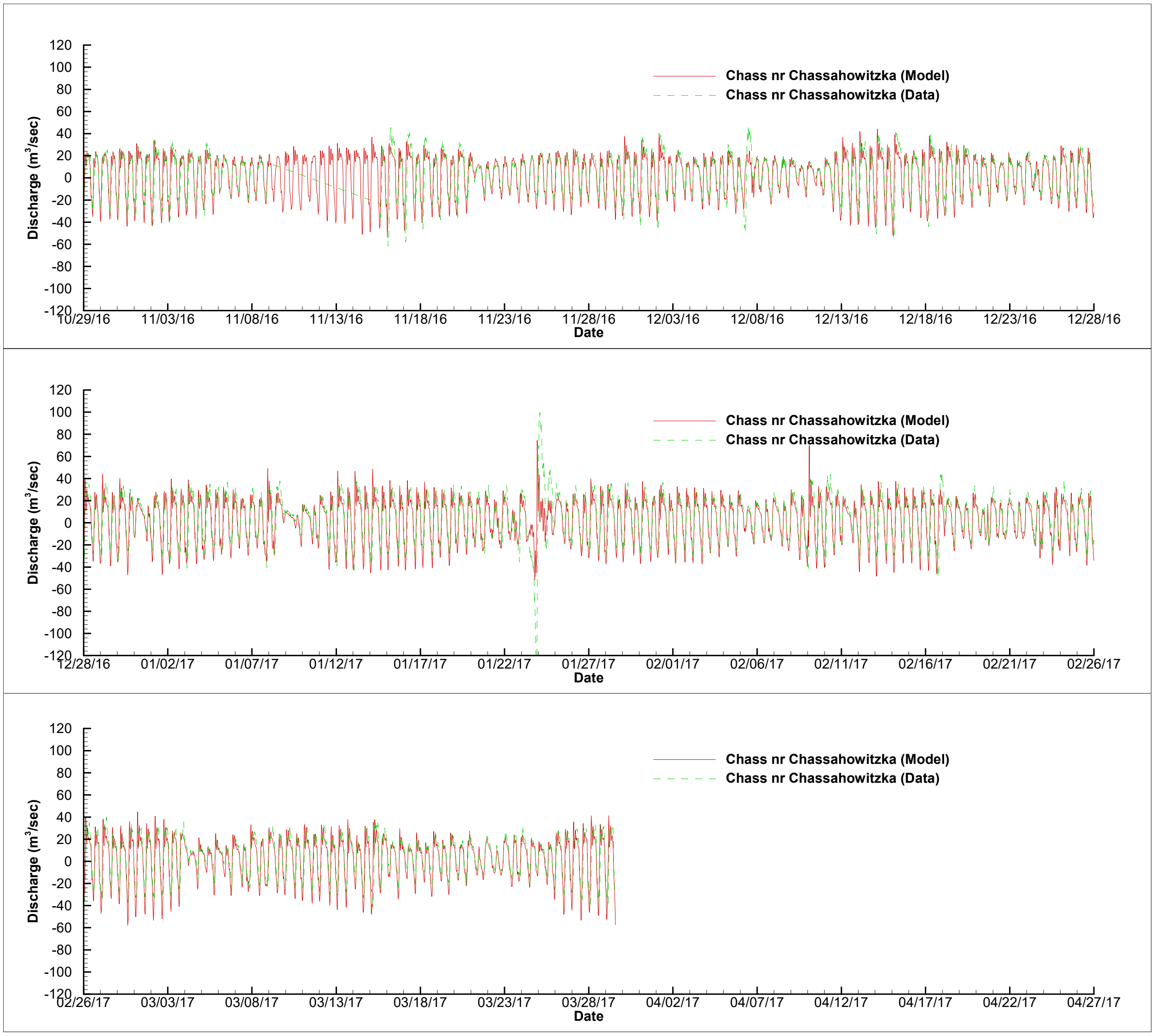

Figure G - 9. Comparisons of simulated (red lines) and measured (dashed green lines) discharges at the Chassahowitzka River near Chassahowitzka station 10/29/2016 - 4/27/2016.

Appendix H. Upstream Boundary Conditions

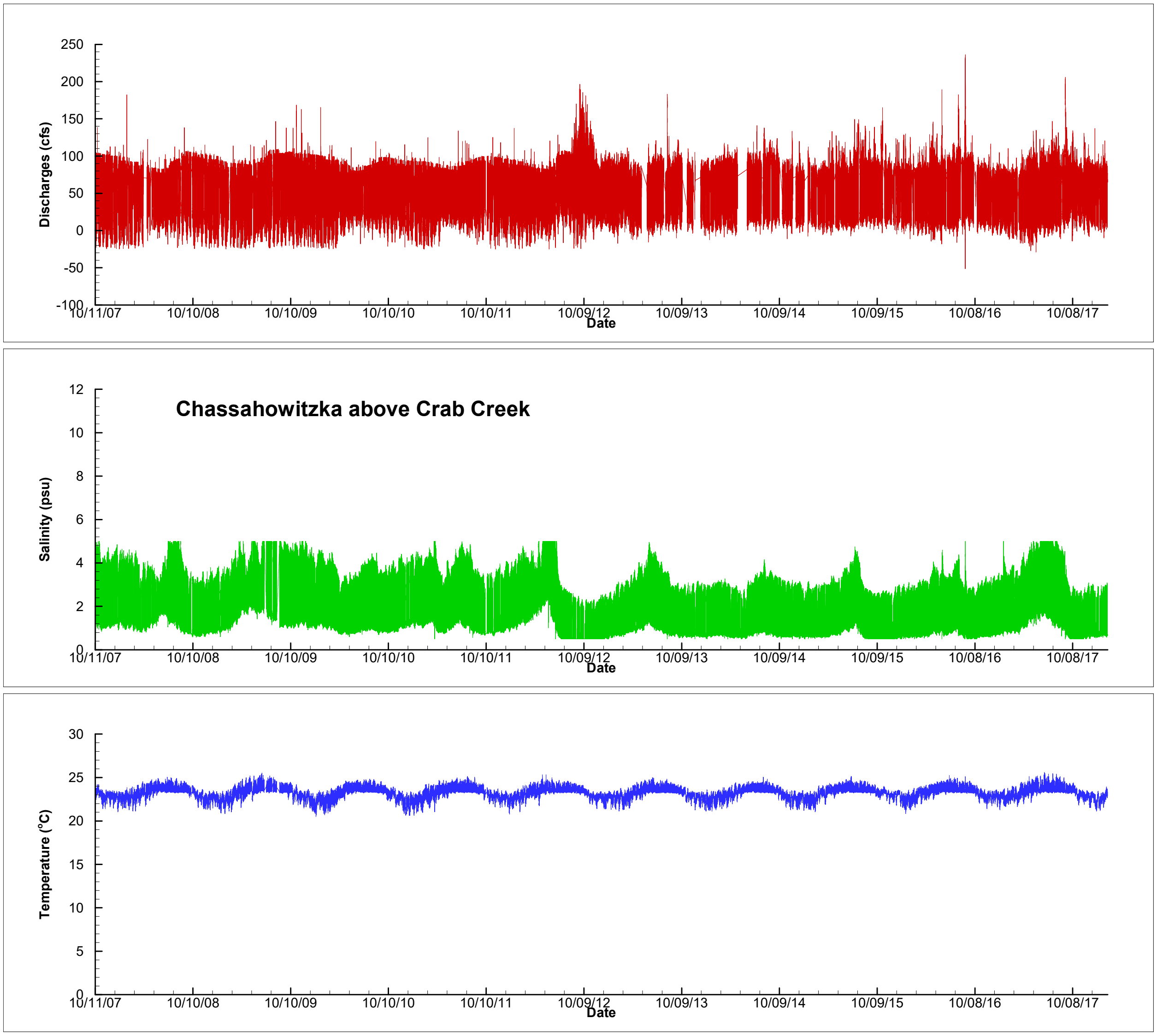

Figure H - 1. Time series plots of flow rate (top panel), salinity (middle panel), and temperature (bottom panel) of submarine groundwater discharge entering the Chassahowitzka River above the Crab Creek during 10/11/2007 through 2/16/2018.

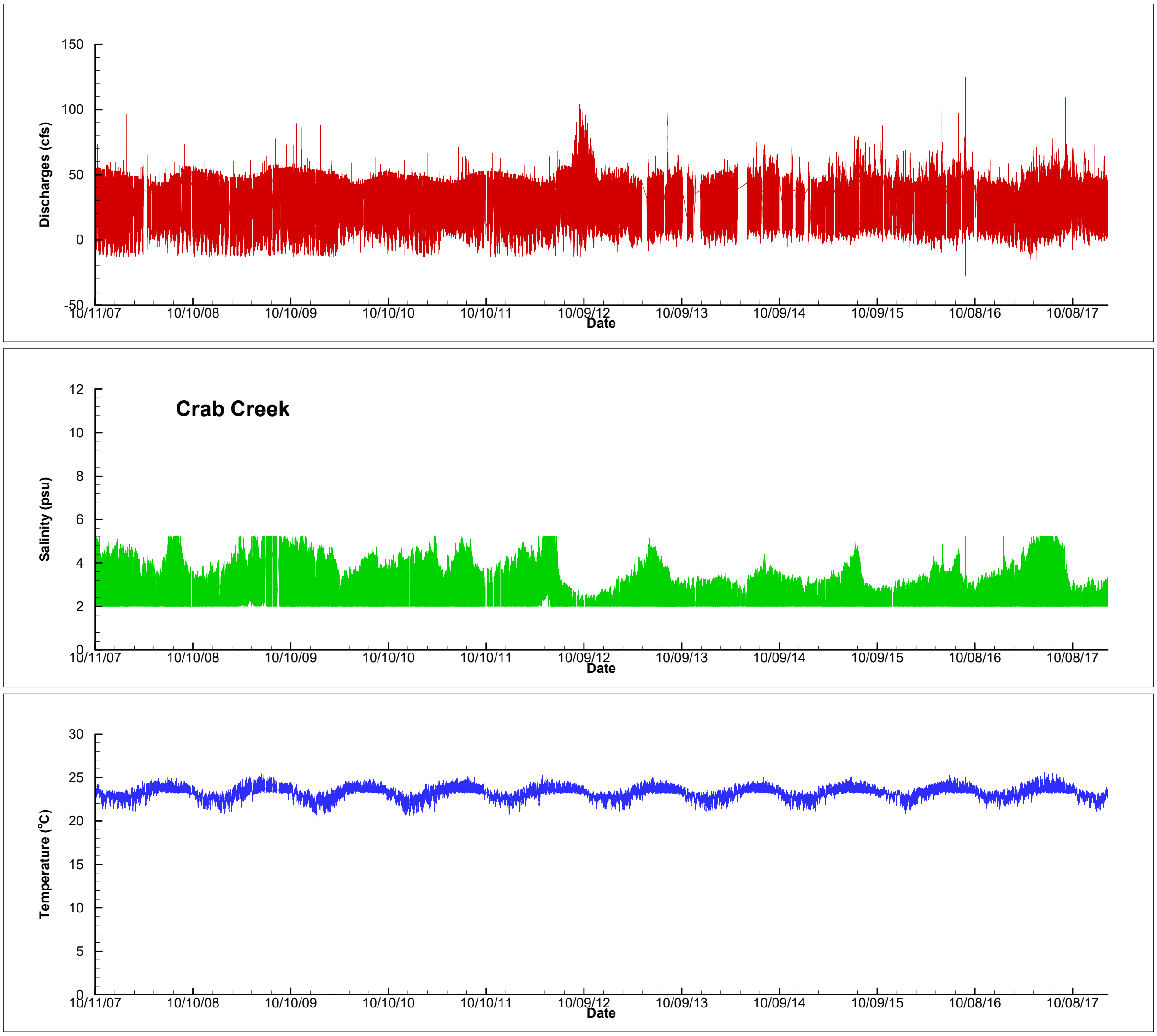

Figure H - 2. Time series plots of flow rate (top panel), salinity (middle panel), and temperature (bottom panel) of submarine groundwater discharge entering the Crab Creek during 10/11/2007 through 2/16/2018.

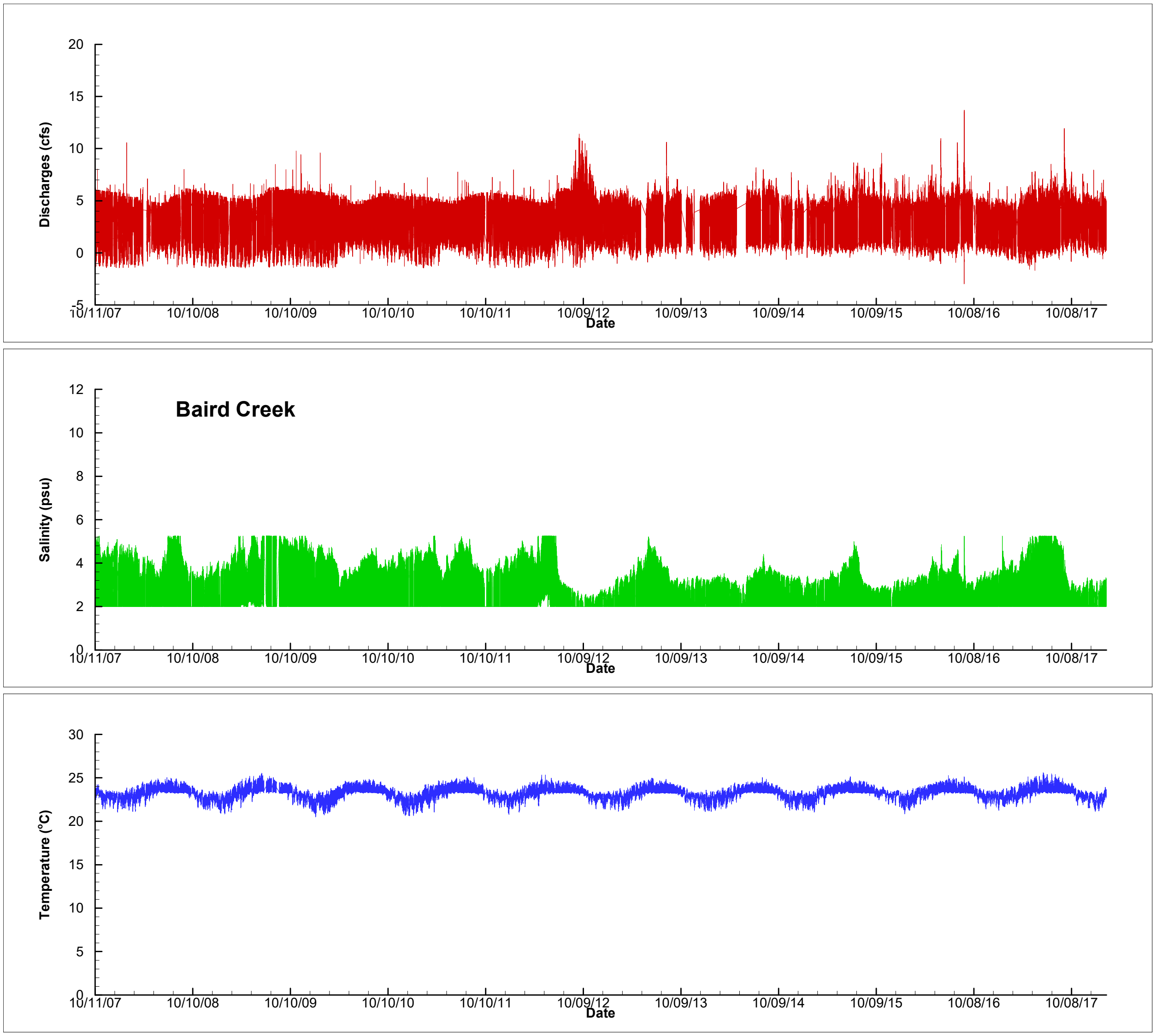

Figure H - 3. Time series plots of flow rate (top panel), salinity (middle panel), and temperature (bottom panel) of submarine groundwater discharge entering the Baird Creek during 10/11/2007 through 2/16/2018.

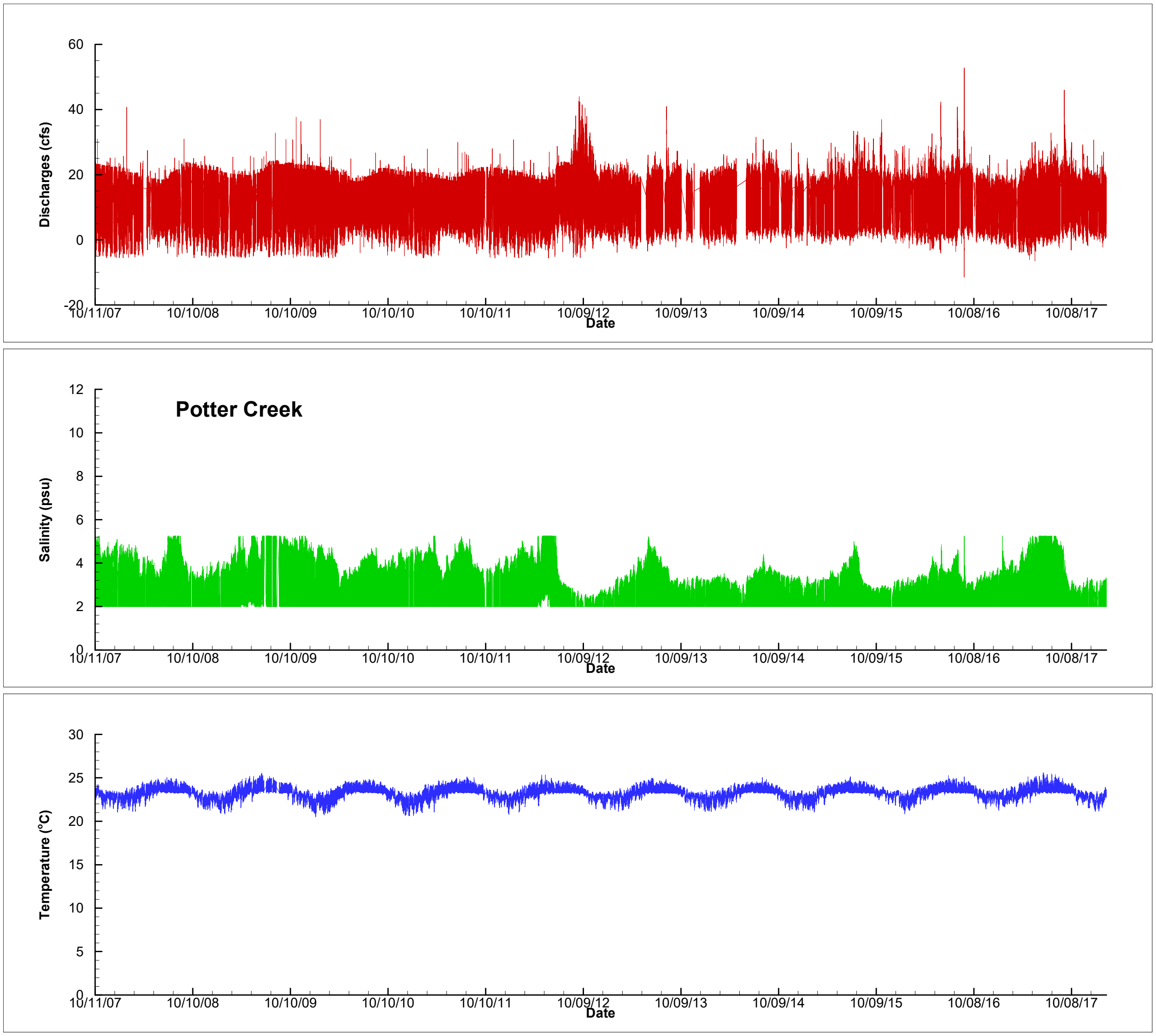

Figure H - 4. Time series plots of flow rate (top panel), salinity (middle panel), and temperature (bottom panel) of submarine groundwater discharge entering the Potters Creek during 10/11/2007 through 2/16/2018.

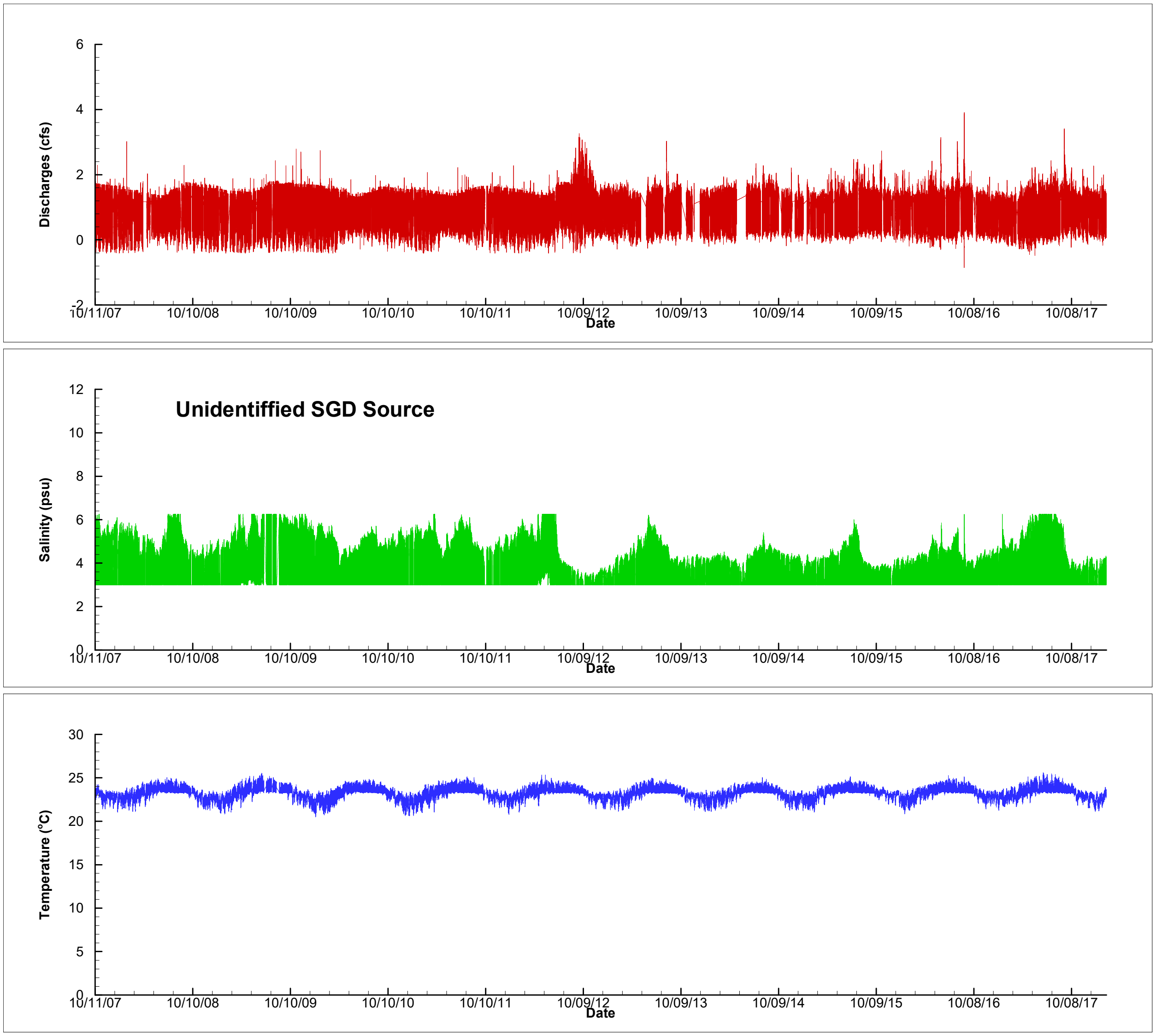

Figure H - 5 Time series plots of flow rate (top panel), salinity (middle panel), and temperature (bottom panel) of submarine groundwater discharge entering the Chassahowitzka River from an unidentified SGD source during 10/11/2007 through 2/16/2018.

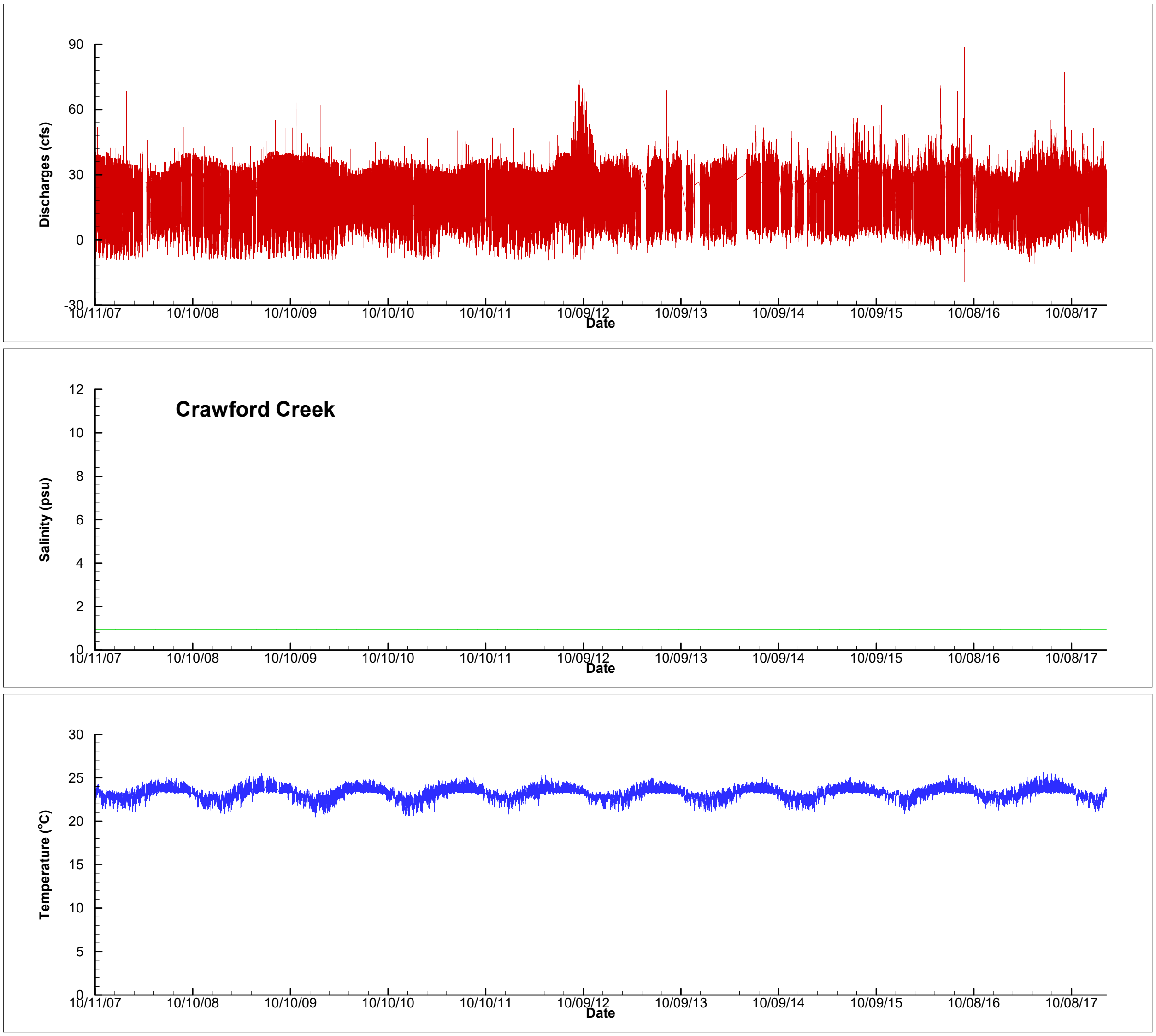

Figure H - 6. Time series plots of flow rate (top panel), salinity (middle panel), and temperature (bottom panel) of submarine groundwater discharge entering the Crawford Creek during 10/11/2007 through 2/16/2018.